ON SEQUENCE DESIGN FOR INTEGRATED RADAR AND COMMUNICATION SYSTEMS

Momin Jamil Sandhu

Blekinge Institute of Technology
Doctoral Dissertation Series No. 2017:07

Department of Creative Technologies

On Sequence Design for Integrated Radar and Communication Systems

Momin Jamil Sandhu

Blekinge Institute of Technology Doctoral Dissertation Series
No 2017:07

On Sequence Design for Integrated Radar and Communication Systems

Momin Jamil Sandhu

Doctoral Dissertation in
Telecommunications

Department of Creative Technologies
Blekinge Institute of Technology
SWEDEN

Department of Creative Technologies
Publisher: Blekinge Institute of Technology
SE-371 79 Karlskrona, Sweden
Printed by Exakta Group, Sweden, 2017
ISBN: 978-91-7295-340-6
ISSN:1653-2090
urn:nbn:se:bth-15009

Abstract

The motivation of having a joint radar and communication system on a single hardware is driven by space, military, and commercial applications. However, designing sequences that can simultaneously support radar and communication functionalities is one of the major hurdles in the practical implementation of these systems. In order to facilitate a simultaneous use of sequences for both radar and communication systems, a flexible sequence design is needed.

The objective of this dissertation is to address the sequence design problem for integrated radar and communication systems. The sequence design for these systems requires a trade-off between different performance measures, such as correlation characteristics, integrated sidelobe ratio, peak-to-sidelobe ratio and ambiguity function. The problem of finding a trade-off between various performance measures is solved by employing meta-heuristic algorithms.

This dissertation is divided into an introduction and three research parts based on peer-reviewed publications. The introduction provides background on binary and polyphase sequences, their use in radar and communication systems, sequence design requirements for integrated radar and communication systems, and application of meta-heuristic optimization algorithms to find optimal sets of sequences for these systems.

In Part I-A, the performance of conventional polyphase pulse compression sequences is compared with Oppermann sequences. In Part I-B, weighted pulse trains with the elements of Oppermann sequences serving as complex-valued weights are utilized for the design of integrated radar and communication systems. In Part I-C, an analytical expression for the cross-ambiguity function of weighted pulse trains with Oppermann sequences is derived. Several properties of the related auto-ambiguity and cross-ambiguity functions are derived in Part I-D. In Part II, the potential of meta-heuristic algorithms for finding optimal parameter values of Oppermann sequences for radar, communications, and integrated radar and communication systems is studied. In Part III-A, a meta-heuristic algorithm mimicking the breeding behavior of Cuckoos is used to locate more than one solution for multimodal problems. Further, the performance of this algorithm is evaluated in additive white Gaussian noise (AWGN). It is shown that the Cuckoo search algorithm can successfully locate multiple solutions

in both non-noise and AWGN with relatively high degree of accuracy. In Part III-B, the cross-ambiguity function synthesization problem is addressed. A meta-heuristic algorithm based on echolocation of bats is used to design a pair of sequences to minimize the integrated square error between the desired cross-ambiguity function and a synthesized cross-ambiguity function.

Preface

In this dissertation, the sequence design problem for integrated radar and communication system is addressed. Firstly, Oppermann sequences have been identified as potential sequences for integrated radar and communication systems. They have been compared against conventional polyphase pulse compression sequences using various performance measures. Secondly, meta-heuristic algorithms have been used to design sequences for radar, communications, as well as for integrated systems. Thirdly, the problem of synthesizing cross-ambiguity functions using a meta-heuristic algorithm based on the echolocation behaviour of bats is considered. In particular, the problem of matching a synthesized cross-ambiguity function to a desired cross-ambiguity function with a pre-defined magnitude over the delay-Doppler plane is solved using a meta-heuristic algorithm. This work has been carried at the Faculty of Computing, Blekinge Institute of Technology, Karlskrona, Sweden. The dissertation consists of an introduction section followed by three research parts as follows.

Introduction

Part I

A Performance Assessment of Polyphase Pulse Compression Codes

B On Integrated Radar and Communication Systems Using Oppermann Sequences

C Cross-Ambiguity Function of Weighted Pulse Trains with Oppermann Sequences

D Properties of Ambiguity Functions for Weighted Pulse Trains With Oppermann Sequences

Part II

Waveform Optimization for Integrated Radar and Communication Systems Using Meta-Heuristic Algorithms

Part III

Acknowledgements

Completing the requirements to receive a Doctor of Philosophy degree demanded a great deal of time, dedication, preparation, training, and a good supervision. It requires a continuous internal drive, immense desire and blessings of God Almighty to see it through.

Firstly, I would like to thank Prof. Hans-Jürgen Zepernick for his guidance, criticism, support, and continued motivation throughout the dissertation. You taught me how to question thoughts and express ideas. Your guidance, patience, and support helped me to overcome many crisis and finish this dissertation. Thank you for encouraging the use of correct grammar and consistent notation in my writings and for carefully reading and commenting on countless revisions of publications and this manuscript. You have been absolute key in the completion of this dissertation.

Secondly, I would like to thank Dr. Xin-She Yang of Middlesex University for introducing me to the topic of meta-heuristic optimization. Thank you for always taking time out from your busy schedule to answer my countless question and stimulating discussions on the topic. Your in-depth insight and continuous support is much appreciated.

Thirdly, I would like to thank Prof. Mats Pettersson and Docent Siamak Khatibi for acting as co-supervisors in the earlier and later stage of the candidacy, respectively.

Although too many to mention by name you know who you are. You've all had an impact on me. However, certain individuals were instrumental. Special thanks to Bringfired and Heidi Wehmeyer and Else Rausch. Your support has been immense and is much appreciated.

To my long-time friends Jacques Cilliers, Daine van Wyk, Frans Marx, Leon Staphorst, Jacques van Wyk, Naeem Abbas, Holger Roos, Michael Zeller, Esslinger Rolf, Axel Westenweller and Zahid Saeed. You all are true and time-tested friends. Thanks to Tariq, Mujahid, and Danish for their unconditional support, you all have been great brothers.

Mom and Dad, you don't live to see the dissertation in this form. Your prayers that something good would finally come of me appears to be giving fruit. Thanks for teaching me to appreciate the value of hard work. I hope, you both might be watching through the holes in the Heaven.

Neelum, you deserve deepest gratitude. Thank you for being with me all these years and putting up with me through thick and thin. Your role in my life was, and remains, immense. Your encouragement is much appreciated and duly noted. It was a great comfort and relief to know that you were willing to provide management of our household activities and taking care of the children while I completed my work. Many heartfelt thanks.

Lastly, to my girls Manaal, Haania and Wiam. You all had a hard time. I have missed many precious moments as I always and constantly worked during the weekdays, weekends, and even in my holidays. You always found me locked up in the study or behind the books or on a laptop for many years. I love you all. Can we play now and have some fun?

Momin Jamil Sandhu
Karlsbad, June 2017

Publication list

Part I is based on:

M. Jamil, H.-J. Zepernick, and M. I. Pettersson, "Performance Assessment of Polyphase Pulse Compression Codes," *IEEE Intl. Symp. on Spread Spectrum Techn. and Its Appl.*, Bologna, Italy, Aug. 2008, pp. 166–172.

M. Jamil, H.-J. Zepernick, and M. I. Pettersson, "On Integrated Radar and Communication Systems Using Oppermann Sequences," *IEEE Military Commun. Conf.*, San Diego, U.S.A., Nov. 2008, pp. 1–6.

M. Jamil, H.-J. Zepernick and M. I. Pettersson, "Cross-Ambiguity Function for Weighted Pulse Trains with Oppermann Sequences," *IEEE Intl. Symp. on Wireless Commun. Syst.*, Siena, Italy, Sept. 2009, pp. 239–243.

M. Jamil, H.-J. Zepernick, and M. I. Pettersson, "Properties of Ambiguity Functions for Weighted Pulse Trains with Oppermann Sequences," *Intl. Conf. on Signal Process. and Commun. Syst.*, Omaha, Nebraska, U.S.A., Sept. 2009, pp. 1–8.

Part II is based on:

M. Jamil and H.-J. Zepernick, "Waveform Optimization for Integrated Radar and Communication Systems Using Meta-Heuristic Algorithms," Book Chapter in *Comput. Optimization and Appl. in Eng. and Ind.*, Springer, Heidelberg, pp. 183–203, 2011.

Part III-A is based on:

M. Jamil and H.-J. Zepernick, "Multimodal Function Optimisation with Cuckoo Search Algorithm," *Int. J. Bio-Inspired Comput.*, vol. 5, no. 2, pp. 73–83, 2013.

Part III-B is based on:

M. Jamil, H.-J. Zepernick, and X.-S. Yang, "Synthesizing Cross-Ambiguity Functions Using Improved Bat Algorithm," Book Chapter in *Recent Advances in Swarm Intell. and Evol. Comput.*, Springer International Publishing, Cham, pp. 179–202, 2015.

Other publications in conjunction with the thesis:

M. Jamil, H.-J. Zepernick, and X.-S. Yang, "Sequence Optimization for Integrated Radar and Communication Systems Using Meta-heuristic Multiobjective Methods," *IEEE Radar Conf.*, Seattle, WA, U.S.A., May 2017.

M. Jamil, H.-J. Zepernick, and X.-S. Yang, "Multimodal Function Optimization Using an Improved Bat Algorithm in Noise-Free and Noisy Environments," Book Chapter in *Nature Inspired Comput. and Optimization - Theory and Appl.*, Springer, Apr. 2017.

M. Jamil and H.-J. Zepernick, "Sequence Design for Radar Applications Using Particle Swarm Optimization," *IEEE Intl. Conf. on Advanced Technol. for Commun.*, Hanoi, Vietnam, Oct. 2016, pp. 210-214.

M. Jamil and H.-J. Zepernick, "Lévy Flights and Global Optimization," Book Chapter in *Swarm Intell. and Bio-Inspired Comput.: Theory and Appl.*, Elsevier, pp. 49–69, May 2013.

M. Jamil and H.-J. Zepernick, "Test Functions for Global Optimization: A Comprehensive Survey," Book Chapter in *Swarm Intell. and Bio-Inspired Comput.: Theory and Appl.*, Elsevier, pp. 193–221, May 2013.

M. Jamil and X.-S. Yang, "A Literature Survey of Benchmark Functions for Global Optimisation Problems," *Int. J. Mathematical Modelling and Numerical Optimisation*, vol. 4, no. 2, pp. 150–194, 2013.

M. Jamil, H.-J. Zepernick, and X.-S. Yang, "Lévy Flight Based Cuckoo Search Algorithm for Synthesizing Cross-Ambiguity Functions," *IEEE Military Commun. Conf.*, San Diego, CA, U.S.A., Nov. 2013, pp. 823–828.

List of Acronyms

AC	Autocorrelation
AAC	Aperiodic Autocorrelation
ACC	Aperiodic Crosscorrelation
AF	Ambiguity Function
AMRFC	Advanced Multifunction Radio Frequency Concept
CAF	Cross-Ambiguity Function
CC	Crosscorrelation
CDMA	Code Division Multiple Access
DS	Direct Sequence
DSP	Digital Signal Processor
DSSS	Direct Sequence Spread-Spectrum
EA	Evolutionary Algorithm
FOM	Figure of Merit
GA	Genetic Algorithm
GNSS	Global Navigation Satellite System
IFF	Identification Friend or Foe
ISLR	Integrated Sidelobe Ratio
LFSR	Linear Feedback Shift Register
LPI/D	Low Probability of Intercept/Detection
MO	Multiobjective
MS	Mean Square

MUI	Multi-User Interference
OVSF	Orthogonal Variable Spreading Factor
PN	Pseudo-Noise
PR	Pseudo-Random
PSLR	Peak-to-Sidelobe Ratio
PSO	Particle Swarm Optimization
RF	Radio Frequency
SNR	Signal-to-Noise Ratio
SSR	Secondary Surveillance Radar
UCHT	Unified Complex Hadamard Transform
V2I	Vehicle-to-Infrastructure
V2V	Vehicle-to-Vehicle
WLAN	Wireless Local Area Network
WSN	Wireless Sensor Network

Contents

Introduction

1 Motivation

Radar systems operate in an environment that is corrupted by noise and may consist of a variety of clutter conditions. Under these conditions, two primary goals of any radar system are parameter estimation and target resolution [1]. The parameter estimation of a target includes information related to its size, motion, and location. The ability of a radar to distinguish between targets that are very close either in range or bearing refers to target resolution [1].

On the other hand, wireless communication systems are required to provide a certain minimum transmission quality in order to meet user demands in speech and mobile multimedia communication applications [2]. Wireless communication systems focus on achieving the best possible transmission quality under noise, spectrum, and transmit power constraints.

Given the application scenarios and operational requirements, radar and wireless communication systems have been traditionally developed and studied as separate research entities. However, by developing a single platform with reconfigurable architecture and flexible software, it is envisaged that such a platform will provide a possibility of maintaining several functions with one single radio frequency (RF) front-end. The integration of various tasks on a single platform will have many benefits such as architecture unification and simplification, functional reconfiguration, efficiency enhancement, reduced costs, weight, and total power consumption.

The motivation of having a joint radar and communication system on a single hardware is driven by a multitude of emerging space, military, and commercial applications. The NASA Space Shuttle Orbiter [3] might be regarded as the first known application of an integrated radar and communication system for space applications. For military applications, the Advanced Multifunction Radio Frequency Concept (AMRFC) proposed in [4] addressed the need of integrating radar, communications, and electronic warfare functions on a single platform. Such systems can simultaneously handle mission-critical and military operations such as electronic surveillance and battlefield communication. By integrating radar, communications, and electronic warfare, it was envisaged to achieve the following goals: (i) decrease the electronic hardware such as topside antennas, (ii) alleviate the problems of antenna blockage, (iii) resolve own-ship electromagnetic interference, and (iv) reduce the stress on maintenance resources.

Recent years have seen a multitude of emerging applications fusing radar and wireless communication functionalities on a single platform [5, 6, 7, 8]. A wireless sensor network (WSN) for positioning and monitoring purposes is one such example [9]. In a WSN, each node detects targets and shares the information with other nodes in a network through wireless communication links. Another example includes connected cars supporting vehicle-to-vehicle (V2V) or vehicle-to-infrastructure (V2I) communication applications. In these systems, a vehicle possesses and exchanges relevant information about its surrounding with others in V2V or V2I systems. In a V2V system, vehicles are able to exchange information to improve road and vehicle safety, enhance collision avoidance systems, support energy conservation, and develop smarter traffic management systems [10, 11]. Vehicles in V2I applications not only receive road, traffic, and weather information from the road side infrastructure but also exchange this information among the vehicles [11, 12]. Yet, another example include research on signals for hybrid receivers for Global Navigation Satellite Systems (GNSS) [13].

Developing a flexible multi-functional system is a complex task. The design of such a system needs to fulfill several stringent requirements such as simple implementation, flexible functional reconfiguration, high power efficiency, fast system response, and low cost. Nowadays, the

operating frequencies for wireless communication applications are of the same magnitude as once used for radar applications. This, in combination with the advancement in digital circuit technology, will help simplifying the RF front-end architectures for integrated radar and communication systems. Further, increasing number of functionalities once realized on hardware components are now being implemented on digital signal processors (DSPs). Therefore, most of the system functions of integrated radar and communication applications can be realized using adaptive and configurable software systems while keeping the same RF front-end architecture.

A design of a flexible integrated radar and communication platform would offer unique possibilities for novel system concepts and applications. One such application is intelligent transportation systems. These systems require both environment sensing and the allocation of an ad-hoc communication link for reliable operation. However, one of the major hurdles in the development and practical implementation of such applications to simultaneously support communication and radar-like functions lies in proper sequence design. In other words, sequence designs for such applications require to cater needs for both radar and communication applications.

In radar applications, it is desirable to have sequences that exhibit an ideal or thumbtack autocorrelation (AC) function, i.e., peak at zero delay and no sidelobes at delays other than zero. However, in practice, the return signal may be corrupted by noise and clutter. Therefore, when a matched radar receiver performs correlation between the return signal and the receiver reference sequence, sidelobes are created in addition to the mainlobe. These sidelobes may block reflections from smaller or weaker targets and let them go undetected, therefore, they are highly undesirable.

For communication systems, a large number of sequences is required to facilitate simultaneous channel access for many users. In this case, sequences with both good AC and good crosscorrelation (CC) would be desirable. A good AC means that a transmitted sequence and its time-shifted versions is nearly uncorrelated and ideally have zero sidelobes at all possible shifts. This is desirable for timing recovery and coherent detection [14, 15]. On the other hand, good CC means that

all the transmitted sequences and their time-shifted replicas are nearly uncorrelated with respect to each other. In order to reduce multi-user interference (MUI), minimizing CC among the transmitted sequences is a major design consideration.

This dissertation addresses the sequence design problem for integrated radar and communication systems by finding trade-offs between AC and CC properties of Oppermann sequences [16, 17]. These sequences are found to be suitable to support joint operation of radar and communication functionalities. The choice of Oppermann sequences for such systems is motivated due to: (i) this family offers a wide range of correlation properties and (ii) may offer better correlation properties compared to other well-known families of polyphase sequences [16, 17].

Further, in this dissertation, population-based meta-heuristic algorithms have been used to find suitable sets of Oppermann sequences for integrated radar and communication systems. It should be emphasized that, even if the investigations presented in this dissertation focus on integrated radar and communication systems, Oppermann sequences can also be employed either in radar or communication systems [17].

The remainder of the introduction is organized as follows. Section 2 gives an overview of binary and polyphase sequences. Section 3 introduces polyphase sequences for radar and communication systems. Sequence design requirements for integrated radar and communication systems are addressed in Section 4. In Section 5, the definitions of the performance measures for radar and communication systems are introduced. Section 6 presents an overview of meta-heuristic algorithms in the context of sequence design for radar and communication systems. Finally, an overview of Lévy flights and a motivation of using Lévy flights to solve global optimization problems is provided in Section 7.

2 Overview of Sequences

A sequence of length N is defined as a vector $\mathbf{u}_k = [u_k(0), u_k(1), \ldots, u_k(N-1)]$ whose elements $u_k(l)$ are drawn from a set $\mathcal{U}$ of size U, where $1 \leq k \leq U$. In general, sequences can be classified into two categories, i.e., real and complex.

Different kinds of sequences can be found throughout the literature, e.g., [14, 15, 18], such as binary, quadriphase, non-binary, periodic, aperiodic, frequency-hopping, optical orthogonal sequences, one or two-dimensional arrays, complementary pairs, and complementary sets.

2.1 Binary Sequences

A sequence $\mathbf{u}_k$ is called binary, if each element of the sequence $\mathbf{u}_k$ takes values from the set $\{0, 1\}$ or $\{-1, 1\}$. If the elements of $\mathbf{u}_k$ take values $\{0, 1\}$, then the sequence is called unipolar. If the elements of $\mathbf{u}_k$ take values $\{-1, 1\}$, the sequence is classified as bipolar.

Binary sequences have been extensively studied and are frequently used in both civilian and military applications [14, 15, 18]. Many applications require to fulfill the contradictory requirement of generating random, yet repeatable finite-length sequences. These applications include system identification, synchronization, spread-spectrum (SS) communication, cryptography, radar, channel estimation, equalization, test measurement, and coded aperture imaging.

Binary sequences that fulfill the following three randomness criteria, namely, the balance criterion, the run criterion, and the correlation criterion are also called pseudo-random (PR) sequences, pseudo-noise (PN) sequences, or optimal binary sequences [14]. Not many families of binary sequences are known to exist that simultaneously fulfill these randomness criterion. These sequences exhibit random-like behaviour and at the same time are generated using deterministic methods.

PR sequences are known to exhibit a multi-level AC function. In general, the AC function is considered as good, if the sidelobes of the AC function are low. Similarly, CC is considered as good, if a pair of sequences in a given set exhibits low values for all possible time shifts. A comprehensive coverage on binary and real-valued sequences can be found in [14] and the references therein. A non-exhaustive list of some notable families of binary sequences is given in Table 1.

The commonly used PN-sequences are maximal-length sequences (m-sequences), Gold and Kasami sequences. The m-sequences are used to generate either Gold or Kasami sequences through linear feedback shift registers (LFSRs).

2.2 Polyphase Sequences

A sequence $\mathbf{u}_k$ is called complex, if its elements are complex numbers. Further, a complex sequence is called polyphase sequence if its elements can be represented as a complex q-th root of unity, i.e.,

$$u_k(l) = e^{j\frac{2\pi}{q}kl}, \quad 0 \leq l \leq q-1 \tag{1}$$

The origin of polyphase sequences dates back to the 1950's [14, 15]. Since then, many new families of polyphase sequences have been proposed, e.g., [14, 15]. The first publicly known work on polyphase sequences was presented in [19]. These sequences give more degrees of freedom for sequence design since each of its elements can be represented by a real and imaginary component. This makes it possible to design sequences with better correlation properties as compared to binary sequences. A non-exhaustive list of some notable families of polyphase sequences is provided in Table 2.

3 Polyphase Sequences for Radar and Communication Applications

Polyphase sequences have been proposed and analyzed for diverse applications such as radar systems and SS communication systems. The advancement in integrated circuit technologies has been paving the way for implementation of polyphase sequences in radar and communication systems. In the sequel, polyphase sequences are considered for potential use in integrated radar and communication systems.

3.1 Polyphase Sequences for Radar Applications

Space and military applications have played a major role in the advent of PN sequences and related signal processing techniques. The following two basic requirements must be satisfied when designing waveforms for radar applications [31, 32, 33]:

Table 1: List of notable binary sequences

Characteristics	Binary sequences	Ref.
Optimal AC	m-sequences	[14]
	Hall sequences	[14]
	GMW sequences	[14]
	Jacobi sequences	[14]
	Legendre sequences	[14]
	Twin prime sequences	[14]
	Biquadratic sequences	[14]
	Octic residue sequences	[14]
Good AC/CC	No sequences	[20]
	BCH sequences	[14]
	Gold sequences	[21, 22]
	Visme sequences	[14]
	Kasami sequences	[23]
	Gold-like sequences	[14]
	Bent function sequences	[14]
	Boztas-Kumar sequences	[24]
	Frank-Chu like sequences	[14]
	Bomer-Antweiler sequences	[14]
	Trajectory derived sequences	[14]

Table 2: List of notable polyphase sequences

Characteristics	Polyphase sequences	Ref.
Ideal periodic AC	Perfect array	[14]
	Chu sequences	[25]
	Frank sequences	[26]
	Milewski sequences	[14]
	Frank-Zadoff sequences	[27]
	Ipatov ternary sequences	[14]
	Generalized Bent sequences	[14]
	Frank-Zadoff-Chu sequences	[14]
Ideal periodic CC	Lüke sequences	[14]
	Helleseth sequences	[14]
	Cubic phase sequences	[14]
	Kumar-Moreno sequences	[14]
	Non-binary Kasami sequences	[14]
	Families of quadriphase sequences	[14, 24, 28]
Good aperiodic AC/aperiodic CC	Chu sequences	[25]
	Frank sequences	[26]
	Huffmann sequences	[14]
	Polyphase Barker sequences	[14]
Special correlation	EOE sequences	[29]
	ABC sequences	[30]
	Oppermann sequences	[16, 17]

- Short duration pulses for good range resolution. A short pulse in time domain requires large bandwidth in the frequency domain.
- The target detection calls for sufficient energy on the target.

The pulse duration of the transmitted radar pulse enables the radar to emit sufficient energy that allows a radar receiver to detect the reflected pulse from the target. The product of transmitter output power and the transmission pulse duration corresponds to the amount of energy that is delivered to a distant target. The maximum detection range of a target is constrained by pulse duration which limits the energy efficiency of a radar system. Pulse compression is a way to increase the energy of the transmitted signal by evenly spreading it over the pulse duration without sacrificing detection range. In this way, energy efficiency of a radar improves significantly. Practical radar systems employ either frequency or phase coding to achieve pulse compression [34].

The matched filter plays an important role in processing pulse compression sequences [32]. The output of a matched filter is equivalent to correlating the received signal with a locally stored copy of the transmitted sequence in a radar receiver. Thus, the output of the matched filter represents an aperiodic autocorrelation (AAC) function of a pulse compression sequence. The performance of a phase coded pulse compression radar depends on the similarity of the matched filter output to an ideal AAC without any sidelobe artifacts at delays other than zero.

Pulse compression sequences exhibiting perfect AAC without any sidelobe artifacts do not exist [32, 34]. The sidelobes are highly undesirable as they spread out to mask the mainlobe response of weaker targets, leaving them undetected. Consequently, much research effort has been directed towards the reduction of sidelobes, either by signal processing techniques or by sophisticated designs of pulse compression sequences [32].

Polyphase sequences provide an alternative to frequency-modulated signals [18, 32] for radar applications. Traditionally, binary sequences such as Barker and m-sequences have been used for radar applications due to their simplistic implementation. However, both Barker and

m-sequences exhibit high sidelobes in range. Therefore, polyphase sequences have been seen as an alternative to binary sequences. Compared to binary sequences, polyphase sequences offer better Doppler tolerance for a broader range-Doppler coverage [31, 32, 33, 34, 35]. A non-exhaustive list of some notable families of polyphase sequences for radar applications is given in Table 3.

3.2 Polyphase Sequences for Communication Applications

SS is a class of methods to modulate information on radio signals [36]. In SS systems, the bandwidth of the transmit signal is spread, resulting in a signal with wider bandwidth. All SS systems make use of spreading sequences to spread the bandwidth of a given signal. This provides a number of advantages, such as interference suppression, multipath resistance, and low probability of intercept/detection (LPI/D). Therefore, it is desirable to design spreading sequences with good correlation characteristics.

The elements of a spreading sequence are called chips. The rate at which the spreading sequence is transmitted is called chip rate T_c. The period of the spreading sequence is given by $T = N \cdot T_c$, where N is the number of chips in the spreading sequence.

In SS systems, a single data bit is replaced with a spreading sequence. The optimal detection of this data bit is possible only if the spreading sequence is known at the receiver. Good correlation properties increase the detection of the desired signal in multipath channels or clutter interference.

The two contradicting design goals of spreading sequence are to have good AC and good CC properties. The good AC improves synchronization and combats multipath fading, while good CC allows multiple users to access the same transmission medium by minimizing the mutual interference among multiple users.

The development of cellular mobile communication systems and SS based radios for indoor communication gave a major boost to the application of PR sequences in the field of communication systems [14, 15]. In particular, the code division multiple access (CDMA) system developed by Qualcomm Incorporated for digital cellular phone

Table 3: List of notable polyphase sequence families for radar applications

Name	**Type**	Ref.
Barker sequences	Phase sequences	[39]
Complementary sequences	Complementary phase sequences	[40]
Huffman sequences	Phase sequences	[41]
Frank sequences	Chirp-like phase sequences	[26, 42]
Zadoff-Chu sequences	Chirp-like phase sequences	[42]
Gold sequences	Binary phase sequences	[21, 22]
Minimum peak-sidelobe sequences	Binary phase sequences	[43, 44]
Welti sequences	Sub-complementary sequences	[45]
P1, P2, P3, P4, Px sequences	Phase sequences	[46, 47, 48]
Frank polyphase sequences	Polyphase sequences	[46, 47]
Costas array	Frequency sequences	[49]
Quadratic congruential coding	Frequency sequences	[50]
Polyphase Barker sequences	Phase sequences	[51]
Biphase perfect sequences	Bi-phase sequences	[52]
Ipatov sequences	Sequences with minimal peak response loss	[53]
P(n,k) sequences	Phase sequences	[54]
PONS based complementary sequences	Complementary sequences	[55]
Orthogonal sequences	Train of orthogonal coded pulses	[56]
Multi-carrier phase coded pulse	Multi-carrier phase coded signals	[32]
Björck sequences	Polyphase sequences based on Legendre symbol	[57]

applications and the family of IEEE 802.11(b/g/n) standards for wireless local area networks (WLANs) [37] have taken the theoretical concepts of SS into practical systems. Walsh-Hadamard sequences [14], m-sequences [14, 15], Barker sequences [14, 15], and complementary sequence keying (CCK) based modulation [37] are the main classes of sequences used within these systems. Advanced SS methods, namely orthogonal variable spreading factor (OVSF) sequences and complex-valued short scrambling sequences, are employed in 3G mobile communication systems [15, 38].

When using a fully digital implementation of these sequences, the signal should be filtered to achieve the required spectral occupancy. This will not only allow the sharing of the available spectrum for satellite, military, and data applications, but also to achieve the desired spectral efficiency. Optimization of the latter directly affects the system capacity which is considered as one of the important design parameters in the development of a communication system employing CDMA. Furthermore, in order for the sequences to be modulatable and to ensure minimum bandwidth occupancy, the filtering technique must be chosen in a way that the correlation properties of the spreading sequence are not adversely affected. Keeping this in mind, the family of spreading sequence presented in [30] eliminates the need for a complex filter in a CDMA system.

4 Sequence Design for Integrated Radar and Communication Applications

The history of digital sequence designs is rich and has been widely discussed in [14, 15, 18] and references therein. However, sequence design with good correlation properties is discussed either in the context of radar or active sensing applications, e.g., [58, 59, 60, 61, 62, 63, 64], or for communication applications, e.g., [17, 30, 38, 65, 66, 67, 68, 69, 70, 71, 72, 73, 74, 75, 76, 77].

The first step towards the implementation of integrated radar and communication applications is to identify sequences that are suitable for both radar and communication applications. According to [31, 32, 33], a good sequence selection will enable the radar to (i) obtain good resolution in delay (range) and Doppler (velocity); (ii) obtain high

signal energy whilst using low peak power; (iii) preferably have a large number of sequences in a given set allowing several radars to operate in close proximity of each other in multiple-input multiple-output (MIMO) radar systems, and (iv) utilize the spectrum efficiently. Therefore, in order to support radar functionality, a sequence should be robust against interference, noise, and distortion due to multipath propagation.

On the other hand, communication applications need to accommodate higher data rates with simultaneous ability to provide a reliable communication link. Sequence design for a radio communication system based on direct sequence spread-spectrum (DSSS) should be designed to mitigate the interference from other users in the system. Also of prime importance is the performance of a sequence over multipath fading channels.

The brief overview of polyphase sequences from the viewpoint of radar and communication applications in Section 3 emphasizes the need for more flexible sequence designs to fulfill the conflicting requirements of these two applications. The work in this dissertation advocates the use Oppermann sequences for integrated radar and communication systems compared to conventional sequence designs. A wide range of correlation properties offered by Oppermann sequences distinguishes it from its peers and makes them suitable candidates for integrated radar and communication systems.

4.1 Oppermann Sequences

For any given sequence length N, Oppermann sequences are defined by three parameters m, n, and p. These parameters offer three degrees of freedom for designing these sequences. As a result, a great variety of trade-offs between AC, CC, and ambiguity function (AF) characteristics can be supported. So far, Oppermann sequences may have been considered mainly for communication applications, i.e., CDMA systems. However, in this dissertation, their suitability for integrated radar and communication applications has been studied.

Let a set $\mathcal{U}(m,n,p)$ of Oppermann sequences of length N be defined as [17]

$$\mathcal{U}(m,n,p) = \left\{ \{u_i^k(m,n,p)\} : \quad 0 \leq i \leq N-1, \quad 1 \leq k \leq N-1 \right\} \quad (2)$$

where the ith element u_i^k of the kth sequence in $\mathcal{U}(m,n,p)$ is given by [17]

$$u_i^k = (-1)^{k(i+1)} \exp\left[\frac{j\pi(k^m(i+1)^p + (i+1)^n)}{N}\right] \quad 0 \le i \le N-1 \tag{3}$$

where k is an integer relatively prime to sequence length N, $j = \sqrt{-1}$, and the parameters m, n, and p are real numbers. The latter three parameters control the correlation characteristics of Oppermann sequences [17]. According to [17], for any triplet (m,n,p), the maximum number of sequences in a set $\mathcal{U}(m,n,p)$ can be achieved only for prime sequence length N and is given by

$$U = N - 1 \tag{4}$$

Given the design flexibility offered by Oppermann sequences, it is possible to construct families of polyphase sequences with specific correlation characteristics.

The magnitude of the AAC function for all sequences in a family of Oppermann sequences is the same for a fixed combination of triplet (m,n,p) [17]. Further, for $p = 1$, the magnitude of the AAC function depends only on n and is given by

$$C_{k,k}(l) = \frac{1}{N}\left|\sum_{i=0}^{N-1-l} \exp\left[\frac{j\pi}{N}\Big((i+1)^n - (i+l+1)^n\Big)\right]\right| \tag{5}$$

for shifts $0 \le l \le N-1$ and $1-N \le l \le 0$, where

$$\Big|C_{k,k}(l)\Big| = \Big|C_{k,k}(-l)\Big| \tag{6}$$

For $l = 0$, the maximum magnitude of AAC becomes

$$\Big|C_{k,k}(0)\Big| = 1 \tag{7}$$

A comprehensive treatment on Oppermann sequences can be found in [15] and references therein.

5 Performance Measures

In this section, the definitions of measures used in the performance assessment of sequences for integrated radar and communication systems are provided.

5.1 Performance Measures for Radar Applications

The commonly used performance measures of sequences in this context are ambiguity function (AF), and sidelobe performance measures, such as integrated sidelobe ratio (ISLR) and peak-to-sidelobe ratio (PSLR).

5.1.1 Ambiguity Function

In the absence of motion between the radar, target, and the environmental interference, i.e., the clutter, the study of radar waveforms is a simple task. However, due to the presence of Doppler shift f_d, the target returns do not represent the true replicas of the transmitted waveform. In addition, the response from a second target or clutter at a slightly different range may appear at the radar receiver output when the desired target response is at its peak value. This overlap of signals occurs when the time extent of the waveform is greater than the differential time delay between the targets. As a result, signals at the radar receiver are characterized by using an AF.

The AF, first proposed by Woodward [78], is considered as an intricate, flexible, and indispensable tool to design and analyze radar sequences. It is particulary useful in analyzing resolution, sidelobe behaviour, ambiguities in both range and Doppler, and range-Doppler coupling for a given sequence [34].

It is worth pointing out that the definition of the AF varies throughout the literature [31, 33, 78, 79]. A standardized and widely accepted definition of the continuous-time AF is given by [80]

$$|\chi(\tau, f_d)|^2 = \left| \int_{-\infty}^{\infty} u(t) u^*(t+\tau) \exp(j2\pi f_d t) dt \right|^2 \tag{8}$$

where $u(t)$ is a transmitted signal, τ corresponds to a time shift, f_d is the Doppler frequency/Doppler shift, operator $(\cdot)^*$ denotes complex

conjugate, and $j = \sqrt{-1}$. A positive Doppler frequency f_d implies that a target is moving towards the radar [32, 80].

The AF describes the correlation between transmitted signal and its replica shifted both in time and frequency by an amount τ and f_d, respectively. According to (8), the AF can be regarded as the output of a matched filter receiver to a target shifted both in time and frequency from a reference target [80]. A matched filter receiver amplifies the received energy and maximizes the signal-to-noise ratio (SNR). The SNR at the radar receiver output is maximized when the receiver is a matched filter with respect to the transmitted waveform [31].

5.1.2 Properties of the Ambiguity Function

The simultaneous resolution in range and Doppler is constrained by the Heisenberg uncertainty principle. Therefore, target position cannot be defined both in time and frequency domain at the same time [79, 81]. As a result, increased resolution in range can be obtained by sacrificing resolution in Doppler and vice versa [31, 33, 78, 79]. In practice, the transmitted signals are of positive duration and have finite energy E. Therefore, any AF must obey certain fundamental properties [79, 81]. Sequence design for radar is an ill-posed problem with no satisfactory technique being available for finding the waveform corresponding to the pre-defined AF. Also, no satisfactory set of rules is known to determine whether a desired AF is, in fact, an AF.

In the context of this dissertation, the following three properties are of main interest [32]:

- **Symmetry Property**: The magnitude of the AF is symmetric with respect to the origin, i.e,

$$|\chi(-\tau, -f_d)| = |\chi(\tau, f_d)| \tag{9}$$

- **Maximum Magnitude Property**: The maximum of the AF magnitude always occurs at the origin, i.e.,

$$|\chi(\tau, f_d)| \leq |\chi(0, 0)| = E \tag{10}$$

- **Volume Property**: The total volume under the ambiguity surface is constant, i.e.,

$$\int_{-\infty}^{\infty}\int_{-\infty}^{\infty}\left|\chi\left(\tau,f_d\right)\right|^2 d\tau df_d = E^2 \tag{11}$$

The symmetry property implies that when studying radar waveforms, it is sufficient to focus only on two adjacent quadrants of the AF [32]. The symmetry property can then be used to deduce the remaining two quadrants of the AF.

The maximum magnitude property implies that the maximum magnitude of the AF occurs at the origin. In other words, the magnitude of an AF can nowhere be higher than at the origin [32].

The volume property gives a strong and important condition necessary for a function to be an AF [82]. This property implies that energy removed from one portion of the delay-Doppler plane will crop up somewhere else within the ambiguity surface [31, 32, 33, 34]. In other words, the volume squeezed out of the peak will appear somewhere else in the delay-Doppler plane.

Integrated Sidelobe Level Ratio

In the context of radar applications, ISLR is used to measure the performance of a given sequence in a distributed clutter and target environment. It measures the total sidelobe energy of a sequence of length N compared to the mainlobe energy of the zero-Doppler cut of the corresponding AF. The zero-Doppler cut of an AF represents the output of a matched filter without Doppler shift f_d and is equal to the AAC of the sequence. Accordingly, the ISLR is defined as

$$ISLR = \frac{\sum\limits_{\substack{l=1-N \\ l\neq 0}}^{N-1}\left|\chi\left(l,0\right)\right|^2}{\left|\chi\left(0,0\right)\right|^2} \tag{12}$$

Figure of Merit

Another commonly used performance measure of a given sequence in radar applications is the figure of merit (FOM). The ratio of the

mainlobe energy to the sidelobes energy of the AAC of a sequence of length N is measured by FOM. It can also be written as the inverse of ISLR, i.e.,

$$FOM = \frac{1}{ISLR} \tag{13}$$

Peak-to-Sidelobe Ratio

For radar applications, the performance of a given sequence for a single point target in a large clutter environment is quantified by the PSLR. The ratio of the amplitude of the central peak to the maximum sidelobe amplitude of the zero-Doppler cut of the AF is measured by PSLR. It is defined as

$$PSLR = \frac{|\chi(0,0)|}{\max\limits_{1 \leq l < N} |\chi(l,0)|} \tag{14}$$

5.2 Performance Measures for Communication Applications

The commonly used performance measures of sequences for communication applications are aperiodic correlation measures such as AAC, ACC and mean square (MS) correlation measures.

5.2.1 Aperiodic Correlation Measures

The degree of similarity between a given sequence and its shifted version or between different sequences from a given set, respectively, is quantified by correlation measures, i.e., AC and CC.

AAC refers to the correlation of a given sequence with itself which is shifted by a discrete offset l, resulting in a nominally non-repetitive AC function. On the other hand, ACC refers to the correlation of pairs of sequences from a given set and their replicas shifted by an offset l with respect to each other.

Let two sequences $\mathbf{u}_x(\cdot)$ and $\mathbf{u}_y(\cdot)$ of length N be defined as

$$\mathbf{u}_x = \left[u_x(0), u_x(1), \ldots, u_x(N-1)\right] \in \mathbb{C}^{1\times N} \tag{15}$$

$$\mathbf{u}_y = \left[u_y(0), u_y(1), \ldots, u_y(N-1)\right] \in \mathbb{C}^{1\times N} \tag{16}$$

Then, ACC at discrete shift l is given as [14, 15]

$$C_{x,y}(l)=\begin{cases}\frac{1}{N}\sum\limits_{i=0}^{N-1-l}u_x(i)u_y^*(i+l), & 0\le l\le N-1\\ \frac{1}{N}\sum\limits_{i=0}^{N-1+l}u_x(i-l)u_y^*(i), & 1-N\le l<0\\ 0, & |l|\ge N\end{cases} \tag{17}$$

where $(\cdot)^*$ denotes the complex conjugate of the argument $(\cdot)$. In case of $\mathbf{u}_x=\mathbf{u}_y$, (17) is referred to as AAC and is denoted as $C_{x,y}(l)=C_{x,x}(l)$.

5.2.2 Mean Square Correlation Measure

Prior to the work reported in [83, 84], the peak values of periodic or aperiodic correlations were the main criteria to compare the performance of different spreading sequences for direct sequence CDMA systems. However, in these systems, incorporating the correlation values at all possible relative shifts rather than only accounting for peak values of AAC or ACC is considered more appropriate [16, 17, 84, 85]. In this context, worst case scenarios may be replaced by MS values. Accordingly, MSAC and MSCC of a given sequence set $\mathcal{U}$ of size U are defined as

$$R_{ac}=\frac{1}{U}\sum_{x=1}^{U}\sum_{\substack{l=1-N\\ l\neq 0}}^{N-1}|C_{x,x}(l)|^2 \tag{18}$$

$$R_{cc}=\frac{1}{U(U-1)}\sum_{x=1}^{U}\sum_{\substack{y=1\\ y\neq x}}^{U}\sum_{l=1-N}^{N-1}|C_{x,y}(l)|^2 \tag{19}$$

where $C_{x,x}(\cdot)$ and $C_{x,y}(\cdot)$ represent the AAC function and ACC function, respectively.

6 Meta-Heuristic Algorithms and Sequence Design

Optimization approaches employed in sequence design for radar and communication systems mainly include iterative algorithms [86, 87],

gradient based optimization algorithms [88], optimization algorithms based on the least square approach, and branch-and-bound algorithm [74] among others. The problem with these methods is that they either require gradient information, or an initial guess, or optimal step size in order to avoid local minima. Another major disadvantage of these algorithms is that they cannot effectively explore the search space simultaneously in different directions. To a large extent, the methods described above are capable of finding local optimum solutions only. As a result, it is difficult for these optimization algorithms to find the global minimum, if the search space contains many local minima.

Optimal sequence set design may be categorized as a non-deterministic polynomial hard (NP-hard) optimization problem. The cost functions in sequence design optimization could be with or without constraints, highly irregular, non-linear, multimodal, noisy and even discontinuous. Further, the exact gradient of the objective function is hard to compute. Therefore, simple computer search and classical optimization algorithms are not suitable to solve these complicated problems. The choice of the right optimizer or algorithm to solve sequence design optimization is critically important. The choice of an algorithm to solve such problems depends largely on the type of problem, the nature of an algorithm, the desired quality of solutions, the available computing resources, and time limit. In fact, there are no guidelines for choosing a particular algorithm for a particular problem and a single efficient algorithm applicable to all types of problems does not exist [89].

In recent years, nature-inspired population based meta-heuristic algorithms have emerged as an alternative where traditional methods have failed or proved inefficient. They are preferred over other methods due to their general applicability, effectiveness, intuitive mathematical formulation, and ability to handle uncertain, stochastic, and dynamic information. They are general purpose methods with the aim to effectively search the solution space without tailoring them to a specific problem.

The use of nature-inspired meta-heuristic algorithms is gaining attention in the sequence design for radar and communication systems, e.g., [71, 72, 73, 75, 76, 77, 90, 91, 92, 93, 94]. A suite of optimal sequences to simultaneously support mission critical multi-tasks such as

ground moving target indication, airborne moving target indication, and synthetic aperture radar imaging were designed using an evolutionary algorithm (EA) [90]. It was shown that optimal sequences can be designed using EA to fulfill objectives such as PSLR, ISLR, pulse integration, and revisit time.

Optimized waveforms with sparse spectrum for radar applications in the high frequency band were reported in [91] by using meta-heuristic algorithms such as genetic algorithm (GA) and particle swarm optimizer (PSO). It is shown that optimal waveforms with acceptable AC sidelobes can be obtained using GA and PSO. In conclusion, it was found that PSO was simpler and faster than the GA.

An approach to design polyphase sequences for direct sequence (DS) CDMA systems using EA has been proposed in [71, 72]. Particularly, a multiobjective (MO) evolutionary approach is proposed to find solutions that can simultaneously satisfy objectives posed on AC and CC properties.

GA was employed to design unified complex Hadamard transform (UCHT) sequences and Oppermann sequences for CDMA applications in [73, 75, 76]. The UCHT, modified UCHT, and Oppermann sequences were designed with reference to optimizing the maximum nontrivial aperiodic and MS correlation values. However, GA requires proper selection of the number of chromosomes, the probability of selection, mutation, and crossover. These parameters may influence the performance of the GA and their proper selection may require some experimentation [95].

A meta-heuristic sequence optimization approach for integrated radar and communication systems was presented in [92]. In this work, meta-heuristic algorithms were used to perform a multidimensional optimization in order to find a trade-off between AC and CC characteristics. The numerical results illustrated that meta-heuristic algorithms are potentially useful in designing sequences for radar, communications, as well as integrated systems.

Most recently, a meta-heuristic algorithm mimicking the echolocation of bats and breeding behaviour of certain species of cuckoos has been used to tackle cross-ambiguity synthesization [93, 94]. In these works, the problem of matching a cross-ambiguity function (CAF) to a predefined desired CAF by minimizing the mean-square distance between

the pre-defined desired CAF and synthesized CAF has been tackled. It has been shown that meta-heuristic approaches can be used as an effective tool in dealing with such problems.

The cost function for sequence design for integrated radar and communication systems might be extremely irregular and might have several local minima. Most meta-heuristic algorithms employ the Gaussian distribution to achieve randomization in order to explore the problem search space [95]. The Gaussian random walkers make small and cautious steps which may lead them to deep troughs (local minima). The small and cautions step sizes hinder the ability of a Gaussian random walker to escape from extrema that are wider than approximately twice the step size [96]. This means that Gaussian random walkers will spend more time in exploiting small portions of the search space. On the other hand, they will rarely visit and explore portions of the problem search space that may contain a potentially better solution. However, the Gaussian distribution may be replaced by Lévy flights based on the Lévy distribution to achieve randomization in meta-heuristic algorithms [93, 94, 95, 96, 97, 98, 99].

7 Lévy Flights and Global Optimization

Animals move in order to find random and sparsely distributed resources in nature. In the absence of prior knowledge about the location of these resources, a forager needs an effective and efficient search strategy to locate these resources in minimum time. A search strategy optimized in terms of search time is often a limiting factor for daily survival of these foragers [100]. A fundamental question faced by foragers is to determine the fastest way of finding non-uniformly distributed resources. This question has triggered several experimental initiatives and theoretical studies, e.g. [101, 102, 103]. These studies show that the search behavior among different foragers is generally based on stochastic search strategies. The foragers start with an active search phase and then randomly alternate to a phase of fast ballistic motion during these sporadic movements. The search strategies vary from cruise strategy (e.g., fish) to ambush or sit-and-wait search. In the latter, a forager remains stationary for a long period (e.g., rattlesnake) [100].

The search strategies of different animal species have been topic of many theoretical and empirical studies. These include animals like fish [103], grey seals [104], microzooplankton [105], reindeer [106], spider monkeys [107], and marine predators [108, 109]. These studies hypothesized that many foragers adopt Lévy flights or Lévy walks as optimal search strategies. According to [109], foragers sometimes switch between Lévy flights and Brownian motion depending on the density of the prey in a search area [109].

In nature, foragers search for food without a priori knowledge about its location. The problem of finding food in natural and dynamical environment may be regarded as a global optimisation (GO) problem. In these problems, sometimes, there is little or no a priori information about the whereabouts of the global optimum (unimodal problems) or optima (multimodal problems). Therefore, stochastic algorithms may require strategies that can effectively and efficiently explore the whole search space of a GO problem. The discussion in the preceding paragraphs provides a strong motivation to incorporate Lévy flights based on the α-stable Lévy distribution as a search strategy in the stochastic algorithms to solve complex real-world problems.

7.1 Lévy Flights

A Lévy flight is a random walk characterized by sequences of many short steps connected by rare longer steps [95, 96, 110, 111]. A Lévy flight in two dimensions will show a typical pattern as illustrated in Figure 1. The term flight means a straight line trip between two points that a moving random walker makes without directional change or pause.

Let the step sizes of a random walker w be represented by independent and identically distributed (i.i.d.) random variables (RVs) $S_1, S_2, \ldots, S_n$. These step sizes represent the displacements of random walker w in the $1\text{st}, 2\text{nd}, \cdots, n\text{th}$ step. According to the generalized central limit theorem (GCLT) [95], if the number of steps are large, the probability density of the sum of step sizes in a Lévy flight converges to an α-stable Lévy probability distribution [95, 96].

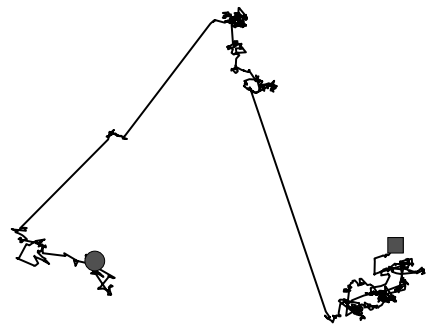

Figure 1: Two-dimensional 500 steps trajectory of a Lévy flight (Start ● and end ■).

The probability density function (PDF) of a symmetric α-stable Lévy RV S is given as [95, 96]

$$L_{\alpha,\beta}(S) = \frac{1}{\pi}\int_0^\infty \exp(-\beta z^\alpha)\cos(zS)dz \tag{20}$$

The parameter α is called stability index, tail index, tail exponent, or characteristic exponent. It measures the thickness of the tails of an α-stable Lévy probability distribution. In other words, it determines the rate at which the tail of the α-stable Lévy probability distribution tapers off. By controlling the value of α, different shapes of the α-stable Lévy probability distribution can be obtained, especially, in the tail region. This provides flexibility to characterize a wide range of impulsive processes. The parameter β determines the width and thus dispersion of a Lévy probability distribution. One may think of β as being similar to the variance of a Gaussian distribution.

A closed-form expression of (20) is known only for a few special cases [95]. Therefore, (20) is computed using numerical methods. For $\alpha = 1$ and $\alpha = 2$, respectively, (20) becomes the Cauchy and Gaussian probability distribution. Lévy probability distributions for different values of α are shown in Figure 2. For different values of $\alpha < 2$, the shape of the α-stable Lévy probability distribution is similar to a Gaussian probability distribution, but the tail of the α-stable Lévy probability distribution falls off much more gently compared to a Gaussian prob-

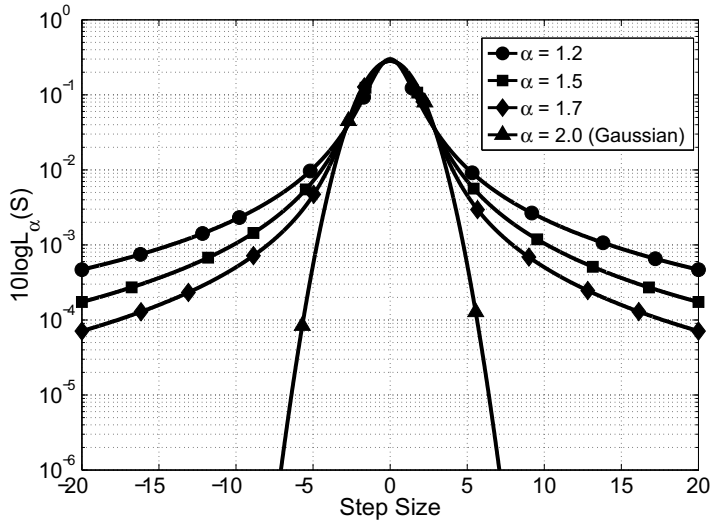

Figure 2: Comparison of Lévy probability distributions for different values of stability index α.

ability distribution.

Thus, in a Lévy flight, the step sizes $S_1, S_2, \ldots, S_n$ of a random walker w are distributed according to an α-stable Lévy probability distribution whose tails follow a power-law distribution and is given as follows [95, 110, 111]:

$$L_\alpha(S) \sim \frac{1}{S^{\alpha+1}}, \quad |S| \gg 1 \tag{21}$$

In Lévy flights, irrespective of the flight length, a random walker w is only at the start point and at the end point and never in between.

In contrast to Lévy flights, in a Lévy walk, the random walker w follows a continuous trajectory from the start to the end position. Thus, in a Lévy walk, the random walker w moves with finite velocity and takes a finite time to complete the walks. The finite and constant velocity results in shorter jumps and pauses between jumps compared to the Lévy flights [110, 111].

7.2 Lévy Flights in Global Optimization

Random walks are an important component of global optimization algorithms. Random walks can be modelled on the animal movement. It has been shown that Lévy flights or Lévy walks are optimal search strategies for foragers or animals searching for food [102, 103, 104, 105, 106, 108, 109]. Randomization in global optimization algorithms can be achieved by using various probability distributions such as uniform, Gaussian, and α-stable Lévy distributions [95, 97].

The purpose of exploration of the problem search space in global optimization is to accomplish the goals of: (i) intensive exploration within search space areas with high quality solutions; and (ii) move to unexplored areas of the search space when necessary. Diversification (exploration) and intensification (exploitation) can be used to achieve these goals [97, 112, 113].

Both diversification and intensification are the two main components of a global optimization algorithm. The overall efficiency of a GO algorithm depends on having a sound balance between them. A simple and efficient method to achieve randomization is to introduce a random starting point for a deterministic algorithm [95, 97, 98, 114]. A good example is the well-known hill-climbing method with random restart.

Diversification (exploration) intends to explore the search space more thoroughly which helps in generating diverse solutions. Too much diversification increases the probability of finding the true optimality globally, but often at much lower convergence rate.

The idea between intensification (exploitation) is that the promising portions of the search space that may contain the best solution or solutions are thoroughly explored. The concept of intensification ensures that the best solution or solutions are found. Too much intensification will make the optimization process converge quickly, which may lead to premature convergence, often to a local optimum. This, in turn, reduces the probability of finding the true global optimum.

In the context of global optimization, Lévy flights are advantageous over Gaussian distribution to achieve randomization due to the following two reasons [95, 96, 97, 98, 114]:

- Lévy flights reduce the probability of revisiting the areas of the

search space that have been previously explored.

- Lévy flights increase the chance of reaching far-off regions of the function landscape in global optimization problems. This is beneficial for the algorithm to escape a local minimum or minima with deep and wide basins.

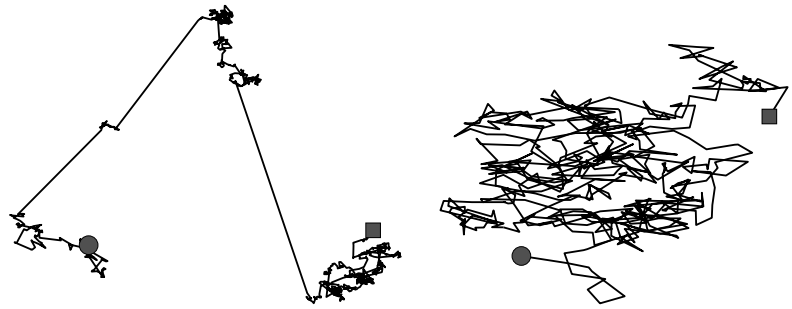

(a) (b)

Figure 3: Trajectories of a random walker w performing: (a) Lévy flights ($\alpha = 1.5$), and (b) Gaussian walk ($\alpha = 2$) (Start ● and end ■).

A random walker w performing a Lévy flight will spend more time in exploiting a large area of the search space (exploration on the global scale) and less time in searching the small local neighborhood. Figure 3 (a) shows that a random walker w performing a Lévy flight will take many small steps within a small area. Then, it takes a long flight to a far-off area, where it again takes many short steps. This will help in reducing the overall number of iterations required to find the optimal solution.

On the other hand (Figure 3 (b)), the same random walker w performing Gaussian walk returns to previously visited locations and spends more time in searching small local neighbourhood areas (exploration on the local scale). This, in turn, will increase the overall number of iterations required to find the optimal solution.

The smaller hill shown in Figure 4 indicates that Lévy flights will spend more time in exploiting a large area of the search space and spend

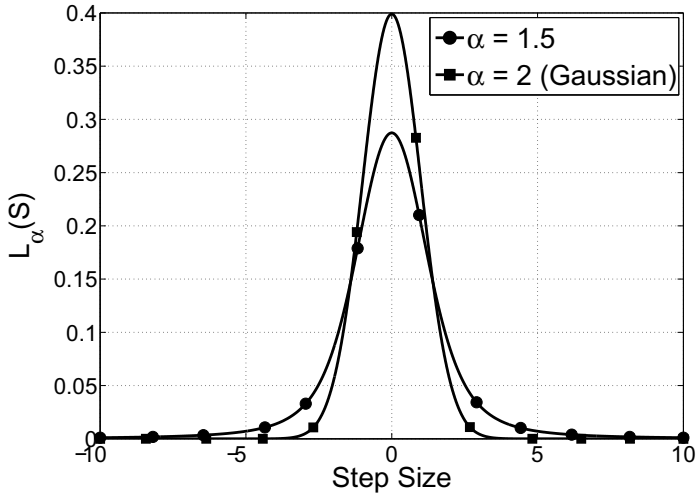

Figure 4: Lévy probability distribution for $\alpha = 1.5$ and for Gaussian probability distribution $\alpha = 2$.

less time in searching the small local neighborhood. The higher peak of the Gaussian distribution means that Lévy flights have a weaker fine-tuning ability compared to the Gaussian distribution for small- to mid-range search regions.

In case of Lévy flights, the upper limit on the number of iterations $N_{\max}$ to find a global minimum with pre-defined level of accuracy δ is far less compared to Gaussian random walks [95]. According to [99], incorporating Lévy flights global optimization techniques instead of Gaussain random walk may reduce the overall number of iterations by about 4 orders $[O(10^4)]$.

8 Dissertation Overview

This dissertation aims at designing sequences for integrated radar and communication systems. Nowadays, the RF front-end architectures for radar and wireless communication technologies are becoming more and more similar. DSPs are replacing an increasing number of functionalities

that were realized on hardware components in the past. The operating frequencies of modern wireless communication systems are becoming of the same order of magnitude as those previously used for radar applications. Given today's technological development, a joint RF platform for radar and communications applications could easily be realized. The first step towards the implementation of these systems is to identify sequences that can simultaneously support both radar and communication applications.

Oppermann sequences have been identified as suitable candidates for integrated radar and communication systems. These sequences are known for their wide range of correlation properties. The three parameters that define Oppermann sequences offer several degrees of freedom for designing these sequences. As a result, a great variety of trade-offs between AC, CC, and AF characteristics can be supported. Up till now, Oppermann sequences were only considered for communication applications, i.e., CDMA systems.

Meta-heuristic algorithms are used to find optimal parameter values to generate sets of Oppermann sequence that can simultaneously support integrated radar and communication applications. The meta-heuristic algorithms are preferred over numerical optimization methods due to their effectiveness and efficiency in handling computationally complex problems, such as sequence design for integrated radar and communication systems. It has been shown that meta-heuristic algorithms are suitable to find the optimal parameters of Oppermann sequences.

8.1 Part I: - Oppermann Sequences for Integrated Radar and Communication Systems

A: Performance Assessment of Polyphase Pulse Compression Codes

Motivated by a wide range of correlation properties offered by Oppermann sequences, in this part, we present a brief overview of conventional polyphase pulse compression sequences such as the Frank, Frank-Zadoff-Chu (FZC), P1, P2, P3, P4, and Px sequences. Then, the performance of these polyphase pulse compression sequences is evaluated and compared with Oppermann sequences. The latter class of sequences has

been considered to date only for applications within the context of CDMA systems. In this part, the performance evaluation of Oppermann sequences is extended to reveal their delay-Doppler characteristics. It is shown that Oppermann sequences can conceptually support integrated radar and communication systems as compared to the P1, P2, P3, P4, and Px sequences. Furthermore, a number of benefits and drawbacks associated with the examined polyphase sequence classes are discussed that may provide additional guidance in the waveform design for modern radar systems.

B: On Integrated Radar and Communication Systems Using Oppermann Sequences

In this part, weighted pulse trains with the elements of Oppermann sequences serving as complex-valued weights are utilized for the design of integrated radar and communication systems. An analytical expression for the ambiguity function is derived for weighted pulse trains with Oppermann sequences. It is shown that the ambiguity function of Oppermann sequences depend only on one sequence parameter. The design of the associated weighted pulse trains is simplified as it constrains the degrees of freedom. In contrast to the single polyphase pulse compression sequences that are typically deployed in radar applications, the families considered in this part form sets of sequences. As such, they readily facilitate also multiple-access in communication systems. The numerical examples shown illustrate the many options offered by Oppermann sequences in the design of integrated radar and communication systems.

C: Cross-Ambiguity Function of Weighted Pulse Trains with Oppermann Sequences

In this part, an analytical expression for the cross-ambiguity function of weighted pulse trains with Oppermann sequences is derived. Further, the auto-ambiguity function is deduced as a special case. In contrast to the auto-correlation and auto-ambiguity function of Oppermann sequences, which depend only on one sequence parameter and are the same for all sequences, the cross-ambiguity function depends on two

parameters. This additional parameter can be used, e.g., to control the spacing of the correlation peaks between pairs of sequences at the zero-Delay cut of the cross-ambiguity function. The analytical expressions obtained and properties summarized may guide waveform designers to formulate a multi-objective performance optimization subject to given requirements of integrated radar and communication systems.

D: Properties of Ambiguity Functions for Weighted Pulse Trains with Oppermann Sequences

In this part, the auto-ambiguity and cross-ambiguity properties of weighted pulse trains with Oppermann sequences are considered. Several properties are examined and proved which in turn allows for reducing the design space for optimization of a particular design. The insights gained from these properties build the foundations in the formulation of a formal framework leading to procedures that can be used for a more structured waveform design. In particular, the two procedures presented for designing weighted pulse trains with respect to auto-correlation and cross-correlation properties, respectively, are linked to the zero-Doppler cut metrics of mean-square auto-correlation and mean-square cross-correlation. Numerical examples are used to illustrate the relationship between sequence parameters and performance characteristics.

8.2 Part II: Waveform Optimization for Integrated Radar and Communication Systems Using Meta-Heuristic Algorithms

In this part, the focus is on the waveform optimization for such integrated systems based on Oppermann sequences. These sequences are defined by a number of parameters that can be chosen to design sequence sets for a wide range of performance characteristics. Firstly, it is shown that meta-heuristic algorithms are well-suited to find the optimal parameters for these sequences. Secondly, given the conflicting requirements on autocorrelation and crosscorrelation characteristics, meta-heuristic algorithms are considered to perform multidimensional optimization. The potential of meta-heuristic algorithms for designing sequences for radar, communications, as well as integrated systems is

illustrated with the help of numerical examples.

8.3 Part III: Multimodal Function Optimization

A: Multimodal Function Optimisation with Cuckoo Search Algorithm

This part studies multimodal function optimization mimicking the breeding behavior of certain species of cuckoos. The multimodal functions have objective functions that exhibit multiple peaks, valleys, and hyperplanes of varying heights. Furthermore, they are non-linear, non-smooth, non-quadratic, and can have multiple satisfactory solutions. In order to select the best solution among several possible solutions that can meet the problem objectives, it is desirable to find many such solutions. For these problems, the gradient information is either not available or not computable within reasonable time. Therefore, solving such problems is a challenging task. Recent years have seen a plethora of activities to solve such multimodal problems using non-traditional methods. These methods are nature-inspired and are becoming popular due to their general applicability and effective search strategies. In this part, we assess the ability of a meta-heustric algorithm mimicking the breeding behavior of certain species of Cuckoos to solve multimodal problems in noise-free and additive white Gaussian noise environments.

B: Synthesizing Cross-Ambiguity Functions Using An Improved Bat Algorithm

In this part, we consider the joint sequence design using a meta-heuristic algorithm based on the echolocation of bats by matching a synthesized cross-ambiguity function to a desired cross-ambiguity function of predefined magnitude over the delay-Doppler plane. A joint design of a pair of sequences such that their cross-ambiguity function approximates a desired cross-ambiguity function is a global optimization problem. This type of problem may be considered as a highly multimodal problem without any a priori information about the location of the optimum solution (unimodal) or solutions (multimodal). By way of four examples, it is shown that the approach based on echolocation of bats can indeed

synthesize a cross-ambiguity function that approximate cross-ambiguity function surfaces having a diagonal ridge and zero value elsewhere as well as cross-ambiguity function surfaces with a clear area around the origin. The results presented in this part indicate that the proposed approach is a promising technique for synthesizing cross-ambiguity functions.

9 Future Works

The research interests presented in this dissertation are mainly in the field of integrated radar and communication systems. Future works in this research field could involve investigation of related hardware architectures using polyphase sequences including Oppermann sequences.

Up until now, Oppermann sequences may have been considered only for communication applications, i.e., CDMA systems. However, given the trade-offs between autocorrelation, crosscorrelation and ambiguity functions supported by Oppermann sequences, the use of Oppermann sequences in MIMO radar, sonar and imaging applications would be an interesting avenue to explore.

Future work in this research field could involve extending the use of polyphase sequences including Oppermann sequences for cognitive radar network systems. Cognitive radar systems incorporate several radars working together in a cooperative manner. Radars working in this manner enhance the remote-sensing capability significantly compared to radar systems working individually. Cognitive radar system design could be extended to implement polyphase sequences including Oppermann sequences for indoor and outdoor channel environments. The use of Oppermann sequences in cognitive radars for biomedical applications like synthesis of body area networks for remotely observing and monitoring the physiological and physical conditions of patients is an interesting topic to explore.

As a widely used tool in radar signal analysis, the minimization of the sidelobes of the ambiguity function in the delay-Doppler plane is a difficult task due to the large number of constraints in the two-dimensional space. There are no systematic approaches for designing sequences that exhibit ambiguity functions with low sidelobe levels in

the delay-Doppler plane. Meta-heuristic algorithms may provide an alternative approach to solve this problem. It is, therefore, an interesting topic to explore.

References

[1] M. I. Skolnik, "*Introduction to Radar Systems*," 3rd Ed., McGraw-Hill, New York, 2001.

[2] A. F. Molisch, "Wireless Communications," 2nd Ed., John Wiley & Sons, Chichester, 2011.

[3] R. H. Cager, Jr., D. T. LaFlame, and L. C. Parode, "Orbiter Ku-Band Integrated Radar and Communication Subsystems," *IEEE Trans. Commun.,* vol. 26, no. 11, pp. 1604–1619, Nov. 1978.

[4] G. C. Tavik, C. L. Hilterbrick, J. B. Evins, J. J. Alter, J. G. Crnkovich Jr., J. W. de Graaf, W. Habicht II, G. P. Hrin, S. A. Lessin, D. C. Wu, and S. M. Hagewood, "The Advanced Multifunction RF Concept," *IEEE Trans. Microw. Theory and Technol.*, vol. 53, no. 3, pp. 1009–1020, Mar. 2005.

[5] D. Garmatyuk, J. Schuerger, Y. Morton, K. Binns, M. Durbin, and J. Kimani, "Feasibility Study of a Multi-Carrier Dual-Use Imaging Radar and Communication System," in *Proc. European Radar Conf.*, Munich, Germany, Oct. 2007, pp. 194–197.

[6] D. Garmatyuk and J. Schuerger, "Conceptual Design of a Dual-Use Radar/Communication System Based on OFDM," in *Proc. IEEE Military Commun. Conf.*, San Diego, U.S.A., Nov. 2008, pp. 1–7.

[7] D. Garmatyuk, J. Schuerger, and K. Kauffman, "Multifunctional Software-Defined Radar Sensor and Data Communication System," *IEEE Sensors J.*, vol. 11, no. 1, pp. 99–106, Jan. 2011.

[8] J. Moghaddasi and K. Wu, "Multifunctional Transceiver for Future Radar Sensing and Radio Communicating Data-Fusion Platform," *IEEE Access*, vol. 4, pp. 818–838, Feb. 2016.

[9] M. Vossiek, L. Wiebking, P. Gulden, J. Wieghardt, C. Hoffmann, and P. Heide, "Wireless Local Positioning," *IEEE Microw. Mag.*, vol. 4, no. 4, pp. 77–86, Dec. 2003.

[10] F. Qu, F.-Y. Wang, and L. Yang, "Intelligent Transportation Spaces: Vehicles, Traffic, Communications, and Beyond," *IEEE Commun. Mag.*, vol. 48, no. 11, pp. 136–142, Nov. 2010.

[11] 5G-PPP, "5G Automotive Vision," pp. 1–67, Oct. 2015, [Available Online]: `https://5g-ppp.eu/wp-content/uploads/2014/02/5G-PPP-White-Paper-on-Automotive-Vertical-Sectors.pdf`

[12] D. J. Glancy, "Sharing the Road: Smart Transportation Infrastructure," *Fordham Urban Law J.*, vol. 41, no. 5, pp. 1617–1664, 2015.

[13] M. S. Grewal, A. P. Andrews, and C. G. Bartone, "*Global Navigation Satellite Systems, Inertial Navigation, and Integration*," John Wiley & Sons, Hoboken, 2013.

[14] P. Fan and M. Darnell, "*Sequence Design for Communication Applications*," Research Studies Press, Taunton, 1996.

[15] H.-J. Zepernick and A. Finger, "*Pseudo Random Signal Processing: Theory and Application*," John Wiley & Sons, Chichester, 2005.

[16] I. Oppermann and B. S. Vucetic, "Complex Valued Spreading Sequences with Good Crosscorrelation Properties," in *Proc. IEEE Intl. Symp. on Spread Spectrum Technol. and Its Appl.*, Sydney, Australia, Jul. 1994, pp. 500–504.

[17] I. Oppermann and B. S. Vucetic, "Complex Spreading Sequences with a Wide Range of Correlation Properties," *IEEE Trans. Commun.*, vol 45, no. 3, pp. 365–375, Mar. 1997.

[18] S. W. Golomb and G. Gong, "*Signal Design for Good Correlation for Wireless Communications, Cryptography and Radar*," Cambridge University Press, Cambridge, 2005.

[19] R. C. Heimiller, "Phase Shift Pulse Codes with Good Periodic Correlation Properties," *IRE Trans. Inf. Theory*, vol. 7, no. 4, pp. 254–257, Oct. 1961.

[20] J.-S. No and P. V. Kumar, "A New Family of Pseudorandom Sequences Having Optimal Correlation Properties and Large Linear Span," in *Proc. IEEE Intl. Conf. on Commun.*, Philadelphia, U.S.A., Jun. 1998, pp. 802–806.

[21] R. Gold, "Optimal Binary Sequences for Spread Spectrum Multiplexing," *IEEE Trans. Inf. Theory*, vol. 13, no. 4, pp. 619–621, Oct. 1967.

[22] R. Gold, "Maximal Recursive Sequences with 3-Valued Recursive Cross-Correlation Function," *IEEE Trans. Inf. Theory*, vol. 14, no. 1, pp. 154–156, Jan. 1968.

[23] T. Kasami, "Weight Distribution Formula for Some Class of Cyclic Codes," Coordinated Science Lab., University of Illinois, Urbana-Champaign, U.S.A., Technical Report (R-285), 1966.

[24] S. Boztas and P. V. Kumar, "Binary Sequences with Gold-Like Correlation but Larger Linear Span," *IEEE Trans. Inf. Theory*, vol. 40, no. 2, pp. 532–537, Mar. 1994.

[25] D. C. Chu, "Polyphase Codes with Good Periodic Correlation Properties," *IEEE Trans. Inf. Theory*, vol. 18, no. 4, pp. 531–532, Jul. 1972.

[26] R. L. Frank, "Polyphasae Codes with Good Non Periodic Correlation Properties," *IEEE Trans. Inf. Theory*, vol. 9, no. 1, pp. 43–45, Jan. 1963.

[27] R. L. Frank and S. A. Zadoff, "Phase Shift Pulse Codes with Good Periodic Correlation Properties," *IRE Trans. Inf. Theory*, vol. 8, no. 6, pp. 381–382, Oct. 1962.

[28] S. M. Korne and D. V. Sarwate, "Quadriphase Sequences for Spread Spectrum Multiple Access Communications," *IEEE Trans. Inf. Theory*, vol. 30, no. 3, pp. 520–529, May 1984.

[29] H. Fukumasa, R. Kohono, and H. Imai, "Design of Pseudonoise Sequences with Good Odd and Even Correlation Properties for

DS/CDMA," *IEEE J. Sel. Areas Commun.*, vol. 12, no. 5, pp. 828–836, Jun. 1994.

[30] M. P. Lötter and L. P. Linde, "A Class of Bandlimited Complex Spreading Sequences with Analytical Properties," in *Proc. IEEE Intl. Symp. on Spread Spectrum Technol. and Its Appl.*, Germany, Sep. 1996, pp. 662–666.

[31] C. E. Cook and M. Bernfeld, "*Radar Signals: An Introduction to Theory and Applications*," Academic Press, New York, 1967.

[32] N. Levanon and E. Mozeson, "*Radar Signals*," John Wiley & Sons, Chichester, 2004.

[33] F. E Nathanson, J. P. Riley, and M. N. Cohen, "*Radar Design Principles: Signal Processing and the Environment*," SciTech Publishing, Mendham, 1999.

[34] M. A. Richards, "*Fundamentals of Radar Signal Processing*," 2nd Ed., McGraw Hill, New York, 2014.

[35] P. E. Pace, "*Detecting and Classifying Low Probability of Intercept Radar*," Artech House, London, 2004.

[36] R. L. Pickholtz, D. L. Schilling, and L. B. Milstein, "Theory of Spread-Spectrum Communications – A Tutorial," *IEEE Trans. Commun.*, vol. 30, no. 5, pp. 855–884, May 1982.

[37] IEEE Std 802.11, "Wireless LAN Medium Access Control (MAC) and Physical Layer (PHY) Specification - Higher-Speed Physical Layer Extension in the 2.4 GHz Band," 2000.

[38] F. Adachi, M. Sawahashi, and K. Okawa, "Tree-structured Generation of Orthogonal Spreading Codes with Different Lengths for Forward Link DS-CDMA Mobile," *IEE Electron. Lett.*, vol. 33, no. 1, pp. 27–28, Jan. 1997.

[39] R. H. Barker, "Group Synchronization of Binary Digital Systems," In: W. Jackson (Ed.), *Communication Theory*, Academic Press, London, pp. 272–287, 1953.

[40] M. J. E. Golay, "Complementary Series," *IRE Trans. Inf. Theory*, vol. 7, no. 2, pp. 82–87, Apr. 1961.

[41] D. A. Huffman, "The Generation of Impulse-Equivalent Pulse Trains," *IRE Trans. Inform. Theory*, vol. 8, no. 5, pp. 10–16, Sept. 1962.

[42] S. A. Zadoff, "Phase Coded Communication System," *US Patent No.* 3,099,796, Jul. 1963.

[43] J. Lindner, "Binary Sequences up to Length 40 with Best Possible Autocorrelation Function," *Electron. Lett.*, vol. 11, no. 21, pp. 507, 1975.

[44] M. N. Cohen, J. M. Baden, and P. E. Cohen, "Biphase Codes with Minimum Peak Sidelobes," in *Proc. IEEE National Radar Conf.*, Dallas, U.S.A., Mar. 1989, pp. 62–66.

[45] R. Sivaswamy, "Digital and Analog Subcomplementary Sequences for Pulse Compression," *IEEE Trans. Aerosp. Electron. Syst.*, vol. 14, no. 2, pp. 343–350, Mar. 1978.

[46] B. L. Lewis and F. F. Kretschmer, "A New Class of Polyphase Compression Codes and Techniques," *IEEE Trans. Aerosp. Electron. Syst.*, vol. 17, no. 3, pp. 364–372, May 1981.

[47] B. L. Lewis and F. F. Kretschmer, "Corrections to: A New Class of Polyphase Compression Codes and Techniques," *IEEE Trans. Aerosp. Electron. Syst.*, vol. 17, no. 5, pp. 726, Sept. 1981.

[48] P. B. Rapajic and R. A. Kennedy, "Merit Factor Based Comparison of New Polyphase Sequences," *IEEE Commun. Lett.*, vol. 2, no. 10, pp. 269–270, Oct. 1998.

[49] J. P. Costas, "A Study of a Class of Detection Waveforms Having Nearly Ideal Range-Doppler Ambiguity Properties," *Proc. IEEE*, vol. 72, no. 8, pp. 996–1009, Aug. 1984.

[50] J. R. Bellegarda and E. L. Titlebaum, "Time-Frequency Hop Codes Based Upon Extended Quadratic Congruences," *IEEE Trans. Aerosp. Electron. Syst.*, vol. 24, no. 6, pp. 726–742, Nov. 1988.

[51] L. Bömer and M. Antweiler, "Polyphase Barker Sequences," *Electron. Lett.*, vol. 25, no. 23, pp. 1577–1579, Nov. 1989.

[52] S. W. Golomb, "Two-valued Sequences with Perfect Periodic Autocorrelation," *IEEE Trans. Aerosp. Electron. Syst.*, vol. 28, no. 2, pp. 383–386, Mar. 1992.

[53] V. P. Ipatov, "*Spread Spectrum and CDMA: Principles and Applications,"* John Wiley & Sons, Chichester, 2005.

[54] T. Felhauer, "Design and Analysis of new P(n,k) Polyphase Pulse Compression Codes," *IEEE Trans. Aerosp. Electron. Syst.*, vol. 30, no. 3, pp. 865–874, Jul. 1994.

[55] P. A. Zulch, M. C. Wicks, B. Moran, S. Suvorova, and J. Byrnes, "A New Complementary Waveform Technique for Radar Signals," in *Proc. IEEE Radar Conf.*, Long Beach, U.S.A., Apr. 2002, pp. 35-40.

[56] E. Mozeson and N. Levanon, "Removing Autocorrelation Sidelobes by Overlaying Orthogonal Coding on Any Train of Identical Pulses," *IEEE Trans. Aerosp. Electron. Syst.*, vol. 39, no. 2, pp. 583–603, Apr. 2003.

[57] G. Björck, "Functions of Modulus 1 on Z_n Whose Fourier Transforms Have Constant Modulus and "Cyclic n-Roots"," In: J. S. Byrnes and J. F. Byrnes (Eds.), *Recent Advances in Fourier Analysis and Its Applications*, pp. 131–140, Kluwer Academic Publishers, Dordrecht, 1990.

[58] H. Deng, "Polyphase Code Design for Orthogonal Netted Radar System," *IEEE Trans. Signal Process.*, vol. 52, no. 11, pp. 3126–3135, Nov. 2004.

[59] H. A. Khan, Y. Zhang, C. Ji, C. J. Stevens, D. J. Edwards, and D. O'Brien, "Optimizing Polyphase Sequences for Orthogonal Netted Radar," *IEEE Signal Process. Lett.*, vol. 13, no. 10, pp. 589–592, Oct. 2006.

[60] B. Friedlander, "Waveform Design for MIMO Radar," *IEEE Trans. Aerosp. Electron. Syst.*, vol. 43, no. 3, pp. 1227–1238, Jul. 2007.

[61] D. R. Fuhrmann and G. San Antonio, "Transmit Beamforming for MIMO Radar System Using Signal Cross-Correlation," *IEEE Trans. Aerosp. Electron. Syst.*, vol. 44, no. 1, pp. 171–186, Jan. 2008.

[62] P. Stoica, J. Li, and X. Zhu, "Waveform Synthesis for Diversity-Based Transmit Beampattern Design," *IEEE Trans. Signal Process.*, vol. 56, no. 6, pp. 2593–2598, Jun. 2008.

[63] Y. Yang and R. S. Blum, "MIMO Radar Waveform Design Based on Mutual Information and Minimum Mean-Square Error Estimation," *IEEE Trans. Aerosp. Electron. Syst.*, vol. 43, no. 1, pp. 330–343, Jan. 2007.

[64] Y. Yang and R. S. Blum, "Minimax Robust MIMO Radar Waveform Design," *IEEE J. Sel. Topics Signal Process.*, vol. 1, no. 1, pp. 147–155, Jun. 2007.

[65] F. E. Marx, "Direct Sequence Spread Spectrum (DSSS) Communication Link Employing Complex Spreading Squences (CSS)," MEng Dissertation, University of Pretoria, Pretoria, South Africa, 1999.

[66] K. Gao and L. Ding, "Adaptive Binary Spreading Sequence Assignment Using Semidefinite Relaxation," *IEEE Wireless Commun. Lett.*, vol. 2, no. 1, pp. 94–97, Dec. 2012.

[67] F. B. Gross and C. M. Elam, "A New Digital Beamforming Approach for SDMA Using Spreading Sequences Array Weights," *Elsevier J. Signal Process.*, vol. 88, no. 10, pp. 2425–2430, Oct. 2008.

[68] M. Jamil, "Comparative Study of Complex Spreading Sequences for CDMA Applications," MEng Dissertation, University of Pretoria, Pretoria, South Africa, 1999.

[69] Y. Jung-Lang, K. Chien-Ming, and L. Chih-Chun, "Blind Channel Estimation for MC-CDMA Systems with Long Spreading Codes,"

Elsevier J. Signal Process., vol. 85, no. 10, pp. 1898–1906, Oct. 2005.

[70] B. J. Wysocki and T. A. Wysocki, "Optimization of Orthogonal Polyphase Spreading Sequences for Wireless Data Applications," in *Proc. IEEE Veh. Technol. Conf.*, Atlantic City, U.S.A., Oct. 2001, pp. 1894–1898.

[71] B. Natarajan, S. Das, and D. Stevens, "Design of Optimal Complex Spreading Codes for DS-CDMA Using an Evolutionary Approach," in *Proc. IEEE Global Telecommun. Conf.*, Dallas, U.S.A., Nov. 2004, pp. 3882–3886.

[72] B. Natarajan, S. Das, and D. Stevens, "An Evolutionary Approach to Designing Complex Spreading Codes for DS-CDMA," *IEEE Trans. Wireless Commun.*, vol. 4, no. 5, pp. 2051–2056, Sep. 2005.

[73] G. Cresp, H. H. Dam, and H.-J. Zepernick, "Design of Modified UCHT Sequences," in *Proc. Joint IST Workshop on Mobile Future and the Symp. on Trends in Commun.*, Bratislava, Slovakia, Jun. 2006, pp. 40–43.

[74] G. Cresp, H.-J. Zepernick, and H. H. Dam, "Design of Sequence Family Subsets Using a Branch and Bound Techniques," *IEEE Trans. Inf. Theory*, vol. 55, no. 8, pp. 3847–3857, Aug. 2009.

[75] H. H. Dam, H.-J. Zepernick, and H. Lüders, "Polyphase Sequence Design Using a Genetic Algorithm," in *Proc. IEEE Veh. Technol. Conf.*, Milan, Italy, May 2004, pp. 1471–1474.

[76] H. H. Dam, H.-J. Zepernick, and H. Lüders, "On the Design of Complex-Valued Spreading Sequences Using a Genetic Algorithm," in *Proc. IEEE Intl. Symp. on Spread Spectrum Technol. and Its Appl.*, Sydney, Australia, Aug. 2004, pp. 704–707.

[77] H. H. Dam, H.-J. Zepernick, S. Nordholm, and J. Nordberg, "Spreading Code Design Using a Global Optimization Method," *Annals of Operations Research – Optimization Theory and Appl., Part II*, vol. 133, no. 1-4, Springer, The Netherlands, pp. 249–264, Jan. 2005.

[78] P. M. Woodward, "*Probability and Information Theory with Applications to Radar*," Reprint: Artech House, Boston, 1980.

[79] A. W. Rihaczek, "*Principles of High-Resolution Radar*," Artech House, Boston, 1996.

[80] A. I. Sinsky and C. P. Wang, "Standardization of the Definition of the Radar Ambiguity Functions," *IEEE Trans. Aerosp. Electron. Syst.*, vol. 10, no. 4, pp. 532–533, Jul. 1974.

[81] B. Price and E. M. Hofstetter, "Bounds on the Volume and Height Distribution of the Ambiguity Function," *IEEE Trans. on Inf. Theory*, vol. 11, no. 2, pp. 207–214, Apr. 1965.

[82] R. E. Blahut, "*Theory of Remote Image Formation*," Cambridge University Press, Cambridge, 2004.

[83] D. V. Sarwate, "Mean-Square Correlation of Shift-Register Sequences," *IEE Proc. on Commun., Radar, and Signal Process.*, Part-F, vol. 131, no. 2, pp. 101–106, Apr. 1984.

[84] A. G. Burr, "Codes for Spread Spectrum Multiple Access System," in *Proc. IEEE Intl. Symp. on Spread Spectrum Technol. and Its Appl.*, London, UK, Sep. 1990, pp. 109–115.

[85] K. H. Kärkkäinen, "Mean-Square Cross-Correlation as a Performance Measure for Spreading Code Families," in *Proc. IEEE Intl. Symp. on Spread Spectrum Technol. and Its Appl.*, Yokohama, Japan, Nov. 2002, pp. 147–150.

[86] S. Ulukus and R. D. Yates, "Iterative Construction of Optimum Signature Sequence Sets in Synchronous CDMA Systems," *IEEE Trans. Inf. Theory*, vol. 47, no. 5, pp. 1989–1998, Jul. 2001.

[87] S. Ulukus and A. Yener, "Iterative Transmitter and Receiver Optimization for CDMA Networks," *IEEE Trans. Wirless Commun.*, vol. 3, no. 6, pp. 1879–1884, Nov. 2004.

[88] G. S. Rajappan and M. L. Honig, "Signature Sequence Adaptation for DS-CDMA With Multipath," *IEEE J. Sel. Areas Commun.*, vol. 20, no. 2, pp. 384–395, Feb. 2002.

[89] D. H. Wolpert and W. G. MacReady, "No Free Lunch Theorems for Optimization," *IEEE Trans. Evol. Comput.*, vol. 1, no. 1, pp. 67–82, Apr. 1997.

[90] V. J. Amuso and J. Enslin, "An Evolutionary Algorithm Approach to Simultaneous Multi-Mission Radar Waveform Design," In: M. Wicks, E. Mokole, S. Blunt, R. Schneible, and V. Amuso, (Eds.) *Principles of Waveform Diversity and Design*, SciTech Publishing, Rayleigh, pp. 110–125, 2011.

[91] W. Liu, Y. L. Lu, and M. Lesturgie, "Evolutionary Algorithms Based Sparse Spectrum Waveform Optimization," In: M. Wicks, E. Mokole, S. Blunt, R. Schneible, V. Amuso, (Eds.) *Principles of Waveform Diversity and Design*, SciTech Publishing, Rayleigh, pp. 152–162, 2011.

[92] M. Jamil and H.-J. Zepernick, "Waveform Optimization for Integrated Radar and Communication Systems Using Meta-Heuristic Algorithms," In: X.-S. Yang and S. Koziel, (Eds.) *Computational Optimization and Applications in Engineering and Industry*, pp. 183–203, Springer, Heidelberg, 2011.

[93] M. Jamil, H.-J. Zepernick, and X.-S. Yang, "Lévy Flight Based Cuckoo Search Algorithm for Synthesizing Cross-Ambiguity Functions," in *Proc. IEEE Military Commun. Conf.*, San Diego, U.S.A., Nov. 2013, pp. 823–828.

[94] M. Jamil, H.-J. Zepernick, and X.-S. Yang, "Synthesizing Cross-Ambiguity Functions Using the Improved Bat Algorithm," In: X.-S. Yang, (Ed.) *Recent Advances in Swarm Intelligence and Evolutionary Computation*, Springer International Publishing, Cham, pp. 179–202, 2015.

[95] X.-S. Yang, "*Engineering Optimization: An Introduction with Metaheuristic Applications*," John Wiley & Sons, London, 2010.

[96] M. Gutowski, "Lévy Flights as an Underlying Mechanism for Global Optimization Algorithms," in *Proc. Nat. Conf. on Evol. Comput. and Global Optimization*, Jastrzębia Góra, Poland, 2001, pp. 79–86.

[97] X.-S. Yang, "*Nature-Inspired Metaheuristic Algorithms*," Luniver Press, London, 2008.

[98] X.-S. Yang and S. Deb, "Cuckoo Search via Lévy Flights," in *Proc. World Cong. on Nature & Biologically Inspired Computing*, Coimbatore, India, Dec. 2009, pp. 210–214.

[99] X.-S. Yang, T. O. Ting, and M. Karamanoglu, "Random Walks, Lévy Flights, Markov Chains and Metaheuristic Optimization," In: H.-K. Jung, T. J. Kim, T. Sahama, and C.-H. Yang (Eds.) *Future Information Communication Technology and Applications*, Springer, Dordrecht, pp. 1055–1064, 2013.

[100] O. Bénicho, M. Coppey, M. Moreau, P. H. Suet, and R. Voituriez, "Optimal Search Strategies for Hidden Targets," *Physical Review Lett.*, vol. 94, no. 19–20, pp. 198101, May 2005.

[101] W. J. Bell, "*Searching Behaviour, The Behavioural Ecology of Finding Resources*," Chapman and Hall, London, 1991.

[102] G. M. Viswanathan, V. Afanasyev, S. V. Buldyrev, E. J. Murphy, P. A. Prince, and H. E. Stanley, "Lévy Flight Search Patterns of Wandering Albatrosses," *Nature*, vol. 381, no. 6581, pp. 413–415, May 1996.

[103] G. M. Viswanathan, "Fish in Lévy-Flight Foraging," *Nature*, vol. 465, no. 7301, pp. 1018–1019, Jun. 2010.

[104] D. Austin, W. D. Bowen, and J. I. McMillan, "Intraspecific Variation in Movement Patterns: Modeling Individual Behaviour in a Large Marine Predator," *Oikos*, vol. 105, no. 1, pp. 15–30, Apr. 2004.

[105] F. Bartumeus, F. Peters, S. Pueyo, C. Marrase, and J. Catalan, "Lévy Walks: Adjusting Searching Strategies to Resource Availability in Microzooplankton," in *Proc. National Academy of Sciences*, U.S.A., vol. 100, no. 22, pp. 12771–12775, Oct. 2003.

[106] A. J. Mårell, P. Ball, and A. Hofgraad, "A Foraging and Movement Paths of Female Reinedeer: Insights from Fractal Analysis, Correlated Random Walks and Lévy Flights," *Canadian J. of Zoology*, vol. 80, no. 5, pp. 854–865, May 2002.

[107] G. Ramos-Frenández, J. L. Mateos, O. Miramontes, G. Cocho, H. Larralde, and B. Ayala-Orozco, "Lévy Walk Patterns in the Foraging Movements of Spider Monkeys (Ateles Geoffroyi)," *Behavioural Ecology and Sociobiology*, vol. 55, no. 3, pp. 223–230, Jan. 2004.

[108] N. E. Humphries, N. Querioz, J. R. M. Dyer, N. G. Pade, M. K. Musyl, K. M. Schaefer, D. W. Fuller, J. M Brunnschweiler, T. K. Doyle, J. D. R. Houghton, G. C. Hays, C. S. Jones, L. R. Noble, V. J. Wearmouth, E. J. Southall, and D. W. Sims, "Environmental Context Explains Lévy and Brownian Movement Patterns of Marine Predators," *Nature*, vol. 451, no. 7301, pp. 1066–1069, Jun. 2010.

[109] D. W. Sims, "Tracking and Analysis Technique for Understanding Free-Ranging Shark Movements and Behaviour," in J. A. Msick, M. R. Heituaus, and J. C. Carrier, (Eds.), *Sharks and Their Relatives II – Biodiversity, Adaptive Physiology and Conservation*, CRC Press, Boca Raton, pp. 351–392, 2010.

[110] M. F. Shlesinger, G. M. Zaslavsky, and J. Klafter, "Strange Kinetics," *Nature*, vol. 363, no. 6424, pp. 31–37, May 1993.

[111] M. F. Shlesinger, G. M Zaslavsky, and U. Frisch (Eds.), "*Lévy Flights and Related Topics in Physics*," Springer, Heidelberg, 1995.

[112] F. Glover, "Tabu Search – Part I," *OSRA J. Computing*, vol. 1, no. 3, pp. 190–206, Summer 1989.

[113] F. Glover, "Tabu Search – Part II," *OSRA J. Computing*, vol. 2, no. 1, pp. 4–32, Winter 1990.

[114] X.-S. Yang, "Review of Metaheuristics and Generalized Evolutionary Walk Algorithm," *Intl. J. of Bio-Inspired Comput.*, vol. 3, no. 2, pp. 77–84, Apr. 2011.

Part I-A

Part I-A

Performance Assessment of Polyphase Pulse Compression Codes

Part I-A is based on:

M. Jamil, H.-J. Zepernick, and M. I. Pettersson, "Performance Assessment of Polyphase Pulse Compression Codes," *IEEE Intl. Symp. on Spread Spectrum Techn. and Its Appl.*, Bologna, Italy, Aug. 2008, pp. 166–172.

Performance Assessment of Polyphase Pulse Compression Codes

Momin Jamil, Hans-Jürgen Zepernick, and Mats I. Pettersson

Abstract

The performance of conventional polyphase pulse compression codes such as the Frank, Frank-Zadoff-Chu (FZC), P1, P2, P3, P4, and Px codes will be compared with Oppermann codes. While the majority of the former code classes focus on radar applications, Oppermann codes have been discussed only within the context of code-division multiple-access (CDMA) systems. In this paper, we therefore consolidate findings on the conventional codes and extent the performance assessment to Oppermann codes by accounting for Doppler shifts as needed in radar applications. It is shown that Oppermann codes can conceptually support integrated radar and communication systems as compared to the P1, P2, P3, P4, and Px codes where this is not readily feasible. The numerical results given here illustrate that Oppermann codes outperform Px codes in the presence of Doppler shifts as supported by the ambiguity function.

1 Introduction

Radar waveform designers have studied polyphase pulse compression codes for many years as an efficient alternative to the different classes of frequency-modulated signals [1, 2]. Polyphase pulse compression codes may be derived from the phase history of chirp or step-chirp analog signals but can be implemented and processed digitally.

Analogously to spread spectrum systems, performance of different polyphase codes in radar applications can be compared in terms of their delay or range tolerance by correlation measures such as the autocorrelation function, the mainlobe-to-total-sidelobe ratio, and the peak-to-sidelobe ratio. Due to potential movement of targets, the tolerance of a design with respect to Doppler shifts has to be evaluated too and can be quantified using the ambiguity function. In practice, radar waveforms may be optimized in a first design step by using correlation measures and subsequently engage the ambiguity function to evaluate the impact of Doppler shifts on the performance.

One of the first polyphase codes that were considered for pulse compression in radar applications have been reported in [3] and are known as Frank codes. However, these chirplike codes can only be designed for perfect square length. Modified versions of the Frank code can be obtained by simply permuting its phase history such as those offered by polyphase pulse compression codes referred to as P1 and P2 codes [4]. Superior performance in terms of the integrated sidelobe levels compared to the Frank and P1 codes is provided by the Px codes that have been introduced by Rapajic and Kennedy [5]. It is noted that the Px code for even square root of code length is defined exactly as the P2 code and hence provides identical performance in this case. The concepts behind Frank codes have later been generalized to facilitate designs of polyphase codes of any length and related work was consolidated in the Frank-Zadoff-Chu (FZC) codes [6, 7]. Similarly, the P3 and P4 codes, derived by Lewis and Kretschmer [8] from a linear frequency modulated waveform, are also applicable for any length. It is noted that P3 and P4 codes can be considered as cyclically shifted and decimated versions of FZC codes.

Several performance aspects of the aforementioned classes of polyphase pulse compression codes have been reported in literature over the years, e.g. [5, 9]. In addition, we will include here also the class of Oppermann codes [10]. These codes were originally introduced within the context of applications for code-division multiple-access (CDMA) systems, while their behavior within radar scenarios have not been considered so far to the best of our knowledge. Given the length of the code, Oppermann codes are defined by three parameters which then

corresponds to a distinct family of codes. For particular values of these parameters, the autocorrelation magnitude of Oppermann codes is controlled by one parameter while a second parameter influences only the phase characteristics. Further, the autocorrelation magnitude is then the same for all Oppermann codes in the family. Thus, this makes it a candidate for the design of integrated radar and communication systems where more than one code is needed.

The paper is organized as follows. Section 2 defines the measures used to facilitate a quantitative performance evaluation and comparison of the considered polyphase codes. Section 3 presents fundamentals on prominent classes of polyphase codes that are used with radar applications and describes the class of Oppermann codes. On this basis, numerical results are given in Section 4 for a number of scenarios. It also illustrates the wide range of options that are offered by Oppermann codes for radar waveform designs. Finally, Section 5 concludes the paper.

2 Performance Measures

Let N denote the length of each polyphase code $\mathbf{u}_k = [u_k(0), u_k(1), \ldots, u_k(N-1)]$ of a given set $\mathcal{U}$ of size U, where $1 \leq k \leq U$. In the sequel, we provide the definitions of the measures [11, 12] used to assist with the performance comparisons of the examined classes of polyphase codes.

2.1 Aperiodic Autocorrelation

The aperiodic autocorrelation $C_k(l)$ at discrete shift l between a polyphase code $\mathbf{u}_k \in \mathcal{K}$ and its shifted version, is defined as

$$C_k(l) = \begin{cases} \frac{1}{N} \sum_{i=0}^{N-1-l} u_k(i) u_k^*(i+l), & 0 \leq l \leq N-1 \\ \frac{1}{N} \sum_{i=0}^{N-1+l} u_k(i-l) u_k^*(i), & 1-N \leq l < 0 \\ 0, & |l| \geq N \end{cases} \tag{1}$$

where $(\cdot)^*$ denotes the complex conjugate of the argument $(\cdot)$.

It is noted that the discrete shift l in the considered radar scenarios is associated with the delay by which a transmitted pulse code signal is received, which in turn translates to the range of a target.

2.2 Figure of Merit

The figure of merit (FOM) of a code $\mathbf{u}_k \in \mathcal{U}$, $1 \leq k \leq U$ of length N with aperiodic autocorrelation function $C_k(l)$ measures the ratio of energy in the mainlobe to that in the sidelobe of the autocorrelation function. It is defined as

$$FOM_k = \frac{C_k(0)}{2\sum_{l=1}^{N-1} |C_k(l)|^2}, \qquad \forall k \tag{2}$$

2.3 Peak-to-Sidelobe Ratio

Similarly, the peak-to-sidelobe ratio (PSLR) of a code $\mathbf{u}_k \in \mathcal{U}$, $1 \leq k \leq U$ of length N with aperiodic autcorrelation function $C_k(l)$ measures the ratio of the inphase value $C_k(0)$ to the maximum sidelobe magnitude $|C_k(l)|$ of the autocorrelation function. It is defined as

$$PSLR_k = \frac{C_k(0)}{\max\limits_{1 \leq l < N} |C_k(l)|} \tag{3}$$

2.4 Ambiguity Function

In this paper, we consider phase-coded pulse trains that can be described by a complex envelope as

$$u_k(t) = \frac{1}{\sqrt{T}} \sum_{i=1}^{N} u_k(i) \operatorname{rect}\left[\frac{t-(i-1)T_c}{T_c}\right] \tag{4}$$

where $T = N\,T_c$ denotes the duration of the kth pulse train and T_c is the duration of each rectangular pulse $\operatorname{rect}(\cdot)$. The elements $u_k(i)$ of the kth polyphase code $\mathbf{u}_k$ of length N are given by

$$u_k(i) = \exp\left[j\varphi_k(i)\right], \qquad j = \sqrt{-1} \tag{5}$$

where the set of N phases $\{\varphi_k(0), \varphi_k(1), \ldots, \varphi_k(N-1)\}$ are referred to as the phase code of $u_k(t)$.

The ambiguity function (AF) represents the output of a matched filter with respect to an examined finite energy signal. It describes the interference that would be caused to a transmitted signal due to the delay/range and/or the Doppler shift compared to a reference signal. In this paper, we utilize the following definition of the ambiguity function [1]

$$|\chi(\tau, f_d)| = \left| \int_{-\infty}^{\infty} u_k(t) u_k^*(t+\tau) \exp(j2\pi f_d t) dt \right| \tag{6}$$

where τ and f_d denote delay and Doppler shift, respectively. The AF facilitates radar designers with a comprehensive tool for comparison of different waveforms with main focus typically being on sidelobes relative to the mainlobe. While other AF definitions based on magnitude square or logarithmic scale would render sidelobes suppressed or amplified, respectively, the selected magnitude definition (6) provides a good trade-off in view of inspecting AF plots or related ambiguity contour plots.

3 Classes of Polyphase Codes

In this section, we will provide the definitions of the considered classes of polyphase pulse compression codes in terms of their phase codes. It should be mentioned that, in this paper, we adopt the term code in favor of the term sequence as it is used in the bulk of radar-related publications while the latter is frequently used with communication systems. In particular, the Frank, FZC, P1, P2, P3, P4, Px, and Oppermann codes will be described along with remarks on some of their beneficial properties for radar applications. Specifically, the positioning of the newly considered Oppermann codes within the other more conventional codes is revealed.

3.1 Frank Codes

The history of complex-valued codes ranges back as far as the 1950s but related concepts were mainly contained in classified documents during

these early years. It is due to the work on phase shift pulse codes reported in [13] that sparked discussions on this type of codes among the broader audience. This work proposed a method of generating codes of so-called perfect square length

$$N = M^2 \tag{7}$$

where M is a prime number. The code elements are arranged to form an $M \times M$ matrix and are given by the Mth roots of unity $w = \exp(j2\pi/M)$. The actual polyphase code of length N is then produced by reading out the matrix of roots of unity row-by-row.

In generalization of the above approach, it has been shown in [6] that sets of polyphase codes of perfect square length $N = M^2$ can be designed for any integer M. The related codes are referred to as Frank codes. The elements $f_k(m,n)$ of the kth Frank code in a given set can be arranged as matrix

$$\mathbf{F}_k = [f_k(m,n)]_{M\times M} = \left[\exp\left(j\frac{2\pi\,k}{M}m\,n\right)\right]_{M\times M} \tag{8}$$

and its phases are defined accordingly as

$$\varphi_k(m,n) = \frac{2\pi}{M}\,k\,m\,n \tag{9}$$

where $1 \le k \le M-1$ and $0 \le m,n \le M-1$ while the greatest common divisor $gcd(k,M) = 1$ is required. Then, the (m,n)th element of (8) can be mapped to the ith element of a code of length N in terms of the phase code as follows:

$$i = m\,M + n: \quad \varphi_k(m,n) \mapsto \varphi_k(i) = \varphi_k(m\,M+n) \tag{10}$$

3.2 P1, P2, and Px Codes

The P1, P2, and Px codes [4, 5] may be regarded as modifications of the Frank codes and can be designed for perfect square length $N = M^2$ only. In particular, the phases of the Frank codes appear rearranged in the P1, P2, and Px codes with the cluster of zero phases placed in the central part of the pulse code and from there symmetrically increase in

value towards start and end of the codes. It is due to this reordering that P1, P2, and Px codes outperform Frank codes with respect to PSLR as reported in [4, 5].

Specifically, the elements $u(i)$ of the P1 and P2 (M even) codes, respectively, are given by

$$u(i) = u(mM+n) = u(m,n) = \exp[j\varphi(m,n)] \tag{11}$$

where $0 \le m,n \le M-1$ and their phases are defined as

$$\text{P1:} \quad \varphi(m,n) = -\frac{2\pi}{M}\left(\frac{M-1}{2}-m\right)(mM+n) \tag{12}$$

$$\text{P2:} \quad \varphi(m,n) = +\frac{2\pi}{M}\left(\frac{M-1}{2}-m\right)\left(\frac{M-1}{2}-n\right) \tag{13}$$

Similarly, the elements $u(i)$ of the Px codes also follow the general expression of (11) and the phases of this class of pulse codes are defined as

$$\text{Px:} \quad \varphi(m,n) = \begin{cases} \frac{2\pi}{M}\left(\frac{M-1}{2}-m\right)\left(\frac{M-1}{2}-n\right) & M \text{ even} \\ \frac{2\pi}{M}\left(\frac{M-1}{2}-m\right)\left(\frac{M-2}{2}-n\right) & M \text{ odd} \end{cases} \tag{14}$$

where $0 \le m,n \le M-1$. Apparently, the elements of the Px code for M even are defined exactly as those of the P2 code.

3.3 Frank-Zadoff-Chu Codes

The FZC codes can be constructed for any length N [6, 7] and are not restricted to perfect square length. In particular, the phase $\varphi_k(i)$ of the ith element $u_k(i)$ of the kth FZC code $\mathbf{u}_k = [u_k(0), u_k(1), \ldots, u_k(N-1)]$ of length N may be defined as

$$\varphi_k(i) = \frac{\pi}{N}\left[k^2(i+1) + k(i+1)N\right] \tag{15}$$

where $0 \le i \le N-1$ and k is an integer relatively prime to N.

3.4 P3 and P4 Codes

As the P1, P2, and Px codes are related to the Frank codes, so can the P3 and P4 codes [8] be considered as cyclically shifted and decimated versions of the FZC code. Accordingly, P3 and P4 codes are not restricted to perfect square length but can also be constructed for any length N. While the P3 code is shown in [8] to be more Doppler tolerant compared to the P1 and P2 codes, the P4 code has also good tolerance for pre-compression bandwidth limitations and offers the same Doppler tolerance as the P3 code.

The elements $u(i)$ of the P3 and P4 codes are given by

$$u(i) = \exp[j\varphi(i)] \tag{16}$$

where $0 \leq i \leq N-1$ and their phases are defined as

$$\text{P3:} \qquad \varphi(i) = \frac{\pi}{N}(i-1)^2 \tag{17}$$

$$\text{P4:} \qquad \varphi(i) = \frac{\pi}{N}(i-1)(i-1-N) \tag{18}$$

3.5 Oppermann Codes

A family of polyphase codes that supports a wide range of correlation properties is proposed in [10]. The phase $\varphi_k(i)$ of the ith element $u_k(i)$ of the kth Oppermann code $\mathbf{u}_k = [u_k(0), u_k(1), \ldots, u_k(N-1)]$ of length N is defined as

$$\varphi_k(i) = \frac{\pi}{N}\left[k^m(i+1)^p + (i+1)^n + k(i+1)N\right] \tag{19}$$

where $1 \leq k \leq N-1$, $0 \leq i \leq N-1$ and integer k is relatively prime to the length N. In this paper, we require N to be a prime, which results in the family being of maximum size $N-1$. The parameters m, n, and p in (19) take real values and define a family of Oppermann codes. For a fixed combination of these three parameters, all the codes have the same autocorrelation magnitude. If $p=1$, this autocorrelation magnitude depends only on n and is given by [10]

$$|C_k(l)| = \left| \frac{1}{N} \sum_{i=0}^{N-1-l} \exp\left\{ \frac{j\pi}{N}\left[(i+1)^n - (i+l+1)^n\right] \right\} \right| \tag{20}$$

In this case, the optimal family in terms of FOM or PSLR as defined in (2) and (3), respectively, can be found by simple search over n. In the sequel, we will therefore concentrate on the case of $p = 1$. Given $p = 1$ and the parameter n associated with the optimal family, the parameter m may be varied to produce favorable phase or crosscorrelation characteristics, for instance. With this parameter setting, the class of Oppermann codes provides us not only with a wide range of correlations but also flexibility to control the ambiguity function at scenarios other than those relating to the zero Doppler cut.

4 Numerical Results

This section aims at illustrating major performance characteristics of the examined classes of polyphase pulse compression codes along with the related benefits and drawbacks. In the first step, performance assessment is based on FOM and PSLR that reflect code characteristics in the absence of Doppler shifts. In the second step, the behavior in non-zero Doppler shifts is evaluated using the ambiguity function as well as the related concept of ambiguity contour plots.

4.1 Figure of Merit and Peak-to-Sidelobe Ratio

Let us first consider FOM and PSLR of polyphase pulse compression codes as the performance measures that reveal the zero-Doppler shift characteristics of the codes.

Figs. 1 and 2 show FOM and PSLR, respectively, for codes of perfect square length $N = M^2$. Apparently, the considered classes of polyphase codes give similar performances with the Px code outperforming the other codes in terms of FOM. It is noted that only Px codes for odd square root M of length N are presented in the figures as their definition for even square root of length is identical to the P2 codes and as such is the related performance.

Figs. 3 and 4 show FOM and PSLR, respectively, for the codes that can be generated for any length N. However, in order to allow for the maximum size of codes in a given Oppermann family, the length has been chosen as a prime number. Further, for each considered length

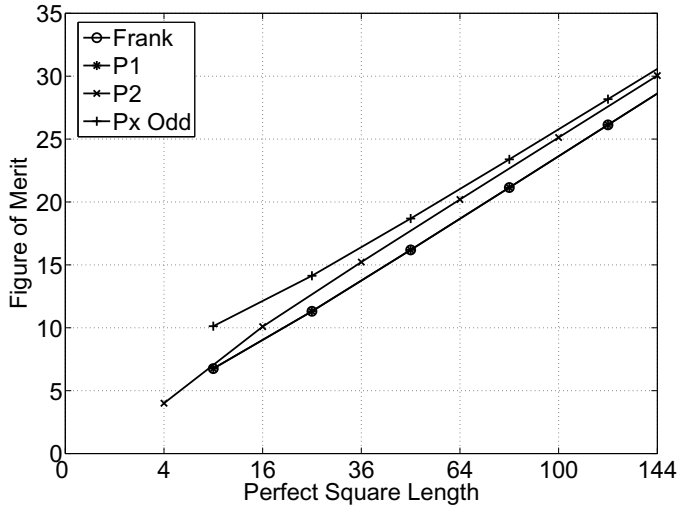

Figure 1: FOM of different polyphase codes of length $N = M^2$.

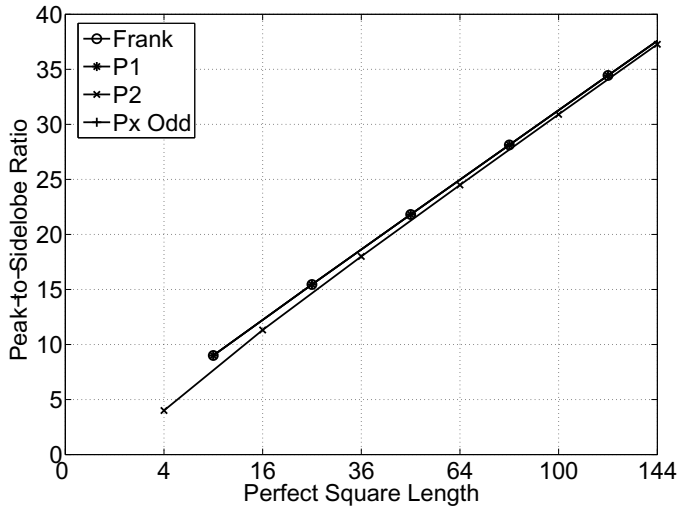

Figure 2: PSLR of different polyphase codes of length $N = M^2$.

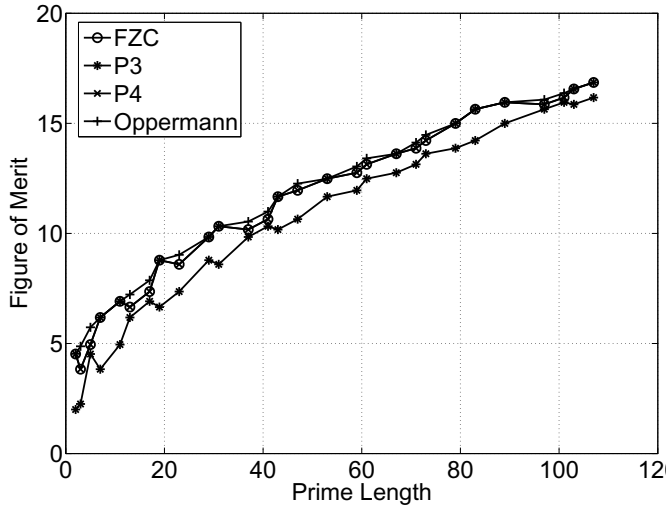

Figure 3: FOM of different polyphase codes of prime length N.

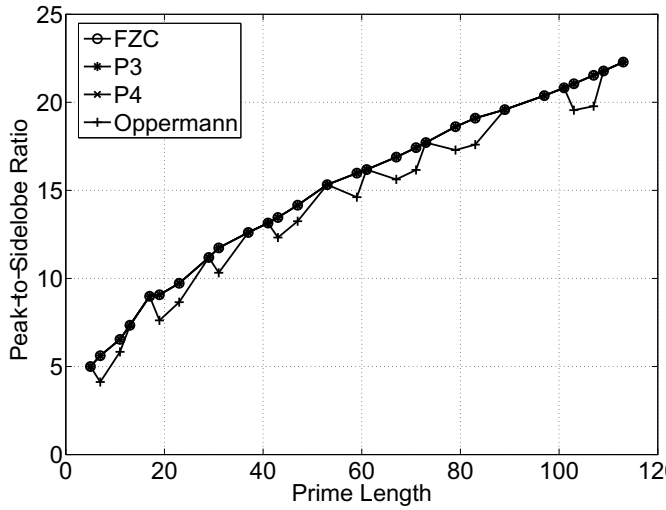

Figure 4: PSLR of different polyphase codes of prime length N.

N, the parameters of the Oppermann codes were selected as $p = 1$ and n such that FOM is maximized. In view of (20), parameter m may assume any real number without having an impact on autocorrelation magnitude or FOM. As far as the set of FZC codes is concerned, the code that offers the highest FOM for a given length has been chosen for each length. Then, the FOM results show that FZC and Oppermann codes behave identical for the considered prime lengths and outperform P3 and P4 codes. In contrast, the Oppermann codes perform slightly inferior in PSLR for some particular prime lengths while FCZ, P3, and P4 codes show identical performance. As can also be seen from the FOM and PSLR results, the penalty for having a smaller granularity in code length compared to being restricted to only perfect square length is an inferior FOM and PSLR performance.

4.2 Autocorrelation Magnitude

To further investigate differences between the classes of FZC and Oppermann codes, which both can be generated for any code length and provide a set of codes, the autocorrelation magnitude shall be consulted. Due to the many possibilities for selecting code parameters, qualitative rather than comprehensive results are given here for FCZ and Oppermann codes of length $N = 31$. In both cases, each of the related sets contain 30 unique codes.

Figs. 5(a)-(b), respectively, show the autocorrelation magnitudes of the first and second FZC code ($k=1$ and $k=2$) in the set of codes. As the autocorrelation magnitude differs with the particular code chosen from the set of FZC codes, not all of them may perform favorable in applications such as integrated radar and communication systems.

Fig. 6 depicts the autocorrelation magnitude of Oppermann codes of length $N = 31$ optimized for maximum FOM. Specifically, the parameters $p = 1$ and $n = 2.007$ relate to the maximum FOM of 9.027 for Oppermann codes of length $N = 31$ while the parameter m has no impact on the autocorrelation magnitude. In fact, all 30 Oppermann codes in the set offer the same autocorrelation magnitude shown in the figure. Accordingly, the radar waveform designer may select a distinct code based on implementation considerations. Furthermore, the additional parameter m may be used to control crosscorrleation properties

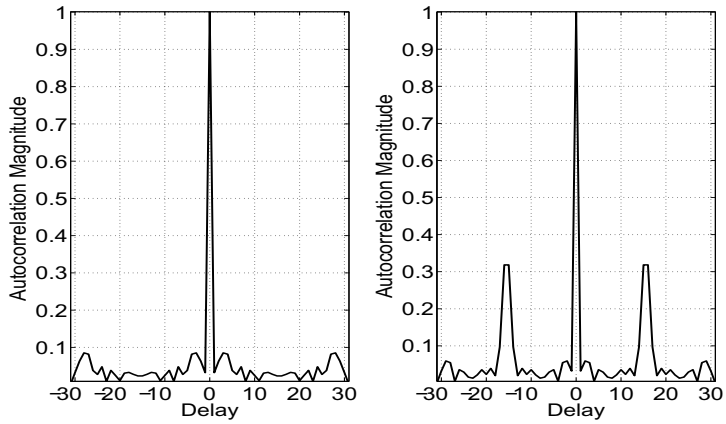

(a) (b)

Figure 5: Autocorrelation of FZC codes of length $N=31$: (a) $k=1$, (b) $k=2$.

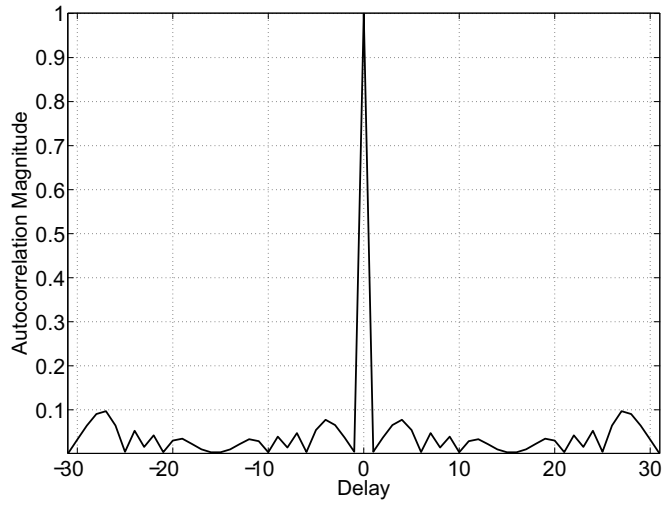

Figure 6: Autocorrelation of Oppermann codes of length $N=31$ with parameters $p=1$, $m=2$, $n=2.007$, $1\leq k\leq 30$.

of the set of Oppermann codes if the design is aimed at integrated radar and communication systems.

4.3 Ambiguity Function

In this section, the ambiguity magnitude of polyphase pulse compression codes is given as a function of normalized delay and normalized Doppler shift. Recall that T_c denotes the duration of a chip in a code of length N or period $T = N\,T_c$. Further, τ denotes the delay that a transmitted signal is returned from a target and f_d denotes the Doppler frequency induced by a moving target. The ratios τ/T_c and $f_d\,T$ are then called normalized delay and normalized Doppler, respectively, which shall hereinafter be referred to as delay and Doppler for brevity.

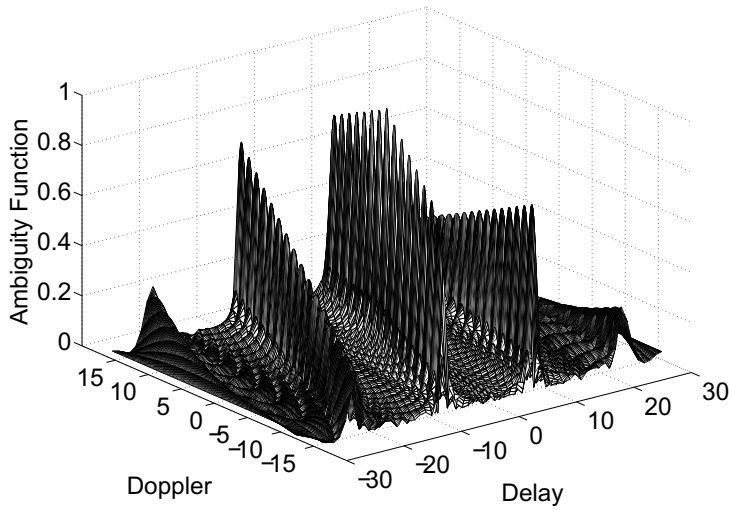

Figure 7: Ambiguity function of second FZC code of length $N = 31$ ($k = 2$).

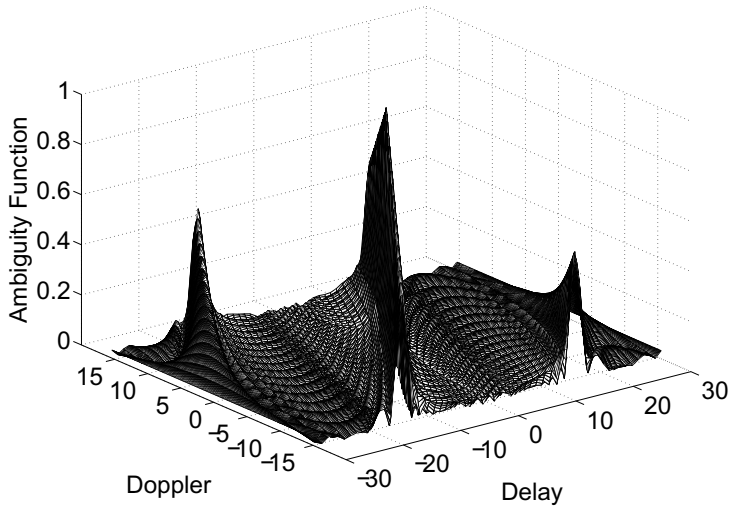

Figure 8: Ambiguity function of Oppermann codes of length $N = 31$ with parameters $p = 1$, $m = 2$, $n = 2.007$ and $1 \leq k \leq 30$.

Figs. 7-8 show the AF of the second FZC code and Oppermann codes with the maximum FOM, respectively, both of length $N = 31$. As for the FZC code, the two distinct peaks in the sidelobes of the autocorrelation shown in Fig. 5(b) translate to two significant ridges on both sides to the diagonal ridge that commences from the third quadrant of the delay-Doppler plane and passes through the origin to the first quadrant of the delay-Doppler plane. In addition, two smaller ridges develop in the second and fourth quadrant of the delay-Doppler plane. Unlike this FZC code, the AF of the examined Oppermann code does not have these undesirable two ridges in relatively close proximity to the diagonal ridge but only induces the smaller ridges in the corners of the second and fourth quadrant of the delay-Doppler plane.

4.4 Ambiguity Contour Plots

In view of the above findings, delay-Doppler performance among the Px, P4, and Oppermann codes will be compared using ambiguity contour

plots deduced from the related AFs. This selection is motivated by the fact that Px codes have been identified as the best choice among the considered polyphase pulse compression codes in terms of FOM performance (see Fig. 1) while P4 codes are know to outperform P3 codes as mentioned in Section 3.4. As for the Oppermann codes, the results presented so far promise waveform designs of any length that can achieve comparable FOM and PSLR as P3 and P4 codes but with the additional benefit of catering for a set of codes instead of only a single code. Again, in this paper we aim at revealing representative behavior rather then a comprehensive performance analyzes for a wide range of parameter sets and hence focus on a selected code length.

Figs. 9-10 show the ambiguity contours of the Px codes of perfect square length $N=25$ and $N=36$, respectively. It can be seen from the figures, that the favorable performance of Px codes with respect to FOM and PSLR does not extend to the delay-Doppler tolerance. Specifically, the diagonal ridge is accompanied by a number of sidelobes. In addition, secondary attenuated ridges builtup in the second and fourth quadrant of the delay-Doppler plane. These characteristics are observed for both length but with the ambiguity contour more focused along the diagonal ridge and the secondary ridges more attenuated for the longer Px code.

Fig. 11 provides the ambiguity contour for the P4 code of length $N = 31$ as a comparison to the examined Px codes. As can be seen from this numerical example, the inferior performance of the P4 code with respect to FOM and PSLR is compensated for by its favorable behavior in the non-zero Doppler shift regime. Specifically, the undesirable sidelobes alongside the diagonal ridge is not present with this P4 code.

Given the length N, the aforementioned polyphase pulse compression codes cater for only one distinct code and may be utilized for the design of a conventional radar system. In order to facilitate integrated radar and communication applications, Oppermann codes shall be examined in the sequel. Here, we consider a set of 30 Oppermann codes of length $N = 31$ defined by the parameters $p = 1$, $m = 2$, and $n=1.8$, 1.9, and 2.007. Figs. 12(a)-(c) show the ambiguity contour for this code with varying n. Clearly, the results indicate that the diagonal ridge is controlled by the value of the parameter n. Specifically, the diagonal ridge rotates counter-clockwise with increasing n to its optim-

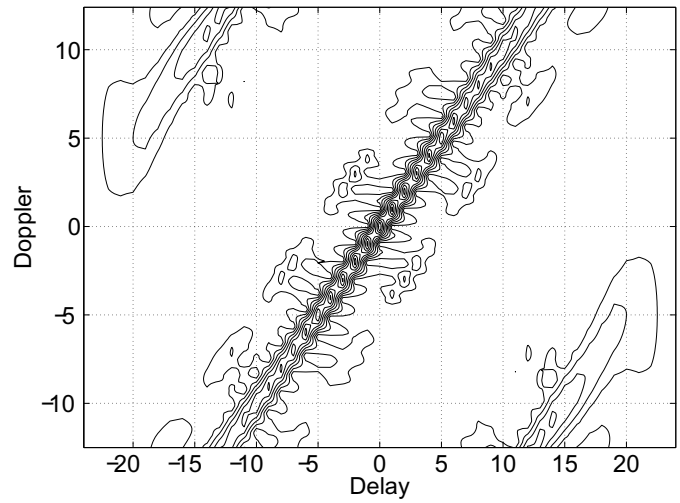

Figure 9: Contour plot of the Px code of length $N = 25$ ($FOM = 14.132$).

um along with the appearance of secondary ridges in the second and fourth quadrant of the delay-Doppler plane. Also, FOM improves with increased n and reaches a maximum of $FOM = 9.027$ for $n = 2.007$. In this case of maximum FOM, the ambiguity contour of the Oppermann codes is very similar to that of the P4 code of the same length.

Additional insights into the impact of the parameter n on the performance of the Oppermann codes can be gained by examining the related power spectrum of these codes as depicted in Figs. 13(a)-(c). Here, the power spectrum of the two Oppermann codes $k = 1$ and $k = 2$ are given for the different values of parameter n. It can be deduced from these figures that overlapping of their power spectrum increases with increasing the parameter n. While the power spectrum of the two codes are well separated for $n = 1.8$, significant crosscorrelation will be caused by the overlapping power spectrum observed for $n = 2.007$. Having shown the wide range of design options offered by Oppermann codes in the radar context, future work on multiobjective optimization is warranted but outside the scope of this paper.

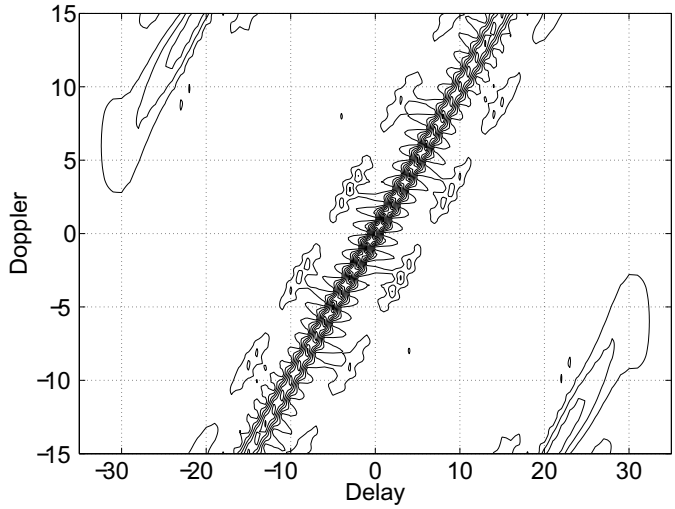

Figure 10: Contour plot of the Px code of length $N = 36$ ($FOM = 15.220$).

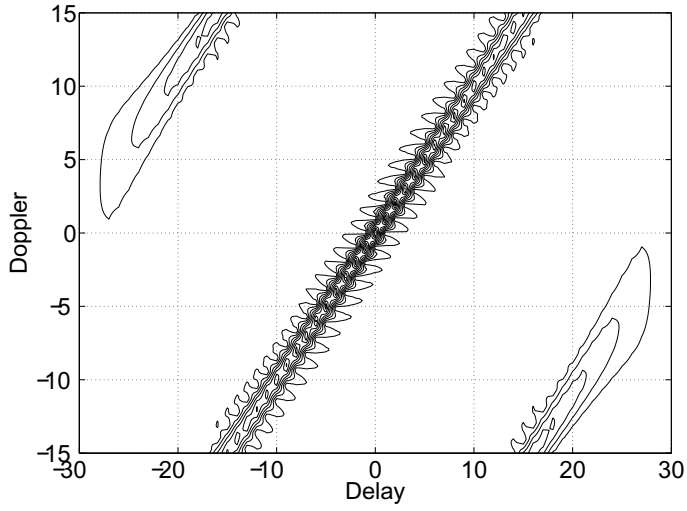

Figure 11: Contour plot of the P4 code of length $N = 31$ ($FOM = 8.595$).

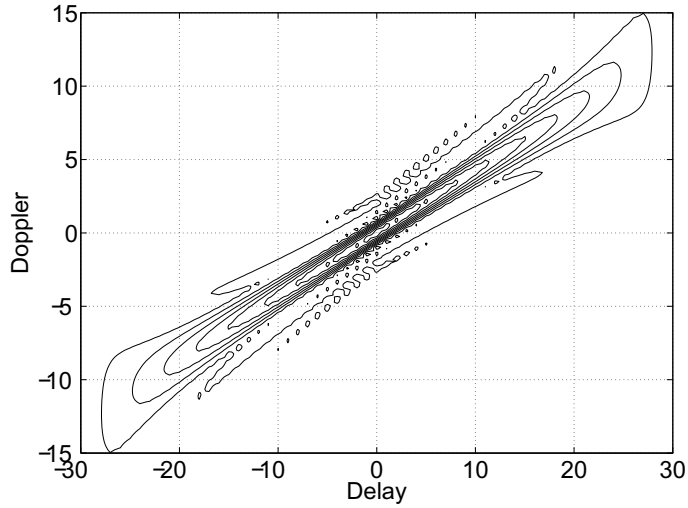
15
10
5
0
−5
−10
−15
Doppler
−30
−20
−10
0
10
20
30
Delay

(a)

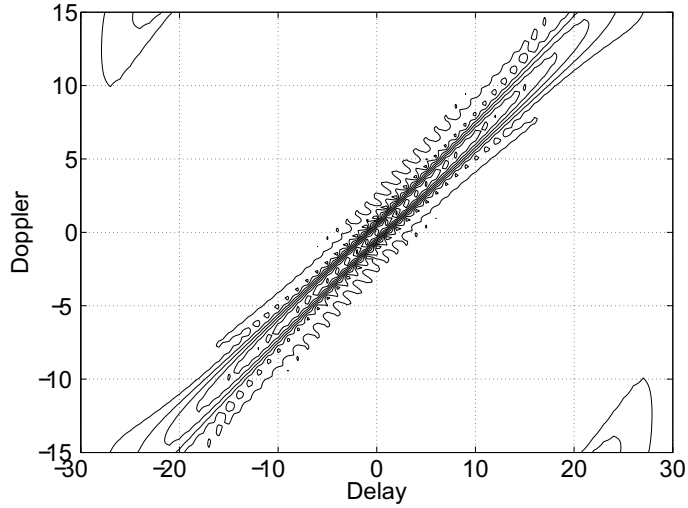
15
10
5
0
−5
−10
−15
Doppler
−30
−20
−10
0
10
20
30
Delay

(b)

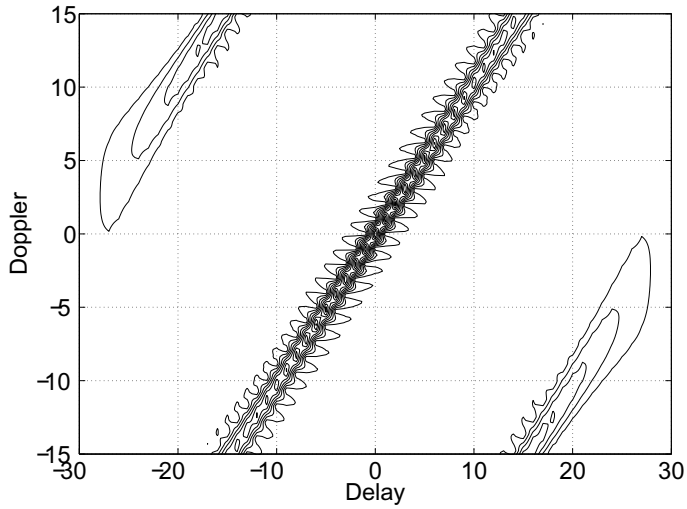

(c)

Figure 12: Contour plots of Oppermann codes of length $N = 31$ with parameters $p = 1$, $m = 2$: (a) $n = 1.8$ ($FOM = 0.772$), (b) $n = 1.9$ ($FOM = 1.943$), (c) $n = 2.007$ (maximum $FOM = 9.027$).

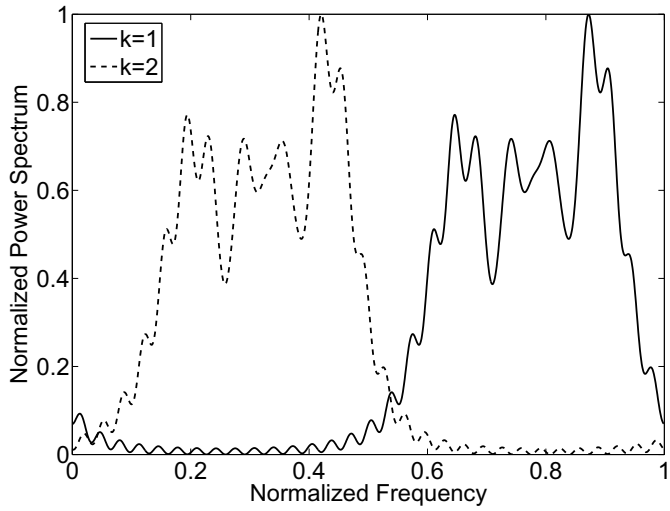

(a)

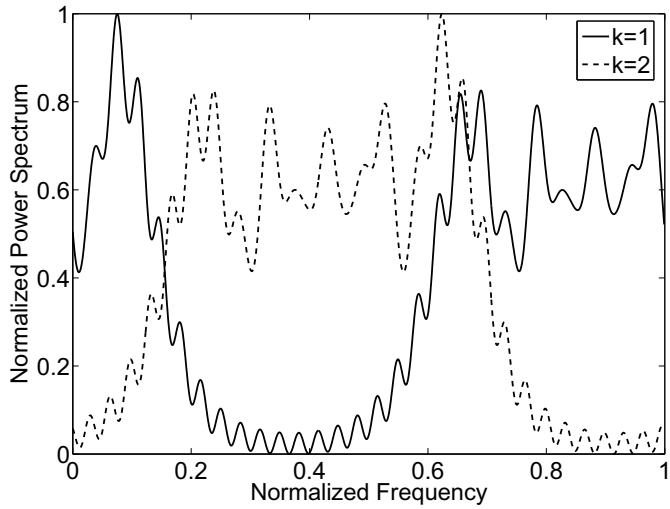

(b)

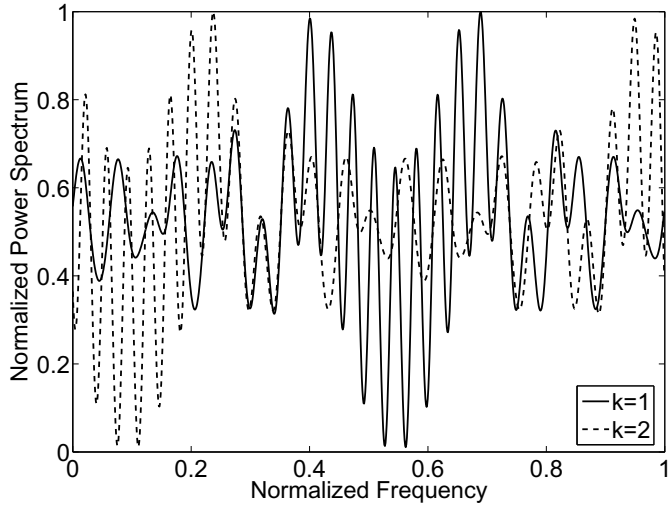

(c)

Figure 13: Normalized power spectrum of Oppermann codes of length $N=31$ with parameters $p=1$, $m=2$: (a) $n=1.8$ ($FOM=0.772$), (b) $n=1.9$ ($FOM=1.943$), (c) $n=2.007$ (maximum $FOM=9.027$).

5 Conclusions

In this paper, we have examined and compared the performance of prominent polyphase pulse compression codes such as Frank, FZC, P1, P2, P3, P4, and Px codes with the performance of Oppermann codes. The latter class of codes has been considered to date only for applications in CDMA systems while their performance evaluation has been extended in this paper to reveal their delay-Doppler characteristics. It was shown by way of example that Oppermann codes can account for a wide range of applications including the design of integrated radar and communication systems. Furthermore, a number of benefits and drawbacks associated with the examined polyphase code classes have been discussed and may be helpful as additional guide in the waveform design for modern radar systems.

References

[1] N. Levanon and E. Mozeson, "Radar Signals," Chichester: John Wiley & Sons, 2004.

[2] S. W. Golomb and G. Gong, "Signal Design for Good Correlation for Wireless Communication, Cryptography, and Radar," Cambridge: Cambridge University Press, 2005.

[3] R. L. Frank, "Polyphase Codes with Good Nonperiodic Correlation Properties," *IEEE Trans. on Inf. Theory*, vol. 9, pp. 43-45, Jan. 1963.

[4] B. L. Lewis and F. F. Kretschmer, "A New Class of Polyphase Pulse Compression Codes and Techniques," *IEEE Trans. on Aerospace and Electronic Systems*, vol. 17, no. 3, pp. 364–372, May 1981.

[5] P. B. Rapajic and R. A. Kennedy, "Merit Factor Based Comparison of New Polyphase Sequences," *IEEE Commun. Letters*, vol. 2, no. 10, pp. 269– 270, Oct. 1998.

[6] R. L. Frank and S. A. Zadoff, "Phase Shift Pulse Codes with Good Periodic Correlation Properties," IEEE Trans. on Inf. Theory, vol. 19, no. 1, pp. 115-120, Jan. 1975.

[7] D. C. Chu, "Polyphase Codes with Good Periodic Correlation Properties," *IEEE Trans. on Inf. Theory*, vol. 18, no. 4, pp. 531-532, July 1972.

[8] B. L. Lewis and F. F. Kretschmer, "Linear Frequency Modulation Derived Polyphase Pulse Compression Codes," *IEEE Trans. on Aerospace and Electronic Systems*, vol. 18, no. 5, pp. 637–641, Sept. 1982.

[9] F. F. Kretschmer and B. L. Lewis, "Doppler Properties of Polyphase Coded Pulse Compression Waveforms," *IEEE Trans. on Aerospace and Electronic Systems*, vol. 19, no. 4, pp. 521-531, July 1983.

[10] I. Oppermann and B. S. Vucetic, "Complex Spreading Sequences with a Wide Range of Correlation Properties," *IEEE Trans. on Commun.*, vol. 45, pp. 365–375, Mar. 1997.

[11] P. Fan and M. Darnell, "Sequence Design for Communications Applications," Somerset: Research Studies Press, 1996.

[12] H.-J. Zepernick and A. Finger, "Pseudo Random Signal Processing: Theory and Application," Chichester: John Wiley & Sons, 2005.

[13] R. C. Heimiller, "Phase Shift Pulse Codes with Good Periodic Correlation Properties" IRE Trans. on Inf. Theory, vol. 7, pp. 254-257, Oct. 1961.

Part I-B

Part I-B

On Integrated Radar and Communication Systems Using Oppermann Sequences

Part I-B is based on:

M. Jamil, H.-J. Zepernick, and M. I. Pettersson, "On Integrated Radar and Communication Systems Using Oppermann Sequences," *IEEE Military Commun. Conf.*, San Diego, USA, 2008, pp. 1–6.

On Integrated Radar and Communication Systems Using Oppermann Sequences

Momin Jamil, Hans-Jürgen Zepernick, and Mats I. Pettersson

Abstract

In this paper, we consider the design of integrated radar and communication systems that utilize weighted pulse trains with the elements of Oppermann sequences serving as complex-valued weights. An analytical expression of the ambiguity function for weighted pulse trains with Oppermann sequences is derived. Given a family of Oppermann sequences, it is shown that the related ambiguity function depends only on one sequence parameter. This property simplifies the design of the associated weighted pulse trains as it constrains the degrees of freedom. In contrast to the single polyphase pulse compression sequences that are typically deployed in radar applications, the families considered in this paper form sets of sequences. As such, they readily facilitate also multiple-access in communication systems. Numerical examples are provided that show the wide range of options offered by Oppermann sequences in the design of integrated radar and communication systems.

1 Introduction

The integration of multiple functions such as navigation and radar tasks with communication applications has attracted substantial interest in recent years and sparked a number of research initiatives. This includes the research on future signals for hybrid receivers for Global Navigation Satellite Systems (GNSS)/communication and others tasks. The many

benefits of multifunctionality in the area of military radio frequency (RF) systems range from reducing costs and probability of intercept to offering tolerable co-site interference.

As far as integration of radar and communications is concerned, the Office of Naval Research in 1996 launched the Advanced Multifunction Radio Frequency Concept (AMRFC) program [1,2]. The AMRFC program was motivated by the lack of integration of radar, communications, and electronic warfare functions and the related significant increase in the number of topside antennas. This in turn increases the ship radar cross section and infrared signature. Further, lack of integration may cause severe problems with antenna blockage, difficulties with own-ship electromagnetic interference, and puts stress on maintenance resources. The concept proposed in the related work aimed at suitable broadband RF apertures that can cope with simultaneous operation of multiple functions and hence is centered on the RF front-end.

A different approach using linear frequency modulated (LFM) waveforms, also referred to as chirps, has been proposed in [3]. In order to enhance orthogonality among the signals of the different functions, it uses up-chirps for the communications component and down-chirps for the radar functionality. The particular composition of the suggested chirp signals allows for the radar and communication data to be simultaneously transmitted and received with some standard antenna array. Noting the inherent connection of the aforementioned chirp-based integration concept to spread spectrum techniques, the work reported in [4,5] investigated the integration of radar and communications based on bipolar pseudo random (PN) sequences, namely m-sequences [6,7]. However, one of the main drawbacks of m-sequences in the radar context is their poor Doppler tolerance [8]. These and related designs such as polyphase Barker sequences are optimized only with respect to the zero Doppler cut of the ambiguity function but produce much higher interference levels in the presence of Doppler shifted waveforms. As for the application to communications, large sets of m-sequences as needed with multiple-access techniques have typically rather poor crosscorrelation properties [6]. As such, they are generally only used as components of more complex designs such as Gold sequences. On the other hand, the large advances in modern integrated circuit technologies would fa-

cilitate an efficient implementation of more advanced sequence designs such as complex-valued sequences.

In view of the above, this paper considers integrated radar and communication systems based on polyphase sequences, especially, Oppermann sequences [9] are utilized. The most prominent sequences that have been advised for radar applications include polyphase pulse compression sequences such as the P1, P2, P3, P4, and Px sequences [8, 10–12]. It shall be mentioned that these sequences may be derived from the phase history of chirp or step-chirp analog signals such as those used in the integration approach discussed in [3] but with the additional benefit of being implemented and processed digitally. Although these sequences perform well in the radar scenarios, they do not readily scale to communications as only a single sequence is provided in contrast to the required sets of sequences with sizes ranging up to the hundreds. In order to account for the waveform design challenges associated with integrated radar and communication systems, we have compared performance and potential application scenarios of different classes of polyphase pulse compression sequences [13], namely P1, P2, P3, P4, Px, Frank-Zadoff-Chu, and Oppermann sequences. Specifically, Oppermann sequences have been revealed in this study to potentially better support the considered integration as these allow for the design not only of families with a wide range of correlations but also support a variety of characteristics with respect to the ambiguity function, i.e. delay-Doppler tolerance.

Motivated by the promising features revealed from this study on the qualitative classification of polyphase pulse compression sequences [13], this paper advances to the quantitative examination of Oppermann sequences along with rigorous formulation and derivation of the related ambiguity function. This provides both an in-depth understanding about the fundamental characteristics of Oppermann sequences for integrated radar and communication applications and establishes the theoretical framework that could guide the waveform designer in phrasing the particular multi-objective optimization with respect to given system constraints. Clearly, the proposed approach moves the technical challenges associated with multifunctionality away from the expensive RF front-end and the less flexible analog domain based on chirp signals

towards the cost effective and highly adaptable discrete domain.

The remainder of this paper is organized as follows. Section 2 describes the measures used to evaluate the performance of the considered weighted pulse trains. In Section 3, the definition of Oppermann sequences and some of their properties are given. An analytical expression of the ambiguity function of weighted pulse trains with Oppermann sequences is derived in Section 4. In Section 5, numerical examples are given to show the wide range of options provided by Oppermann sequences in the design of integrated radar and communication systems. Finally, Section 6 concludes the paper.

2 Performance Measures

Let N denote the length of each polyphase code $\mathbf{u}_k = [u_k(0), u_k(1), \ldots, u_k(N-1)]$ of a given set $\mathcal{U}$ of size U, where $1 \leq k \leq U$. In this section, we provide the definitions of measures [6, 14] used to evaluate the performance of the considered family of Oppermann sequences.

2.1 Aperiodic Autocorrelation Function

The aperiodic autocorrelation function $C_k(l)$ at discrete shift l between the kth complex-valued sequence $\mathbf{u}_k \in \mathcal{U}$ and its shifted version, is defined as

$$C_k(l) = \begin{cases} \frac{1}{N} \sum_{i=0}^{N-1-l} u_k(i) u_k^*(i+l), & 0 \leq l \leq N-1 \\ \frac{1}{N} \sum_{i=0}^{N-1+l} u_k(i-l) u_k^*(i), & 1-N \leq l < 0 \\ 0, & |l| \geq N \end{cases} \tag{1}$$

where $(\cdot)^*$ denotes the complex conjugate of the argument $(\cdot)$.

2.2 Figure of Merit

The figure of merit (FOM) of a sequence $\mathbf{u}_k \in \mathcal{U}$, $1 \leq k \leq U$ of length N with aperiodic autocorrelation function $C_k(l)$ measures the ratio of

energy in the mainlobe to that in the sidelobe of the autocorrelation function. It is defined as

$$FOM_k = \frac{C_k(0)}{2\sum_{l=1}^{N-1} |C_k(l)|^2} \tag{2}$$

2.3 Ambiguity Function

In this paper, we consider weighted pulse trains that can be described by a complex envelope as

$$U_k(t) = \frac{1}{\sqrt{T}} \sum_{i=0}^{N-1} u_k(i) \operatorname{rect}\left(\frac{t - iT_c}{T_w}\right) \tag{3}$$

where $T = NT_c$ is the duration of the kth pulse train while T_c and $T_w \leq T_c$, respectively, denote the repetition period and the width of each rectangular pulse

$$\operatorname{rect}\left(\frac{t}{T_w}\right) = \begin{cases} 1 & \text{for} \quad -\frac{T_w}{2} \leq t \leq \frac{T_w}{2} \\ 0 & \text{otherwise} \end{cases} \tag{4}$$

The elements $u_k(i)$, $i = 0, 1, \ldots, N-1$, of the kth complex-valued sequences $\mathbf{u}_k$ of length N represent the weights of the pulse train in (3).

The ambiguity function (AF) represents the output of a matched filter with respect to an examined finite energy signal. It describes the interference that would be caused to a transmitted signal due to the delay/range and/or the Doppler shift compared to a reference signal. In this paper, we utilize the following definition of the ambiguity function [8]

$$|\chi(\tau, f_d)| = \left| \int_{-\infty}^{\infty} U_k(t) U_k^*(t + \tau) \exp(j2\pi f_d t) dt \right| \tag{5}$$

where τ and f_d denote delay and Doppler shift, respectively.

3 Oppermann Sequences

A family of polyphase sequences that supports a wide range of correlation properties is proposed in [9]. The ith element $u_k(i)$ of the kth Oppermann sequence $\mathbf{u}_k = [u_k(0), u_k(1), \ldots, u_k(N-1)]$ of length N is defined as

$$u_k(i) = (-1)^{k(i+1)} \exp\left\{\frac{j\pi[k^m(i+1)^p + (i+1)^n]}{N}\right\} \tag{6}$$

where $1 \leq k \leq N-1$, $0 \leq i \leq N-1$ and integer k is relatively prime to the length N. Hereafter, we require N to be a prime, which results in the family being of maximum size $N-1$ [9]. The parameters m, n, and p in (6) take real values and define a family of Oppermann sequences. For a fixed combination of these three parameters, all the sequences have the same autocorrelation magnitude. If $p=1$, this autocorrelation magnitude depends only on n and is given by [9]

$$|C_k(l)| = \left|\frac{1}{N}\sum_{i=0}^{N-1-l} \exp\left\{\frac{j\pi}{N}\left[(i+1)^n - (i+l+1)^n\right]\right\}\right| \tag{7}$$

In this case, the optimal family in terms of FOM as defined in (2) can be found by simple search over n. In the sequel, we will therefore concentrate on the case of $p = 1$. Given $p = 1$ and the parameter n associated with the optimal family, the parameter m may be varied to produce favorable phase or crosscorrelation characteristics, for instance. With this parameter setting, the class of Oppermann sequences provides us not only with a wide range of correlations but also flexibility to control the ambiguity function at scenarios other than those relating to the zero Doppler cut.

A number of properties that turn out to be beneficial in supporting a wide range of correlations and ambiguity properties are summarized as follows [9]:

- The autocorrelation magnitude depends only on n if parameter $p = 1$.
- The parameter m controls the location of the power spectra associated with each sequence and hence controls the crosscorrelation properties.

- The size of a set of Oppermann sequences is maximal if the length N is a prime and then given as $N-1$.

In view of the above, an optimized sequence set design can be based on performance measures such as auto- and crosscorrelations, the FOM, the peak-to-sidelobe ratio, and the ambiguity function.

4 Ambiguity Function of Weighted Pulse Trains With Oppermann Sequences

Let us consider a weighted pulse train $U_k(t)$ as defined in (3), where the pulse weights $u_k(i)$, $i=0,1,\ldots,N-1$, are the ith elements of the kth Oppermann sequence as given in (6). The ambiguity function (without the absolute value operator $|\cdot|$ for ease of exposition) of such a weighted pulse train can then be written as

$$\begin{aligned}\chi(\tau, f_d) &= \int_{-\infty}^{\infty} \sum_{r=0}^{N-1}\sum_{s=0}^{N-1} u_k(r)u_k^*(s) \\ &\quad \times \operatorname{rect}\left(\frac{t-rT_c}{T_w}\right)\operatorname{rect}\left(\frac{t+\tau-sT_c}{T_w}\right) \\ &\quad \times \exp(j2\pi f_d t)dt \\ &= \frac{1}{T}\sum_{r=0}^{N-1}\sum_{s=0}^{N-1} u_k(r)u_k^*(s) \\ &\quad \times \int_{-\infty}^{\infty} \operatorname{rect}\left(\frac{t-rT_c}{T_w}\right)\operatorname{rect}\left(\frac{t+\tau-sT_c}{T_w}\right) \\ &\quad \times \exp(j2\pi f_d t)dt \\ &= \frac{1}{T}\sum_{r=0}^{N-1}\sum_{s=0}^{N-1} u_k(r)\, u_k^*(s)\, \mathcal{I}_1 \end{aligned} \tag{8}$$

where the integral $\mathcal{I}_1$ is introduced for brevity as

$$\mathcal{I}_1 = \int_{-\infty}^{\infty} \operatorname{rect}\left(\frac{t-rT_c}{T_w}\right)\operatorname{rect}\left(\frac{t+\tau-sT_c}{T_w}\right)\exp(j2\pi f_d t)\,dt \tag{9}$$

Making the change of variables $t_1 = t - rT_c$, and integrating over the range $(-\infty, \infty)$, (9) can be expressed as

$$\mathcal{I}_1 = \exp(j2\pi f_d r T_c)\chi_1[\tau + (r-s)T_c, f_d] \tag{10}$$

where $\chi_1[\tau, f_d]$ denotes the triangular ambiguity function of a rectangular pulse and represents the output of a matched filter for a single pulse.

By substituting (10) into (8), the ambiguity function can be written as

$$\chi(\tau, f_d) = \frac{1}{T}\sum_{r=0}^{N-1}\sum_{s=0}^{N-1} u_k(r)\, u_k^*(s) \times \exp(j2\pi f_d r T_c)\, \chi_1[\tau + (r-s)T_c, f_d] \tag{11}$$

Utilizing the relation $q = r - s$ and collecting terms centered at the same shift $\tau = qT_c$, the double sum in (11) can be rewritten according to [15] as

$$\sum_{r=0}^{N-1}\sum_{s=0}^{N-1} = \sum_{q=0}^{N-1}\sum_{s=0}^{N-1-q}\Bigg|_{r=s+q} + \sum_{q=-(N-1)}^{-1}\sum_{r=0}^{N-1-|q|}\Bigg|_{s=r-q} \tag{12}$$

The ambiguity function $\chi(\tau, f_d)$ of the considered weighted pulse train $U_k(t)$, where the elements $u_k(i)$ of the kth Oppermann sequence $\mathbf{u}_k$ are used as weights, can then be written with (12) as a series of shifted ambiguity functions $\chi_1(\tau, f_d)$ of the rectangular pulse as

$$\chi(\tau, f_d) = \frac{1}{T}\sum_{q=0}^{N-1}\chi_1(\tau + qT_c, f_d)\, \exp(j2\pi f_d q T_c)\, \mathcal{S}_1 + \frac{1}{T}\sum_{q=0}^{N-1}\chi_1(\tau + qT_c, f_d)\, \mathcal{S}_2 \tag{13}$$

where the two sums $\mathcal{S}_1$ and $\mathcal{S}_2$, respectively, are defined as

$$\mathcal{S}_1 = \sum_{s=0}^{N-1-q} u_k(s+q)u_k^*(s)\exp(j2\pi f_d s T_c) \tag{14}$$

$$\mathcal{S}_2 = \sum_{r=0}^{N-1-|q|} u_k(r) u_k^*(r-q) \exp(j2\pi f_d r T_c) \tag{15}$$

Using the definition of the elements of Oppermann sequences in (6) and performing some elementary algebra, (14) and (15), respectively, can be written as follows:

$$\begin{aligned}\mathcal{S}_1 = (-1)^{kq} \exp\left(j\frac{\pi}{N}k^m q\right) \\ \times \sum_{s=0}^{N-1-q} \exp\left\{-j\frac{\pi}{N}\left[(s+1)^n - (s+q+1)^n\right]\right\} \\ \times \exp(j2\pi f_d s T_c)\end{aligned} \tag{16}$$

$$\begin{aligned}\mathcal{S}_2 = (-1)^{kq} \exp\left(j\frac{\pi}{N}k^m q\right) \\ \times \sum_{s=0}^{N-1-|q|} \exp\left\{j\frac{\pi}{N}\left[(r+1)^n - (r-q+1)^n\right]\right\} \\ \times \exp(j2\pi f_d r T_c)\end{aligned} \tag{17}$$

Let us further assume that the ratio of pulse width to pulse repetition period is less than 50%, i.e. $T_w/T_c < 0.5$, then magnitudes of the series of ambiguity functions in (13) are non-overlapping. Accordingly, the magnitude of the ambiguity function of a weighted pulse train using Oppermann sequences is given by

$$\begin{aligned}|\chi(\tau, f_d)| = \frac{1}{T}\sum_{q=0}^{N-1} |\chi_1(\tau + qT_c, f_d)| \\ \times \left|\sum_{s=0}^{N-1-q} \exp\left\{-j\frac{\pi}{N}\left[(s+1)^n - (s+q+1)^n\right]\right\}\right. \\ \left.\times \exp(j2\pi f_d s T_c)\right| \\ + \frac{1}{T}\sum_{q=-(N-1)}^{1} |\chi_1(\tau + qT_c, f_d)|\end{aligned}$$

$$\times \left| \sum_{r=0}^{N-1-|q|} \exp\left\{ j\frac{\pi}{N}\left[(r+1)^n - (r-q+1)^n\right]\right\} \right.$$

$$\left. \times \exp(j2\pi f_d r T_c) \right| \tag{18}$$

As can be seen from the analytical expression in (18), the ambiguity function of the examined type of weighted pulse trains with Oppermann sequences depend only on the parameter n for $p = 1$. As with the autocorrelation magnitude of the Oppermann sequences, all sequences have the same ambiguity functions for a fixed parameter set.

5 Numerical Examples

This section provides a number of numerical examples to illustrate the wide range of options offered by Oppermann sequences in the design of integrated radar and communication systems. It will also show the relationships of the different sequence parameters on performance characteristics.

Figure 1 depicts the progression of FOM as a function of the parameter n for different prime length N. It can be seen from the figure that for the considered lengths, the maximum FOM is achieved for parameter values $n \in (1.9, 2.1)$. In addition, it is observed that the maximum FOM tends to be more distinct with the longer sequences and less tolerant to variations of n around the optimal value. Although the FOM does not depend on the parameter m for the considered case of $p=1$, the parameter m controls the phase characteristics of the Oppermann sequences and as such the arrangement of the associated power spectra of the sequences. This is illustrated in Fig. 2 for sequences of length $N=31$, where the normalized power spectrum of the second Oppermann sequence ($k = 2$) is shifted towards higher normalized frequencies with the parameter m increasing from 1 to 4. This characteristic may be used to control crosscorrelation between the sequences in a design for integrated radar and communication systems by varying m while the ambiguity functions remains the same for all sequences in the set for given n.

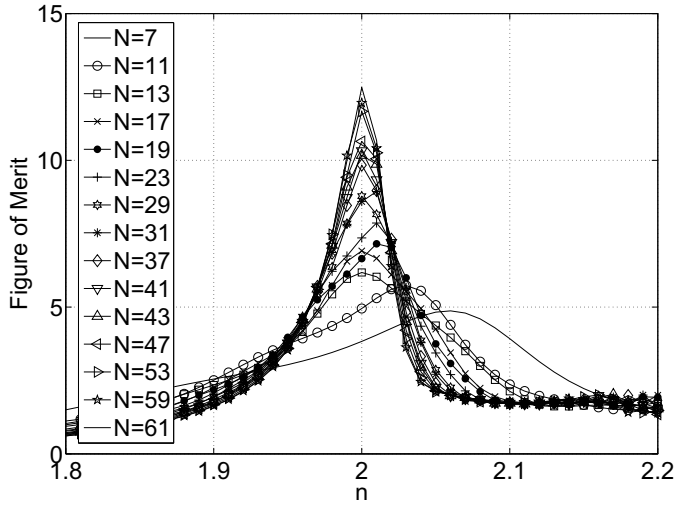

Figure 1: Figure of merit as a function of parameter n for Oppermann sequences of prime length N ($p = 1$, $m = 2$).

Let us now consider sets of Oppermann sequences of prime length $N = 31$ and parameter $p = 1$. Accordingly, parameters m and n are available for an optimized sequence set design. Figs. 3(a)-(d) show the ambiguity function, ambiguity contour plot, autocorrelation magnitude, and normalized power spectrum, respectively, for a design aimed at minimizing the out-of-phase average mean-square aperiodic autocorrelation. This reflects requirements of many radar applications with focus being on maximum FOM and good delay-Doppler tolerance. Clearly, the distinct autocorrelation peak at the zero Doppler cut is obtained at the expense of overlapping and hence interfering power spectra.

Similarly, Figs. 4(a)-(d) show the results for a design aiming at minimizing the average mean-square aperiodic crosscorrelation. In this case, the autocorrelation mainlobe broadens significantly which results in a poor FOM and inferior delay-Doppler tolerance. However, the normalized power spectrum of the different sequences are well separated and thus support multiple-access in a communications context.

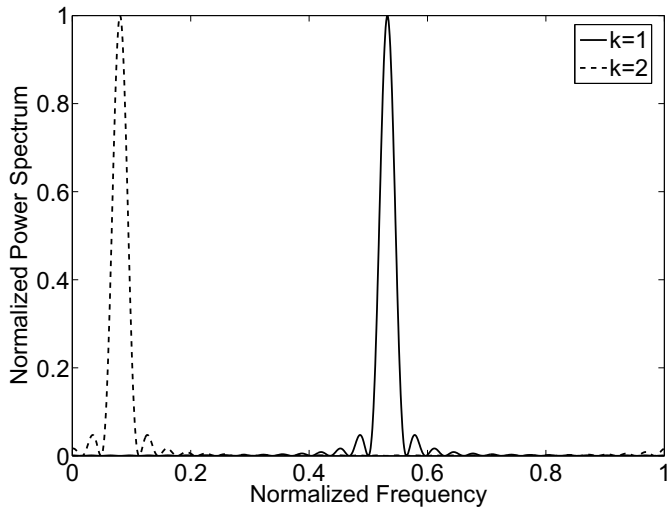

(a)

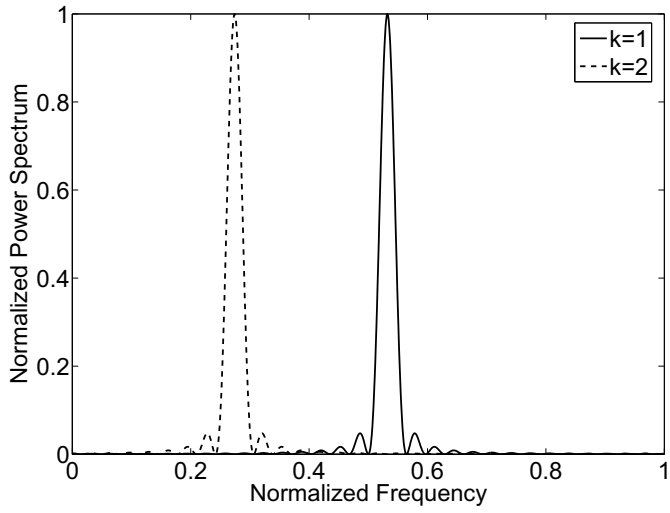

(b)

Figure 2: Normalized power spectrum of Oppermann sequences ($N=31$, $p=1$, $n=2.007$): (a) $m=1$, (b) $m=4$.

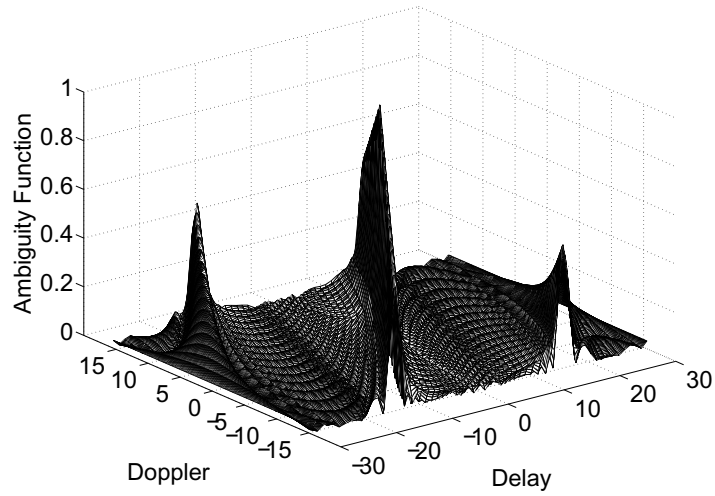
Ambiguity Function
1
0.8
0.6
0.4
0.2
0
15
10
5
0
−5
−10
−15
Doppler
−30
−20
−10
0
10
20
30
Delay

(a)

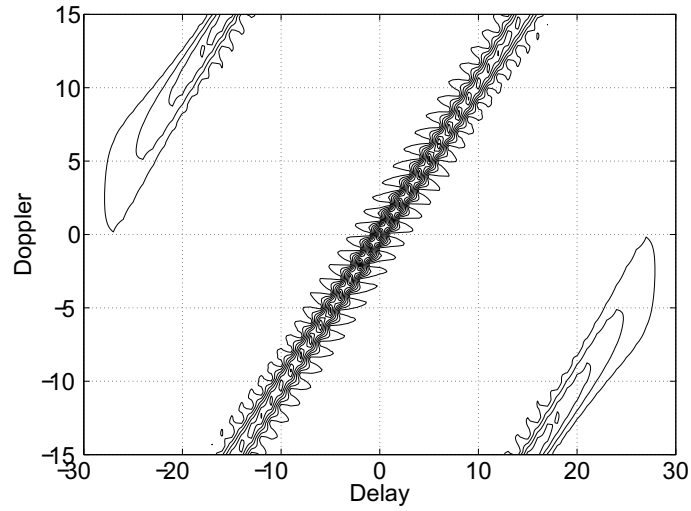
Doppler
15
10
5
0
−5
−10
−15
−30
−20
−10
0
10
20
30
Delay

(b)

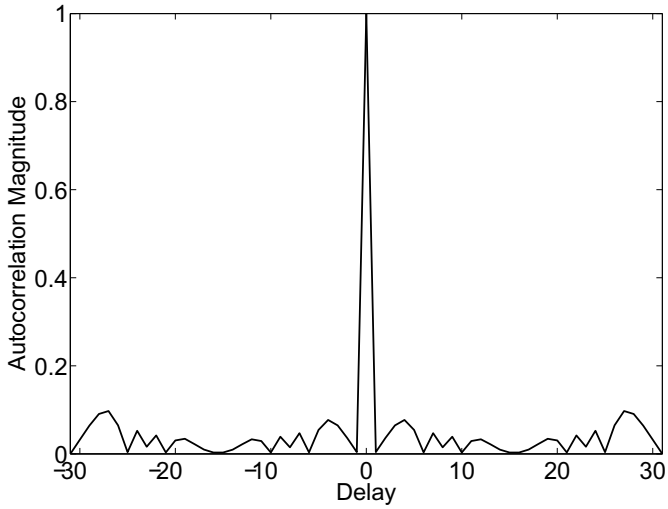

(c)

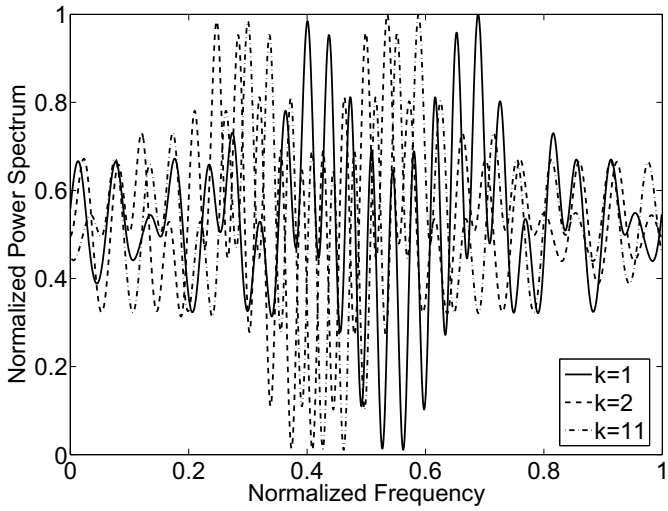

(d)

Figure 3: Performance of Oppermann sequences for optimized mean-square out-of-phase aperiodic autocorrelation ($N=31$, FOM $=9.0287$): (a) Ambiguity function, (b) Ambiguity contour plot, (c) Autocorrelation magnitude, (d) Normalized power spectrum.

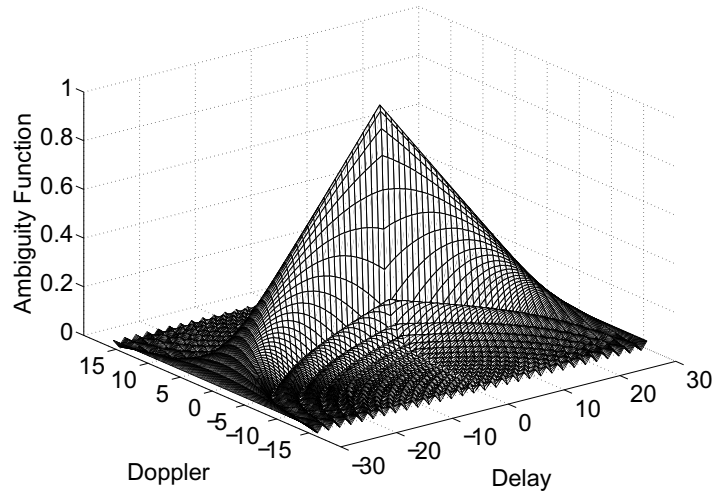
Ambiguity Function
1
0.8
0.6
0.4
0.2
0
15
10
5
0
−5
−10
−15
Doppler
−30
−20
−10
0
10
20
30
Delay

(a)

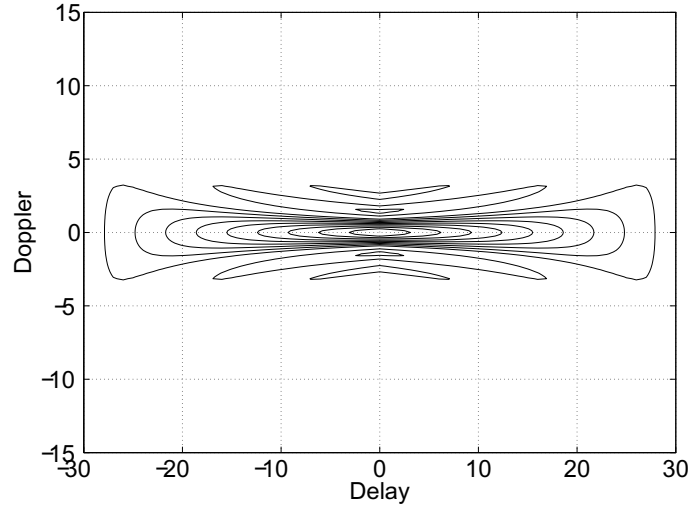
Doppler
15
10
5
0
−5
−10
−15
−30
−20
−10
0
10
20
30
Delay

(b)

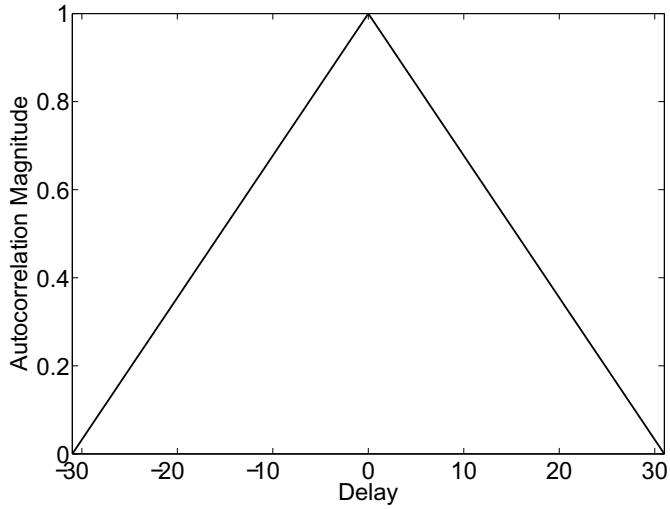

(c)

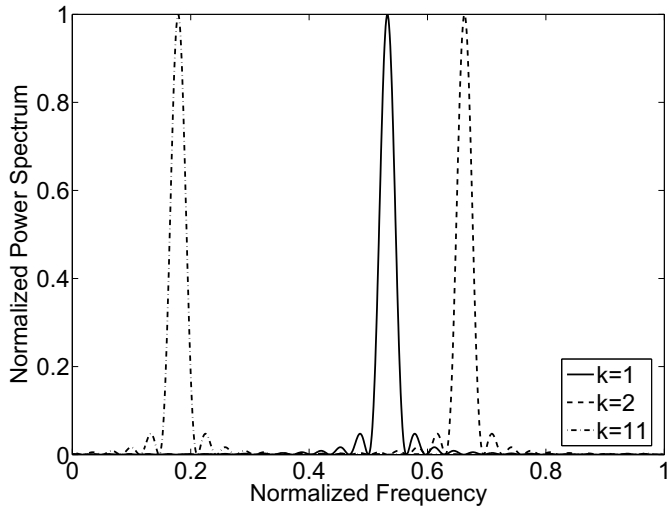

(d)

Figure 4: Performance of Oppermann sequences for optimized mean-square aperiodic crosscorrelation ($N = 31$, FOM $= 0.0508$): (a) Ambiguity function, (b) Ambiguity contour plot, (c) Autocorrelation magnitude, (d) Normalized power spectrum.

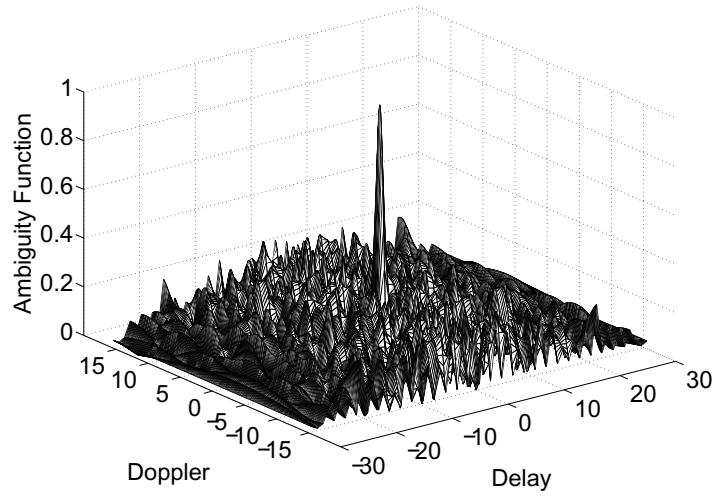
Ambiguity Function
1
0.8
0.6
0.4
0.2
0
15
10
5
0
−5
−10
−15
Doppler
−30
−20
−10
0
10
20
30
Delay

(a)

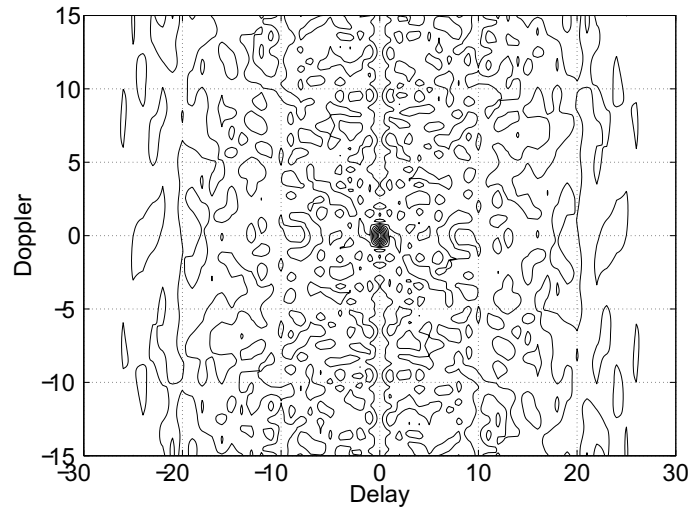
Doppler
15
10
5
0
−5
−10
−15
−30
−20
−10
0
10
20
30
Delay

(b)

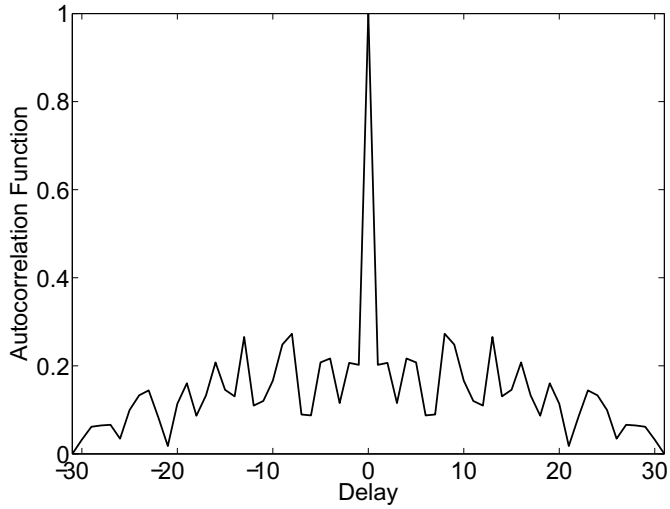

(c)

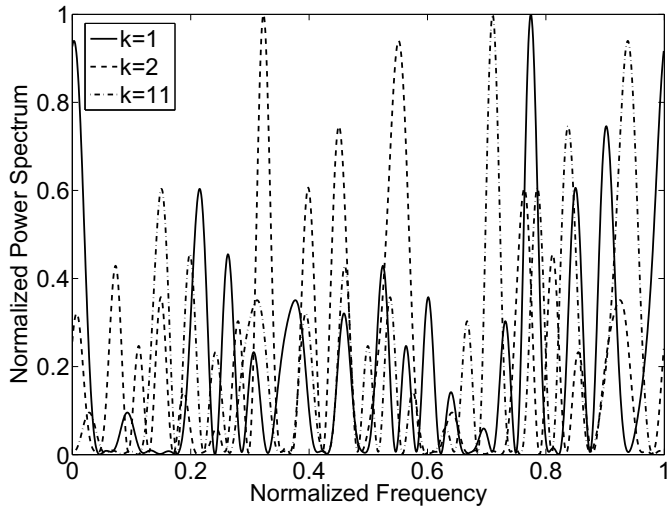

(d)

Figure 5: Performance of Oppermann sequences with $n > n_{optimum}$ with respect to maximum FOM ($N=31$, FOM$=0.7372$): (a) Ambiguity function, (b) Ambiguity contour plot, (c) Autocorrelation magnitude, (d) Normalized power spectrum.

In view of applications for integrated radar and communication systems, a trade-off may be established among the multiple objectives of such scenarios. For example, the parameter n may be increased beyond the optimal value for maximum FOM as shown in Fig. 5. In this case, the ambiguity function shows a distinct peak while the normalized power spectra are still somewhat distinguishable.

6 Conclusion

In this paper, we have considered the design of integrated radar and communication systems using Oppermann sequences for the generation of weighted pulse trains. An analytical expression of the related ambiguity function was derived, which turned out to depend only on one sequence parameter. As with the autocorrelation magnitude, the ambiguity function is the same for all sequences in a given family of Oppermann sequences. This simplifies the design methodology for integrated radar and communication system as Doppler and delay characteristics may be considered one after the other. The numerical examples shown illustrate the many options offered by Oppermann sequences in the design of integrated radar and communication systems.

References

[1] P. K. Hughes and J. Y. Choe, "Overview of Advanced Multifunction RF System (AMRFS)," IEEE Int. Conf. on Phased Array Systems and Technology, Dana Point, U.S.A., pp. 21–24, May 2000.

[2] G. C. Tavik, et al., "The Advanced Multifunction RF Concept," *IEEE Trans. Microw. Theory and Techn.*, vol. 53, pp. 1009–1020, Mar. 2005.

[3] M. Roberton and E. R. Brown, "Integrated Radar and Communications based on Chirped Spread-Spectrum Techniques," IEEE MTT-S Int. Microwave Symp., Philadelphia, U.S.A., pp. 611–614, June 2003.

[4] S. J. Xu, Y. Chen, and P. Zhang, "Integrated Radar and Communication based on DS-UWB," IEEE Ultrawideband and Ultrashort Impulse Signals, Sevastopol, Ukraine, pp. 142–144, Sept. 2006.

[5] S. J. Xu, B. Chen, and P. Zhang, "Radar-Communication Integration based on DSSS Techniques," IEEE Int. Conf. on Signal Processing, Beijing, China, pp. 16–20, Nov. 2006.

[6] H.-J. Zepernick and A. Finger, "Pseudo Random Signal Processing: Theory and Application," Chichester: John Wiley & Sons, 2005.

[7] S. W. Golomb and G. Gong, "Signal Design for Good Correlation for Wireless Communication, Cryptography, and Radar," Cambridge: Cambridge University Press, 2005.

[8] N. Levanon and E. Mozeson, "Radar Signals," Chichester: John Wiley & Sons, 2004.

[9] I. Oppermann and B. S. Vucetic, "Complex Spreading Sequences with a Wide Range of Correlation Properties," *IEEE Trans. on Commun.*, vol. 45, no. 3, pp. 365–375, Mar. 1997.

[10] B. L. Lewis and F. F. Kretschmer, "A New Class of Polyphase Pulse Compression Codes and Techniques," *IEEE Trans. on Aerospace and Electronic Systems*, vol. 17, no. 3, pp. 364–372, May 1981.

[11] B. L. Lewis and F. F. Kretschmer, "Linear Frequency Modulation Derived Polyphase Pulse Compression Codes," *IEEE Trans. on Aerospace and Electronic Systems*, vol. 18, no. 5, pp. 637–641, Sept. 1982.

[12] P. B. Rapajic and R. A. Kennedy, "Merit Factor Based Comparison of New Polyphase Sequences," *IEEE Commun. Letters*, vol. 2, no. 10, pp. 269–270, Oct. 1998.

[13] M. Jamil, H.-J. Zepernick, and M. I. Pettersson, "Performance Assessment of Polyphase Pulse Compression Codes," IEEE Int. Symp. on Spread Spect. Techn. and Appl., Bologna, Italy, pp. 161–165, Aug. 2008.

[14] P. Fan and M. Darnell, "Sequence Design for Communications Applications," Somerset: Research Studies Press, 1996.

[15] R. L. Mitchell and A. W. Rihaczek, "Clutter Suppression Properties of Weighted Pulse Trains," IEEE Trans. Aerospace and Electr. Systems, vol. AES-4, no. 6, pp. 822–828, Nov. 1968.

Part I-C

Part I-C

Cross-Ambiguity Function of Weighted Pulse Trains with Oppermann Sequences

Part I-C is based on:

M. Jamil, H.-J. Zepernick, and M. I. Pettersson, "Cross-Ambiguity Function of Weighted Pulse Trains with Oppermann Sequences," *IEEE Intl. Symp. on Wireless Commun. Syst.*, Siena, Italy, Sept. 2009, pp. 239–243.

Cross-Ambiguity Function of Weighted Pulse Trains with Oppermann Sequences

Momin Jamil, Hans-Jürgen Zepernick, and Mats I. Pettersson

Abstract

The design of integrated radar and communication systems may be based on sets of polyphase sequences such as Oppermann sequences. In this paper, we derive an analytical expression for the cross-ambiguity function of weighted pulse trains with Oppermann sequences. Further, the auto-ambiguity function is deduced from this as a special case. Numerical examples are provided to illustrate the relationship between sequence parameters and performance characteristics.

1 Introduction

The problem of integrating communication functions with radar systems has received considerable attention in recent years. An important research area essential for the development of such systems includes the design of signals and sequence sets that can cope with the often stringent demands posed on delay resolution, Doppler tolerance, and multi-access interference suppression.

In a recent publication [1] chirps have been proposed to support integrated radar and communication systems. Noting the relationship of chirp-based integration concepts to spread spectrum techniques, the work in [2, 3] examines integration of radar and communications using m-sequences [4, 5]. However, m-sequences are known to have poor Doppler tolerance [6]. In particular, these and related designs such

as polyphase Barker sequences are optimized only with respect to the zero-Doppler cut of the ambiguity function but produce much higher interference levels in the presence of Doppler shifts. On the other hand, large sets of m-sequences as needed with multiple-access techniques in communication systems have typically rather poor cross-correlation properties [4]. Given the large advances in modern integrated circuit technologies, it may be advised to consider more advanced sequence designs such as polyphase sequences.

Sequences that have been advised for radar applications include polyphase pulse compression sequences such as the P1, P2, P3, P4, and Px sequences [6–9]. Although these perform well in radar scenarios, they do not readily scale to communication systems as only a single sequence is provided. In view of integrated radar and communication systems, we have therefore compared performance and potential application scenarios of different classes of polyphase pulse compression sequences [10], namely P1, P2, P3, P4, Px, FZC, and Oppermann sequences [11]. This comparison revealed that Oppermann sequences potentially better support the considered integration as these allow for the design of families that offer a wide range of correlations as well as a variety of characteristics with respect to the ambiguity function, i.e. delay-Doppler tolerance. Given the qualitative classification of polyphase pulse compression sequences [10], the work in [12] advances to a quantitative examination of Oppermann sequences including the derivation of the related auto-ambiguity function.

In this paper, we consider the more generic problem of deriving an analytical expression for the cross-ambiguity function of weighted pulse trains with Oppermann sequences comprising the auto-ambiguity function as a special case. Along with this theoretical framework, a number of properties of the correlations, auto-ambiguity function, and cross-ambiguity function are summarized. This facilitates not only a more structured understanding about the relationship between sequence parameters and the corresponding performance characteristics but would also enable the waveform designer to pose and solve a multi-objective performance optimization subject to given system requirements.

The remainder of the paper is organized as follows. Section 2 describes the measures used to evaluate the performance of the considered weighted pulse trains. In Section 3, the definition of Oppermann sequences is given. An analytical expression for the cross-ambiguity function of weighted pulse trains with Oppermann sequences is derived in Section 4. On this basis, the special case of an auto-ambiguity function is deduced in Section 5. In Section 6, numerical examples are given to illustrate the relationship between sequence parameters and performance characteristics. Finally, Section 7 concludes the paper.

2 Performance Measures

In this section, we provide the definitions of performance measures [4] used to evaluate the performance of the considered family of Oppermann sequences. For this purpose, let N denote the length of each sequence $\mathbf{u}_x = [u_x(0), u_x(1), \ldots, u_x(N-1)]$ of a given set $\mathcal{U}$ of size U, where $1 \leq x \leq U$.

2.1 Aperiodic Cross-correlation

In view of applications such as integrated radar and communication systems, we consider aperiodic correlation measures. The aperiodic cross-correlation $C_{xy}(l)$ at discrete shift l between the xth complex-valued sequence $\mathbf{u}_x \in \mathcal{U}$ and the yth complex-valued sequence $\mathbf{u}_y \in \mathcal{U}$ is defined as

$$C_{xy}(l) = \begin{cases} \frac{1}{N} \sum_{i=0}^{N-1-l} u_x(i) u_y^*(i+l), & 0 \leq l \leq N-1 \\ \frac{1}{N} \sum_{i=0}^{N-1+l} u_x(i-l) u_y^*(i), & 1-N \leq l < 0 \\ 0, & |l| \geq N \end{cases} \tag{1}$$

where $(\cdot)^*$ denotes the complex conjugate of the argument $(\cdot)$. The aperiodic auto-correlation $C_x(l)$ of $\mathbf{u}_x$ at shift l is the aperiodic cross-correlation of $\mathbf{u}_x$ with itself, $C_{xx}(l)$.

2.2 Mean Squared Aperiodic Correlations

A quantification of the cross-correlation properties with respect to all possible shifts and all possible sequences in a given set is provided by the mean squared aperiodic cross-correlation (MSCC). In particular, for a given set $\mathcal{U}$ of size U, the MSCC is defined as

$$R_{cc} = \frac{1}{U(U-1)} \sum_{\substack{x,y \in \mathcal{U} \\ x \neq y}} \sum_{l=1-N}^{N-1} |C_{xy}(l)|^2 \tag{2}$$

Similarly, the out-of-phase mean squared aperiodic auto-correlation (MSAC) is defined as

$$R_{ac} = \frac{1}{U} \sum_{x \in \mathcal{U}} \sum_{\substack{l=1-N \\ l \neq 0}}^{N-1} |C_x(l)|^2 \tag{3}$$

which measures the energy in the sidelobes of the auto-correlation for lags different to zero.

2.3 Cross-Ambiguity Function

In this paper, we consider weighted pulse trains that can be described by a complex envelope as

$$U_x(t) \;=\; \frac{1}{\sqrt{T}} \sum_{i=0}^{N-1} u_x(i)\, \mathrm{rect}\left(\frac{t - iT_c}{T_w}\right) \tag{4}$$

where $T = N\,T_c$ is the duration of the xth pulse train while T_c and $T_w \leq T_c$, respectively, denote the repetition period and the width of each rectangular pulse

$$\mathrm{rect}\left(\frac{t}{T_w}\right) = \begin{cases} 1 & \text{for} \quad -\frac{T_w}{2} \leq t \leq \frac{T_w}{2} \\ 0 & \text{otherwise} \end{cases} \tag{5}$$

The elements $u_x(i)$, $i = 0, 1, \ldots, N-1$, of the xth complex-valued sequences $\mathbf{u}_x$ of length N represent the weights of the pulse train in (4).

The cross-ambiguity function represents the output of a matched filter with respect to an examined finite energy signal. It describes the interference that would be caused by a received signal $U_y(t)$ due to the delay/range and/or the Doppler shift compared to a reference signal $U_x(t)$. In this paper, we utilize the following definition of the cross-ambiguity function

$$|\chi_{xy}(\tau, f_d)| = \left| \int_{-\infty}^{\infty} U_x(t) U_y^*(t+\tau) \exp(j2\pi f_d t) dt \right| \tag{6}$$

where τ and f_d denote delay and Doppler shift, respectively. The auto-ambiguity function $|\chi_x(\tau, f_d)|$ of $U_x(t)$ is the cross-ambiguity function of $U_x(t)$ with itself, $|\chi_{xx}(\tau, f_d)|$.

3 Oppermann Sequences

A family of polyphase sequences that supports a wide range of correlation properties is proposed in [11]. The ith element $u_x(i)$ of the xth Oppermann sequence $\mathbf{u}_x = [u_x(0), u_x(1), \ldots, u_x(N-1)]$ of length N is defined as

$$u_x(i) = (-1)^{x(i+1)} \exp\left\{ \frac{j\pi[x^m(i+1)^p + (i+1)^n]}{N} \right\} \tag{7}$$

where $1 \leq x \leq N-1$, $0 \leq i \leq N-1$ and integer x is relatively prime to the length N. The parameters m, n, and p in (7) take on real values and define a family of Oppermann sequences. A number of known properties shall be summarized as follows [11]:

Property 1. The size of a set of Oppermann sequences is maximal if the length N is a prime and then given as $N-1$.

Property 2. For a fixed combination of m, n, and p, all the sequences have the same auto-correlation magnitude.

Property 3. The auto-correlation magnitude depends only on n if parameter $p = 1$ and is given as [11]

$$|C_k(l)| = \left| \frac{1}{N} \sum_{i=0}^{N-1-l} \exp\left\{ \frac{j\pi}{N} \left[(i+1)^n - (i+l+1)^n \right] \right\} \right| \tag{8}$$

Property 4. The parameter m controls the location of the power spectra associated with each sequence and hence controls the cross-correlation properties.

4 Cross-Ambiguity Function of Weighted Pulse Trains With Oppermann Sequences

In view of Property 3, we will concentrate on the case of $p = 1$. Then, let us consider two weighted pulse trains $U_x(t)$ and $U_y(t)$ as defined in (4), where the pulse weights $u_x(i)$ and $u_y(i)$, $i = 0, 1, \ldots, N-1$, respectively, are the ith elements of the xth and yth Oppermann sequence as given in (7). The cross-ambiguity function (without the absolute value operator $|\cdot|$ for ease of exposition) of such a pair of weighted pulse trains can then be written as

$$\begin{aligned}\chi_{xy}(\tau, f_d) &= \frac{1}{T}\sum_{r=0}^{N-1}\sum_{s=0}^{N-1} u_x(r)u_y^*(s) \\ &\quad \times \int_{-\infty}^{\infty} \text{rect}\left(\frac{t - rT_c}{T_w}\right) \text{rect}\left(\frac{t + \tau - sT_c}{T_w}\right) \\ &\quad \times \exp(j2\pi f_d t)dt \\ &= \frac{1}{T}\sum_{r=0}^{N-1}\sum_{s=0}^{N-1} u_x(r)\, u_y^*(s)\, \mathcal{I}_1 \end{aligned} \tag{9}$$

where

$$\mathcal{I}_1 = \int_{-\infty}^{\infty} \text{rect}\left(\frac{t - rT_c}{T_w}\right) \text{rect}\left(\frac{t + \tau - sT_c}{T_w}\right) \exp(j2\pi f_d t)\, dt \tag{10}$$

In order to solve (10), we make the change of variables $t_1 = t - rT_c$, and then integrate over the range $(-\infty, \infty)$:

$$\mathcal{I}_1 = \exp(j2\pi f_d r T_c)\chi_{rect}[\tau + (r - s)T_c, f_d] \tag{11}$$

where $\chi_{rect}[\tau, f_d]$ denotes the triangular ambiguity function of a rectangular pulse rect$(\cdot)$ and represents the output of a matched filter for a single pulse.

By substituting (11) into (9), the cross-ambiguity function can be written as

$$\chi_{xy}(\tau, f_d) = \frac{1}{T} \sum_{r=0}^{N-1} \sum_{s=0}^{N-1} u_x(r)\, u_y^*(s) \times \exp(j2\pi f_d r T_c)\, \chi_{rect}[\tau + (r-s)T_c, f_d] \tag{12}$$

Utilizing the relation $q = r - s$ and collecting terms centered at the same shift $\tau = qT_c$, the double sum in (12) can be rewritten according to [13] as

$$\sum_{r=0}^{N-1} \sum_{s=0}^{N-1} = \sum_{q=0}^{N-1} \sum_{s=0}^{N-1-q} \Bigg|_{r=s+q} + \sum_{q=-(N-1)}^{-1} \sum_{r=0}^{N-1-|q|} \Bigg|_{s=r-q} \tag{13}$$

The cross-ambiguity function $\chi_{xy}(\tau, f_d)$ between the considered weighted pulse trains $U_x(t)$ and $U_y(t)$, respectively, where the elements $u_x(i)$ and $u_y(i)$ of the xth and yth Oppermann sequence $\mathbf{u}_x$ and $\mathbf{u}_y$ are used as weights, can then be written with (13) as a series of shifted ambiguity functions $\chi_{rect}(\tau, f_d)$ of the rectangular pulse as

$$\chi_{xy}(\tau, f_d) = \frac{1}{T} \sum_{q=0}^{N-1} \chi_{rect}(\tau + qT_c, f_d)\, \exp(j2\pi f_d q T_c)\, \mathcal{S}_1 + \frac{1}{T} \sum_{q=0}^{N-1} \chi_{rect}(\tau + qT_c, f_d)\, \mathcal{S}_2 \tag{14}$$

where the two sums $\mathcal{S}_1$ and $\mathcal{S}_2$, respectively, are defined as

$$\mathcal{S}_1 = \sum_{s=0}^{N-1-q} u_x(s+q) u_y^*(s) \exp(j2\pi f_d s T_c) \tag{15}$$

$$\mathcal{S}_2 = \sum_{r=0}^{N-1-|q|} u_x(r) u_y^*(r-q) \exp(j2\pi f_d r T_c) \tag{16}$$

Using the definition of the elements of Oppermann sequences in (7) and performing some elementary algebra, (15) and (16), respectively,

can be written as

$$\mathcal{S}_1 = \sum_{s=0}^{N-1-q} (-1)^{x(s+q+1)+y(s+1)} \times \exp\left\{j\frac{\pi}{N}\left[x^m(s+q+1) - y^m(s+1)\right]\right\} \times \exp\left\{j\frac{\pi}{N}\left[(s+q+1)^n - (s+1)^n\right]\right\} \times \exp(j2\pi f_d s T_c) \tag{17}$$

$$\mathcal{S}_2 = \sum_{s=0}^{N-1-|q|} (-1)^{x(r+1)+y(r-q+1)} \times \exp\left\{j\frac{\pi}{N}\left[x^m(r+1) - y^m(r-q+1)\right]\right\} \times \exp\left\{j\frac{\pi}{N}\left[(r+1)^n - (r-q+1)^n\right]\right\} \times \exp(j2\pi f_d r T_c) \tag{18}$$

Assuming that $T_w/T_c < 0.5$, then magnitudes of the series of ambiguity functions in (14) are non-overlapping. As such, the cross-ambiguity function between weighted pulse trains with Oppermann sequences is given by

$$|\chi_{xy}(\tau, f_d)| = \frac{1}{T}\sum_{q=0}^{N-1} |\chi_{rect}(\tau + qT_c, f_d)| \times \left| \sum_{s=0}^{N-1-q} (-1)^{x(s+q+1)+y(s+1)} \times \exp\left\{j\frac{\pi}{N}\left[x^m(s+q+1) - y^m(s+1)\right]\right\} \times \exp\left\{j\frac{\pi}{N}\left[(s+q+1)^n - (s+1)^n\right]\right\} \times \exp(j2\pi f_d s T_c)\right|$$

$$+ \frac{1}{T} \sum_{q=-(N-1)}^{-1} |\chi_{rect}(\tau + qT_c, f_d)|$$

$$\times \left| \sum_{r=0}^{N-1-|q|} (-1)^{x(r+1)+y(r-q+1)} \right.$$

$$\times \exp\left\{ j\frac{\pi}{N} \left[x^m(r+1) - y^m(r-q+1) \right] \right\}$$

$$\times \exp\left\{ j\frac{\pi}{N} \left[(r+1)^n - (r-q+1)^n \right] \right\}$$

$$\left. \times \exp(j2\pi f_d r T_c) \right| \tag{19}$$

Property 5. The cross-ambiguity function is anti-symmetric, i.e. $|\chi_{xy}(\tau, f_d)| = |\chi^*_{xy}(-\tau, -f_d)|$.

Property 6. The volume under the cross-ambiguity function is constant. For the case $p = 1$ and parameter n given, correlation peaks can be shifted in the delay-Doppler plane through parameter m (see example shown in Figs. 1(c)-(d)).

5 Auto-Ambiguity Function of Weighted Pulse Trains With Oppermann Sequences

In order to verify the analytical expression for the cross-ambiguity function $|\chi_{xy}(\tau, f_d)|$ given in (19), we examine whether it comprises the special case of an auto-ambiguity function $|\chi_x(\tau, f_d)|$ as reported in [10]. For this purpose, we re-write the cross-ambiguity function for weighted pulse trains $U_x(t)$ and $U_y(t) = U_x(t)$ as

$$|\chi_x(\tau, f_d)| = \frac{1}{T} \sum_{q=0}^{N-1} |\chi_{rect}(\tau + qT_c, f_d)|$$

$$\times \left| \sum_{s=0}^{N-1-q} (-1)^{x(s+q+1)+x(s+1)} \right.$$

$$\times \exp\left\{j\frac{\pi}{N}\left[x^m(s+q+1)-x^m(s+1)\right]\right\}$$
$$\times \exp\left\{j\frac{\pi}{N}\left[(s+q+1)^n-(s+1)^n\right]\right\}$$
$$\times \exp(j2\pi f_d s T_c)|$$
$$+\frac{1}{T}\sum_{q=-(N-1)}^{-1}|\chi_{rect}(\tau+qT_c,f_d)|$$
$$\times\left|\sum_{r=0}^{N-1-|q|}(-1)^{x(r+1)+x(r-q+1)}\right.$$
$$\times \exp\left\{j\frac{\pi}{N}\left[x^m(r+1)-x^m(r-q+1)\right]\right\}$$
$$\times \exp\left\{j\frac{\pi}{N}\left[(r+1)^n-(r-q+1)^n\right]\right\}$$
$$\times \exp(j2\pi f_d r T_c)| \tag{20}$$

The bipolar factor under the respective sums can be simplified by accumulating even powers as

$$(-1)^{x(s+q+1)+x(s+1)} = (-1)^{xq} \tag{21}$$
$$(-1)^{x(r+1)+x(r-q+1)} = (-1)^{-xq} \tag{22}$$

Furthermore, the arguments of the exponential functions containing the sequence number x can be simplified as

$$\exp\left\{j\frac{\pi}{N}[x^m(s+q+1)-x^m(s+1)]\right\}=\exp\left[j\frac{\pi}{N}(x^m q)\right] \tag{23}$$
$$\exp\left\{j\frac{\pi}{N}[x^m(r+1)-x^m(r-q+1)]\right\}=\exp\left[j\frac{\pi}{N}(x^m q)\right] \tag{24}$$

Substituting (21), (22), (23), and (24) into (20) and subsequently taking suitable magnitudes in the different terms, we obtain the auto-ambiguity function in agreement with [10] as

$$
\begin{aligned}
|\chi_x(\tau, f_d)| = \frac{1}{T} \sum_{q=0}^{N-1} & |\chi_{rect}(\tau + qT_c, f_d)| \\
& \times \left| \sum_{s=0}^{N-1-q} \exp\left\{ j \frac{\pi}{N} \left[(s+q+1)^n - (s+1)^n \right] \right\} \right. \\
& \left. \times \exp(j 2\pi f_d s T_c) \right| \\
& + \frac{1}{T} \sum_{q=-(N-1)}^{-1} |\chi_{rect}(\tau + qT_c, f_d)| \\
& \times \left| \sum_{r=0}^{N-1-|q|} \exp\left\{ j \frac{\pi}{N} \left[(r+1)^n - (r-q+1)^n \right] \right\} \right. \\
& \left. \times \exp(j 2\pi f_d r T_c) \right| \qquad (25)
\end{aligned}
$$

Property 7. All sequences have the same auto-ambiguity function for a fixed parameter set (m, n, p).

Property 8. The auto-ambiguity function of the examined type of weighted pulse trains with Oppermann sequences depends only on the parameter n for $p = 1$.

6 Numerical Examples

To illustrate the impact of sequence parameters on the performance of a design, consider Oppermann sequences of length $N = 31$ and $p = 1$. According to Property 1, the family size is $U = 30$. In view of Properties 3, 7, and 8, auto-correlation and auto-ambiguity function are the same for all sequences and depend only on parameter n.

Fig. 1(a) shows the mean squared aperiodic correlations MSAC and MSCC for a design aiming at optimal MSCC, which is obtained for parameters $m = 1$ and $n = 1$ as $R_{cc,opt} = 0.344$. Although R_{ac} does not depend on m, a large impact of m on R_{cc} can be observed.

Given $(m, n, p) = (1, 1, 1)$, a family of Oppermann sequences is defined. Pairs of sequences may be selected such that small cross-correlation values are produced. The minimum of the maximum cross-correlation value among all sequence pairs and possible shifts is obtained here for sequences $x = 1$ and $y = 2$. Fig. 1(b) shows the contour plots of the auto-ambiguity function, which holds for all sequences in the family, and the cross-ambiguity function for sequences $x = 1$ and $y = 2$. The ratios τ/T_c and $f_d T$ represent normalized delay and normalized Doppler, respectively, which are referred to in the sequel as delay and Doppler for brevity. Clearly, auto-ambiguity (solid) and cross-ambiguity (dashed) are well separated with respect to the zero-Delay cut and thus support discrimination of the desired sequence over the interfering sequence. Note that a design for optimal MSAC instead of optimal MSCC would produce a more distinct auto-correlation function at the expense of cross-correlation properties but this shall not be considered here due to space limitations.

To reveal the impact of m on the Doppler tolerance of the cross-ambiguity function (see also Property 6), Fig. 1(c) and (d), respectively, show the zero-Delay cut related to optimal MSCC with $m = 1$ and a non-optimal case with $m = 0.5$. Similar as parameter m controls the power spectrum density associated with each sequence and hence the cross-correlation properties of a design (Property 4), the optimal parameter $m = 1$ produces a favorable spacing of the characteristics in the zero-Delay cut for the different sequence pairs (Fig. 1(c)). Clearly, the pair $x = 1$ and $y = 2$ (dashed) incurs the smallest overlap with the desired sequence (solid). For the non-optimal case of $m = 0.5$, the curves for the different sequence pairs are more clustered (Fig. 1(d)), which may cause challenges in distinguishing different moving objects.

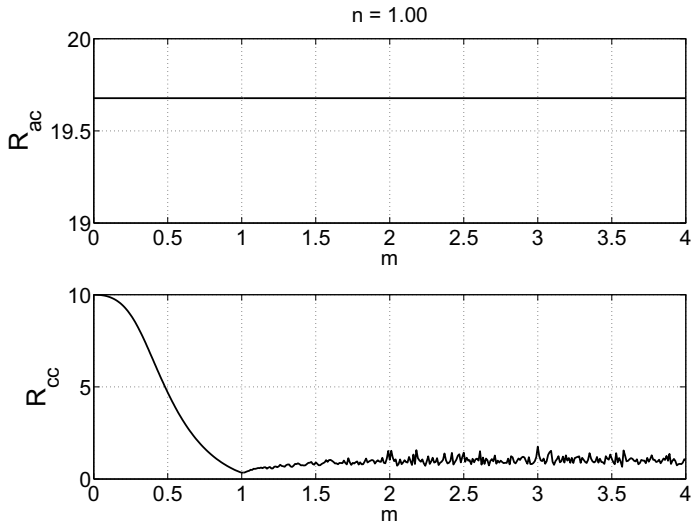
n = 1.00
20
19.5
19
R_{ac}
0
0.5
1
1.5
2
2.5
3
3.5
4
m
10
5
0
R_{cc}
0
0.5
1
1.5
2
2.5
3
3.5
4
m

(a)

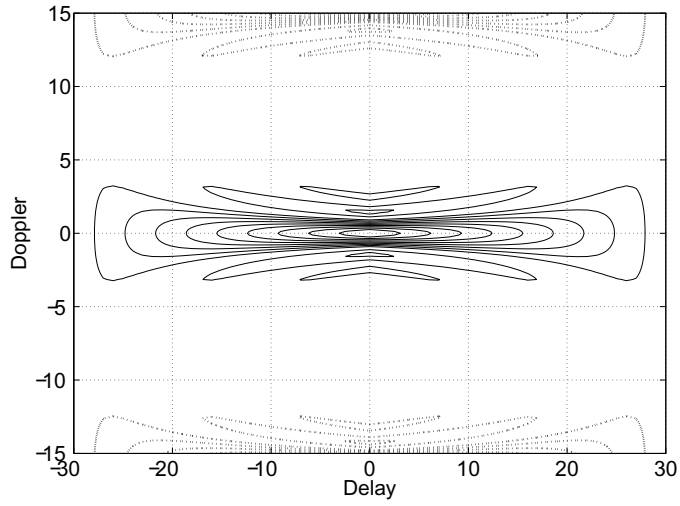
15
10
5
0
−5
−10
−15
Doppler
−30
−20
−10
0
10
20
30
Delay

(b)

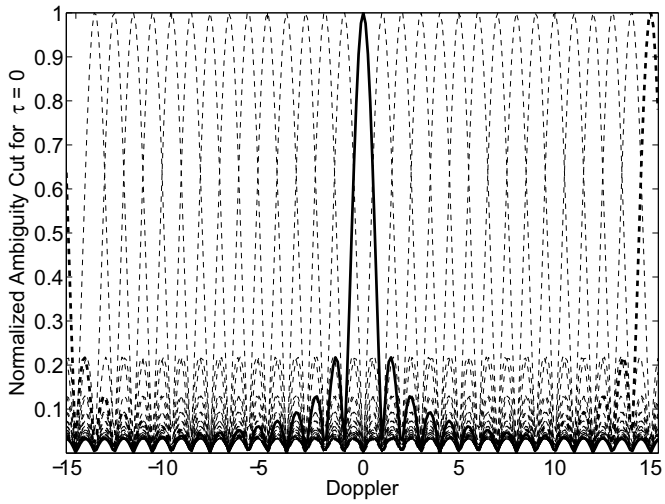

(c)

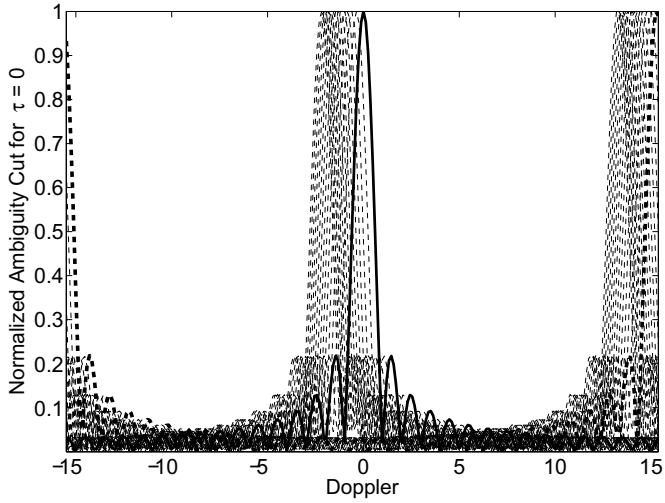

(d)

Figure 1: Performance for optimized $R_{cc,opt} = 0.344$ ($N = 31$, $n = 1$, $m = 1$): (a) R_{ac} and R_{cc} versus m; (b) Auto-ambiguity (solid) and cross-ambiguity (dashed, optimal sequence pair $x = 1, y = 2$); Normalized ambiguity cut for $\tau = 0$ and (c) $m = 1$, (d) $m = 0.5$.

7 Conclusions

In this paper, we have derived an analytical expression for the cross-ambiguity function of weighted pulse trains with Oppermann sequences comprising the auto-ambiguity function as a special case. In contrast to the auto-correlation and auto-ambiguity function of Oppermann sequences, which depend only on one sequence parameter and are the same for all sequences, the cross-ambiguity function depends on two parameters. This additional parameter can be used, e.g., to control the spacing of the correlation peaks between pairs of sequences at the zero-Delay cut of the cross-ambiguity function. The analytical expressions obtained and properties summarized may guide waveform designers to formulate a multi-objective performance optimization subject to given requirements of integrated radar and communication systems.

References

[1] M. Roberton and E. R. Brown, "Integrated Radar and Communications based on Chirped Spread-Spectrum Techniques," IEEE MTT-S Int. Microwave Symp., Philadelphia, U.S.A., pp. 611–614, June 2003.

[2] S. J. Xu, Y. Chen, and P. Zhang, "Integrated Radar and Communication based on DS-UWB," IEEE Ultrawideband and Ultrashort Impulse Signals, Sevastopol, Ukraine, pp. 142–144, Sept. 2006.

[3] S. J. Xu, B. Chen, and P. Zhang, "Radar-Communication Integration based on DSSS Techniques," IEEE Int. Conf. on Signal Processing, Beijing, China, pp. 16–20, Nov. 2006.

[4] H.-J. Zepernick and A. Finger, "Pseudo Random Signal Processing: Theory and Application," Chichester: Wiley, 2005.

[5] S. W. Golomb and G. Gong, "Signal Design for Good Correlation for Wireless Communication, Cryptography, and Radar," Cambridge: Cambridge University Press, 2005.

[6] N. Levanon and E. Mozeson, "Radar Signals," Chichester: Wiley, 2004.

[7] B. L. Lewis and F. F. Kretschmer, "A New Class of Polyphase Pulse Compression Codes and Techniques," *IEEE Trans. on Aerospace and Electronic Systems*, vol. 17, no. 3, pp. 364–372, May 1981.

[8] B. L. Lewis and F. F. Kretschmer, "Linear Frequency Modulation Derived Polyphase Pulse Compression Codes," *IEEE Trans. on Aerospace and Electronic Systems*, vol. 18, no. 5, pp. 637–641, Sept. 1982.

[9] P. B. Rapajic and R. A. Kennedy, "Merit Factor Based Comparison of New Polyphase Sequences," *IEEE Commun. Letters*, vol. 2, no. 10, pp. 269–270, Oct. 1998.

[10] M. Jamil, H.-J. Zepernick, and M. I. Pettersson, "Performance Assessment of Polyphase Pulse Compression Codes," IEEE Int. Symp. on Spread Spect. Techn. and Appl., Bologna, Italy, pp. 161–165, Aug. 2008.

[11] I. Oppermann and B. S. Vucetic, "Complex Spreading Sequences with a Wide Range of Correlation Properties," *IEEE Trans. on Commun.*, vol. 45, no. 3, pp. 365–375, Mar. 1997.

[12] M. Jamil, H.-J. Zepernick, and M. I. Pettersson, "On Integrated Radar and Communication Systems Using Oppermann Sequences," IEEE Military Communications Conference, San Diego, U.S.A., Nov. 2008.

[13] R. L. Mitchell and A. W. Rihaczek, "Clutter Suppression Properties of Weighted Pulse Trains," IEEE Trans. Aerospace and Electr. Systems, vol. AES-4, no. 6, pp. 822–828, Nov. 1968.

Part I-D

Part I-D

Properties of Ambiguity Functions for Weighted Pulse Trains with Oppermann Sequences

Part I-D is based on:

M. Jamil, H.-J. Zepernick, and M. I. Pettersson, "Properties of Ambiguity Functions for Weighted Pulse Trains with Oppermann Sequences," *Intl. Conf. on Signal Process. and Commun. Syst.*, Omaha, Nebraska, USA, Sept. 2009, pp. 1–8.

Properties of Ambiguity Functions for Weighted Pulse Trains with Oppermann Sequences

Momin Jamil, Hans-Jürgen Zepernick, and Mats I. Pettersson

Abstract

In this paper, we consider properties of the auto-ambiguity and cross-ambiguity functions of weighted pulse trains with Oppermann sequences. Several properties are examined and proved which in turn allows for reducing the design space for optimization of a particular design. The insights gained from these properties are consolidated in a formal framework leading to procedures that can be used for a more structured waveform design. Numerical examples are provided to illustrate the relationship between sequence parameters and performance characteristics.

1 Introduction

In recent years, there has been increased attention given to research towards receiver structures that support for the integration of radio communication functions with radar, positioning, and navigation applications. The benefits of exploring synergies of such combined receivers and systems include reduced costs, reduced multi-access interference (MAI), and tolerable co-site interference. Also, hybrid data fusion can increase coverage and accuracy. An important research area essential for the development of such integrated receivers and systems includes the design of sequence sets that can cope with the often stringent demands posed on delay resolution, Doppler tolerance, and required MAI suppression.

In view of the above context, we have compared the performance of different classes of polyphase pulse compression sequences in [1], namely P1, P2, P3, P4, Px, FZC, and Oppermann sequences [2–6]. This work revealed that Oppermann sequences potentially better support the considered integration as this class allows for the design of families that offer a wide range of correlations as well as a variety of characteristics with respect to the ambiguity functions, i.e. delay-Doppler tolerance. Given the qualitative classification of polyphase pulse compression sequences, the work in [7, 8], respectively, advances to a quantitative examination of Oppermann sequences including the derivation of the related auto-ambiguity and cross-ambiguity function.

In this paper, we consider the properties of the auto-ambiguity and cross-ambiguity function of weighted pulse trains with Oppermann sequences. Several properties are examined and proved such as the evolved symmetry property, which in turn allows for reducing the design space for optimization of a particular design. The insights gained from these properties are consolidated in a formal framework leading to procedures that can be used for a more structured waveform design with respect to cost functions and system constraints.

The rest of the paper is organized as follows. Section 2 describes measures used for the performance assessment of the considered weighted pulse trains. Section 3 contains the definition of Oppermann sequences. The analytical expression for the related cross-ambiguity and auto-ambiguity functions are given in Section 4 along with their properties and selected proofs. In Section 5, two design procedures are outlined and examples are given to illustrate the application of selected properties. The examples also provide insights into the relationship between sequence parameters and performance characteristics.

2 Performance Measures

Let N denote the length of each sequence $\mathbf{u}_x = [u_x(0), u_x(1), \ldots, u_x(N-1)]$ of a given set $\mathcal{U}$ of size U, where $1 \leq x \leq U$.

2.1 Aperiodic Cross-Correlation

The aperiodic cross-correlation $C_{xy}(l)$ at discrete shift l between the xth complex-valued sequence $\mathbf{u}_x \in \mathcal{U}$ and the yth complex-valued sequence $\mathbf{u}_y \in \mathcal{U}$ is defined as

$$C_{xy}(l) = \begin{cases} \frac{1}{N} \sum_{i=0}^{N-1-l} u_x(i) u_y^*(i+l), & 0 \le l \le N-1 \\ \frac{1}{N} \sum_{i=0}^{N-1+l} u_x(i-l) u_y^*(i), & 1-N \le l < 0 \\ 0, & |l| \ge N \end{cases} \tag{1}$$

where $(\cdot)^*$ denotes the complex conjugate of the argument $(\cdot)$. The aperiodic auto-correlation $C_x(l)$ of $\mathbf{u}_x$ at shift l is the aperiodic cross-correlation of $\mathbf{u}_x$ with itself, $C_{xx}(l)$.

2.2 Mean Squared Aperiodic Correlations

For a given set $\mathcal{U}$ of size U, the mean squared aperiodic cross-correlation (MSCC) and out-of-phase mean squared aperiodic auto-correlation (MSAC), respectively, are defined as

$$R_{cc} = \frac{1}{U(U-1)} \sum_{\substack{x,y \in \mathcal{U} \\ x \ne y}} \sum_{l=1-N}^{N-1} |C_{xy}(l)|^2 \tag{2}$$

$$R_{ac} = \frac{1}{U} \sum_{x \in \mathcal{U}} \sum_{\substack{l=1-N \\ l \ne 0}}^{N-1} |C_x(l)|^2 \tag{3}$$

2.3 Cross-Ambiguity Function

In the sequel, we consider weighted pulse trains that can be described by a complex envelope as

$$U_x(t) = \frac{1}{\sqrt{T}} \sum_{i=0}^{N-1} u_x(i) \operatorname{rect}\left(\frac{t - iT_c}{T_w}\right) \tag{4}$$

where $T = N\,T_c$ is the duration of the xth pulse train while T_c and $T_w \leq T_c$, respectively, denote the repetition period and the width of each rectangular pulse

$$\text{rect}\left(\frac{t}{T_w}\right) = \begin{cases} 1 & \text{for} \quad -\frac{T_w}{2} \leq t \leq \frac{T_w}{2} \\ 0 & \text{otherwise} \end{cases} \tag{5}$$

The elements $u_x(i) \in \mathbb{C}$, $i = 0, 1, \ldots, N-1$, of the xth sequence $\mathbf{u}_x$ are the weights of the pulse train in (4).

In this paper, the following definition of the cross-ambiguity function between two signals $U_x(t)$ and $U_y(t)$ is used:

$$|\chi_{xy}(\tau, f_d)| = \left| \int_{-\infty}^{\infty} U_x(t) U_y^*(t+\tau) \exp(j2\pi f_d t) dt \right| \tag{6}$$

where τ and f_d denote delay and Doppler shift, respectively. The auto-ambiguity function $|\chi_x(\tau, f_d)|$ of $U_x(t)$ is the cross-ambiguity function of $U_x(t)$ with itself, $|\chi_{xx}(\tau, f_d)|$.

3 Oppermann Sequences

The ith element $u_x(i)$ of the xth Oppermann sequence $\mathbf{u}_x = [u_x(0), u_x(1), \ldots, u_x(N-1)]$ of length N is defined as [6]

$$u_x(i) = (-1)^{x(i+1)} \exp\left\{ \frac{j\pi[x^m(i+1)^p + (i+1)^n]}{N} \right\} \tag{7}$$

where $1 \leq x \leq N-1$, $0 \leq i \leq N-1$ and integer x is relatively prime to the length N. The parameters m, n, and p in (7) take on real values and define a family of Oppermann sequences. Some known properties are as follows [6]:

Property 1. The size of a set of Oppermann sequences is maximal if the length N is a prime and is then given as $N-1$.

Property 2. For a fixed combination of m, n, and $p = 1$, all the sequences have the same auto-correlation magnitude.

Property 3. The auto-correlation magnitude depends only on n if parameter $p = 1$ and is given as [6]

$$|C_x(l)| = \left| \frac{1}{N} \sum_{i=0}^{N-1-l} \exp\left\{ \frac{j\pi}{N} \left[(i+1)^n - (i+l+1)^n \right] \right\} \right| \tag{8}$$

Property 4. The parameter m controls the location of the power spectra associated with each sequence and hence controls the cross-correlation properties.

4 Ambiguity Functions and Their Properties

4.1 Cross-Ambiguity Function

In view of Property 3, we focus on the case of $p = 1$. On this basis, we consider two weighted pulse trains $U_x(t)$ and $U_y(t)$ as defined in (4), where the pulse weights $u_x(i)$ and $u_y(i)$, $i = 0, 1, \ldots, N-1$, respectively, are the ith elements of the xth and yth Oppermann sequence as given in (7).

Property 5. Given $T_w/T_c < 0.5$, the cross-ambiguity function of a pair of weighted pulse trains $U_x(t)$ and $U_y(t)$ with Oppermann sequences is given by [8]

$$\begin{aligned} |\chi_{xy}(\tau, f_d)| = \frac{1}{T} \sum_{q=0}^{N-1} & |\chi_{rect}(\tau + qT_c, f_d)| \\ & \times \left| \sum_{s=0}^{N-1-q} (-1)^{x(s+q+1)+y(s+1)} \right. \\ & \times \exp\left\{ \frac{j\pi}{N} \left[x^m(s+q+1) - y^m(s+1) \right] \right\} \\ & \left. \times \exp\left\{ \frac{j\pi}{N} \left[(s+q+1)^n - (s+1)^n \right] \right\} \right| \end{aligned}$$

$$
\begin{aligned}
&\times \exp(j2\pi f_d s T_c)| \\
&+ \frac{1}{T} \sum_{q=-(N-1)}^{-1} |\chi_{rect}(\tau + qT_c, f_d)| \\
&\times \left| \sum_{r=0}^{N-1-|q|} (-1)^{x(r+1)+y(r-q+1)} \right. \\
&\times \exp\left\{ \frac{j\pi}{N} \left[x^m (r+1) - y^m (r-q+1) \right] \right\} \\
&\times \exp\left\{ \frac{j\pi}{N} \left[(r+1)^n - (r-q+1)^n \right] \right\} \\
&\times \exp(j2\pi f_d r T_c)| \qquad (9)
\end{aligned}
$$

where $\chi_{rect}(\tau, f_d)$ denotes the triangular ambiguity function of a rectangular pulse rect$(\cdot)$.

Property 6. The cross-ambiguity function is anti-symmetric w.r.t. the origin, i.e. $|\chi_{xy}(\tau, f_d)| = |\chi^*_{yx}(-\tau, -f_d)|$.

Proof: Let us commence with the definition of the cross-ambiguity function given in (6) in modified form using negative arguments, reversed order of sequences, i.e., yx instead of xy and without operator $|\cdot|$ as

$$
\chi_{yx}(-\tau, -f_d) = \int_{-\infty}^{\infty} U_y(t) U_x^*(t-\tau) \exp(-j2\pi f_d t) dt \qquad (10)
$$

where the weighted pulse trains are given by

$$
U_x(t) = \frac{1}{\sqrt{T}} \sum_{r=0}^{N-1} u_x(r) \operatorname{rect}\left(\frac{t - rT_c}{T_w} \right) \qquad (11)
$$

$$
U_y(t) = \frac{1}{\sqrt{T}} \sum_{s=0}^{N-1} u_y(s) \operatorname{rect}\left(\frac{t - sT_c}{T_w} \right) \qquad (12)
$$

Further, let us first proof the property for general weighted pulse trains and subsequently narrow the result to the considered scenario of

using Oppermann sequences. For this purpose, we make a change of variable in (10) as $t_1 = t - \tau$ and obtain

$$\begin{aligned}\chi_{yx}(-\tau, -f_d) &= \exp(-j2\pi f_d \tau) \\ &\quad \times \int_{-\infty}^{\infty} U_y(t+\tau) U_x^*(t) \exp(-j2\pi f_d t) dt \end{aligned} \tag{13}$$

Noting that integration is a linear operation, we can exploit the fact that an integral of a conjugate is equivalent to the conjugate of the integral. Thus, we may write

$$\begin{aligned}\chi_{yx}(-\tau, -f_d) &= \exp(-j2\pi f_d \tau) \\ &\quad \times \left[\int_{-\infty}^{\infty} U_x(t) U_y^*(t+\tau) \exp(j2\pi f_d t) \right]^* dt \\ &= \exp(-j2\pi f_d \tau) \times \chi_{xy}^*(\tau, f_d) \end{aligned} \tag{14}$$

Taking the conjugate of both sides in (14) and calculating the magnitude completes the general proof of Property 6 as

$$|\chi_{yx}^*(-\tau, -f_d)| = |\chi_{xy}(\tau, f_d)| \tag{15}$$

Rephrasing the proof with respect to the specific type of weighted pulse trains with Oppermann sequences, we substitute (11) and (12) in (10) giving

$$\chi_{yx}(-\tau, -f_d) = \frac{1}{T} \sum_{s=0}^{N-1} \sum_{r=0}^{N-1} u_y(s) u_x^*(r) \times \mathcal{I}_1 \tag{16}$$

where the following notation has been used for brevity

$$\mathcal{I}_1 = \int_{-\infty}^{\infty} \text{rect}\left[\frac{t - sT_c}{T_w}\right] \text{rect}\left[\frac{t - \tau - rT_c}{T_w}\right] \exp(-j2\pi f_d t) dt \tag{17}$$

Similar as in the derivation of the auto-ambiguity function and the cross-ambiguity function in [7] and [8], respectively, we make the change of variable in (17) as $t_1 = t - sT_c$ and then obtain after some elementary derivations the expression

$$\mathcal{I}_1 = \chi_{rect}\left[-\tau - (s-r)T_c, -f_d\right] \times \exp(-j2\pi f_d s T_c) \tag{18}$$

where $\chi_{rect}(\cdot,\cdot)$ denotes the auto-ambiguity function of a rectangular pulse and is defined as

$$\chi_{rect}(\tau, f_d) = \int_{-\infty}^{\infty} \text{rect}\left[\frac{t}{T_w}\right] \text{rect}\left[\frac{t+\tau}{T_w}\right] \exp(j2\pi f_d t) dt \tag{19}$$

By substituting (17) in (16) and changing the order of the sums over r and s, we obtain

$$\begin{aligned} \chi_{yx}(-\tau, -f_d) \; = \; & \frac{1}{T} \sum_{r=0}^{N-1} \sum_{s=0}^{N-1} u_x^*(r) u_y(s) \\ & \times \exp(-j2\pi f_d s T_c) \\ & \times \chi_{rect}\left[-\tau - (r-s)T_c, -f_d\right] \end{aligned} \tag{20}$$

According to [9] and utilizing a change of variable in the form of $q = r - s$, the double sum in (20) can be rewritten as

$$\sum_{r=0}^{N-1} \sum_{s=0}^{N-1} = \sum_{q=0}^{N-1} \sum_{s=0}^{N-1-q} \Bigg|_{r=s+q} + \sum_{q=-(N-1)}^{-1} \sum_{r=0}^{N-1-|q|} \Bigg|_{s=r-q} \tag{21}$$

and (20) may hence be expressed as

$$\begin{aligned} \chi_{yx}(-\tau, -f_d) = & \frac{1}{T} \sum_{q=0}^{N-1} \chi_{rect}(-\tau - qT_c, -f_d) \\ & \times \sum_{s=0}^{N-1-q} u_x^*(s+q) u_y(s) \exp(-j2\pi f_d s T_c) \\ & + \\ & \frac{1}{T} \sum_{q=-(N-1)}^{-1} \chi_{rect}\left[-\tau - qT_c, -f_d\right] \\ & \times \exp(-j2\pi f_d q T_c) \end{aligned} \tag{22}$$

$$\times \sum_{r=0}^{N-1-|q|} u_x^*(r)u_y(r-q)\exp(-j2\pi f_d r T_c)$$

In order to specialize (22) for Oppermann sequences, let us consider the sums over s and r, respectively, as follows:

$$\mathcal{S}_1 = \sum_{s=0}^{N-1-q} u_x^*(s+q)u_y(s)\exp(-j2\pi f_d s T_c) \tag{23}$$

$$\mathcal{S}_2 = \sum_{r=0}^{N-1-|q|} u_x^*(r)u_y(r-q)\exp(-j2\pi f_d r T_c) \tag{24}$$

Using the definition of Oppermann sequences given in (7) for the considered case of $p = 1$, we have

$$u_x(i) = (-1)^{x(i+1)}\exp\left\{\frac{j\pi}{N}[x^m(i+1)+(i+1)^n]\right\} \tag{25}$$

$$u_y(i) = (-1)^{y(i+1)}\exp\left\{\frac{j\pi}{N}[y^m(i+1)+(i+1)^n]\right\} \tag{26}$$

Let us focus on (23) by solving the respective product obtained from multiplying (25) with the complex conjugate of (26) as

$$\begin{aligned} u_x^*(s+q)u_y(s) = {} & (-1)^{x(s+q+1)}(-1)^{y(s+1)} \\ & \times \exp\left\{\frac{-j\pi}{N}[x^m(s+q+1)+(s+q+1)^n]\right\} \\ & \times \exp\left\{\frac{j\pi}{N}[y^m(s+1)+(s+1)^n]\right\} \end{aligned} \tag{27}$$

which results after some rearrangement of terms in

$$\begin{aligned} u_x^*(s+q)u_y(s) = {} & (-1)^{x(s+q+1)+y(s+1)} \\ & \times \exp\left\{\frac{-j\pi}{N}[x^m(s+q+1)-y^m(s+1)]\right\} \\ & \times \exp\left\{\frac{-j\pi}{N}[(s+q+1)^n-(s+1)^n]\right\} \end{aligned} \tag{28}$$

By substituting (28) in (23), we obtain

$$\begin{aligned}\mathcal{S}_1 = \sum_{s=0}^{N-1-q} & (-1)^{x(s+q+1)+y(s+1)} \\ & \times \exp\left\{\frac{-j\pi}{N}\left[x^m(s+q+1) - y^m(s+1)\right]\right\} \\ & \times \exp\left\{\frac{-j\pi}{N}\left[(s+q+1)^n - (s+1)^n\right]\right\} \\ & \times \exp(-j2\pi f_d s T_c) \end{aligned} \tag{29}$$

The similar derivation can be performed for (24), which eventually leads to the expression

$$\begin{aligned}\mathcal{S}_2 = \sum_{r=0}^{N-1-|q|} & (-1)^{x(r+1)+y(r-q+1)} \\ & \times \exp\left\{\frac{-j\pi}{N}\left[x^m(r+1) - y^m(r-q+1)\right]\right\} \\ & \times \exp\left\{\frac{-j\pi}{N}\left[(r+1)^n - (r-q+1)^n\right]\right\} \\ & \times \exp(-j2\pi f_d r T_c) \end{aligned} \tag{30}$$

At this point, we return to the calculation of the cross-ambiguity function $\chi_{yx}(-\tau, -f_d)$ and substitute for $\mathcal{S}_1$ and $\mathcal{S}_2$ the expressions given in (29) and (30), respectively, in (22):

$$\begin{aligned}\chi_{yx}(-\tau, -f_d) = \frac{1}{T} \sum_{q=0}^{N-1} & \chi_{rect}(-\tau - qT_c, -f_d) \\ & \times \sum_{s=0}^{N-1-q} (-1)^{x(s+q+1)+y(s+1)} \\ & \times \exp\left\{\frac{-j\pi}{N}\left[x^m(s+q+1) - y^m(s+1)\right]\right\} \\ & \times \exp\left\{\frac{-j\pi}{N}\left[(s+q+1)^n - (s+1)^n\right]\right\} \\ & \times \exp(-j2\pi f_d s T_c) \\ & + \frac{1}{T} \sum_{q=-(N-1)}^{-1} \chi_{rect}(-\tau - qT_c, -f_d) \end{aligned}$$

$$\times \exp(-j2\pi f_d q T_c)$$
$$\times \sum_{r=0}^{N-1-|q|} (-1)^{x(r+1)+y(r-q+1)}$$
$$\times \exp\left\{\frac{-j\pi}{N}\left[x^m(r+1)-y^m(r-q+1)\right]\right\}$$
$$\times \exp\left\{\frac{-j\pi}{N}\left[(r+1)^n-(r-q+1)^n\right]\right\}$$
$$\times \exp(-j2\pi f_d r T_c) \tag{31}$$

In order to perform the complex conjugate of the cross-ambiguity function shown in (31), we take advantage of the fact that complex numbers form a field and the related identities for sum and product, respectively, of $(a+b)^* = a^* + b^*$ and $(a \cdot b)^* = a^* \cdot b^*$. Then, we have

$$\chi^*_{yx}(-\tau, -f_d) = \frac{1}{T}\sum_{q=0}^{N-1} \chi^*_{rect}(-\tau - qT_c, -f_d)$$
$$\times \sum_{s=0}^{N-1-q} (-1)^{x(s+q+1)+y(s+1)}$$
$$\times \exp\left\{\frac{j\pi}{N}\left[x^m(s+q+1)-y^m(s+1)\right]\right\}$$
$$\times \exp\left\{\frac{j\pi}{N}\left[(s+q+1)^n-(s+1)^n\right]\right\}$$
$$\times \exp(j2\pi f_d s T_c)$$
$$+ \frac{1}{T}\sum_{q=-(N-1)}^{-1} \chi^*_{rect}(-\tau - qT_c, -f_d)$$
$$\times \exp(j2\pi f_d q T_c)$$
$$\times \sum_{r=0}^{N-1-|q|} (-1)^{x(r+1)+y(r-q+1)}$$
$$\times \exp\left\{\frac{j\pi}{N}\left[x^m(r+1)-y^m(r-q+1)\right]\right\}$$
$$\times \exp\left\{\frac{j\pi}{N}\left[(r+1)^n-(r-q+1)^n\right]\right\}$$

$$\times \exp(j2\pi f_d r T_c) \tag{32}$$

Given $T_w/T_c < 0.5$, the magnitude of (32) is given by

$$\begin{aligned}
|\chi^*_{yx}(-\tau,-f_d)| = \frac{1}{T}\sum_{q=0}^{N-1} |\chi^*_{rect}(-\tau - qT_c,-f_d)| \\
\times \Bigg| \sum_{s=0}^{N-1-q} (-1)^{x(s+q+1)+y(s+1)} \\
\times \exp\left\{\frac{j\pi}{N}\left[x^m(s+q+1) - y^m(s+1)\right]\right\} \\
\times \exp\left\{\frac{j\pi}{N}\left[(s+q+1)^n - (s+1)^n\right]\right\} \\
\times \exp(j2\pi f_d s T_c)| \\
+ \frac{1}{T}\sum_{q=-(N-1)}^{-1} |\chi^*_{rect}(-\tau - qT_c,-f_d)| \\
\times \Bigg| \sum_{r=0}^{N-1-|q|} (-1)^{x(r+1)+y(r-q+1)} \\
\times \exp\left\{\frac{j\pi}{N}\left[x^m(r+1) - y^m(r-q+1)\right]\right\} \\
\times \exp\left\{\frac{j\pi}{N}\left[(r+1)^n - (r-q+1)^n\right]\right\} \\
\times \exp(j2\pi f_d r T_c)|
\end{aligned} \tag{33}$$

Comparing (33) with (9) reveals that the following has to be shown in order to complete the proof for the special case of Oppermann sequences:

$$|\chi_{rect}(\tau + qT_c, f_d)| \quad = \quad |\chi^*_{rect}(-\tau - qT_c, -f_d)| \tag{34}$$

For this purpose, let us recall that

$$\begin{aligned}
\chi_{rect}(-\tau - qT_c, -f_d) \quad = \quad & \int_{-\infty}^{\infty} \mathrm{rect}\left[\frac{t}{T_w}\right] \mathrm{rect}\left[\frac{t-\tau-qT_c}{T_w}\right] \\
& \times \exp(-j2\pi f_d t)dt
\end{aligned} \tag{35}$$

Applying a change of variable as $t_2 = t - \tau - qT_c$ gives

$$\begin{aligned}\chi_{rect}(-\tau - qT_c, -f_d) &= \exp[-j2\pi f_d(\tau + qT_c)] \\ &\quad \times \int_{-\infty}^{\infty} \text{rect}\left[\frac{t+\tau+qT_c}{T_w}\right] \text{rect}\left[\frac{t}{T_w}\right] \\ &\quad \times \exp(-j2\pi f_d t)dt \end{aligned} \tag{36}$$

with the conjugate being

$$\begin{aligned}\chi^*_{rect}(-\tau - qT_c, -f_d) &= \exp[j2\pi f_d(\tau + qT_c)] \\ &\quad \times \int_{-\infty}^{\infty} \text{rect}\left[\frac{t}{T_w}\right] \text{rect}\left[\frac{t+\tau+qT_c}{T_w}\right] \\ &\quad \times \exp(j2\pi f_d t)dt \end{aligned} \tag{37}$$

Taking the magnitude of (37) completes the proof. □

4.2 Auto-Ambiguity Function

Property 7. The auto-ambiguity function $|\chi_x(\tau, f_d)|$ of weighted pulse train $U_x(t)$ is given by [7]

$$\begin{aligned}|\chi_x(\tau, f_d)| = \frac{1}{T} &\sum_{q=0}^{N-1} |\chi_{rect}(\tau + qT_c, f_d)| \\ &\times \left| \sum_{s=0}^{N-1-q} \exp\left\{ j\frac{\pi}{N}\left[(s+q+1)^n - (s+1)^n\right]\right\} \right. \\ &\left. \times \exp(j2\pi f_d s T_c) \right| \\ + \quad \frac{1}{T} &\sum_{q=-(N-1)}^{-1} |\chi_{rect}(\tau + qT_c, f_d)| \\ &\times \left| \sum_{r=0}^{N-1-|q|} \exp\left\{ j\frac{\pi}{N}\left[(r+1)^n - (r-q+1)^n\right]\right\} \right. \\ &\left. \times \exp(j2\pi f_d r T_c) \right| \end{aligned} \tag{38}$$

Property 8. All sequences have the same auto-ambiguity function $|\chi_x(\tau, f_d)|$ for a fixed parameter set m, n, and $p = 1$.

Proof: It can be seen from inspection of (38) that the auto-ambiguity function $|\chi_x(\tau, f_d)|$ does not depend on x and hence is independent of the sequence for fixed $(m, n, 1)$. □

Property 9. The auto-ambiguity function $|\chi_x(\tau, f_d)|$ of the examined type of weighted pulse trains with Oppermann sequences depends only on the parameter n for $p = 1$.

Proof: It can be seen from simple inspection of (38) that the auto-ambiguity function $|\chi_x(\tau, f_d)|$ does not depend on m for $p = 1$ but only on the parameter n. □

Property 10. The auto-ambiguity function is symmetric w.r.t. the origin, i.e. $|\chi_x(\tau, f_d)| = |\chi_x^*(-\tau, -f_d)|$.

Proof: Given $T_w/T_c < 0.5$, this property can be proved by setting $y = x$ in (33) and proceeding as follows:

$$
\begin{aligned}
|\chi_x^*(-\tau, -f_d)| = \frac{1}{T} \sum_{q=0}^{N-1} & |\chi_{rect}^*(-\tau - qT_c, -f_d)| \\
& \times \left| \sum_{s=0}^{N-1-q} (-1)^{x(s+q+1)+x(s+1)} \right. \\
& \times \exp\left\{ \frac{j\pi}{N} \left[x^m(s+q+1) - x^m(s+1) \right] \right\} \\
& \times \exp\left\{ \frac{j\pi}{N} \left[(s+q+1)^n - (s+1)^n \right] \right\} \\
& \left. \times \exp(j2\pi f_d s T_c) \right| \\
+ \quad \frac{1}{T} \sum_{q=-(N-1)}^{-1} & |\chi_{rect}^*(-\tau - qT_c, -f_d)| \\
& \times \left| \sum_{r=0}^{N-1-|q|} (-1)^{x(r+1)+x(r-q+1)} \right.
\end{aligned}
$$

$$\times \exp\left\{\frac{j\pi}{N}\left[x^m(r+1)-x^m(r-q+1)\right]\right\}$$
$$\times \exp\left\{\frac{j\pi}{N}\left[(r+1)^n-(r-q+1)^n\right]\right\}$$
$$\times \exp(j2\pi f_d r T_c)| \tag{39}$$

Then, rearranging and summing common terms gives

$$|\chi_x^*(-\tau,-f_d)| = \frac{1}{T}\sum_{q=0}^{N-1}|\chi_{rect}^*(-\tau-qT_c,-f_d)|$$
$$\times|(-1)^{xq}|\left|\exp\left\{\frac{j\pi}{N}x^m q\right\}\right|$$
$$\times\left|\sum_{s=0}^{N-1-q}\exp\left\{\frac{j\pi}{N}\left[(s+q+1)^n-(s+1)^n\right]\right\}\right.$$
$$\times \exp(j2\pi f_d s T_c)|+$$
$$\frac{1}{T}\sum_{q=-(N-1)}^{-1}|\chi_{rect}^*(-\tau-qT_c,-f_d)|$$
$$\times|(-1)^{-xq}|\left|\exp\left\{\frac{j\pi}{N}x^m q\right\}\right|$$
$$\times\left|\sum_{r=0}^{N-1-|q|}\exp\left\{\frac{j\pi}{N}\left[(r+1)^n-(r-q+1)^n\right]\right\}\right.$$
$$\times \exp(j2\pi f_d r T_c)| \tag{40}$$

which simplifies by taking the respective magnitudes under the summation over variable q as

$$|\chi_x^*(-\tau,-f_d)| = \frac{1}{T}\sum_{q=0}^{N-1}|\chi_{rect}^*(-\tau-qT_c,-f_d)|$$
$$\times\left|\sum_{s=0}^{N-1-q}\exp\left\{\frac{j\pi}{N}\left[(s+q+1)^n-(s+1)^n\right]\right\}\right.$$

$$
\begin{aligned}
& \times \exp(j2\pi f_d s T_c)| \\
+ \quad & \frac{1}{T} \sum_{q=-(N-1)}^{-1} |\chi^*_{rect}(-\tau - qT_c, -f_d)| \\
& \times \left| \sum_{r=0}^{N-1-|q|} \exp\left\{ \frac{j\pi}{N} \left[(r+1)^n - (r-q+1)^n \right] \right\} \right. \\
& \left. \times \exp(j2\pi f_d r T_c) \right| \qquad (41)
\end{aligned}
$$

As $|\chi_{rect}(\tau + qT_c, f_d)| = |\chi^*_{rect}(-\tau - qT_c, -f_d)|$ has been proved in the context of Property 6, the proof is complete. □

5 Design Procedure and Numerical Examples

In this section, we provide procedures that may be deployed for the design of sequence sets with particular auto-ambiguity and cross-ambiguity properties depending on the specific scenario under study. The numerical examples are thought to provide additional insights on how the sequence parameters relate to different performance characteristics.

5.1 Design procedure with focus on auto-ambiguity

A hierarchically structured framework for systematically designing weighted pulse trains with Oppermann sequences and focus on auto-ambiguity characteristics may take advantage of Properties 1–3 and 7–10. In this case, a formal procedure may be suggested as follows.

Clearly, Procedure 1 is based on the zero-Delay cut of the auto-ambiguity function. Accordingly, optimization of performance metrics other than the MSAC may be utilized in Step 2 such as the figure of merit or maximum out-of-phase autocorrelation value [10]. In all these cases, the designed weighted pulse trains will have the same auto-ambiguity function for all sequences in the set (see Properties 2 and 8). However, cross-correlation among pairs of sequence may be large as this type of characteristic is not taken into account by Procedure 1.

Procedure 1. *Auto-ambiguity based on MSAC*

Step 1: *Choose the sequence length N as a prime number in order to obtained the largest set size of $N-1$ (see Property 1).*

Step 2: *Minimize R_{ac}, for example, by varying parameter n using a sufficiently small increment.*

Step 3: *Calculate the auto-ambiguity function $|\chi_x(\tau, f_d)|$, e.g., for normalized delay τ/T_c being in the interval $[-(N-1), (N-1)]$ and for normalized Doppler f_dT being in the interval $[0, C]$, where C denotes a constant (see Property 10).*

Step 4: *End of procedure.*

5.2 Design procedure with focus on cross-ambiguity

Similar as with the auto-ambiguity, a design procedure for weighted pulse trains with Oppermann sequences and focus on cross-ambiguity characteristics may take advantage of Properties 4 and 5–6. In this case, a formal procedure may be suggested as follows.

Apparently, Procedure 2 is based on the zero-Delay cut of the auto-ambiguity and cross-ambiguity functions. Similar optimization problems as those possed in Step 2 of Procedure 2 may be formulated for metrics pairs other than MSAC and MSCC such as maximum out-of-phase autocorrelation value and maximum crosscorrelation value. The actual optimization may be performed, for example, by using the global optimization method proposed in [11].

Alternatively, optimization may be performed in a more brute force manner similar as outlined in Step 2 of Procedure 1 for the auto-ambiguity function. For example, the bound value α of the MSAC may be searched for by varying parameter n using a sufficiently small increment. Subsequently, given the value of parameter n, the minimum of the MSCC may be obtained by varying parameter m also using a sufficiently small increment.

Procedure 2. *Cross-ambiguity based on MSCC*

Step 1: *Choose the sequence length N as a prime number in order to obtained the largest set size of $N-1$ (see Property 1).*

Step 2: *Minimize R_{cc} for a given bound α on R_{ac}, that is*

$$\begin{cases} \min_{m,n} R_{cc} \\ \textit{subject to } R_{ac} \leq \alpha \end{cases}$$

or, alternatively, minimize R_{ac} for a given bound β on R_{cc}, that is

$$\begin{cases} \min_{m,n} R_{ac} \\ \textit{subject to } R_{cc} \leq \beta \end{cases}$$

Step 3: *Calculate the cross-ambiguity function $|\chi_{xy}(\tau, f_d)|$ for a desired pair x and y of sequence, e.g., for normalized delay τ/T_c being in the interval $[-(N-1), (N-1)]$ and for normalized Doppler $f_d T$ being in the interval $[0, C]$, where C denotes a constant (see Property 6).*

Step 4: *End of procedure.*

5.3 Design examples

To illustrate the application of selected ambiguity function properties in the waveform design process, let us consider Oppermann sequences of length $N = 31$ and $p = 1$. According to Property 1, the family is of maximum size offering $U = 30$ distinct sequences. In view of Properties 2, 3, 9, and 10, auto-correlation and auto-ambiguity function are the same for all sequences and depend only on parameter n.

Let us further consider an optimized design using Procedure 2 with respect to minimum MSAC, which is obtained as $R_{ac,opt} = 0.1107$ for $n = 2.0072$. While $R_{ac,opt}$ does not depend on m, the MSCC, R_{cc}, can be kept small for $m \geq 0.92$ and assumes the minimum of $R_{cc} = 0.9984$ for $m = 2.92$. As mentioned above, optimization may be performed either by using the method described in [11] or the brute force approach by varying n in small increments to minimize R_{ac} and then varying m in small increments to minimize R_{cc}.

Fig. 1a shows the contour plot of the auto-ambiguity function for this design, which holds for all sequences in the family (see Properties 9 and 10). As can be seen from the plot and in view of Property 10, it is sufficient to consider two quadrants in an optimization while the shape of the ambiguity function for the remaining quadrants can be obtained from the symmetry property. It is noted that the ratios τ/T_c and f_dT represent normalized delay and normalized Doppler, respectively, which are referred to as delay and Doppler for brevity.

Fig. 1b depicts the zero-Delay cut related to optimal MSAC and reveals insights into the Doppler tolerance of an integrated receiver design. As can be seen from the plot, the optimal parameter $m = 2.92$ produces a favorable spacing of the characteristics in the zero-Delay cut for the different sequence pairs. In particular, sequences pairs may be selected such that different moving objects can be easily distinguished.

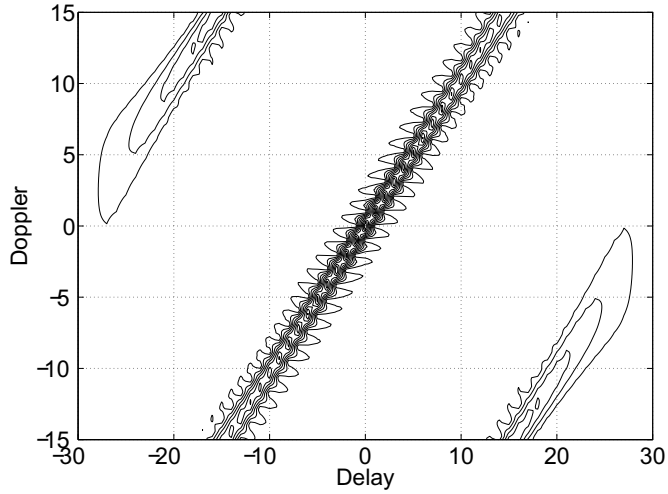

(a)

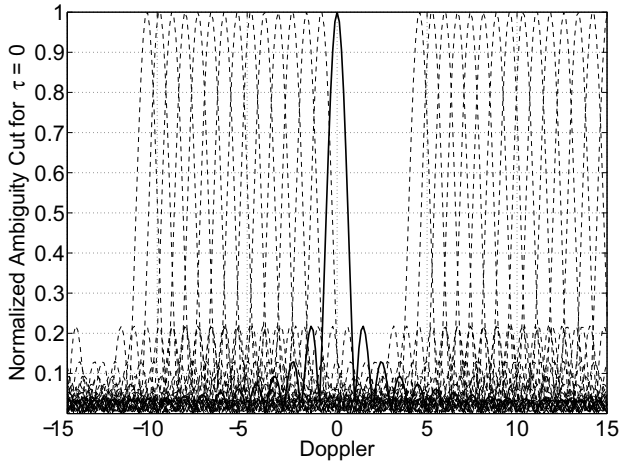

(b)

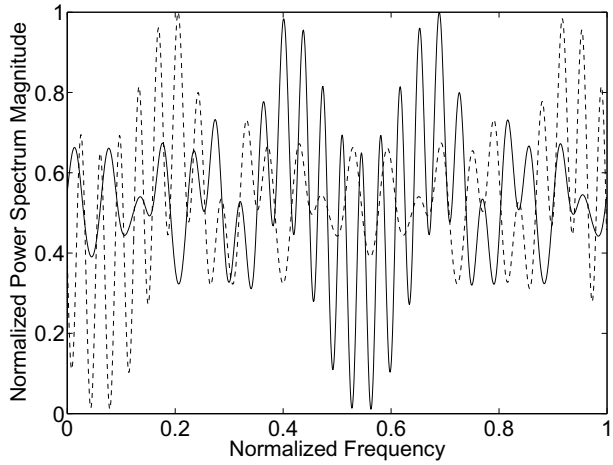

(c)

Figure 1: Performance for optimized $R_{ac,opt} = 0.1107$ ($N = 31$, $n = 2.0072$, $m = 2.92$): (a) Auto-ambiguity function, (b) Normalized auto-ambiguity cut (solid) and cross-ambiguity cut (dashed) for $\tau = 0$, (c) Normalized power spectrum magnitudes for sequences $\mathbf{u}_1$ (solid) and $\mathbf{u}_2$ (dashed).

Fig. 1c shows the power spectrum magnitudes of sequence pair $\mathbf{u}_1$ and $\mathbf{u}_2$, i.e. $x = 1$ and $y = 2$. This pair turns out to results in the smallest interference among the possible pairs and hence may be selected to serve communication functions. Additional sequences may be selected for the designed set accordingly such that MAI remains small.

Clearly, the waveform design for an integrated receiver may be optimized to trade-off auto-correlation and auto-ambiguity characteristics, respective, for cross-correlation and cross-ambiguity characteristics. In other words, the design may balance the constraints given by communications as well as radar, positioning, or navigation objectives.

6 Conclusions

In this paper, we have considered several properties of the auto-ambiguity and cross-ambiguity function of weighted pulse trains with Oppermann sequences. A number of important properties have been examined and proved which in turn allows for reducing the design space for optimization of a particular design. The insights gained from these properties build the foundations in the formulation of a formal framework leading to procedures that can be used for a more structured waveform design. In particular, the two procedures presented for designing weighted pulse trains with respect to auto-correlation and cross-correlation properties, respectively, are linked to the zero-Doppler cut metrics of MSAC and MSCC. Numerical examples are provided to illustrate the relationship between sequence parameters and performance characteristics.

References

[1] M. Jamil, H.-J. Zepernick, and M. I. Pettersson, "Performance Assessment of Polyphase Pulse Compression Codes," IEEE Int. Symp. on Spread Spect. Techn. and Appl., Bologna, Italy, pp. 161–165, Aug. 2008.

[2] N. Levanon and E. Mozeson, "Radar Signals," Chichester: Wiley, 2004.

[3] B. L. Lewis and F. F. Kretschmer, "A New Class of Polyphase Pulse Compression Codes and Techniques," *IEEE Trans. on Aerospace and Electronic Systems*, vol. 17, no. 3, pp. 364–372, May 1981.

[4] B. L. Lewis and F. F. Kretschmer, "Linear Frequency Modulation Derived Polyphase Pulse Compression Codes," *IEEE Trans. on Aerospace and Electronic Systems*, vol. 18, no. 5, pp. 637–641, Sept. 1982.

[5] P. B. Rapajic and R. A. Kennedy, "Merit Factor Based Comparison of New Polyphase Sequences," *IEEE Commun. Letters*, vol. 2, no. 10, pp. 269–270, Oct. 1998.

[6] I. Oppermann and B. S. Vucetic, "Complex Spreading Sequences with a Wide Range of Correlation Properties," *IEEE Trans. on Commun.*, vol. 45, no. 3, pp. 365–375, Mar. 1997.

[7] M. Jamil, H.-J. Zepernick, and M. I. Pettersson, "On Integrated Radar and Communication Systems Using Oppermann Sequences," IEEE Military Commun. Conf., San Diego, U.S.A., Nov. 2008.

[8] M. Jamil, H.-J. Zepernick, and M. I. Pettersson, "Cross-Ambiguity Function of Weighted Pulse Trains with Oppermann Sequences," IEEE Int. Symp. Wireless Commun. Sys., Siena, Italy, Sept. 2009.

[9] R. L. Mitchell and A. W. Rihaczek, "Clutter Suppression Properties of Weighted Pulse Trains," IEEE Trans. Aerospace and Electr. Systems, vol. AES-4, no. 6, pp. 822–828, Nov. 1968.

[10] P. Fan and M. Darnell, "Sequence Design for Communications Applications," Somerset: Research Studies Press, 1996.

[11] H. H. Dam, et al., "Spreading Code Design Using a Global Optimization Method," Annals of Operations Research, Springer, vol. 133, no. 1-4, Jan. 2005, pp. 249-264.

Part II

Part II

Waveform Optimization for Integrated Radar and Communication Systems Using Meta-Heuristic Algorithms

Part II is based on:

M. Jamil and H.-J. Zepernick, "Waveform Optimization for Integrated Radar and Communication Systems Using Meta-Heuristic, Algorithms," In: X.-S. Yang and S. Koziel (Eds.), *Comput. Optimization and Appl. in Eng. and Ind.*, vol. 359, Studies in Comput. Intell., Springer, Berlin Heidelberg, pp. 183–203, 2011.

Waveform Optimization for Integrated Radar and Communication Systems Using Meta-Heuristic Algorithms

Momin Jamil and Hans-Jürgen Zepernick

Abstract

Integration of multiple functions such as navigation and radar tasks with communication applications has attracted substantial interest in recent years. In this chapter, we therefore focus on the waveform optimization for such integrated systems based on Oppermann sequences. These sequences are defined by a number of parameters that can be chosen to design sequence sets for a wide range of performance characteristics. It will be shown that meta-heuristic algorithms are well-suited to find the optimal parameters for these sequences. The motivation behind the use of biologically inspired heuristic and/or meta-heuristic algorithms is due to their ability to solve large, complex, and dynamic problems.

1 Introduction

In recent years, integration of multiple functions such as navigation and radar tasks with communication applications has sparked a number of research initiatives. This includes research on future signals for hybrid receivers for Global Navigation Satellite Systems (GNSS)/communication and others tasks. The many benefits of multi-functionality range from reducing costs and probability of intercept to offering tolerable

co-site interference. While navigation and radar applications require waveform designs that offer excellent autocorrelation characteristics, the target for communication applications is on sets of waveforms with minimum crosscorrelation among the sequences in the set. In the former case, typically only a single sequence is needed while in the latter case many sequences are required to support access of multiple users to the common transmission medium. As excellent autocorrelation properties come at the expense of crosscorrelation characteristics and vice versa, a related waveform optimization problem has to be posed and solved taking into account these conflicting requirements. As far as the integration of radar and communication functionalities are concerned, the Office of Naval Research in 1996 launched the Advanced Multifunction Radio Frequency Concept (AMRFC) program [18,52]. This major program was motivated by the lack of integration of radar, communications, and electronic warfare functions which resulted in a significant increase of the number of topside antennas. Furthermore, it was realized that the lack of integration may also cause severe problems with antenna blockage and difficulties with own-ship electromagnetic interference. Also, a large number of antennas puts stress on maintenance resources. The concepts developed within the AMRFC program are centered around suitable broadband RF apertures that can cope with simultaneous operation of multiple functions and as such focuses on the rather expensive radio frequency (RF) front-end. A different approach on the basis of linear frequency modulated (LFM) waveforms, also known as chirps, has been proposed in [48]. In order to enhance the orthogonality among the signals and to support distinct separation of the different functions, it uses up-chirps for the communications component and down-chirps for the radar functionality of the integrated system. In this way, the suggested chirp signals allow for the radar and communication data to be simultaneously transmitted and received using some standard antenna array. Noting the inherent connection of the chirp-based integration concept to spread spectrum techniques, the work of [58, 59] investigated integrated radar and communication systems with the help of bipolar pseudo noise (PN) sequences, namely m-sequences [14,62]. However, one of the severe drawbacks of m-sequences with respect to radar applications is their poor Doppler tolerance [32]

and related problems of detecting multiple targets. These and related designs such as polyphase Barker sequences are optimized only with respect to the zero Doppler cut of the ambiguity function but produce much higher interference levels in the presence of Doppler shifted waveforms. As for the application to communications, large sets of m-sequences that would be needed to support multiple-access of many users have typically rather poor crosscorrelation properties [62]. As a consequence, they are generally only used as components of more complex designs such as Gold sequences. On the other hand, the large advances in modern integrated circuit technologies would facilitate an efficient implementation of more advanced sequence designs such as complex-valued sequences. Clearly, efficient optimization methods are needed to find suitable waveform and sequence designs for different applications.

Over the last few decades, researchers around the world have developed a vast number of algorithms to solve different optimization problems. Many of these algorithms are based on numerical linear and non-linear programming methods. As a result, the related algorithms require substantial gradient information and try to improve the solution in the proximity of an initial starting point. As a consequence, these methods provide useful strategies to find the global optimum for rather ideal and simple models. However, if the objective function and constraints have multiple or sharp peaks, these methods tend to become unstable. Most of the real world problems turn out to be too complex and difficult to solve using numerical based optimization methods as these tend to fail or are even unable to solve them. There exist also several direct search approaches which use no gradient information such as the Hooke and Jeeves method [17], Nelder-Mead simplex method [43], the Powell method [46], and the Rosenbrock method [49]. Common to these methods is that they take some basic approach of heading downhill from an arbitrary starting point but differ in deciding in which direction to and how far to move. Accordingly, the final outcome depends somewhat on the initial guess of the starting point. This would not be a major shortcoming if the parameter space is well behaved, i.e. if it contains a single, well-defined minimum. However, if the parameter space contains many local minima, as may be the case in

waveform optimization, it can be more difficult for such traditional approaches to find the global minimum. In contrast to population based algorithms, these direct searches cannot explore the search space effectively in different directions simultaneously. Successive improvements can be made to speed up the downhill movement of the algorithms but this does not improve the algorithms ability to find the global minimum instead of converging to a local minimum.

The drawbacks of numerical methods motivated researchers to adopt ideas from nature and to translate them to solve problems in engineering sciences. This has led to the inception of many biologically inspired heuristic or meta-heuristic algorithms to solve challenging optimization problems. The word "meta" means beyond or higher and "heuristic" means to find or to discover by trial and error. These methods have proven to be efficient in handling computationally complex problems. They aim at defining effective general purpose methods to explore the solution space and avoid tailoring them to a specific problem. Due to their general purpose nature, they can be applied to a wide range of problems. Meta-heuristic algorithms are also referred to as black-box algorithms as they exploit limited knowledge about the problem to be solved. As no gradient or Hessian matrix information is required for their operation, they are also referred to as derivative-free or zero-order algorithms [5]. The term zero-order implies that only the function values are used to establish the search vector. Moreover, the function to be optimized does not necessarily have to be continuous or differentiable and may also be accompanied by a set of constraints. The choice of method for solving a particular problem depends primarily on the type and characteristics of the problem at hand. It must be stressed that the goal of a particular method used is to find the "best" solution of some sort to a problem compared to finding the optimal solution. In this context, the term "best" refers to an acceptable or satisfactory solution to the problem. This could be the absolute best solution from a set of candidate solutions or may be any of the candidate solutions. The requirements and characteristics of the problem determine if the overall best solution can be found [10, 53].

Nature has an evolution span of millions or even billions of years. In all these years, it has mastered the art of finding a perfect solution

to almost all the problems it has been confronted with. As mentioned above, the development of nature inspired optimization algorithms has been an area of active research during recent years and resulted in many approaches such as genetic algorithms (GA), ant colony optimization (ACO), bee algorithms (BA), artificial bee algorithms (ABC), particle swarm optimization (PSO), simulated annealing (SA), harmony search (HS), firefly algorithms (FA), and artificial immune systems (AIS). The interested reader may be referred to [4, 10, 15, 31, 50, 55, 61] and the reference therein for more details and discussions on these topics.

Given the vast amount of available optimization methods, their application in waveform design also stretches from simple searches over more sophisticated and computational demanding realizations to the use of meta-heuristic algorithms. A simple computer search has been used in [44] to obtained sets of sequences with various combinations of sequence parameters. In [57], the optimization of orthogonal polyphase spreading sequences for wireless data applications is reported. It uses a built-in standard 'fmin' function provided in the numerical computing environment MATLAB. In particular, the related functions support multidimensional unconstrained nonlinear minimization including the Nelder-Mead direct search method. As the utilized cost functions in terms of average mean-square autocorrelation and crosscorrelation are very irregular and may have several local minima, the authors report the dependency of the optimization outcome on the starting point and corresponding convergence to different local minima. A similar optimization problem for complex-valued spreading sequences has been investigated in [9] using a global optimization method based on a modified bridging method. In order to solve the related complex optimization problem having a non-linear cost function and a non-linear constraint, a bridged function is used in the search for the global minimum such that the algorithm does not get stuck in a local minimum. Given that cost functions in waveform optimization are often highly irregular with many local minima or are even discontinuous, evolutionary algorithms have gained increased attention in the design of waveforms with respect to communication and radar applications. An evolutionary approach for designing complex spreading codes for direct sequence code-division multiple-access (DS-CDMA) systems has been proposed in [41, 42]. In

particular, a multi-objective evolutionary approach is used to search for solutions that satisfy simultaneous objectives posed on autocorrelation and crosscorrelation properties. This approach turned out to be beneficial in the communications field for designing large number of spreading sequence sets with a wide range of correlation properties. In [7], genetic algorithms have been used to design PN sequence families with bounded correlation properties. It is claimed that this approach can produce sequences of any length and superior performance compared to the well-known Gold sequences. A number of recent works has also been reported for the use of evolutional algorithms in the field of radar applications. In [2], an evolutionary algorithm is applied to determine a suite of optimal waveforms to simultaneously perform different surveillance missions such as ground moving target indication, airborne moving target indication, and synthetic aperture radar. The authors have shown that evolutionary algorithms are well suited to design optimal waveforms for multi-mission objectives such as peak sidelobe levels, integrated sidelobe levels, pulse integration, and revisit time. The work reported in [37] used meta-heuristic algorithms to optimize waveforms with sparse spectrum for radar applications in the high frequency band. In particular, a genetic algorithm and particle swarm optimization are used to produce optimal waveforms with acceptable autocorrelation sidelobes. It is concluded that the particle swarm optimization is simpler and faster than the genetic algorithm. They are of the opinion that computational efficiency of particle swarm optimization is comparable or would be even better than the adaptive method of [39].

In view of the above, this chapter considers integrated radar and communication systems based on waveforms known as polyphase sequences. In order to account for the waveform design challenges associated with such integrated systems, we have compared performance and potential application scenarios of different classes of polyphase pulse compression sequences in our earlier studies reported in [25, 26]. Specifically, Oppermann sequences have been revealed in these studies to potentially better support the considered integration as these allow for the design not only of families with a wide range of correlations but also support a variety of characteristics with respect to the ambi-

guity function, i.e. delay-Doppler tolerance. These sequences provide a number of parameters that can be chosen to design sequences for a wide range of performance characteristics. It will be shown that meta-heuristic algorithms are well-suited to find the optimal parameters for these sequences. Numerical results will be provided for optimal Oppermann sequences obtained with meta-heuristic algorithms.

The rest of this chapter is organized as follows. In Section 2, an overview of meta-heuristic algorithms is presented. A brief discussion of polyphase sequences and the definition of Oppermann sequences is provided in Section 3. In Section 4, performance measures are introduced. Numerical examples are given in Section 5. In Section 6, conclusions are drawn.

2 Meta-Heuristic Algorithms

Meta-heuristic algorithms, also referred to as meta-heuristics for brevity, belong to a branch of stochastic optimization. They are utilized by both engineers and scientists wishing to optimize solutions to problems that are intractable by conventional methods. Meta-heuristic methods consist of two major components known as randomization and selection of the best solutions. The first component avoids that an algorithm gets trapped in a local optimum but also increases the diversity of the potential solutions while the latter component ensures convergence towards the optimal value [10, 60, 61]. A good combination of these two components usually ensures that the global optimum is achievable. The popularity of these algorithms stems from their ability to solve large, complex and dynamic problems. The efficiency of these algorithms or solutions they provide is a measure of their ability to reach an acceptable solution within a reasonable time frame.

The applications of meta-heuristics are broad, versatile and diverse. Application areas include controller design, applied mathematics, power systems, physics, data mining, fuzzy systems and many others. In this chapter, we will apply some of these algorithms to pseudo random signal processing with focus on waveform design for integrated radar and communication systems. For this purpose, meta-heuristic algorithms may be classified as being either population-based

or flight/trajectory-based. Genetic algorithms, for example, can be classified as a population-based method while particle swarm optimization utilizes multiple particles to reach the optimal solution. On the other hand, simulated annealing uses a single solution that moves through the search space or design space in a piecewise manner. The essence of the algorithm is always to accept a better solution, whereas a not-so-good solution is accepted with certain probability. In the sequel, selected state-of-the-art zero order and meta-heuristic algorithms are presented.

2.1 Particle Swarm Optimization

The PSO is a population-based stochastic optimization technique which has been inspired by social behavior of a flock of birds, school of fishes and swarm of bees as proposed by Eberhart and Kennedy [30]. Since its inception, there have now as many as about 20 different variants of PSO been proposed while remaining still an active area of research. It shares many similarities with genetic and virtual ant algorithms including concepts such as population initialization with random solutions and search for a global optimum solution in successive generations. However, the evolution operators like mutation and crossover as well as encoding or decoding of the parameters into binary strings are not used with PSO algorithms. Instead, it uses a real-number randomness and global communication among the swarm population. Accordingly, each member in the swarm adapts its search patterns by learning from its own experiences of the other members. A member in the swarm is referred to as a particle and represents a potential solution which is a point in the search space. The global optimum is regarded as the location of food [36]. Each particle has a fitness value and a velocity to adjust its flying direction by learning from the best experiences of the swarm to search for the global optimum in the D-dimensional solution space. In our case, the dimension D of the problem is given by the number of parameters that are available for optimization for a given class of sequences. In order to avoid haphazard movements of the particles in the search space, upper and lower bounds are usually specified on the velocity. If the velocity v falls below the specified lower bound, it is set to v_{min} as a measure to prevent in-sufficient exploration of the

search space. On the other hand, if the velocity exceeds the specified upper bound, it is set to v_{max} in order to avoid particles moving away from or past a good solution. Similarly, the actual search range for a D-dimensional problem is usually also constrained to a given interval $[x_{min}, x_{max}]^D$, in order to restrain the particles moving on the search boundary.

The standard PSO uses both the personal best, *pbest*, with respect to the location achieved by an individual particle and the global best, *gbest*, referring to the best solution/location among all particles in the swarm [10, 30]. The concept of personal best is primarily used to increase the diversity in finding a solution and to avoid pulling all the particles to the global best. This may cause the algorithm to converge prematurely without finding the overall best solution. However, such diversity can also be simulated by using some kind of randomness [60, 61]. Based on this observation, [61] argues that there is no need to use the personal best, unless the optimization problem is highly nonlinear and multi-modal. This version of the PSO is known as accelerated PSO (APSO) [60, 61].

2.2 Harmony Search

A new of a heuristic optimization algorithms known as harmony search (HS) was developed by Lee and Geem [31]. It formalizes the musician improvisation process, i.e. inventing music while performing, into a quantitative optimization process. It comprises of the following parts: (1) Usage of harmony; (2) pitch adjustment; and (3) randomization. In an HS algorithm, each musician (decision variable) plays (generates) a note (value) for finding a best harmony (global optimum). In other words, a harmony translates to an optimization solution vector and the musician's improvisation corresponds to local and global search schemes in terms of optimization. Solutions of the optimization process correspond to a musician while the harmony of the notes generated by a musician corresponds to the fitness of the solution. The pitch adjustment rate $r_{pa} \in [0.1, 0.5]$ and so-called harmony memory $r_{accept} \in [0.7, 0.95]$ ensure that the best harmonies established at some point will be carried over to a new harmony memory. For a detailed discussion on harmony search, the interested reader is referred to [31, 60, 61] and

the references therein.

2.3 Adaptive Simulated Annealing

The classical SA algorithm [10,53,60,61] relies on the Boltzmann sampling distribution. It comprises of components such as the probability density function of the state space $g(\gamma)$ with γ being the current solution, an acceptance probability function $h(\Delta E)$ with respect to the difference in system energy ΔE between two design vectors, and an annealing schedule for temperature $T(k)$ with annealing time k using Boltzmann annealing. An enhanced version of the classical SA known as adaptive SA (ASA) has been proposed in [20–23] including comparisons, test case studies and applications. In contrast to SA, the annealing schedule for temperature $T(k)$ decreases exponentially in annealing time k. In addition, re-annealing and quenching is introduced with ASA that allows for adaptation to changing sensitivities in multidimensional parameter spaces.

2.4 Artificial Bee Colony Algorithm

The ABC algorithm was proposed by Karaboga [27] in 2005. It simulates the foraging behavior associated with bee colonies. A colony of honey bees can extend itself over long distances, sometimes more than 10 kilometers and in multiple directions simultaneously to exploit a large number of food sources. In a bee colony, tasks are divided among the specialized individuals or bees, namely employed, onlooker and scout bees. The population in a bee colony is divided into two halves. The first half of the population is comprised of employed bees while the second half includes the onlooker bees. The foraging process begins in a colony by scout bees being sent to search for promising food sources. Scout bees move from one food source to another in a random fashion. Employed bees perform duties of exploiting the possible food sources and passing on the information about the quality of the food source to the onlookers bee. The decision taken by onlooker bees to exploit a potential food source depends on the information provided by the employed bees. ABC algorithms have been used to solve both unconstrained and constrained optimization problems [3, 27–29].

It requires only a few control parameters such as the colony size and maximum number of cycles [29].

2.5 Preliminaries for Waveform Design

From this point onwards, we will consider two-dimensional optimization problems unless otherwise specified. In the context of waveform design using Oppermann sequences, the term swarm in APSO, harmonies in HS, bees in ABC and candidate points in ASA relate to the parameters m and n which define a specific sequence family. In all these algorithms, the control parameters are defined in the initialization phase. Initially, all the algorithms start with a population randomly distributed except for ASA, which starts with the initial guess in the search space. In each step of the algorithms, there is always a solution or a set of solutions, representing the current state of the algorithm. These solutions are used to generate phases of the Oppermann sequences (see Section 3). In order to distinguish good waveform designs from inferior designs, waveform characteristics such as aperiod correlations, figure of merit, and integrated sidelobe measures are computed. The interested reader can find pseudo code of HS in [61], ASA in [51], and ABC in [27] while details of the APSO can be found in [60, 61].

3 Polyphase Sequences and Their Applications

The history of complex-valued sequences ranges back as far as the 1950s when polyphase sequences where considered in many research laboratories. As the related research outcomes were reported mainly in classified documents with limited access, a broader audience was first reached with the work in [16] on phase shift pulse sequences. In the following decades, many complex-valued sequences have been proposed and analyzed with their applications ranging from radar systems to spread-spectrum communication systems. In particular, polyphase sequences have gained increased attention due to their ability to match regular phase shift keying modulation schemes. In addition, the advances in integrated circuit technologies have paved the way for moving from simple binary sequences to implementations of complex-valued sequences

and related more involved pseudo random signal processing. In the sequel, we consider polyphase sequences and will shed some light on their potential to serve in integrated radar and communication systems. In particular, the family of Oppermann sequences [44] are considered in more detail as they offer the system designer large sets of sequences with a wide range of correlation properties compared to other classes of polyphase sequences.

3.1 Polyphase Sequences for Radar Systems

Pseudo random sequences and the related signal processing have emerged from space and military applications. In this context, the concept of pulse compression, i.e. expanded pulses with large time-bandwidth products, has been utilized in radar systems. This type of signals offer high range resolution as they can obtain high pulse energy and large pulse width. As an alternative to frequency-modulated signals, pulse compression sequences have been subject of many studies [14,32]. Polyphase sequences are known to have better Doppler tolerance for a broader range-Doppler coverage than binary sequences [8, 32, 40, 45]. These sequences can be derived from the phase history of chirp or step chirp analog signals and can be processed digitally [35]. In radar applications, the performance of different polyphase sequences can be compared in terms of delay or range tolerance using measures such as the autocorrelation function, mainlobe-to-total-sidelobe ratio and peak-to-sidelobe ratio. The sensitivity of a particular waveform design towards Doppler shifts in case of moving targets can be characterized by using the ambiguity function. As there exist no analytical method that would allow for synthesizing the desired waveform given its desired ambiguity function, more practical optimization approaches are needed to facilitate such designs. For example, the design of a particular radar waveform may be first aiming for optimization of autocorrelation properties with respect to range characteristics followed by evaluating the ambiguity function to identify the Doppler tolerance of the deduced sequence.

As far as radar applications are concerned, Frank sequences [12] were the first polyphase sequences used in pulse compression radar [45]. They can only be designed for perfect square lengths, therefore, they

have limited family size. Later in [33] modified versions of Frank sequences were obtained by permuting their phase history. The modified versions are referred to as P1 and P2 sequences. Rapajic and Kennedy in [47] proposed a new class of sequences, known as Px sequences. These sequences have superior performance in terms of integrated sidelobe levels compared to Frank, P1, and P2 sequences. However, for even square root sequence lengths, their performance is the same as for P2 sequences. In [34], the families of P3 and P4 sequences were proposed that can be constructed for any length. The authors of [6, 13] generalized the ideas behind Frank sequences resulting in Frank-Zadoff-Chu (FZC) sequences which can also be designed for any length. Several performance aspects of the aforementioned classes of polyphase sequences with respect to radar applications have been discussed in literature [33, 35, 47].

3.2 Polyphase Sequences for Communication Systems

A major boost for the application of pseudo random sequences in the field of communication systems was given by the development of cellular mobile communication systems and spread-spectrum based radios for indoor communication. In particular, the CDMA system for digital cellular phone applications by Qualcomm Incorporated and the family of IEEE802.11 standards for wireless local area networks (WLANs) has taken the theoretical concepts into practical systems. The main classes of sequences used with these systems are Walsh-Hadamard sequences [11, 54], m-sequences [11, 62], Barker codes [11, 62], and complementary code keying based modulation [19]. Subsequently, with the advent of the third generation of mobile communication systems, more advanced spread-spectrum techniques such as orthogonal variable spreading factor sequences [1] and complex-valued short scrambling sequences have been utilized. In contrast to radar applications where it is usual sufficient to have a single sequence with good autocorrelation characteristics, communication systems require a set of sequences to facilitate simultaneous channel access to a number of users. Clearly, minimum crosscorrelation among the sequences is a major design consideration in this case. Given the large advances in modern integrated circuit technologies, it has become feasible to implement complex-valued se-

quence designs including polyphase sequences such as Frank sequences, FZC sequences, and Oppermann sequences.

3.3 Application of Oppermann Sequences for Integrated Radar and Communication Systems

Given the insights from the brief overview on polyphase sequences from the viewpoint of radar and communication applications, it can be concluded that more flexible waveform designs are needed to address the conflicting objectives of these two applications. Our earlier research [25, 26] on this topic has revealed that Oppermann sequences may serve favorable in such integrated radar and communication systems compared to conventional waveform designs. This is mainly due to the fact that families of Oppermann sequences can be designed for a wide range of correlation properties. For any given sequence length, Oppermann sequences are defined by three parameters. These parameters can be used in an optimization process to control the progression of the autocorrelation function, crosscorrelation function, the power spectral density and characteristics of the ambiguity function. Due to space limitations, however, we will concentrate here on range (autocorrelation) and multiple access (crosscorrelation) characteristics. On the other hand, inclusion of moving targets and the related Doppler shifts into the framework of meta-heuristic algorithms may be addressed in our future research considering ambiguity and cross-ambiguity functions.

In this chapter, we consider weighted pulse trains that can be described by a complex envelope as

$$U_x(t) \quad = \quad \frac{1}{\sqrt{T}} \sum_{i=0}^{N-1} u_x(i)\, \mathrm{rect}\left(\frac{t - iT_c}{T_w}\right) \tag{1}$$

where $T = N\,T_c$ is the duration of the xth pulse train while T_c and $T_w \leq T_c$, respectively, denote the repetition period and the width of each rectangular pulse

$$\mathrm{rect}\left(\frac{t}{T_w}\right) = \begin{cases} 1 & \text{for} \quad -\frac{T_w}{2} \leq t \leq \frac{T_w}{2} \\ 0 & \text{otherwise} \end{cases} \tag{2}$$

The elements $u_x(i)$, $i = 0, 1, \ldots, N-1$, of the xth complex-valued sequence $\mathbf{u}_x$ of length N represent the weights of the pulse train in (1). In general, these elements are given for a polyphase sequence as

$$u_x(i) = \exp\left[j\varphi_x(i)\right], \qquad j = \sqrt{-1} \tag{3}$$

where the set of N phases $\{\varphi_x(0), \varphi_x(1), \ldots, \varphi_x(N-1)\}$ are referred to as phase sequence. In particular, the phase $\varphi_x(i)$ of the ith element $u_x(i)$ of the xth Oppermann sequence $\mathbf{u}_x = [u_x(0), u_x(1), \ldots, u_x(N-1)]$ of length N taken from a family or set $\mathscr{U}$ of sequences is given as

$$\varphi_x(i) = \frac{\pi}{N}\left[x^m(i+1)^p + (i+1)^n + x(i+1)N\right] \tag{4}$$

where $1 \leq x \leq N-1$, $0 \leq i \leq N-1$ and integer x is relatively prime to the length N. The maximum size of a family $\mathscr{U}$ of Oppermann sequences is obtained as $N-1$ when the length N of the sequences is a prime number. A particular family of Oppermann sequences is defined by the real-valued parameters m, n, and p. All the sequences in a family have the same magnitude of the autocorrelation function for a fixed combination of these three parameters. In [44], it has been shown that the magnitude of the autocorrelation function depends only on the parameter n if the parameter $p = 1$. For this case, the autocorrelation magnitude follows the expression

$$|C_x(l)| = \left| \frac{1}{N} \sum_{i=0}^{N-1-l} \exp\left\{ \frac{j\pi}{N}\left[(i+1)^n - (i+l+1)^n\right] \right\} \right| \tag{5}$$

In the sequel, we therefore focus on the case of $p = 1$ which leaves us with m and n as free parameters for use in an optimized waveform design.

Due to the general definition of Oppermann sequences, they include some more specific sequences. For example, for the parameters $m = 2$, $n = -\infty$, $p = 1$, FZC sequences can be generated. As such, application of the considered meta-heuristic algorithms to these more specific sequences is straightforward.

4 Performance Measures

In the following sections, the definitions of the measures used in the performance comparison of the considered Oppermann sequences will be given. Specifically, let an Oppermann sequence of length N be denoted as $\mathbf{u}_x = [u_x(0), u_x(1), \ldots, u_x(N-1)]$ where subscript $1 \leq x \leq U$ relates to the xth sequence $\mathbf{u}_x$ taken from a given set $\mathscr{U}$ of size U.

4.1 Aperiodic Correlation Measures

In order to quantify the degree of similarity between different sequences from a given set or between a given sequence and a shifted version of it, respectively, autocorrelation and crosscorrelation measures are usual considered. In many fields, aperiodic signals need to be processed which occur only once within a considerable time span and appear to the application as more or less singular events. Accordingly, the aperiodic crosscorrelation (ACC) between two complex-valued sequences $\mathbf{u}_x = [u_x(0), u_x(1), \ldots, u_x(N-1)]$ and $\mathbf{u}_y = [u_y(0), u_y(1), \ldots, u_y(N-1)]$ of length N at discrete shift l is given as [11, 62]

$$C_{xy}(l) = \begin{cases} \frac{1}{N} \sum\limits_{i=0}^{N-1-l} u_x(i) u_y^*(i+l), & 0 \leq l \leq N-1 \\ \frac{1}{N} \sum\limits_{i=0}^{N-1+l} u_x(i-l) u_y^*(i), & 1-N \leq l < 0 \\ 0, & |l| \geq N \end{cases} \tag{6}$$

where $(\cdot)^*$ denotes the complex conjugate of the argument $(\cdot)$. In case of $\mathbf{u}_x = \mathbf{u}_y$, (6) is referred to as aperiodic autocorrelation (AAC) and is denoted as $C_x(l) = C_{xx}(l)$.

In addition to ACC and AAC, it is often more realistic to incorporate the whole range of possible correlation values into the performance evaluation of a given set of sequences rather than considering only peak values of aperiodic correlations. In this context, mean-square values from AAC and ACC may be used in favor of worst case scenarios. For this purpose, let us introduce the mean-square out-of-phase autocorrelation (MSAC), R_{ac}, and mean-square crosscorrelation (MSCC), R_{cc}, respectively, of a given set $\mathscr{U}$ of size U as

$$R_{ac} = \frac{1}{U}\sum_{x=1}^{U}\sum_{\substack{l=1-N \\ l\neq 0}}^{N-1}|C_x(l)|^2 \tag{7}$$

$$R_{cc} = \frac{1}{U(U-1)}\sum_{x=1}^{U}\sum_{\substack{y=1 \\ y\neq x}}^{U}\sum_{l=1-N}^{N-1}|C_{xy}(l)|^2 \tag{8}$$

4.2 Sidelobe Measures

The figure of merit (FOM) of a sequence $\mathbf{u}_x \in \mathscr{U}$, $1 \leq x \leq U$ of length N with aperiodic autocorrelation function $C_x(l)$ measures the ratio of energy in the mainlobe to the energy in the sidelobe of the autocorrelation function. It is defined as

$$FOM_x = \frac{C_x(0)}{2\sum_{l=1}^{N-1}|C_x(l)|^2}, \qquad \forall x \tag{9}$$

Alternatively, the integrated sidelobe level (ISL) is often used for radar applications in the context of distributed target environments. The ISL of a sequence $\mathbf{u}_x \in \mathscr{U}$, $1 \leq x \leq U$ of length N is defined as

$$ISL_x = \frac{1}{FOM_x}, \qquad \forall x \tag{10}$$

Another important measure in relation to radar applications is the peak-to-sidelobe ratio (PSLR) which relates to the ability of detecting targets without masking interfering targets. For example, if an AAC has large sidelobes, it will mask nearby targets and leave them undetected. Specifically, the PSLR of a sequence $\mathbf{u}_x$ measures the ratio of the in-phase value $C_x(0)$ to the maximum sidelobe magnitude $|C_x(l)|$ of the periodic autocorrelation function $C_x(l)$. It is defined as

$$PSLR_x = \frac{C_x(0)}{\max\limits_{1\leq l<N}|C_x(l)|}, \qquad \forall x \tag{11}$$

5 Numerical Examples

In the sequel, some numerical examples are provided to illustrate the application of meta-heuristic algorithms for waveform optimization for integrated radar and communication systems. For this purpose, we consider the class of Oppermann sequences as defined in (4) of length $N = 31$. It is noted that the maximum number of $N-1 = 30$ sequences in the designed set is obtained as N is chosen as a prime number. Furthermore, the considered sequence family offers parameters m and n for optimization given the case of parameter $p = 1$. Accordingly, the following optimization problems may be posed:

$$P1: \quad \min_{n\in[n_1,n_2]} ISL(\mathscr{U}) \tag{12}$$

$$P2: \quad \max_{n\in[n_1,n_2]} PSLR(\mathscr{U}) \tag{13}$$

$$P3: \quad \min_{m\in[m_1,m_2],n\in[n_1,n_2]} [R_{ac}(\mathscr{U}) + \alpha R_{cc}(\mathscr{U})] \tag{14}$$

where $m \in [m_1, m_2]$ and $n \in [n_1, n_2]$ are the search regions for m and n, respectively, and α is a weighting factor. While problems $P1$ and $P2$ given in (12) and (13), respectively, relate strongly to radar applications, problem $P3$ formulated in (14) can be used to find a trade-off between conflicting objectives of radar and communication applications. Especially, the weighting factor α may be chosen with respect to desirable system specifications. In contrast to [25], where we have used a two-step approach to first optimize autocorrelation properties by a simple brute-force search over parameter n followed by tuning m towards favorable delay-Doppler properties, we consider here two-dimensional optimization to simultaneously find the optimal values of n and m for problem $P3$. On the other hand, in view of the independence of the autocorrelation of Oppermann sequences on parameter m as shown in (5), problems $P1$ and $P2$ remain one-dimensional as PSLR and ISL only involve the aperiodic autocorrelation.

In order to solve the problems formulated in (12)-(14), we use APSO, HS ASA and ABC. The two-dimensional search space was constrained to the interval $m \in [0, 4]$ and $n \in [0, 4]$. The algorithms were executed on a laptop computer with Intel Pentium M 740 Processor

running at 1.73 GHz and 2048 Megabytes of RAM. With the exception of ASA, where we used a C-routine called from MATLAB, all the other algorithms have been implemented in MATLAB. As for the translation of the notions from meta-heuristics to the optimization problem at hand, the following interpretation can be given.

- **APSO:** Initially, particles in a swarm are randomly distributed in a D-dimensional search space. In APSO, the parameter D refers to the dimension of the problem, swarm refers to a population, and particle is similar to an individual. Alternatively, each solution (or particle) flies through the search space and looks for an optimal position to land. In terms of Oppermann sequences, particles are represented by the values of m and n in a two-dimensional search space and are used to generate the phases of Oppermann sequences as defined in (4). The search for the optimal landing position, i.e. finding optimal values of m and n will continue until the criteria selected from (7) to (11) are met.

- **HS:** Initially, harmonies are randomly generated in a D-dimensional space and are stored in a harmony memory (HM). The use of HM ensures that the best harmonies will be carried over to the HM. As for the optimization of Oppermann sequences, the parameters m and n are represented by the obtained harmonies to generate phases as defined in (4). Then, pitch adjustment is used to control the convergence of the algorithm. Randomization introduced in the algorithm drives the algorithm to search previously unexplored areas in the search space until the criteria selected from (7) to (11) are met.

- **ASA:** This algorithm starts with the initial guess of the parameters in the D-dimensional search space. In terms of Oppermann sequences, the initial guess represents values of the parameters m and n. Each step of the ASA algorithm replaces the current solution by a random nearby solution. The obtained solutions are used to generate Oppermann sequences. The process of finding optimal values of m and n continues by generating feasible points in the search space and acceptance probability including anneal-

ing and re-annealing temperatures until criteria selected from (7) to (11) are met.

- **ABC:** It is recalled that food sources are randomly distributed in the D-dimensional search space at the start of the search. Here, bees refer to a population of bees (employed, onlookers and scout) which are in the search of the best food position. Employed bees search for new food sources within their neighborhood that have more nectar compared to the food sources they have previously visited. These food sources represent the values of the parameters m and n of Oppermann sequences to generate the phases defined in (4). If during the optimization process the criteria set for (7) to (11) are not met, it will represent abandoned food source or bad sequence designs. The search for the final food position represent optimal values of m and n that satisfy the criteria set for (7) to (11).

Figure 1 compares the performance of Oppermann sequences obtained through meta-heuristics in terms of PSLR with the brute-force search method with fixed step size reported in [25]. Clearly, the random search strategy employed in meta-heuristics widens the search area allowing the particles to explore the search space more effectively compared to an optimization using fixed step size. As can be seen from the figure, PSLR values can be improved for those prime length that would have inferior performance using brute-force search with fixed increment on n. In this case, meta-heuristic algorithms improve the performance of the designed set of Oppermann sequences to be comparable to other families such as the FZC sequences (see also [25]).

The convergence behavior of the considered algorithms for the example of optimizing PSLR is illustrated in Fig. 2. It can be seen from the progressions in terms of iterations shown in the figure that ASA achieves the fastest convergence to the optimal values followed by APSO, ABC and HS. The fast convergence of ASA may be attributed to the fact that exponential annealing permits the algorithm to adaptively re-anneal and pacing the convergence in the search space in all dimensions. It should be mentioned that the similar convergence behavior and ranking among the algorithms can be observed when applied

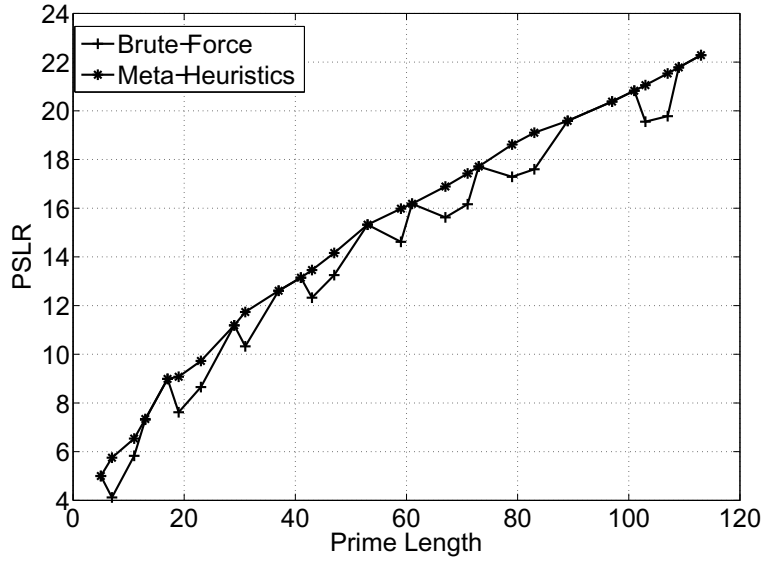

Figure 1: Performance comparisons between brute-force search with fixed increment and meta-heuristic algorithms in terms of PSLR.

to optimize FOM, ISL, and mean-square aperiodic correlation measures.

Tables 1(a)-(e) show numerical results of optimal designs for Oppermann sequences of length $N = 31$ with respect to the optimization problems posed in (12), (13), and (14) using APSO, HS, ASA, ABC. As for the optimal designs presented in Table 1(a) and Table 1(b) for PSLR and ISL, respectively, it is sufficient to consider only the parameter n as these metrics involve only the AAC (see also (10) and (11)). It is recalled that according to (5), the AAC is independent of the parameter m for the considered case of parameter $p = 1$. Also, all $N - 1 = 30$ Oppermann sequences in an optimized set achieve the same PSLR and ISL. Clearly, all considered meta-heuristic algorithms converge towards very similar results for these two classical design objectives of radar systems.

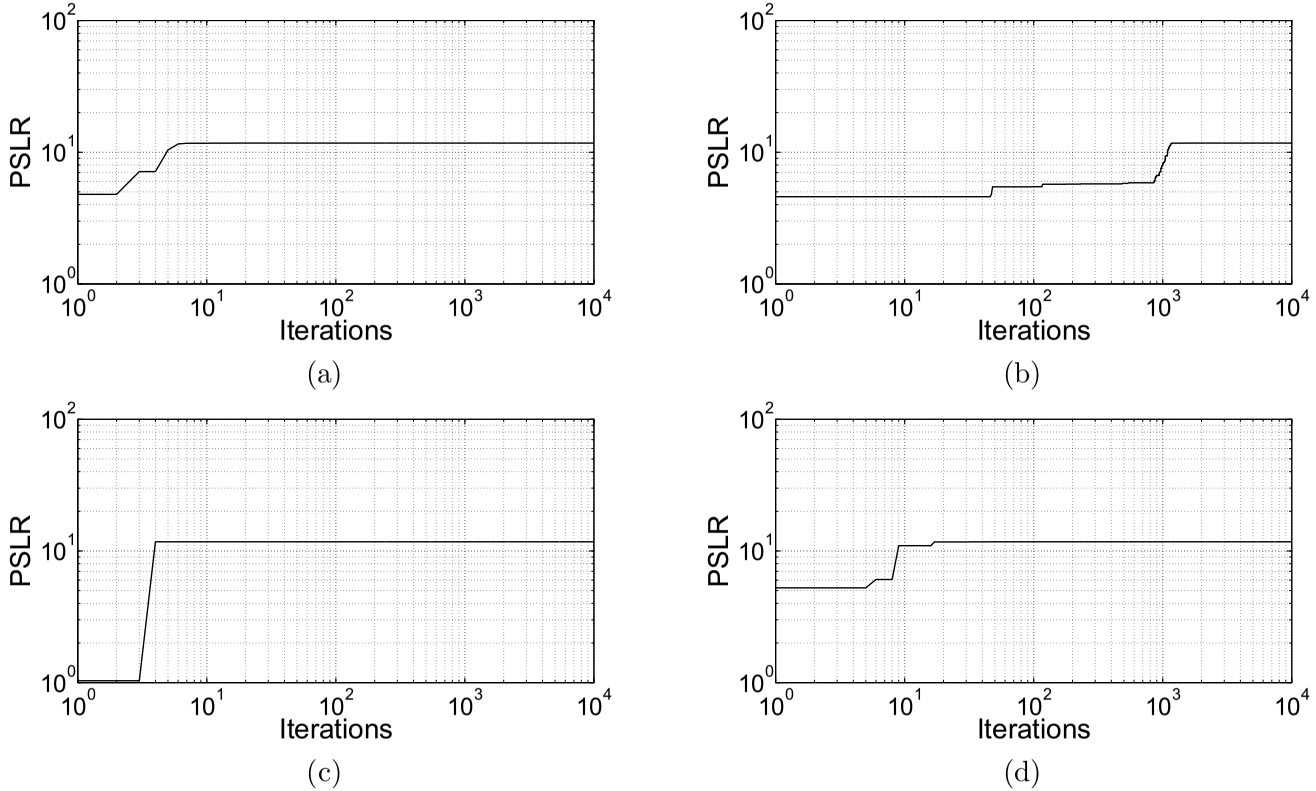

Figure 2: Convergence of different meta-heuristic algorithms towards optimal PSLR: (a) APSO, (b) HS, (c) ASA, (d) ABC.

Table 1: Optimal designs for Oppermann sequences of length $N = 31$.

(a) Peak-to-sidelobe ratio

Algorithm	n	PSLR
APSO	2.000	11.735
HS	2.000	11.734
ASA	2.000	11.735
ABC	2.000	11.735

(b) Integrated sidelobe level

Algorithm	n	ISL
APSO	2.007	0.110
HS	2.007	0.110
ASA	2.000	0.116
ABC	2.007	0.110

(c) MSAC; $\alpha = 0$

Algorithm	m	n	R_{ac}	R_{cc}
APSO	2.597	2.007	0.110	1.000
HS	2.744	2.007	0.110	1.001
ASA	2.000	2.000	0.116	1.000
ABC	0.614	2.007	0.110	1.005

(d) MSCC; $\alpha = 60$

Algorithm	m	n	R_{ac}	R_{cc}
APSO	1.003	1.002	19.676	0.341
HS	1.003	1.000	19.677	0.341
ASA	1.000	1.000	19.677	0.344
ABC	1.003	1.000	19.677	0.341

(e) MSAC+MSCC; $\alpha = 1$

Algorithm	m	n	R_{ac}	R_{cc}
APSO	0.930	2.007	0.110	0.997
HS	1.000	2.007	0.110	0.996
ASA	1.000	2.000	0.116	0.996
ABC	0.999	2.007	0.110	0.996

In order to illustrate the trade-off in waveform optimization for integrated radar and communication systems, let us focus now on the results presented in Tables 1(c)-(e) with respect to the optimization problem posed in (14). In particular, we have chosen $\alpha = 0$ relating to radar systems, $\alpha = 60$ emphasizing on communication systems, and $\alpha = 1$ as an example of an integrated radar and communication scenario. Clearly, the autocorrelation properties indicated by the small R_{ac} values in Table 1(c) are beneficial for radar systems and are independent of parameter m. On the other hand, good crosscorrelation characteristics are shown Table 1(d) for use with communication systems but these come at the expense of poor autocorrelation properties quantified by high values of R_{ac}. The results of the trade-off example shown in Table 1(e) may perform favorable with integrated radar and communication systems keeping autocorrelation values low and driving crosscorrelation values smaller. An additional increase of α would result in an increase of autocorrlelation values and further reduce crosscorrelation values. Also, all four considered meta-heuristic algorithms provide very similar outcomes to the different optimization problems.

6 Conclusions

In this chapter, we have focused on the waveform optimization for integrated radar and communication systems. Given the conflicting requirements on autocorrelation and crosscorrelation characteristics, meta-heuristic algorithms are considered to basically perform a multi-dimensional optimization. Specifically, the selected class of Oppermann sequences allows for designing families with a wide range of correlations with respect to a two-dimensional search space. The numerical results illustrate the potential of meta-heuristic algorithms for designing sequences for radar, communications, as well as integrated systems. By way of example with respect to PSLR, it is shown that meta-heuristics can improve performance compared to search methods with fixed increment.

References

[1] Adachi, F., Sawahashi, M., Okawa, K.: Tree-structured Generation of Orthogonal Spreading Codes with Different Lengths for Forward Link DS-CDMA Mobile. IEE Electronics Letters 33(1), 27–28 (1997)

[2] Amuso, V. J., Enslin, J.: An Evolutionary Algorithm Approach to Simultaneous Multi-Mission Radar Waveform Design. In: Wicks, M., Mokole, E., Blunt, S., Schneible, R., Amuso, V. (eds.) Principles of Waveform Diversity and Design, pp. 110–125, SciTech Publishing, Rayleigh (2011)

[3] Basturk, B., Karaboga, D: An Artificial Bee Colony (ABC) Algorithm for Numeric Function Optimization. In: IEEE Swarm Intelligence Symposium, Indianapolis, USA (2006)

[4] Bergh, F.: An Analysis of Particle Swarm Optimizers. Ph.D. thesis, University of Pretoria, Pretoria, South Africa (2001)

[5] Brent, R. P.: Algorithms for Minimization without Derivatives. Prentice Hall, Englewood Cliffs (1973)

[6] Chu, D. C.: Polyphase Codes with Good Periodic Correlation Properties. IEEE Trans. on Inf. Theory 18(4), 531–532 (1972)

[7] Cinteza, M., Marghescu, I., Radulescu, T.: Design of PN Sequence Families with Bounded Correlation Properties Using Genetic Algorithms. In: IEEE EUROCON, Belgrade, Serbia and Montenegro, pp. 1362–1365 (2005)

[8] Cook, C. E., Bernfeld, M.: Radar Signals: An Introduction to Theory and Applications. Academic Press, New York (1967)

[9] Dam, H. H., Zepernick, H.-J., Nordholm, S.: Spreading Code Design Using a Global Optimization Method. In: Annals of Operations Research, **123**, pp. 249–264 Springer, New York (2005)

[10] Engelbrecht, A. P.: Fundamentals of Computational Swarm Intelligence. John Wiley & Sons, Chichester (2005)

[11] Fan, P., Darnell, M.: Sequence Design for Communications Applications. Research Studies Press, Taunton (1996)

[12] Frank, R. L.: Polyphase Codes with Good Nonperiodic Correlation Properties. IEEE Trans. on Inf. Theory 9(1), 43–45 (1963)

[13] Frank, R. L., Zadoff, S. A.: Phase Shift Pulse Codes with Good Periodic Correlation Properties. IEEE Trans. on Inf. Theory 19(1), 115–120 (1975)

[14] Golomb, S. W., Gong, G.: Signal Design for Good Correlation for Wireless Communications, Cryptography and Radar. Cambridge University Press, Cambridge (2005)

[15] Haupt, R. L., Haupt, S. E.: Practical Genetic Algorithms. John Wiley & Sons, Chichester (2004)

[16] Heimiller, R. C.: Phase Shift Pulse Codes with Good Periodic Correlation Properties. IRE Trans. on Inf. Theory 7(10), 254–257 (1961)

[17] Hooke, R., Jeeves, T. A.: Direct Search Solution of Numerical and Statistical Problems. Journal of the ACM 8, 212–229 (1961)

[18] Hughes, P. K., Choe, J. Y.: Overview of Advanced Multifunction RF System (AMRFS). IEEE International Conference on Phased Array Systems and Technology, Dana Point, USA, pp. 21–24 (2000)

[19] IEEE Std 802.11. Wireless LAN Medium Access Control (MAC) and Physical Layer (PHY) Speccification - Higher-Speed Physical Layer Extension in the 2.4 GHz Band (2000)

[20] Ingber, L.: Adaptive Simulated Annealing (ASA): Global Optimization C-Code, Technical Report, Caltech Alumni Association (1993)

[21] Ingber, L.: Adaptive Simulated Annealing (ASA): Lessons learned. Control and Cybernetics 25, 33–54 (1996)

[22] Ingber, L.: Adaptive Simulated Annealing (ASA) and Path-Integral Algorithms: Generic Tools for Complex Systems. Technical Report, Chicago, USA (2001)

[23] Ingber, L., Rosen, B.: Genetic Algorithms and Very Fast Simulated Reannealing: A Comparison. Mathematical Computer Modeling 16(11), 87–100 (1992)

[24] Ipatov, V. P.: Spread Spectrum and CDMA: Principles and Applications. John Wiley & Sons, Chichester (2005)

[25] Jamil, M., Zepernick, H.-J., Pettersson, M. I.: Performance Assessment of Polyphase Pulse Compression Codes. In: IEEE International Symposium on Spread Spectrum Techniques and Applications, Bologna, Italy, pp. 166–172 (2008)

[26] Jamil, M., Zepernick, H.-J., Pettersson, M. I.: On Integrated Radar and Communication Systems. In: IEEE Military Communications Conference, San Diego, USA, pp. 1–6 (2008)

[27] Karaboga, D.: An Idea Based on Honey Bee Swarm for Numerical Optimization. Technical Report TR06, Erciyes University, Turkey (2005)

[28] Karaboga, D., Basturk, B.: A Powerful and Efficient Algorithm for Numerical Function Optimization: Artificial Bee Colony (ABC) algorithm. Journal of Global Optimization, 39(3), 459–471 (2007)

[29] Karaboga, D., Basturk, B.: On the Performance of Artificial Bee Colony (ABC) Algorithm. Applied Soft Computing 8(1), 687–697 (2008)

[30] Kennedy, J., Eberhart, R. C.: Particle Swarm Optimization. IEEE International Conference on Neural Networks, Piscataway, USA, pp. 1942–1948 (1995)

[31] Lee, K. S., Geem, Z. W.: A New Meta-heuristic Algorithm for Continuous Engineering Optimization: Harmony Search Theory and Practice. Computer Methods Appl. Mech. Eng. 194, 3902–3933 (2005)

[32] Levanon, N., Mozeson, E.: Radar Signals. John Wiley & Sons, Chichester (2004)

[33] Lewis, B. L., Kretschmer, F. F.: A New Class of Polyphase Pulse Compression Codes and Techniques. IEEE Trans. on Aerospace and Electronic Systems 17(3), 364–372 (1981)

[34] Lewis, B. L., Kretschmer, F. F.: Linear Frequency Modulation Derived Polyphase Compression Codes. IEEE Trans. on Aerospace and Electronic Systems 18(4), 637–641 (1982)

[35] Lewis, B. L., Kretschmer, F. F., Shelton, W. W.: Aspects of Radar Signal Processing. Artech House, London (1986)

[36] Liang, J. J., Qin, A. K., Suganthan, P. N., Baskar, S.: Comphrehensive Learning Particle Swarm Optimizer for Global Optimization of Multimodal Functions. IEEE Trans. on Evolutionary Computation 10(3), 281–295 (2006)

[37] Liu, W., Lu, Y. L., Lesturgie, M.: Evolutionary Algorithms Based Sparse Spectrum Waveform Optimization. In: Wicks, M., Mokole, E., Blunt, S., Schneible, R., Amuso, V. (eds.) Principles of Waveform Diversity and Design, pp. 152–162, SciTech Publishing, Rayleigh, (2011)

[38] Luke, S.: Essentials of Metaheuristics, `http://cs.gmu.edu/~sean/book/metaheuristics`.

[39] Michael, J. J.: Sparse Frequency Transmit and Receive Waveform Design. IEEE Trans. on Aerospace and Electronic Systems, 40(3), 851–861 (2004)

[40] Nathanson, F. E., Riley, J. P., Cohen, M. N.: Radar Design Principles: Signal Processing and the Environment. SciTech Publishing, Mendham (1999)

[41] Natarajan, B., Das, S., Stevens, D.: Design of Optimal Complex Spreading Codes for DS-CDMA using an Evolutionary Approach. In: IEEE Global Telecommunications Conference, Dallas, USA, pp. 3882-3886 (2004)

[42] Natarajan, B., Das, S., Stevens, D.: An Evolutionary Approach to Designing Complex Spreading Codes for DS-CDMA. IEEE Trans. on Wireless Communications, 4(5), 2051–2056 (2005)

[43] Nelder, J. A., Mead, R.: A Simplex Method for Function Minimization. Computer Journal 7, 308-313 (1965)

[44] Oppermann, I., Vucetic, B. S.: Complex Spreading Sequences with a Wide Range of Correlation Properties. IEEE Trans. on Commun. 45(3), 365–375 (1997)

[45] Pace, P. E.: Detecting and Classifying Low Probability of Intercept Radar. Artech House, London (2004)

[46] Powell, M. J. D.: An Efficient Method for Finding the Minimum of a Function of Several Variables Without Calculating Derivatives. Computer Journal 7, 152-162 (1964)

[47] Rapajic, P. B., Kennedy, R. A.: Merit Factor Based Comparison of New Polyphase sequences. IEEE Commun. Letters 2(10), 269–270 (1998)

[48] Roberton, M., Brown, E. R.: Integrated Radar and Communications based on Chirped Spread-Spectrum Techniques. In: IEEE International Microwave Symposium, Philadelphia, USA, pp. 611–614 (2003)

[49] Rosenbrock, H. H.: An Automatic Method for Finding the Greatest or Least Value of a Function. Computer Journal, 3(3), 175–184 (1960)

[50] Sumathi, S., Surekha, P.: Computational Intelligence Paradigms: Theory and Application with Matlab. CRC Press, Boca Raton (2010)

[51] Tantar, A.-A., Melab, N., Talbi, El-G.: A Grid-Based Hybrid Hierarchical Genetic Algorithm for Protien Structure Predicition. In: de Vega F.F., Cantú-Paz, E. (eds.) Parallel and Distributed Comptutational Intelligence, vol. 269, pp. 291–319, Springer, Heidelberg (2010)

[52] Tavik, G. C., et al.: The Advanced Multifunction RF Concept. IEEE Trans. Microw. Theory and Techn., 53(3), 1009–1020 (2005)

[53] Venkataraman, P.: Applied Optimization with Matlab Programming. John Wiley & Sons, Chichester (2009)

[54] Walsh, J. L.: A Closed Set of Normal Orthogonal Functions. Am. J. Math. 45, 5–24 (1923)

[55] Weise, T.: Global Optimization Algorithms - Theory and Applications (Self-Published), `http://www.it-weise.de`.

[56] Woodward, P. M.: Probability and Information Theory with Applications to Radar. Artech House, London (1980)

[57] Wysocki, B. J., Wysocki, T. A.: Optimization of Orthognonal Polyphase Spreading Sequences for Wireless Data Applications. In: IEEE Vehicular Technology Conference, Atlantic City, USA, pp. 1894–1898 (2001)

[58] Xu, S. J., Chen, Y., Zhang, P.: Integrated Radar and Communication based on DS-UWB. In: IEEE Ultrawideband and Ultrashort Impulse Signals, Sevastopol, Ukraine, pp. 142–144 (2006)

[59] Xu, S., Chen, B., Zhang, P.: Radar-Communication Integration Based on DSSS Techniques. In: IEEE International Confonference on Signal Processing, Beijing, China, pp. 16–20 (2006)

[60] Yang, X.-S.: Introduction to Mathematical Optimization: From Linear Programming to Metaheuristics. Cambridge International Science Publishing, Cambridge (2008)

[61] Yang, X.-S.: Engineering Optimization: An Introduction with Metaheuristics Applications. John Wiley & Sons, Chichester (2010)

[62] Zepernick, H.-J., Finger, A.: Pseudo Random Signal Processing: Theory and Application. John Wiley & Sons, Chichester (2005)

Part III-A

Part III-A

Multimodal Function Optimisation With Cuckoo Search Algorithm

Part III-A is based on:

M. Jamil and H.-J. Zepernick, "Multimodal Function Optimisation With Cuckoo Search Algorithm," *Int. J. Bio-Inspired Comput.*, vol. 5, no. 2, pp. 73–83, 2013.

Multimodal Function Optimisation With Cuckoo Search Algorithm

Momin Jamil and Hans-Jürgen Zepernick

Abstract

Modern engineering and scientific optimisation problems are becoming complicated. In order to cope with the increasing level of difficulty of these problems, optimisation methods are required to find more than one solution to these problems. The aim of this paper is to gain an insight into the ability of Cuckoo Search to locate more than one solutions for multimodal problems. We also study the performance of this algorithm in the additive white Gaussian noise. Numerical results are presented to show that the Cuckoo search algorithm can successfully locate multiple solutions in both non-noise and additive white Gaussian noise with relatively high degree of accuracy.

Keywords: Cuckoo Search, Additive White Gaussian Noise, Multimodal Optimisation

1 Introduction

Traditional optimisation methods are unsuitable to solve optimisation problems encountered in business, economics, medicine, applied sciences, and engineering. The objective function of these problems could exhibit multiple peaks, valleys, flat hyper-planes of varying heights and are non-linear, non-smooth, non-quadratic or unimodal in nature. For

these problems, the gradient information is either missing, or not computeable. Therefore, solving such problems to optimality poses a major challenge for many researchers around the world.

During the past few years, nature-inspired population based metaheuristic algorithms have replaced traditional optimisation methods to solve modern optimisation problems due to their general applicability and effectiveness. The population-based metaheuristic algorithms use population members to explore the search space for possible solutions using effective search strategies. These strategies are selected in such a way that a dynamic balance between intensification and diversification is maintained. The maintenance of this balance serves two purposes:

1 to identify high-quality solutions in the search space

2 void exploring those areas that lack quality solutions or have already been explored.

In short, search strategies consist of controlled randomization, efficient local search, and selection of the best solution. Usually, randomization is drawn from a uniform or Gaussian distribution.

Algorithms such as tabu search (Glover, 1989) and sequential niche technique (Beasley et al., 1993) have been used to find multiple solutions of a multimodal function. These methods use various techniques that prohibit the convergence to the same solution by preventing the algorithm from exploring again those portions of the search space that have been already explored. In multimodal optimisation problems having multiple optima, it is desirable to find all the possible solutions. Algorithms such as differential evolution (DE), evolutionary strategy (ES), genetic algorithm (GA) and particle swarm optimisation (PSO) have been extensively used to solve such problems. It is shown in Saha and Deb (2010) that these algorithms tend to loose the diversity and converge to global best solution due to genetic drift. The application of these algorithms poses two main challenges to solve multimodal problems with multiple solutions :

1 to maintain adequate population diversity so that multiple optimum solutions can be found

2 a method to preserve and maintain the discovered solution from one generation to another.

Therefore, a *niching* has also been proposed to address the above mentioned challenges in order to solve multimodal problems. Several niching methods have been proposed in the context of metaheuristic algorithms, namely, crowding (DeJong, 1975; Mahfoud, 1995), fitness sharing (Mahfoud, 1995; Goldberg and Richardson, 1987), clearing (Petrowski, 1996), clustering (Tasoulis et al., 2005), stretching and deflation (Parsopolos et al., 2001; Parsopolos and Vrahatis, 2004), parallelisation (Zaharie, 2004), restricted tournament selection (Harik, 1995; Qu and Suganthan, 2010) and speciation (Li et al., 2002).

Flight behavior of animals and insects have been a subject of many studies. These studies have shown that flight behavior of many animals and insects demonstrate the typical characteristics of Lévy flight (Brown et al., 2007; Reynolds and Frey, 2007; Pavlyukevich, 2007). These studies show that animals search for food in a random or quasi-random manner. The foraging path of an animal, in general, is random walk. The next move in the foraging path is based on the current location and the transition probability to the next location. A study conducted in Reynolds and Frey (2007) has shown a Lévy flight style free scale search pattern by fruit flies in their quest for food. They use a series of straight flight paths punctuated by sudden 90 degree turn, a typical characteristic of Lévy flights.

Recently, Lévy flights have been proposed within the context of metaheuristics algorithms to solve optimisation problems (Yang and Deb, 2009, 2010; Yang, 2010). Cuckoo Search (CS) with Lévy flights, is a relatively new metaheursitic optimisation method (Yang and Deb, 2009). It has shown better performance compared to GA and PSO on a limited set of test functions both in 2 and higher dimensional problems (Yang and Deb, 2009, 2010). The purpose of this study is thus two folds:

1 to determine if CS can perform optimisation better than those algorithms in which motion is either simulated by using Gaussian or uniform distributions in case of multiple solution problems

2 to evaluate its ability to locate multiple solutions in additive white Gaussian noise (AWGN) environments.

The rest of the paper is organized as follow. Section 2 presents an overview of CS algorithms. In Section 3, experimental results are presented. In Section 4, we present experimental results on the performance of CS in noisy environment. Finally, Section 5 concludes the paper.

2 Cuckoo Search Algorithm

CS, a relatively new metaheuristic algorithm is inspired by the reproduction strategy of cuckoos and was proposed by Yang and Deb (2009). Some species of cuckoos lay their eggs in the nests of different cuckoo species. When the host bird discovers eggs different than its owns, it either destroys the eggs or abandons the nest all together. This has resulted in the evolution of the cuckoo eggs which mimic the eggs of local hosts (Payne, 2005). In order to apply this to solve the optimisation problems, the algorithm proposed in Yang and Deb (2009) is based on the following three idealized rules:

- Each cuckoo lays a single egg at one time. This egg represents a solution in a problem search space. Cuckoo dumps this egg in randomly chosen nest.
- A fraction of high quality eggs (best eggs or solutions) will be carried over to next generation.
- The host nests are fixed in number and an alien egg can be found in a host nest with a probability of $p_a \in [0, 1]$. If an alien egg is found in a host nest, host bird can either throw away an alien egg or abandon the nest. In such a case cuckoo builds a new nest in a new location which represents a potentially better solution in the problem search space.

According to Yang and Deb (2009), the last assumption can be approximated by a fraction p_a of N nests being replaced by new nests.

This means that new random solutions are generated at new locations in the problem search space. CS uses Lévy flights as a search mechanism for local and global solutions in the problem search space. The Lévy flight is a random walk characterized by a series of instantaneous jumps which obeys a power-law distribution with a heavy tail.

Several optimisation algorithms based on Lévy flights have appeared throughout the literature (Yang and Deb, 2010; Pavlyukevich, 2007; Lee and Yao, 2004). Accordingly, when a new egg (solution) is generated, a Lévy flight is performed starting at the position of a randomly selected egg (solution). If the objective function value at the new solution is better than another randomly selected solution, then the solution is moved to the location (nest). The scale of the random search is controlled by multiplying the generated Lévy flight by a step size α. The step size is related to the domain size of the problem of interest and in most cases $\alpha = 1$ can be used (Yang and Deb, 2009). Therefore, in line with the work of Yang and Deb (2009), we have used $\alpha = 1$ in this paper.

3 Cuckoo Search for Multimodal Problems

In this section, we present the results obtained by applying CS on a set of multimodal functions with multiple solutions. The effectiveness of the CS to handle multimodal problems is verified on a set of benchmark functions having different characteristics.

3.1 Parameter Settings

In Yang and Deb (2009), the number of host nests or population size N was chosen between 15 to 25. However, during this study, we have found that this value is not suitable for functions with multiple solutions scattered throughout the search space. Therefore, selecting a suitable value of N for multimodal functions with multiple solutions needs some experimentation. We have used different values of $N = 50, 100, 150, 200$ and found that $N = 100$ seems to be sufficient for most multimodal optimisation problems with multiple solutions. For tougher problems, larger N can be used, though excessively large N should not be used

unless there is no better alternative, as it is more computationally expensive (Yang and Deb, 2010).

According to Yang and Deb (2009), the parameter p_a, i.e., the fraction of the nests to abandon, is not strongly related to the convergence rate of the algorithm and recommended to use $p_a = 0.25$. We have found that $p_a = 0.25$ is suitable for unimodal optimisation problems, but does not work well for multimodal problems. We have used different values of p_a and tested them on a small set of benchmark functions. The value that produced the best result was chosen and subsequently used for all the test functions. We have found that $p_a = 0.75$ seems to be a suitable choice for most multimodal problems with multiple solutions. Therefore, we will use the following set of parameters for all the experiments, unless we mention new settings for one or other parameters:

- Number of Cuckoos: $N = 100$
- Number of Generation: $G = 1500$
- Number of Runs: $R = 100$
- Fraction of worse nests to be abandoned: $p_a = 0.75$

3.2 Numerical Results

In various applications, the objective function exhibit multiple global minima. Ideally, an optimisation algorithm must be able to find all the global minima or solutions (Rönkkönen, 2009). In general, CS can find global solutions even in higher dimensions (Yang and Deb, 2009, 2010), but its performance for test functions with multiple global minima having few or no local minima has not been evaluated. There are many benchmark test functions in the literature to test the performance of optimisation algorithms (GAMS World, Global Library, http://www.gamsworld.org/global/globallib.html). In this section, we perform an experimental evaluation of CS by using ten well-chosen test functions with multiple global minima and with few or many local minima. The global minimum of the objective functions were known *a priori*. These functions include two

functions with two global optima [Yang (2008) multimodal and test-tube holder (Mishra, 2006)], one function each with three [Brannin (http://www-optima.amp.i.kyoto-u.ac.jp/member/student/hedar/Hedar_files/TestGO_files/Page364.htm)], six (Root 6) and nine global minima [Henrik (Madsen and Žilinskas, 2000)] and four functions with four global minima [Carrom table (Mishra, 2006), Himmelblau (Brits et al., 2007), holder table 1 (Mishra, 2006) and pen holder (Mishra, 2006)].

Several different performance measures have appeared in the literature to evaluate the performance of global optimisation algorithms (Rahnamayan et al., 2008). In practice, for stochastic methods, the results are reported as averages from certain number of independent runs. We have examined the mean, standard deviation (SD) and standard error of mean (SEM) attained with a certain population size and number of generations. The algorithm was executed 100 times with different random seeds for all considered functions. The best fitness value produced by the algorithm after each run was recorded. The mean fitness values, standard deviation and SEM for these functions are presented in Table 1. The number of function evaluations (NFE) required by the CS to converge to a solution averaged over the number of independent runs is also reported. From the results presented in Table 1, it can be seen that CS performs equally well on almost all of the functions tested. The only exception being the Root 6 which shows a small deviation of 10^{-3} from the known global minima.

Figures 1 and 2 show the contour plots of Deb 3 and Parsopoulos functions. Deb 3 have 25 global minima that are unevenly placed in the function landscape (Brits et al., 2007). On the other hand, for Parsopoulos function the number of global minima depend on the problem domain size (Parsopolos and Vrahatis, 2002). For a given domain size of $[-5, 5]^D$, where D represents the problem dimension, it has 12 global minima scattered throughout the function landscape. The $'+'$ sign in the Figures 1 and 2 represents the global minima (solutions) located by the CS in 100 independent runs with the parameter settings mentioned in Section 3.1. From the results in Table 1 and representative figures for Deb 3 and Parsopoulos functions, we can see that CS can locate global minimum with relatively high degree of accuracy.

Table 1: Statistical results of 100 runs obtained by CS for 2-D functions.

Function	Known Min.	Mean NFE		CS
Yang multimodal	0.8512	32380	Mean	0.8512
			SD	$1.2274e-15$
			SEM	$1.2774e-16$
Testtube holder	-10.8723	29469	Mean	-10.8723
			SD	$1.7853e-15$
			SEM	$1.7853e-16$
Brannin	0.39788	22927	Mean	0.3979
			SD	$5.579e-17$
			SEM	$5.579e-18$
Carrom table	-24.1568	18611	Mean	-24.1568
			SD	$1.7853e-14$
			SEM	$1.7853e-15$
Himmelblau	0	14902	Mean	0
			SD	0
			SEM	0
Holder Table 1	-19.2085	18080	Mean	-19.2085
			SD	$2.8565e-14$
			SEM	$2.8565e-15$
Pen holder	-0.9635	17145	Mean	-0.9635
			SD	$2.23116e-15$
			SEM	$2.2316e-16$
Root 6	-1	5569	Mean	-0.9997
			SD	$1.6506e-04$
			SEM	$1.6506e-05$
Hansen	-176.5417	21980	Mean	-176.5417
			SD	$5.7130e-14$
			SEM	$5.7130e-15$
Henrik		18886	Mean	-24.0624
			SD	$1.0712e-14$
			SEM	$1.0712e-015$

Notes: Mean NFE: mean of number of function evaluations
Mean: mean of fitness value
SD: standard deviation of the fitness values
SEM: standard error of mean

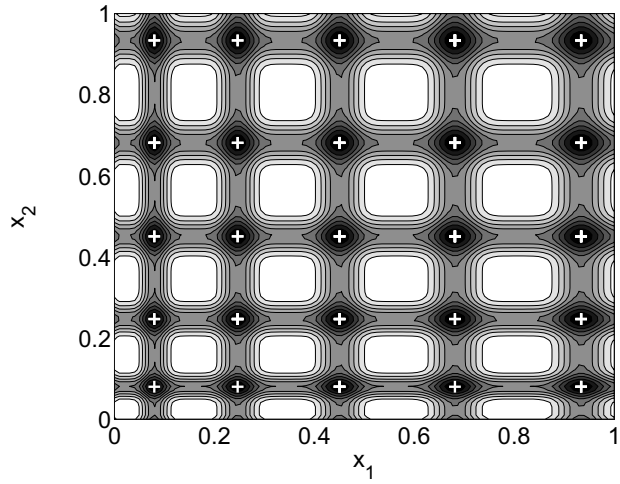

Figure 1: Contour plot of Deb 3 function (25 global minima indicated by $'+'$ found by CS after 100 independent runs).

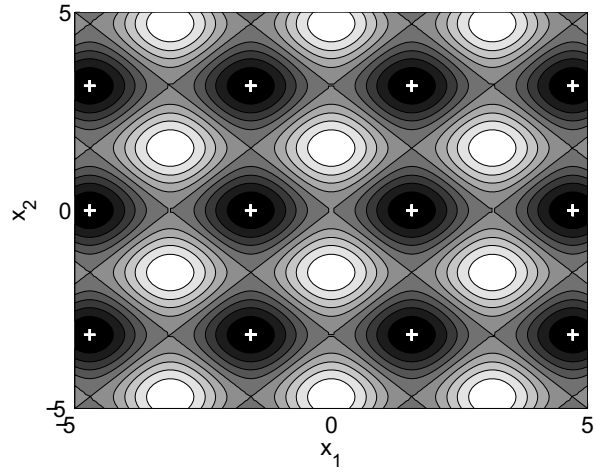

Figure 2: Contour plot of Parsopoulos function (12 global minima indicated by $'+'$ found by CS after 100 independent runs).

In order to measure *accuracy*, i.e., the ability and effectiveness of the CS to accurately locate all of the multiple minima, a *level of accuracy*, $\epsilon \in (0, 1]$ is defined. The computed solution will be considered as a global optimum, if the Euclidean distance of a computed solution to a known global optimum is less than a pre-defined *level of accuracy* ϵ. The *% Converged* in Table 2 signifies the number of the independent runs converged on the solutions. From the results presented in Table 2, it can be seen that CS could find all the solutions for a specified value of ϵ. These results also demonstrate the *performance consistency* of the algorithm. This is a measure of ability of the algorithm to consistently locate all the solutions for each function for a given set of parameters.

From the results presented in this section, we can attribute the ability of CS in handling unimodal and multimodal to:

1 a fine balance of randomization and intensification

2 relatively fewer number of control parameters.

A prerequisite for any metaheuristic algorithm is to maintain a good balance between intensive local search and efficient exploration of the function landscape. There are three ways to carry out randomization:

1 uniform randomization

2 random walks

3 Lévy flights based on heavy tail distributions.

Lévy flights are considered the most suitable for randomization on global scale (Yang and Deb, 2009, 2010; Yang, 2010). The ability of CS to find or locate multiple solutions to multimodal problems can be attributed to Lévy flights which keep dynamic balance between the exploitation of the accumulated search experience (intensification) and exploration of the search space (diversification). Lévy flights are based on the fact that the power law distribution of Lévy distribution at large step lengths will induce an exploration at any stage of the convergence. This enables the CS to explore the search space more effectively and thus enabling the CS to escape local minima. On the other hand, there are only two control parameters in the CS, i.e., the population size (number of cuckoos) N and fraction of worse nests to be abandoned

Table 2: CS performance on test function for $\epsilon = 10^{-5}$

		% Number of Runs Converged on Solutions								
Function	Solutions	1 Sol	2 Sol	3 Sol	4 Sol	5 Sol	6 Sol	7 Sol	8 Sol	9 Sol
Yang multimodal	2	47	53	–	–	–	–	–	–	–
Testtube holder	2	46	54	–	–	–	–	–	–	–
Brannin	3	25	41	34	–	–	–	–	–	–
Carrom table	4	25	27	30	18	–	–	–	–	–
Himmelblau	4	32	17	31	20	–	–	–	–	–
Holder Table 1	4	32	24	28	16	–	–	–	–	–
Pen holder	4	26	28	22	24	–	–	–	–	–
Root 6	6	8	5	10	8	40	29	–	–	–
Hansen	9	5	8	15	14	16	16	10	10	6
Henrik	9	10	13	9	8	20	12	8	8	12

p_a. Fixing the value of N, p_a essentially controls the elitism and the balance of randomization and local search (Yang and Deb, 2009, 2010).

4 CS for Noisy Environments

The function optimization in a noisy environment occurs in various applications such as experimental optimization. The problem of locating either minima or maxima of a function is vital in many physical applications such as spectral analysis and radio-astronomy (Parsopolos and Vrahatis, 2002). Optimization of functions in noise is traditionally carried out using the simplex method by Fletcher (1987) and Nelder and Mead (1965). The advantages and limitations of this algorithm in noisy and noiseless environment are well documented in a literature. Different variants of this method have been proposed to overcome the deficiencies of the original algorithm (Torczon, 1991). More sophisticated methods and extensive studies in this direction are discussed in Arnold (2001). Different population based algorithms, e.g., PSO have also been used to optimize functions in additive and multiplicative noise environments (Parsopolos and Vrahatis, 2002).

Information about the function $f(x)$ is obtained in the form of $f^{\eta}(x)$, where $f^{\eta}(x)$ is an approximation to the true function value $f(x)$, corrupted by a small amount of noise η. The influence of additive white Gaussian noise on the values of the objective functions was simulated according to Elster and Neumaier (1997), and is given as

$$f^{\eta} = f\left(x\right) + \eta, \qquad \eta \sim N\left(0, \sigma^2\right) \tag{1}$$

where $\eta \sim N(0, \sigma^2)$ is a Gaussian distributed random variable with zero mean and standard deviation σ^2.

4.1 Numerical Results

In this section, the influence of AWGN on nine optimization benchmark test problems in two dimensions are investigated. However, these problems can also be extended to dimensions greater than 2. These problems include three functions with single

global optima [Lévy 5 (Parsopolos and Vrahatis, 2002), Michaelwicz (Yang, 2008) and periodic (GAMS World, Global Library, http://www.gamsworld.org/global/globallib.html)] and six problems with multiple global optima [Carrom table (4) (Mishra, 2006), Holder Table 1 (4) (Mishra, 2006), Modified Ackley(2) (Rönkkönen, 2009), Yang mutimodal(2) (Yang, 2008), Parsopoulos (12) (Parsopolos and Vrahatis, 2002) and Root function(6)]. The term enclosed in the brackets indicates the number of global optima for these problems. Experiments were carried out for three different levels of noise variances $\sigma^2 = 0.025, 0.05$ and 0.09. At each function evaluation, noise was added to the actual function according to (1) for different values of variances. For each variance value, 100 independent runs of CS were performed. The other set of parameters N, G, R and p_a were kept the same as specified in Section 3.

Based on the MAPE results presented in Table 3, it can be seen that the increasing value of variance σ^2 deteriorates the ability of CS to locate global minimum/minima for unimodal (Michalewicz and periodic) and multimodal (Yang multimodal and Root 6) functions. A performance degradation of more than 40%, 30% and around 20%, respectively, can be observed for Yang multimodal, periodic and Michaelwicz functions. Both Yang multimodal and periodic functions are strong multimodal function with many local minima. They are considered to be challenging functions to optimize for any optimization algorithm even in the absence of noise. Their challenging nature can be seen from the respective plots in Figures 3(a), 3(b), 4(a) and 4(b).For both of these function, the global minimum (periodic) and mimima (Yang multimodal) are surrounded by large number of local minima. The periodic function has only a single global minimum which is surrounded by 49 local minima as shown in Figure 4(a).For clarity, the periodic function in one dimension is also shown in Figure 4. The deteriorating effect of AWGN variance $\sigma^2 = 0.025$ on Yang multimodal function is shown in Figure 5. This becomes aggravated with an increasing value of variance σ^2.

Next, in Tables 4 and 5, we compare the mean Euclidean distance (the difference between the obtained and actual global minimum) of the computed solution from known *a priori* solution for three level of

variances. The term enclosed in the brackets in front of the function names represent the number of global minimum for these functions. From the results presented in Tables 4 and 5, we can see that as the value of σ^2 increases, the ability of the CS to locate global minima decreases significantly for Yang multimodal and periodic functions. For these two functions, the largest difference between the obtained and actual global minimum can be observed. The results in Tables 4 and 5 also demonstrate the performance consistency of the CS to locate all the solutions for each function for a given set of parameters even in the presence of noise. The success rate of the algorithm on all functions is 100% in the presence of noise. Figure 6 depicts a notoriously difficult Levy 3 (18 global minima) function in the presence of AWGN with variance $\sigma^2 = 0.09$. This shows that the CS has an exceptional ability to find all of the minima for this function.

Interestingly, in case of functions with more that two global minima (with the exception of Yang multimodal) such as Carrom Table, Levy 5, Hansen, Holder Table and Modified Ackley) with few or many local minima, CS seems to perform relatively well in the additive noise environment even for the highest value of variance σ^2. It seems that the noise plays a positive role for these multimodal functions by helping the CS to escape local minima of the objective function. For these multimodal functions, the performance degradation is significantly low for the highest value of variance σ^2. One possible explanation for the unimodal functions performance deterioration could be that high values of variance σ^2 can create deep troughs (for minimization problems) or crests (for maximization problems) in the function landscape that are mistaken by the CS or any other optimisation algorithm as a global minimum or maximum.

Table 3: Statistical results of 100 runs obtained by CS for 2-D functions in AWGN

Function	Known Minima		$\sigma^2 = 0.025$	$\sigma^2 = 0.05$	$\sigma^2 = 0.09$
Carrom table	-24.1568	Mean	-24.2585	-24.3652	-24.5259
		StdDev	0.0074	0.0165	0.0245
		SEM	$7.2571e-04$	0.0017	0.0024
		MAPE	0.4207	0.8628	1.5280
Holder Table 1	-19.20850	Mean	-19.3123	-19.4164	-19.5822
		StdDev	0.0068	0.0131	0.0280
		SEM	$6.8064e-04$	0.0013	0.0028
		MAPE	0.5401	1.0825	1.9455
Hansen	-176.5418	Mean	-176.6375	-176.7328	-176.8925
		StdDev	0.0070	0.0131	0.0294
		SEM	$6.9731e-04$	0.0013	0.0029
		MAPE	0.0542	0.1082	0.1986
Lévy 5	-176.1375	Mean	-176.2284	-176.3208	-176.4724
		StdDev	0.0074	0.0148	0.0293
		SEM	$7.4028e-04$	0.0015	0.0029
		MAPE	0.0516	0.1041	0.1902
Michaelwicz	-1.8013	Mean	-1.9031	2.0075	-2.1634
		StdDev	0.0066	0.0149	0.0221
		SEM	$6.5815e-04$	0.0015	0.0022
		MAPE	5.6538	11.4447	20.1011
Modified Ackley	-4.59012	Mean	-4.6917	-4.7954	-4.9619
		StdDev	0.0066	0.0150	0.0244

continued on next page

continued from previous page					
		SEM	$6.5623e-04$	0.0015	0.0024
		MAPE	2.2119	4.4722	8.1001
Yang multimodal	-0.851	Mean	-0.9519	-1.0573	-1.2211
		StdDev	0.0068	0.0157	0.0268
		SEM	$6.8131e-04$	0.0016	0.0027
		MAPE	11.8607	24.2425	43.4872
Periodic	0.9	Mean	0.8114	0.7237	0.5877
		StdDev	0.0088	0.0154	0.0254
		SEM	$8.799e-04$	0.0015	0.0025
		MAPE	9.8407	19.5857	34.5851
Root 6	-1	Mean	-1.0982	-1.1943	-1.3435
		StdDev	0.0067	0.0133	0.0256
		SEM	$6.714e-04$	0.0013	0.0026
		MAPE	9.8166	19.4323	34.3513

Notes: Mean: mean of fitness value
SD: standard deviation of the fitness values
SEM: standard error of mean
MAPE: mean absolute percentage error

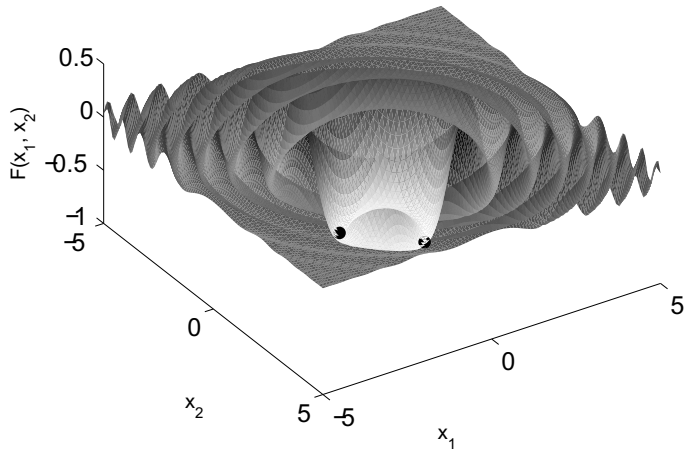

(a)

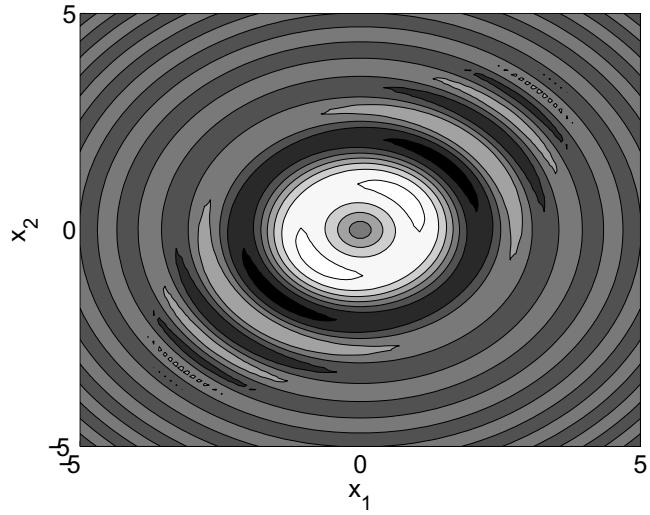

(b)

Figure 3: Plot of Yang multimodal function: (a) 3-D view (the global minima are represented by two solid black •) and (b) contour plot.

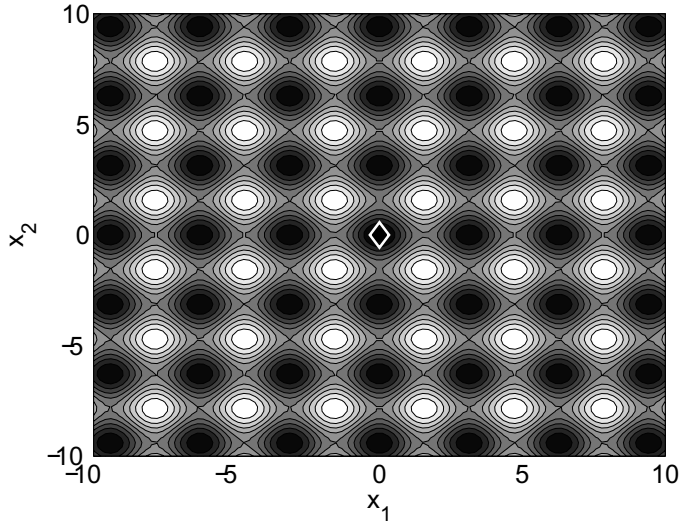

(a)

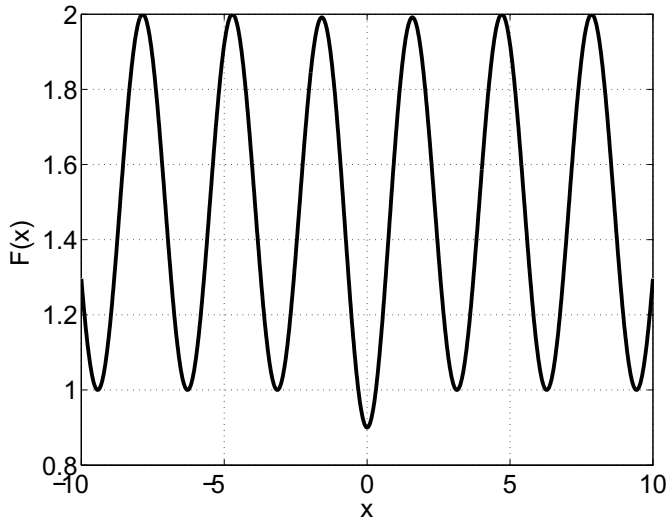

(b)

Figure 4: Periodic function: (a) Contour plot (global minimum marked with ⋄) (b) periodic function in 1-D.

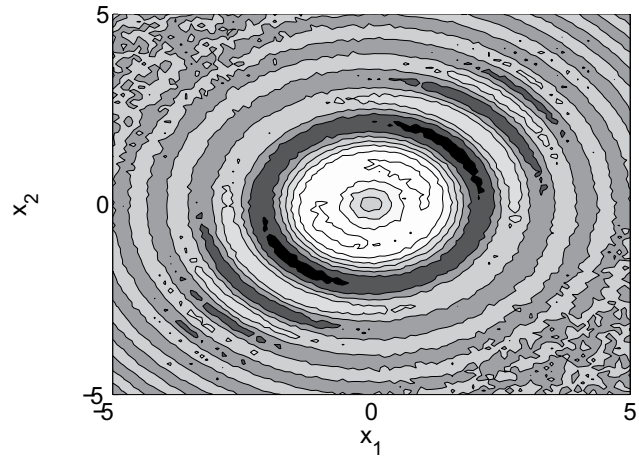

Figure 5: Contour plot of Yang multimodal function corrupted by AWGN with $\sigma^2 = 0.025$.

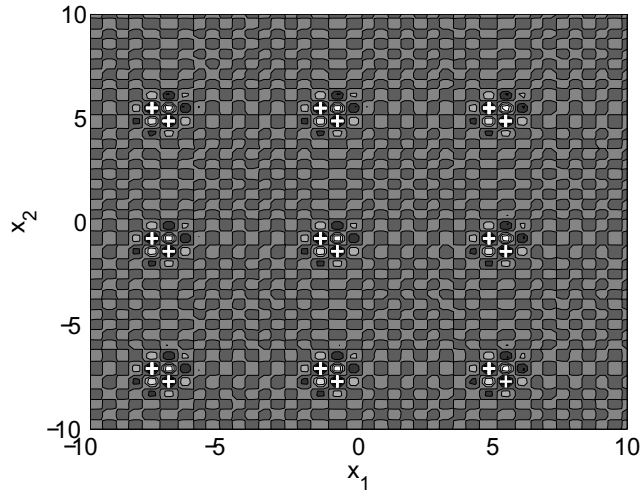

Figure 6: Contour plot of Lévy 3 function with 18 global minima indicated by $'+'$ found by CS after 100 independent runs in the presence of AWGN with $\sigma^2 = 0.09$.

Table 4: CS Performance on test function with AWGN with variances $\sigma^2 = 0.025, 0.05$, and 0.09

		Mean Euclidean Distance of Computed Solution from Known Solution								
Function	σ^2	1 Sol	2 Sol	3 Sol	4 Sol	5 Sol	6 Sol	7 Sol	8 Sol	9 Sol
Lévy 5 (1)	0	$6.6975e-05$	–	–	–	–	–	–	–	–
	0.025	0.0021	–	–	–	–	–	–	–	–
	0.05	0.0025	–	–	–	–	–	–	–	–
	0.09	0.0036	–	–	–	–	–	–	–	–
Michaelwicz (1)	0	$4.1552e-04$	–	–	–	–	–	–	–	–
	0.025	0.0123	–	–	–	–	–	–	–	–
	0.05	0.0166	–	–	–	–	–	–	–	–
	0.09	0.0224	–	–	–	–	–	–	–	–
Periodic (1)	0	$6.9775e-05$	–	–	–	–	–	–	–	–
	0.025	0.0699	–	–	–	–	–	–	–	–
	0.05	0.0830	–	–	–	–	–	–	–	–
	0.09	1.9558	–	–	–	–	–	–	–	–
Yang multimodal (2)	0	$6.5892e-05$	$6.8507e-05$	–	–	–	–	–	–	–
	0.025	0.1472	0.1674	–	–	–	–	–	–	–
	0.05	0.2102	0.1981	–	–	–	–	–	–	–
	0.09	0.3723	0.3047	–	–	–	–	–	–	–
Modified Ackley (2)	0	$7.3868e-05$	$6.4704e-05$	–	–	–	–	–	–	–
	0.025	0.0235	0.0237	–	–	–	–	–	–	–
	0.05	0.0335	0.0343	–	–	–	–	–	–	–
	0.09	0.0376	0.0490	–	–	–	–	–	–	–
Carrom table (4)	0	$6.2865e-05$	$6.2362e-05$	$7.0380e-05$	$6.3661e-05$	–	–	–	–	–
	0.025	0.0121	0.0112	0.0108	0.0133	–	–	–	–	–
	0.05	0.0155	0.0161	0.0174	0.0152	–	–	–	–	–
	0.09	0.0193	0.0223	0.0109	0.0231	–	–	–	–	–
Holder table 1 (4)	0	$6.8236e-05$	$6.1328e-05$	$6.0586e-05$	$8.2733e-05$	–	–	–	–	
	0.025	0.0214	0.0185	0.0163	0.0171	–	–	–	–	–
	0.05	0.0204	0.0262	0.0195	0.0221	–	–	–	–	–
	0.09	0.0298	0.0349	0.0328	0.0339	–	–	–	–	–

Table 5: CS Performance for Hansen function in AWGN with variances $\sigma^2 = 0.025, 0.05$, and 0.09

Solution	$\sigma^2 = 0$	$\sigma^2 = 0.025$	$\sigma^2 = 0.05$	$\sigma^2 = 0.09$
1 Sol	$5.9062e-05$	0.0022	0.0017	0.0024
2 Sol	$6.993e-05$	0.0019	0.0022	0.0034
3 Sol	$5.8877e-05$	0.0019	0.0033	0.0038
4 Sol	$6.9006e-05$	0.0016	0.0033	0.0032
5 Sol	$6.1915e-05$	0.0015	0.0017	0.0034
6 Sol	$7.06995e-05$	0.0021	0.0021	0.0029
7 Sol	$6.5163e-05$	0.0021	0.0019	0.0032
8 Sol	$6.5163e-05$	0.0015	0.0025	0.0034
9 Sol	$6.3339e-05$	0.0017	0.0020	0.0047

5 Conclusion

Population based algorithms such as CS, present a viable alternative to existing numerical optimisation techniques. Population based algorithms can search the function landscape effectively. In this paper, the ability of CS to solve unimodal and mutimodal problems in non-noise and additive white Gaussian noise was investigated. Performance results were reported for a set of test functions with varying level of difficulty, number of minima and different level of noise variances. The experimental results indicate that CS is very stable and efficient in the presence of noise. It is a very noise-tolerant method and can be used for minimization or maximization of noisy functions. It has performed exceptionally well even in the presence of noise with high standard deviation. Conclusively, CS appears to be a very useful technique for solving global optimisation problems, and offers a good alternative where other techniques fail. Although, further research may be required to fully comprehend the dynamics and the potential limits of the CS.

References

Arnold, D. V. (2001), *Local Performance of Evolution Strategies in the Presence of Noise*, PhD thesis, Department of Computer Science, Uni. of Dortmund, Germany.

Beasley, D., Bull, D. R. and Martin, R. R. (1993), 'A sequential niche technique for multimodal function optimization', *Evol. Comput.,* Vol. 1, No. 2, pp. 101–125.

Brits, R., Engelbrecht, A. P. and van den Bergh, F. (2007), 'Locating multiple optima using particle swarm pptimization', *Applied Mathematics and Computation,* Vol. 189, No. 12, pp. 129–138.

Brown, C., Liebovitch, L. S. and Glendon, R. (2007), 'Lévy flights in dobe ju/'hoansi foraging patterns', *Human Ecology, Time and African Land Use: Ethnography and Remote Sensing* Vol. 35, No. 1, pp. 129–138.

DeJong, K. A. (1975), *An Analysis of the Behavior of a class of Genetic Adaptive System*, PhD thesis, PhD Thesis, Uni. of Michigan, USA.

Elster, C. and Neumaier, A. (1997), 'A method of trust region type for minimizaing noisy functions', *Computing,* Vol. 58, No. 1, pp. 31–46.

Fletcher, R. (1987), *Practical Methods of Optimization*, Wiley-Interscience, New York, NY, USA.

GAMS World (2000), 'Global Library', [online] http://www.gamsworld.org/global/globallib.html.

Glover, F. (1989), 'Tabu search – Part 1', *ORSA J. on Computing,* Vol. 1, No. 3, pp. 190–206.

Goldberg, D. E. and Richardson, J. (1987), 'Genetic algorithms with sharing for multimodal function optimization', *Proc. Int. Conf. on Genetic Algorithms and Their Application*, Hillsdale, NJ, USA, pp. 41–49.

Harik, G. R. (1995), 'Finding multimodal solutions using resticted tournament selection', *Proc. Int. Conf. on Genetic Algorithms and Their Application*, San Francisco, USA, pp. 24–31.

Lee, C. Y. and Yao, X. (2004), 'Evolutionary programming using mutations based on lévy probability distribution', *EEE Trans. on Evol. Comput.* Vol. 8 No. 1, pp. 1–13.

Li, J., Balazs, M. E., Parks, G. T. and Clarkson, P. J. (2002), 'A species conserving genetic algorithm for multimodal function optimization', *Evol. Comput.* Vol. 10 No. 2, pp. 207–234.

Madsen, K. and Žilinskas, J. (2000), 'Testing branch-and-bound methods for global optimization', [online] http://www2.imm.dtu.dk/documents/ftp/tr00/tr05_00.pdf. (accessed 31 March 2012).

Mahfoud, S. W. (1995), *Niching Methods for Gentic Algorithms*, PhD thesis, Uni. of Illinois at Urbana-Champaign, IL, USA.

Mishra, S. (2006), 'Some new test functions for global optimization and performance of repulsive particle swarm method', [Online] http://mpra.ub.uni-muenchen.de/2718. (accessed 31 March 2012).

Nelder, J. A. and Mead, R. (1965), 'A simplex method for function minimization', *Computer J.,* Vol. 7, No. 4, pp. 308–313.

Parsopolos, K. and Vrahatis, M. (2002), 'Recent approaches to global optimization problems through particle swarm optimization', *Natural Computing,* Vol. 1, No. 2–3, pp. 235–306.

Parsopolos, K. and Vrahatis, M. (2004), 'On the compuation of all minima through particle swarm optimization', *IEEE Trans. on Evol. Comput.,* Vol. 8, No. 3, pp. 211–224.

Parsopolos, K., Plagianakos, V., Magoulas, G. and Vrahatis, M. (2001), 'Objective function "stretching" to alleviate convergence to local minima', *Nonlinear Analysis,* Vol. 47, No. 5, pp. 3419–3424.

Pavlyukevich, I. (2007), 'Lévy flights, non-local search and simulated annealing', *J. Comput. Phys.,* Vol. 226, No. 2, pp. 1830–1844.

Payne, R. B. (2005), *The Cuckoos*, Oxford University Press, New York, USA.

Petrowski, A. (1996), 'A clearing procedure as a Niching method for genetic algorithms', *IEEE Int. Conf. on Evol. Comput.*, Nagoya, Japan, pp. 798–803.

Qu, B.-Y. and Suganthan, P. (2010), 'Novel multimodal problems and differential evolution with ensemble of restricted tournament selection', *IEEE Cong. on Evol. Comput*, Barcelona, Spain, pp. 1–7.

Rahnamayan, S., Tizhoosh, H. R. and Salama, M. M. A. (2008), 'Opposition-based differential evolution', *IEEE Trans. Evol. Comput.,* Vol. 12, No. 1, pp. 64–79.

Reynolds, A. M. and Frey, M. A. (2007), 'Free-flight odor tracking in dorsophila is consistent with an optimal intermittent scale-free search', *PLoS One,* Vol. 2, No. 4, pp. e354.

Rönkkönen, J. (2009), *Continuous Multimodal Global Optimization with Differential Evolution-Based Methods*, PhD thesis, Lappeenranta University of Technology, Finland.

Saha, A. and Deb, K. (2010), 'A bi-criterion approach to multimodal optimization: Self-adaptive approach', *Proc. Int. Conf. on Simulated Evolution and Learning*, Kanpur, India, pp. 95–104.

Tasoulis, D., Plagianakos, V. and Vrahatis, M. (2005), 'Clustering in evolutionary algorithms to effectively compute simultaneously local and global minima', Vol. 2, *IEEE Cong. on Evol. Comput*, Edinburgh, UK, pp. 1847–1854.

Torczon, V. (1991), 'On the convergence of the multidimensional search algorithm', *SIAM J. Optimization,* Vol. 1, No. 1, pp. 123–145.

Yang, X.-S. (2008), *Introduction to Mathematical Optimization:From Linear Programming to Metaheuristics*, Cambridge International Science Publishing, Cambridge, UK.

Yang, X. S. (2010), Firefly algorithm, Lévy flights and global optimization, *in* M. Bramer, R. Ellis and M. Petridis, eds, 'Research and Development in Intelligent Systems', Vol. XXV1, Springer, pp. 209–218.

Yang, X. S. and Deb, S. (2009), 'Cuckoo search via Lévy flights', *Proc. World Congress on Nature and Biological Inspired Computing*, Coimbatore, India, pp. 210–214.

Yang, X. S. and Deb, S. (2010), 'Engineering optimization by cuckoo search', *Int. J. Mathematical Modelling and Numerical Optimization,* Vol. 1, No. 4, pp. 330–343.

Zaharie, D. (2004), 'Extension of differential evolution algorithm for multimodal optimization', *Int. Symp. on Symbolic and Numeric Algorithms for Scientific Computing*, Timisoara, Romania, pp. 523–534.

Part III-B

Part III-B

Synthesizing Cross-Ambiguity Functions Using An Improved Bat Algorithm

Part III-B is based on:

M. Jamil, H.-J. Zepernick, and X.-S. Yang, "Synthesizing Cross-Ambiguity Functions Using Improved Bat Algorithm," Book Chapter in *Recent Advances in Swarm Intell. and Evol. Comput.*, vol. 585, Studies in Comput. Intell., Springer International Publishing, Switzerland, pp. 179–202, 2015.

Synthesizing Cross-Ambiguity Functions Using An Improved Bat Algorithm

Momin Jamil, Hans-Jürgen Zepernick, and Xin-She Yang

Abstract

The cross-ambiguity function (CAF) relates to the correlation processing of signals in radar, sonar, and communication systems in the presence of delays and Doppler shifts. It is a commonly used tool in the analysis of signals in these systems when both delay and Doppler shifts are present. In this chapter, we aim to tackle the CAF synthesization problem such that the synthesized CAF approximates a desired CAF. A CAF synthesization problem is addressed by jointly designing a pair of waveforms using a metaheuristic approach based on the echolocation of bats. Through four examples, it is shown that such an approach can be used as an effective tool in synthesizing different types of CAFs.

Keywords Cross-ambiguity function · Metaheuristic algorithm · Improved bat algorithm · CAF synthesization

1 Introduction

In a conventional matched filter receiver, the internal reference waveform is a duplicate of the transmitted signal, i.e., the receiver reference waveform is matched to the transmitted signal [1]. However, in radar applications, the appropriate time delay and compression must be taken into account at the receiver side. Therefore, in a conventional matched filter receiver, the receiver waveform is a replica of the transmitted

signal with appropriate time delay and time compression. However, a conventional receiver is not able to take care of clutter or jamming suppression. In a radar system, clutter appears as signal echoes with different delays or Doppler shifts compared to the signal of interest. In order to suppress impairments due to clutter and interference, it is desirable to minimize these effects at the receiver side. Accordingly, a joint design of the transmit signal and receive filter is desirable such that the signal-to-clutter-plus-interference ratio (SCIR) of the receiver output is maximized at the time of target detection [2]. As a result, an alternative to conventional receivers, known as a general or optimum receiver, was proposed in [1]. This receiver can be used as a trade-off between the signal-to-noise ratio (SNR) for improved SCIR [1]. In an optimum receiver, the internal or reference waveforms (or equivalent filter) may be deliberately mismatched to reduce the sidelobes in the delay-Doppler plane.

The aforementioned joint design for clutter/interference suppression has been addressed in [2–9] and the references therein. However, a joint design of the mismatched filter at the receiver side and the transmit signal leads to a more complex optimization problem that involves either assessing cross-correlation (CC) properties with respect to delay in the case of negligible Doppler shifts or focusing on cross-ambiguity function (CAF) characteristics in the delay-Dopper plane otherwise [4, 10].

A performance measure frequently used to assess waveforms for radar, sonar, and communication applications in the presence of delay and Doppler shifts, known as ambiguity function (AF), was proposed in [11]. An AF is a function of two variables representing correlation properties of a signal in the delay-Doppler plane. It provides a mathematical representation of the response of a matched filter to a received waveform. The waveform design that would yield an optimum AF has been on the forefront of research for many years. In an ideal case, an AF would have the shape of a spike at the origin and zero elsewhere in the delay-Doppler plane. Although such an AF is certainly desirable, in practice, it is not realizable for signals having finite energy. As a result, large efforts have been given to waveform designs that relax the zero sidelobe constraint throughout the delay-Doppler plane to uniformly

low sidelobes, while still maintaining a reasonable large value at the origin. In practice, radar waveforms are often designed by minimizing the sidelobes of an auto-correlation function (ACF), i.e., by basically matching pre-defined specifications only to the zero-Doppler cut of an AF [12].

In [11], the importance of signal designs using waveform synthesis for radar and sonar applications has been stressed. Nevertheless, the search for practical solutions to the synthesis problem still poses a challenge to radar system engineers. A first known mathematical solution to the synthesization problem was presented in [13]. However, this solution has two drawbacks: (i) it requires that the shape of a desired ambiguity function is given in analytical form, (ii) it does not cope with settings where only certain parts of the ambiguity surface are to be approximated, e.g., clear area in and around a large neighbourhood of the origin. As a consequence, this solution is of limited interest to practical radar applications. In practice, radar engineers typically have a general idea about the desirable shape of an AF rather than an exact expression of it as a mathematical function. Furthermore, in many scenarios, it is not even necessary to specify the shape of an AF for the entire delay-Doppler plane. In other words, the region where an AF is required to produce small values very much depends on the particular radar application. For example, the Doppler shift may be much smaller compared to the bandwidth of the transmitted waveform which can be in the order of several megahertz. In this case, the AF for Doppler shifts beyond the maximum induced shifts is not required. An alternative approach of constructing a waveform with optimal ambiguity surface in a region around the main lobe of an AF using well-know Hermite waveforms has been presented in [14].

In single-input single-output (SISO) radar systems, the problem becomes to synthesize a single radar waveform that approximates a desired auto-ambiguity function (AAF) of pre-defined magnitude over the delay-Doppler plane. On the other hand, multiple-input multiple-output (MIMO) radar systems or communication systems involve pairs of signals rather than a single waveform. Accordingly, the synthesis problem focuses on the CAF between a pair of signals. In the considered context, the CAF describes the receiver response to a mis-

matched signal as a function of time and Doppler shift. In particular, the continuous-time CAF is defined as

$$\chi(\tau, f_d) = \int_{-\infty}^{\infty} a(t) b^*(t+\tau) \exp(j2\pi f_d t) dt \tag{1}$$

where $a(t)$ and $b(t)$ are arbitrary waveforms as a function of time t, τ is delay, f_d denotes Doppler frequency/Doppler shift, $(\cdot)^*$ denotes complex conjugate, and $j = \sqrt{-1}$. In practice, the CAF is applicable for a SISO radar system when $a(t)$ is the transmit signal and $b(t)$ represents the receive filter [15]. Similarly, the CAF is used for a MIMO radar system when both $a(t)$ and $b(t)$ are different transmit signals [16]. In a conventional matched filter receiver, where the receiver reference waveform is matched to the transmitted signal [1], i.e. $a(t) = b(t)$, the CAF becomes an AAF.

Let us now consider, two signals $a(t)$ and $b(t)$, consisting of a train of N pulses $s_i(t)$ and $s_j(t)$, respectively, as

$$a(t) = \sum_{i=1}^{N} a_i s_i(t) \tag{2}$$

$$b(t) = \sum_{j=1}^{N} b_j s_j(t) \tag{3}$$

where the coefficients a_i and b_i can be expressed as column vectors of length N as

$$\mathbf{a} = (a_1, a_2, \ldots, a_N)^T \tag{4}$$

$$\mathbf{b} = (b_1, b_2, \ldots, b_N)^T \tag{5}$$

and $s_k(t)$; $k = i, j$ denotes a pulse shaping function. For example, a rectangular pulse shaping function is defined as

$$s_k(t) = \frac{1}{\sqrt{T_c}} s\Big[\frac{t-(k-1)T_c}{T_c}\Big], \quad k = 1, 2, \ldots, N \tag{6}$$

where T_c denotes the pulse duration and

$$s(t) = \begin{cases} 1, & 0 \le t \le T_c \\ 0, & \text{elsewhere} \end{cases} \tag{7}$$

Substituting (2), (3), and (6) in (1), the CAF comprising of pulse shaping functions with respective shifted pulses and corresponding coefficients a_i and b_j can be obtained as

$$\chi(\tau, f_d) = \sum_{i=1}^{N}\sum_{j=1}^{N} a_i b_i^* \int_{-\infty}^{\infty} s_i(t) s_j^*(t+\tau)\exp(j2\pi f_d t)dt \quad (8)$$

where the integral represents the CAF between pairs of pulse shaping functions, i.e.,

$$\hat{\chi}_{i,j}(\tau, f_d) = \int_{-\infty}^{\infty} s_i(t) s_j^*(t+\tau)\exp(j2\pi f_d t)dt \quad (9)$$

Clearly, synthesizing a CAF such that it matches a desired CAF of pre-defined magnitude over the delay-Doppler plane is a difficult task. As a result, not many methods, other than solutions based on least square approaches exist, see, e.g., [14,17–21]. Recently, in [22], an algorithm has been proposed to match a synthesized CAF to a desired CAF of pre-defined magnitude over the delay-Doppler plane. More specifically, this algorithm proposes a joint design of a pair of signals $a(t)$ and $b(t)$, or sequences $\mathbf{a}$ and $\mathbf{b}$ to tackle the CAF synthesization problem. Furthermore, in [23], Jamil. et. al. proposed a Lévy flight based cuckoo search for a joint sequence design such that their CAF approximates a desired CAF indicating the potential of metaheuristic approaches to solve such challenging sequence design problems.

In view of the above, this chapter considers a joint sequence design using the improved bat algorithm (IBA) of [24] to address the problem of matching a synthesized CAF to a desired CAF of pre-defined magnitude over the delay-Doppler plane. We hypothesize that a joint design of a pair of sequences $\mathbf{a}$ and $\mathbf{b}$ such that their CAF approximates a desired CAF is a global optimization problem (GOP). Apparently, this type of problem is a highly multimodal problem without any *a priori* information about the location of the optimum solution (unimodal) or solutions (multimodal). Traditional optimization methods that require either an initial guess or gradient information are unsuitable to solve such problems to optimality. Therefore, nature-inspired population methods mimicking the behaviour of different species of animals have

been proposed to solve such problems [25–27]. Due to their general applicability and effectiveness, these algorithms have been a popular choice to solve modern optimization problems. These population-based algorithms use population members to explore the problem search space for a possible solution or solutions by maintaining a balance between intensification (exploitation) and diversification (exploration). However, intensification (exploitation) and diversification (exploration) are usually based on a uniform or Gaussian distribution. Lévy flights (LFs) based on the Lévy distribution have been proposed as an alternative to achieve exploitation and exploration strategies.

The remainder of this chapter is organized as follows. In Section 2, we briefly introduce the Lévy probability distribution. Section 3 presents the motivation of using LFs in metaheuristic algorithms. In Section 4, the formulation and solution to the considered synthesis problem is presented. Numerical results are presented in Section 5. Finally, Section 6 concludes the chapter.

2 Lévy Probability Distribution

A random process is called stable if the sum of a given number of independent random variables, $X_1, X_2, \ldots, X_N$, has the same probability density function (PDF) up to location and scale parameters as the individual random variables. A well-known example of a stable random process is a Gaussian process, i.e., the sum of Gaussian random variables also produces a Gaussian distribution which in addition has a finite second moment. A stable random process with infinite second moment produces a so-called α-stable distribution. An α-stable random variable S is defined by its characteristic function as follow [28]:

$$\Phi_{\alpha,\beta} = \mathrm{E}\big[\exp(jzS)\big] = \exp(-\beta^{\alpha}|z|^{\alpha}) \tag{10}$$

where $\mathrm{E}[\cdot]$ denotes the expectation operator, $j = \sqrt{-1}$, $z \in \mathbb{R}$, $\alpha \in (0, 2]$ and $\beta \geq 0$. The Lévy probability distribution belongs to a special class of symmetric α-stable distributions. According to [28], the PDF of a symmetric α-stable random variable is given by the inverse Fourier

transform of (10) as

$$L_{\alpha,\beta}(S) = \frac{1}{\pi}\int_0^{\infty} \exp(-\beta z^{\alpha})\cos(zS)dz \tag{11}$$

In (11), the parameters α and β control the shape and the scale of the distribution, respectively. The parameter α takes values in the interval $0 < \alpha \leq 2$ and controls the heaviness of the distribution, i.e., the decay of the tail. The smaller the value of α, the more the accumulation of data in the tails of the distribution. In other words, the random variable values are more likely to be far away from the mean of the distribution. On the other hand, the larger the value of α, the more the accumulation of data near the mean of the distribution. Except for a few special cases, a closed-form expression of integral in (11) is not known for general α. The integral in (11) becomes a Cauchy distribution and Gaussian distribution for $\alpha = 1$ and 2, respectively.

3 Lévy Flight Based Metaheuristic Algorithms

In recent years, a number of theoretical and empirical studies have tried to explain that foragers such as grey seals [29], microzooplankton [30, 31], reindeer [32], wandering albatrosses [33], fish [34], among many others, adapt LF as an optimal search strategy in search of food. However, it should be mentioned that foragers adapt their search strategy based on the density of prey, sometimes switching between LF and Brownian motion (BM). In metaheuristic and stochastic optimization algorithms, random walks play an important and central role in the exploration of the problem search space. The search performed by metaheuristic algorithms (MAs) is carried out in a way that it can accomplish goals of intensively explored areas of the search space with high-quality solutions and move to unexplored areas of the search space when necessary. Intensification and diversification [35, 36] are two key ingredients to achieve these goals. By maintaining a fine balance between these two components define the overall efficiency of MA. In fact, Lévy flights have already been used to enhance metaheuristic algorithms with promising results in the literature [23, 25, 26].

An alternative to a uniform or Gaussian distribution to realize randomization in MA is offered by the Lévy distribution. Not only does the power law behavior of a Lévy distribution reduce the probability of returning to previously visited sites in the problem search space, but it also provides an effective and efficient exploration of the far-off regions of the function landscape.

3.1 Improved Bat Algorithm

The MA mimicking the echolocation behavior of certain species of bats was presented in [27] and is based on the following set of rules and assumptions:

1. All bats know the difference between food/prey, background barriers, and use echolocation to sense the proximate distance from the prey;

2. In search mode, bats fly randomly with a frequency $f_{\min}$ with velocity $\mathbf{v}_i$ at position $\mathbf{x}_i$. During search mode, bats vary wavelength λ (or frequency f) and loudness A_0. Depending on the proximity from the target, bats can automatically adjust the wavelength (or frequency) for their emitted pulses and adjust the rate of pulse emission $r \in [0, 1]$;

3. It is further assumed that the loudness varies from a large (positive A_0) to a minimum value of $A_{\min}$;

4. Ray tracing is not used in estimating the time delay and three dimensional topography;

5. The frequency f is considered in a range $[f_{\min}, f_{\max}]$ corresponding to the range of wavelengths $[\lambda_{\min}, \lambda_{\max}]$;

6. For simplicity, frequency is assumed in the range $f \in [0, f_{\max}]$.

According to [27], by making use of the above rules and assumptions, the standard bat algorithm (SBA) will always find the global optimum. However, in SBA, the bats rely purely on random walks drawn from a Gaussian distribution, therefore, speedy convergence may not be guaranteed [27].

In this section, a brief overview of the IBA [24] is presented which constitutes an improved version of SBA [27]. In IBA, the random motion of bats is replaced by LF instead of using a Gaussian distribution. The motivation for this choice is that the power-law behavior of the Lévy distribution will produce some members of the random population in the distant regions of the search space, while other members will be concentrated around the mean of the distribution. The power-law behavior of the Lévy distribution also helps to induce exploration at any stage of the convergence, making sure that the system will be not trapped in local minima. The Lévy distribution also reduces the probability of returning to the previously visited sights, while the number of visitations to new sights is increased [24,25,27]. For a comprehensive review of the bat algorithm and its variant, please refer to [37].

3.2 Motion of the Bats

In IBA, the position or location of each bat is given as $\mathbf{x}_i^t$ and it flies through the D-dimensional search space or solution space with a velocity $\mathbf{v}_i^t$. The position and velocity for bat i are updated at time t, respectively, as

$$\mathbf{v}_i^t = \mathbf{v}_i^{t-1} + (\mathbf{x}_i^{t-1} - \mathbf{x}_i^{\text{best}}) f_i \tag{12}$$

$$\mathbf{x}_i^t = \mathbf{x}_i^{t-1} + \mathbf{v}_i^t \Delta t \tag{13}$$

where Δt represents the discrete time step of the iteration. However, in mathematical optimization, emphasis is often given to dimensionless variables, and therefore, Δt can be implicitly chosen as 1. Furthermore, the pulse frequency f_i for bat i at position $\mathbf{x}_i$ is given by

$$f_i = f_{min} + (f_{max} - f_{min})\beta \tag{14}$$

and vectors $\mathbf{x}_i$ and $\mathbf{v}_i$ represent the position and velocity of bat i. In (14), $\beta \in [0, 1]$ is a random number drawn from a uniform distribution, f_{min} and f_{max} denote the minimum and maximum frequency of the emitted pulse [27]. The symbol $\mathbf{x}_i^{\text{best}}$ in (12) represents the current best solution found by bat i by comparing all the solutions among all the NP bats.

In IBA [24], once a best solution is selected among the current best solutions, a new solution for each bat is generated using an LF that is based on a Lévy distribution according to

$$\mathbf{x}_i^t = \mathbf{x}_i^{\text{best}} + \gamma \cdot \mathbf{L}_\alpha(S) \tag{15}$$

Here, vector $\mathbf{L}_\alpha(S)$ represents a random walk that is generated based on the Lévy distribution for each i (bat) with parameter α. The parameter $\gamma > 0$ scales the random step length and is related to the scales of the problem [25–27]. Specifically, the step size S of the random walk is drawn from a Lévy distribution with infinite mean and variance which is often given in terms of a power-law formula given as [25, 26, 28]

$$L_\alpha(S) \sim \frac{1}{S^{\alpha+1}} \quad |S| >> 0 \tag{16}$$

where α determines the probability of obtaining Lévy random numbers in the tail of the distribution.

3.3 Variation of Loudness and Pulse Rates

In IBA, we use the originally proposed approach of controlling the exploration and exploitation in bats as proposed in [27], i.e., variation of loudness and pulse rates. In order to switch to the exploitation stage when necessary, each bat i varies its loudness A_i and pulse emission rate r_i iteratively as follows:

$$A_i^{t+1} = \Upsilon A_i^{t_0} \tag{17}$$

$$r_i^{t+1} = r_i^{t_0}[1 - \exp(-\Gamma t)] \tag{18}$$

where $A_i^{t_0}$, A_i^{t+1}, $r_i^{t_0}$, and r_i^{t+1}, respectively, represent initial loudness, updated loudness, initial pulse emission rate, and updated pulse emission rate after each iteration for bat i. Furthermore, Υ and Γ are constants.

4 Problem Formulation

In practice, infinite energy signals do not exist, therefore, ambiguity surfaces that produce a Dirac impulse or a function with ideal delay-Doppler characteristics do not exist. Thus, it is often desirable to design

waveforms that exhibit a peak at the origin and produce an almost flat surface in and around a large neighborhood of the origin.

The problem of matching a CAF to a desired CAF can be formulated as a minimization problem and can be solved by using the cyclic approach proposed in [22]. Accordingly, such an optimization problem can be formulated as

$$\min_{\mathbf{a},\mathbf{b}} C(\mathbf{a},\mathbf{b}) = \int_{-\infty}^{\infty}\int_{-\infty}^{\infty} w(\tau, f_d)\cdot\left[d(\tau, f_d) - \left|\mathbf{b}^H\mathbf{X}(\tau, f_d)\mathbf{a}\right|\right]^2 d\tau df_d \quad (19)$$

where $w(\tau, f_d)$ is a weighting function that specifies which area of the CAF in the delay-Doppler plane needs to be emphasized and $(\cdot)^H$ denotes Hermitian transpose. The modulus of the desired CAF is denoted by $d(\tau, f_d)$ which is positive and real-valued, $\mathbf{a}$ and $\mathbf{b}$ are different sequences. In view of (9), the cross-ambiguity matrix of the pulse shaping functions can be written as

$$\mathbf{X}(\tau, f_d) = \begin{bmatrix} \hat{\chi}_{1,1}(\tau, f_d) & \cdots & \hat{\chi}_{1,N}(\tau, f_d) \\ \vdots & \ddots & \vdots \\ \hat{\chi}_{N,1}(\tau, f_d) & \cdots & \hat{\chi}_{N,N}(\tau, f_d) \end{bmatrix} \quad (20)$$

where $\hat{\chi}_{i,j}(\tau, f_d)$ denotes the CAF between the i-th and j-th pulse shaping function given by (9). Furthermore, the term under the absolute value operator $|\cdot|$ in (19) represents the CAF in (8) in a more compact form as

$$\chi(\tau, f_d) = \mathbf{b}^H\mathbf{X}(\tau, f_d)\mathbf{a} \quad (21)$$

Due to phase incoherencies, the magnitude of the ambiguity function contains all the information about a signal pertinent to system performance [20]. In order to solve the ambiguity function synthesis problem, the indirect approach introduced in [20, 38] can be used. Accordingly, auxiliary phases are introduced to the desired ambiguity function $d(\tau, f_d)$ in (19), that is

$$\tilde{C}(\mathbf{a},\mathbf{b},\theta(\tau,f_d)) = \int_{-\infty}^{\infty}\int_{-\infty}^{\infty} w(\tau,f_d)\cdot\left|d(\tau,f_d)e^{j\theta(\tau,f_d)} - \mathbf{b}^H\mathbf{X}(\tau,f_d)\mathbf{a}\right|^2 d\tau df_d \quad (22)$$

Introducing auxiliary phases $\theta(\tau,f_d)$ makes the integrand in (22) real and positive everywhere. The minimization problem in (22) can then be solved by fixing two arguments of $\tilde{C}(\cdot,\cdot,\cdot)$ and minimizing $\tilde{C}(\cdot,\cdot,\cdot)$ with respect to the third variable [22].

First, let us fix a pair of sequences $\mathbf{a}$ and $\mathbf{b}$ which leads to the auxiliary phase $\theta(\tau,f_d)$ being expressed as [20,38]

$$\theta(\tau,f_d) = \arg\{\mathbf{b}^H\mathbf{X}(\tau,f_d)\mathbf{a}\} \quad (23)$$

Second, by fixing the auxiliary phases $\theta(\tau,f_d)$ and sequence $\mathbf{b}$, the criterium $\tilde{C}(\cdot,\cdot,\cdot)\rightarrow\tilde{C}(\mathbf{a})$ can be written as [20,38]

$$\begin{aligned}\tilde{C}(\mathbf{a}) &= \mathbf{a}^H\mathbf{D}_1\mathbf{a} - \mathbf{a}^H\mathbf{D}_2\mathbf{b} - \mathbf{b}^H{\mathbf{D}_2}^H\mathbf{a} + \int_{-\infty}^{\infty}\int_{-\infty}^{\infty} w(\tau,f_d)\left|d(\tau,f_d)\right|^2 d\tau df_d \\ &= (\mathbf{a}-\mathbf{D}_1^{-1}\mathbf{D}_2\mathbf{b})^H\mathbf{D}_1(\mathbf{a}-\mathbf{D}_1^{-1}\mathbf{D}_2\mathbf{b}) + C \quad (24)\end{aligned}$$

where constant C does not depend on sequence $\mathbf{a}$ and therefore can be ignored. It follows from (24) that the minimizer $\mathbf{a}$ is given as

$$\mathbf{a} = \mathbf{D}_1^{-1}\mathbf{D}_2\mathbf{b} \quad (25)$$

where $\mathbf{D}_1\in\mathbb{C}^{N\times N}$ and $\mathbf{D}_2\in\mathbb{C}^{N\times N}$, respectively, are given as

$$\mathbf{D}_1 = \int_{-\infty}^{\infty}\int_{-\infty}^{\infty} w(\tau,f_d)\mathbf{X}^H(\tau,f_d)\mathbf{b}\mathbf{b}^H\mathbf{X}(\tau,f_d)d\tau df_d \quad (26)$$

$$\mathbf{D}_2 = \int_{-\infty}^{\infty}\int_{-\infty}^{\infty} w(\tau,f_d)d(\tau,f_d)e^{\theta(\tau,f_d)}\mathbf{X}^H(\tau,f_d)d\tau df_d \quad (27)$$

Third, by fixing the auxiliary phases $\theta(\tau, f_d)$ and sequence $\mathbf{a}$, the criterium $\tilde{C}(\cdot,\cdot,\cdot) \rightarrow \tilde{C}(\mathbf{b})$ can be formulated as [20, 38]

$$\begin{aligned}\tilde{C}(\mathbf{b}) &= \mathbf{b}^H\mathbf{D}_3\mathbf{b} - \mathbf{b}^H\mathbf{D}_2\mathbf{a} - \mathbf{a}^H\mathbf{D_2}^H\mathbf{b} \\ &\quad + \int_{-\infty}^{\infty}\int_{-\infty}^{\infty} w(\tau, f_d)\big|d(\tau, f_d)\big|^2 d\tau df_d \\ &= (\mathbf{b} - \mathbf{D}_3^{-1}\mathbf{D}_2^H\mathbf{a})^H\mathbf{D}_3(\mathbf{b} - \mathbf{D}_3^{-1}\mathbf{D}_2^H\mathbf{a}) + C \qquad (28)\end{aligned}$$

where constant C does not depend on sequence $\mathbf{b}$ and therefore can be ignored. Then, in view of (28), the minimizer $\mathbf{b}$ can be obtained as

$$\mathbf{b} = \mathbf{D}_3^{-1}\mathbf{D}_2^H\mathbf{a} \qquad (29)$$

where $\mathbf{D}_3 \in \mathbb{C}^{N\times N}$ is given as

$$\mathbf{D}_3 = \int_{-\infty}^{\infty}\int_{-\infty}^{\infty} w(\tau, f_d)\mathbf{X}(\tau, f_d)\mathbf{a}\mathbf{a}^H\mathbf{X}^H(\tau, f_d)d\tau df_d \qquad (30)$$

4.1 Proposed Approach

In the proposed approach, the phases of the elements of sequence $\mathbf{a} \in \mathbb{C}^{N\times 1}$ and sequence $\mathbf{b} \in \mathbb{C}^{N\times 1}$, respectively, are denoted by column vectors of length N as

$$\phi_{\mathbf{a}} = [\phi_a(1), \phi_a(2), \ldots, \phi_a(N)]^T \qquad (31)$$

$$\phi_{\mathbf{b}} = [\phi_b(1), \phi_b(2), \ldots, \phi_b(N)]^T \qquad (32)$$

In the context of IBA, each element of the column vectors $\phi_{\mathbf{a}}$ and $\phi_{\mathbf{b}}$ in (31) and (32), respectively, is considered as a single bat generated randomly in the interval $[0, 2\pi]$. The population size (bats) is equal to the length N of the sequences. Then, the corresponding sequences $\mathbf{a}$ and $\mathbf{b}$, respectively, are given as

$$\mathbf{a} = [e^{\phi_a(1)}, e^{\phi_a(2)}, \ldots, e^{\phi_a(N)}]^T \qquad (33)$$

$$\mathbf{b} = [e^{\phi_b(1)}, e^{\phi_b(2)}, \ldots, e^{\phi_b(N)}]^T \qquad (34)$$

Given the above notion of sequence elements being bats, the pseudocode to solve the CAF synthesization problem using IBA can be formulated as in Procedure 1.

Procedure 1: Pseudocode of IBA for CAF synthesization

1. Objective function $\tilde{C}(\theta(\tau, f_d), \mathbf{a}, \mathbf{b})$
2. Initialize A_i,f_i, and r_i.
3. Generate the cross-ambiguity matrix using (20).

for all NP bats

4. Generate an initial population of NP bats (solutions) to generate sequences $\mathbf{a}$ and $\mathbf{b}$ using (33) and (34), respectively, or use initially generated sequences.
5. $\theta(\tau, f_d) = \arg\{\mathbf{b}^H \mathbf{X}(\tau, f_d)\mathbf{a}\}$
6. Start with initially generated sequence in Step 4 by applying (25) to generate $\mathbf{a}$.
7. Start with initially generated sequence in Step 4 by applying (29) to generate $\mathbf{b}$.
8. Evaluate the objective function using (22).

end

9. Store the best objective function value.
10. Keep the current best sequences $\mathbf{a}$ and $\mathbf{b}$.

$t = 1$

while (t < MaxGeneration) or (stop criterion)

$t = t + 1$

11. Update pulse emission rate and loudness using (17) and (18).
12. Update the velocity and frequency using (12) and (14).
13. $\theta(\tau, f_d) = \arg\{\mathbf{b}^H \mathbf{X}(\tau, f_d)\mathbf{a}\}$
14. Start with sequences generated in Step 6 and 7 to generate $\mathbf{a}'$ and $\mathbf{b}'$ by applying (25), (29), and (13).
15. **if** (rand > r)
    Start with sequences in Step 10 to generate $\mathbf{a}'$ and $\mathbf{b}'$ by performing LF using (25), (29), and (15).
    end
16. Apply problem bound constraints, if the sequences generated in Step 14 or Step 15 are outside the interval $[0, 2\pi]$.
17. Re-evaluate the objective function using (22).
18. **if** ($\tilde{C}_{\text{Step 16}} \leq \tilde{C}_{\text{Step 8}}$ | rand < A)
    Replace the sequences in Step 6 and Step 7 with $\mathbf{a}'$ and $\mathbf{b}'$.
    $\tilde{C}_{\text{Step 8}} \leftarrow \tilde{C}_{\text{Step 17}}$

end

19. **if** $\tilde{C}_{\text{Step 17}} \leq \tilde{C}_{\text{Step 9}}$

Replace the sequences in Step 10 with $\mathbf{a}'$ and $\mathbf{b}'$.

$\tilde{C}_{\text{Step 9}} \leftarrow \tilde{C}_{\text{Step 17}}$

end

end while

4.2 Parameter Settings

Universal values of the parameters A^{t_0}, r^{t_0}, Γ, and Υ do not exist for the problems that will be discussed in Section 5. This is due to the fact that each problem has a different landscape and dimension. Hence, an effective set of initial values of these parameters require some experimentation. Accordingly, the initial values for these parameters were obtained from trial experiments on the optimization problems that will be considered in Section 5. Different initial values for loudness A and pulse emission rate r were taken in the range $[0, 1]$ with increments of 0.1. For each optimization problem, the selected values of A^{t_0}, r^{t_0}, Γ, and Υ produced slightly different rates of convergence as each optimization problem has a different landscape.

In reality, bats increase pulse emission rate r_i and decrease loudness A_i after potential prey has been detected and their approach towards the prey has commenced. In the context of optimization, prey refers to a solution of the problem. As such, an update of loudness A_i and pulse emission rate r_i in (17) and (18), respectively, takes place in the IBA only if a new solution is found. This implies that the virtual bats are moving towards the optimal solution.

The above experimental approach was also adapted to select the values of constants Υ and Γ. The best combination of Υ and Γ was found to be $\Upsilon = \Gamma = 0.5$. The results that will be presented subsequently in Section 5 show that this choice of parameters seems to be appropriate for the optimization problems considered. In summary, the parameter settings listed in Table 1 are used in the simulations.

Table 1: Parameter setting for IBA

Parameter	Value
Number of Bats (Population Size), NP	depending on the length of the sequence to be synthesized
Number of Generations, G	200
Initial Loudness, A^{t_0}	0.1
Initial Pulse Emission Rate, r^{t_0}	0.1
Constants, $\Upsilon = \Gamma$	0.5
Lévy Step Length, S	1.5
Minimum Frequency, f_{min}	0
Maximum Frequency, f_{max}	dependents on the problem domain size

4.3 Calculation of Lévy Step Size

A CAF synthesization problem can be considered as multimodal optimization problem without any *a priori* information regarding the location of an optimal solution. LFs can be used to generate the random step length S of a random walk drawn from a Lévy distribution. The choice of α in (16) determines the probability of obtaining a Lévy random number in the tail of the Lévy distribution. Given that each optimization problem is unique, i.e., has different dimension and landscape, the task of choosing a favorable value of α that generates a suitable step length S becomes difficult. In particular, the search ability of an MA can be severely hampered, if an improper value of α is used to generate S.

Given the complex nature of the CAF synthesization problem, a universal value of α required to generate S for guiding virtual bats in IBA without getting trapped in a local minimum does not exist. Therefore, it is appropriate to carry out a series of experiments in order to find a suitable value of α. For this purpose, four values of $\alpha = 1.3, 1.4, 1.5$, and 1.6 were selected. For each of these values, 10 independent trials for a fixed number of iterations were performed to minimize (22) for the problems that will be discussed in Section 5. It

turned out that $\alpha = 1.5$ produces the best value of criterium (22) in average over the number of trails. Therefore, this value has been used to generate the random step length S for all problems considered in Section 5.

4.4 Selection of Scaling factor

The parameter γ in (15) determines how far the virtual bats in IBA can travel in the search space. An excessively large value of γ causes new solutions to jump outside of the feasible search space and even to fly off to far regions. On the other hand, the search is confined to a rather narrow region, if γ is too small. In the former case, the LF becomes too aggressive, whereas, in the latter case, the LF is not efficient. Therefore, some sort of strategy is needed to scale step length S such that an efficient search process is maintained. In order to avoid the particles flying too far, a small value of parameter γ can be more efficient [25, 26]. A small value of γ may apply for unimodal problems. We hypothesize that the location of an optimal solution to a multimodal problem such as CAF synthesization is not known. As such, selecting a small value of γ will hinder the search process.

Therefore, in order to select an appropriate value of γ, we have adopted the experimental approach described in Section 4.3 and conducted a series of trials with different values of γ. We have conducted 10 independent trails for a fixed number of iterations that were performed to minimize (22) for Example 2 in Section 5 using $\gamma = 0.01, 0.05, 0.1, 0.5, 0.7$ and 0.9. The best peak-to-average power ratio (PAR) for each of these values produced by IBA for each run was recorded. It was found that $\gamma = 0.05$ produces the best PAR and hence was subsequently used as a basis for the examples presented in Section 5.

5 Numerical Results

Let us consider sequences of length $N = 50$ for Examples 1 and 2, sequence length $N = 53$ for Example 3 and sequence length $N = 31$ for Example 4. Each element of the considered sequences corresponds to the phase-coded amplitude of a rectangular pulse shape function of duration T_c. Thus, the duration of a sequence is given as $T = N \cdot T_c$. Furthermore, τ denotes the delay by which a transmitted signal is returned from a target and f_d denotes the Doppler frequency induced by a moving target. In the sequel, we utilize normalized delay τ/T_c and normalized Doppler frequency $f_d \cdot T$, respectively. In what follows, we illustrate by way of four examples that IBA is able to jointly design sequences **a** and **b** such that a desired CAF is synthesized.

5.1 Example 1

In this example, we aim at synthesizing a CAF with a diagonal ridge while being zero elsewhere. This type of CAF is desirable when a filter bank is too expensive to cope with different Doppler frequencies and tolerance to Doppler shifts is needed. The weighting function is $w(\tau, f_d) = 1$ for all (τ, f_d) in (19) and the sequence **a** has constant modulus, i.e., each element of **a** takes on the value of one and hence PAR = 1. The desired CAF is shown in Fig. 1 and the corresponding synthesized CAF obtained by using IBA is shown in Fig. 2. As can be seen from Fig. 2, the CAF synthesized by IBA approximates the desired CAF in Fig. 1.

5.2 Example 2

The synthesization of an ideal thumbtack CAF, i.e., narrow peak at the origin and zero sidelobes in the rest of the delay-Doppler plane is not possible due to the volume property of CAFs. Therefore, in this example, we aim at synthesizing a CAF with a clear area in and around a large neighbourhood of the origin using the following CAF modulus:

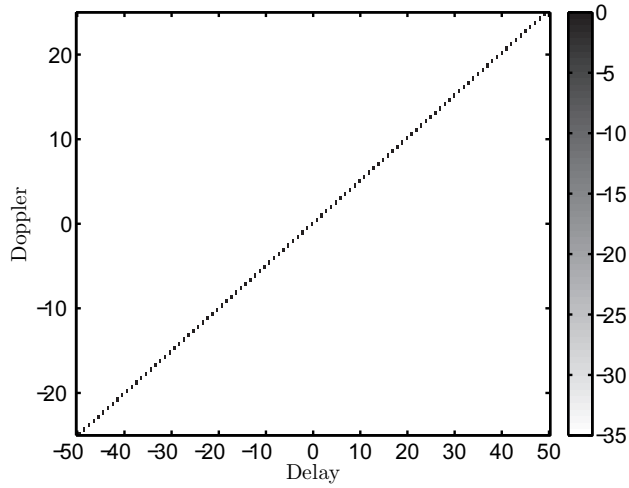

Figure 1: Desired CAF with diagonal ridge.

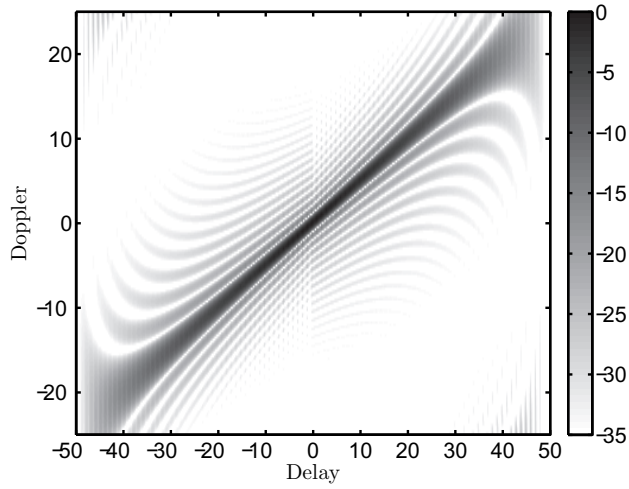

Figure 2: Synthesized CAF using IBA for $\gamma = 0.05$ (PAR = 1).

$$d(\tau, f_d) = \begin{cases} N, & \text{for } (\tau, f_d) = (0,0) \\ 0, & \text{elsewhere} \end{cases}$$

and weighting function

$$w(\tau, f_d) = \begin{cases} 1, & \text{for } (\tau, f_d) \in \Omega_{ds} \backslash \Omega_{\sim ds} \\ 0, & \text{elsewhere} \end{cases}$$

where $\Omega_{ds} = \{[-10T_c, 10T_c] \times [-\frac{2}{T_c}, \frac{2}{T_c}]\}$ is the selected region of interest of the synthesized CAF. In order to compensate for sharp changes in the desired CAF $d(\tau, f_d)$ near the origin, the area of the main lobe $\Omega_{\sim ds} = \{[-T_c, T_c] \backslash \{0\} \times [-\frac{1}{T_c}, \frac{1}{T_c}] \backslash \{0\}\}$ near the origin has to be excluded [22]. Recall that the Doppler shift f_d induced on the signal in practice is often much smaller compared to the bandwidth of the transmitted signal. Therefore, the weighting function $w(\tau, f_d)$ outside the maximum induced Doppler shift f_d can be set to zero.

The need of this type of CAF arises in applications such a geolocation of signals, where the CAF is used to calculate the time of difference of arrival and frequency difference of arrival of the emitted signal using two receivers [39]. The two collector architecture offers the opportunity to compare the reception of a likely similar radar pulse using cross-correlation concepts with respect to delay. Thus, one collector will see the radar pulse as $a(t)$ and the other collector will see it as $b(t + \tau)$. Also, it is assumed that one collector is moving with some relative velocity to the other collector which supports measuring the frequency of the received pulse at slightly different frequencies [39].

Furthermore, a CAF with a clear area around a large neighbourhood of the origin also arises in situations, when it is not possible to design a sequence or set of sequences that yield zero sidelobes over the entire delay-Doppler plane. Therefore, it is desirable to design a reference waveform or equivalent filter at the radar receiver end. Such a receiver, is called optimum receiver [1] in which the internal or reference waveform (or equivalent filter) is deliberately mismatched compared to the transmitted waveform in order to reduce the sidelobes in the delay-Doppler plane.

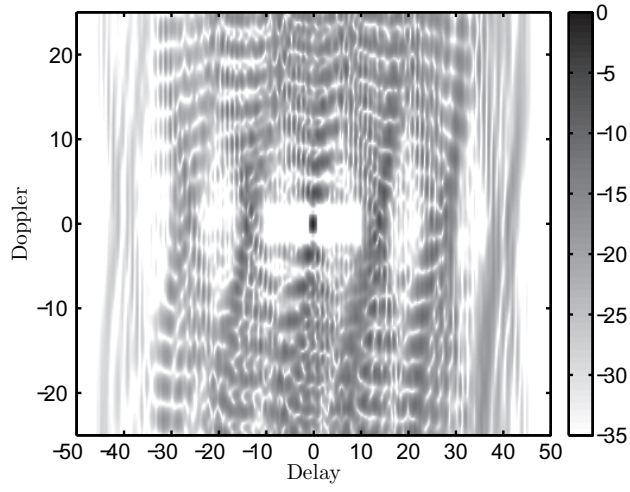

(a)

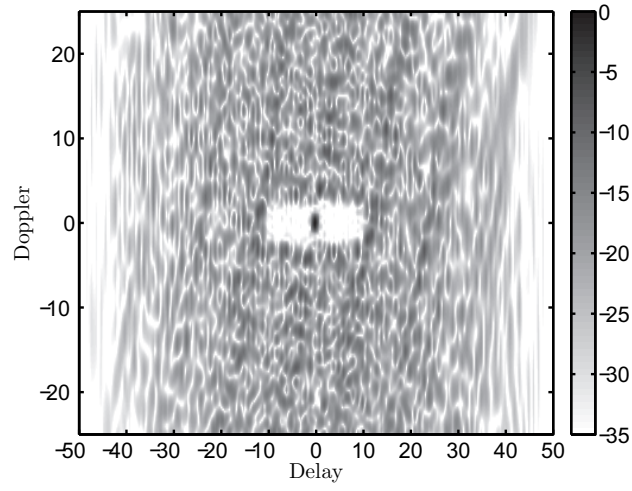

(b)

Figure 3: CAF synthesization without and with PAR constraint (35) for $\gamma = 0.05$: (a) Synthesized CAF of random sequences of length N = 50 (PAR = 3.9), (b) Synthesized CAF of random sequences of length N = 50 (PAR = 1).

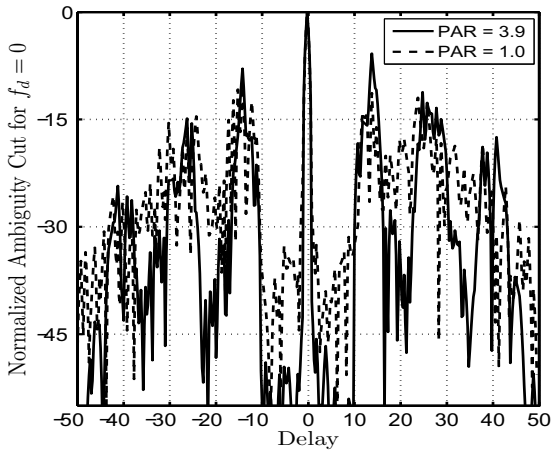

Figure 4: Normalized zero-Doppler cut of the CAFs of Fig. 3(a) and (b) without and with constraint (35), respectively.

Fig. 3 shows the CAF of sequences **a** and **b** generated by IBA with $\gamma = 0.05$. The desired sidelobe free area can be observed within the rectangular area close and around the origin. The sidelobe free region in Fig. 3(a) is due to the fact that the amplitude of the generated sequences **a** or **b** is not constrained. This may result in sequences with relatively high PAR and relatively low sidelobe levels. The PAR of sequences **a** and **b** for the CAF shown in Fig. 3(a) were found to be $\mathrm{PAR}_{\mathbf{a}} = 3.9$ and $\mathrm{PAR}_{\mathbf{b}} = 7.2$, respectively.

It is noted that low sidelobe levels are desirable in radar applications to avoid masking of main peaks of secondary targets, even if the targets are well separated. Moreover, in case of a multiple target environment, the sum of all sidelobes may build up to a level sufficient to mask even relatively strong targets.

The widespread use of solid state power amplifiers and digitization have a significant impact on the overall performance of radar, sonar, and communication systems. For example, transmission of a signal or a waveform of arbitrary amplitude is not possible due to limitations of power amplifiers and analog-to-digital converters. As a result, it is often desirable that transmit signals or waveforms have a constant amplitude or a low PAR. One of the possibilities that allows the consideration of

waveforms with variable amplitude is to work with a pair of waveforms, i.e., the transmitted signal of constant amplitude and the reference signal of arbitrary amplitude that is used during signal processing at the receiver [40]. Therefore, to constrain the PAR of a transmit waveform with PAR=1, the following additional operation may be employed in the IBA algorithm in Procedure 1 after Step 14 (see also [22]):

$$s_n \leftarrow \exp[j \arg(s_n)] \tag{35}$$

However, inducing such a constraint further complicates the design of waveforms with prescribed ambiguity surfaces. Using (35), somewhat higher sidelobes can be observed in the results shown in Fig. 3(b). The normalized zero-Doppler cut through the CAF for the unconstrained design (PAR > 1) and constrained design (PAR $= 1$) are shown in Fig. 4.

5.3 Example 3

In this example, we aim at synthesizing a CAF for Björck sequences of length $N = 53$. In particular, Björck sequences of length $N = P$, where P is a prime number and $P \equiv 1(\text{mod } 4)$, are defined as

$$\mathbf{B}(k) = \exp\left(j2\pi\theta\left(\frac{k}{P}\right)\right), \qquad \theta = \arccos\left(\frac{1}{1+\sqrt{P}}\right) \tag{36}$$

where $(\frac{k}{P})$ denotes the Legendre symbol which is defined as

$$\left(\frac{k}{P}\right) = \begin{cases} 1, & \text{if } \mathrm{k} \equiv 0 \pmod{\mathrm{P}} \\ 1, & \text{if } \mathrm{k} \equiv m^2 \pmod{\mathrm{P}} \text{ for } \mathrm{m} \in \mathbb{Z} \\ -1, & \text{if } \mathrm{k} \not\equiv m^2 \pmod{\mathrm{P}} \text{ for } \mathrm{m} \in \mathbb{Z} \end{cases}$$

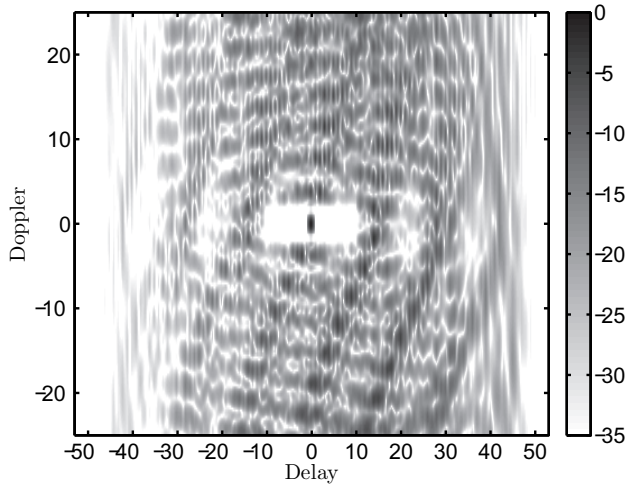

(a)

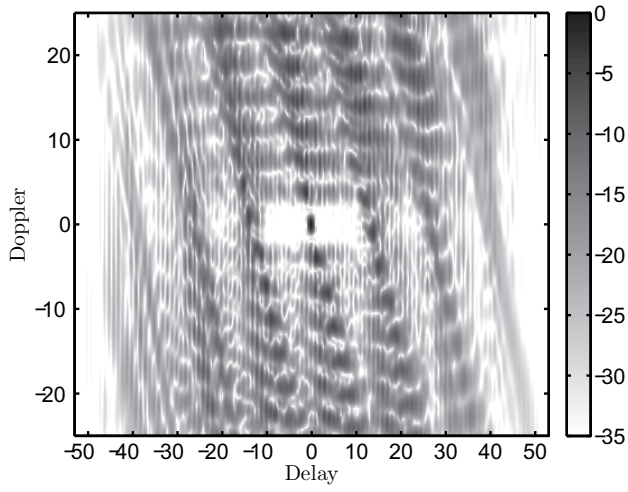

(b)

Figure 5: CAF synthesization without and with (35) for $\gamma = 0.05$: (a) Synthesized CAF for Björck sequence of length N=53 (PAR=4.9), (b) Synthesized CAF for Björck sequence of length N=53 (PAR = 1).

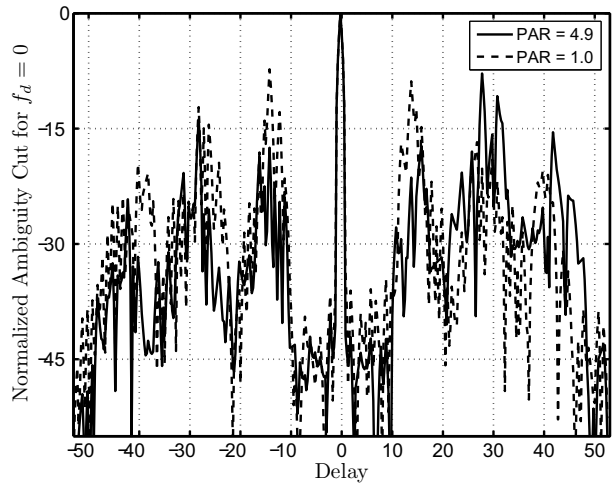

Figure 6: Normalized zero-Doppler cut of the CAFs shown in Fig. 5(a) and (b) without and with constraint (35), respectively.

The synthesized CAFs for the case of Björck sequences which approximates a desired thumbtack CAF without and with using constraint (35) are shown in Fig. 5(a) and (b), respectively. The normalized zero-Doppler cuts through the CAFs for the unconstrained design (PAR > 1) and the constrained design (PAR $= 1$) are shown in Fig. 6. A sidelobe level below -45dB respective -30dB can be observed for these cases.

5.4 Example 4

Finally, we synthesize a CAF for the case of Oppermann sequences [41] of length $N = 31$. The phase $\varphi_k(i)$ of the i-th element $u_k(i)$ of the k-th Oppermann sequence $\mathbf{u}_k = [u_k(0), u_k(1), \cdots u_k(N-1)]$ of length N is defined as

$$\varphi_k(i) = \frac{\pi}{N}[k^m(i+1)^p + (i+1)^n + k(i+1)N] \tag{37}$$

where $1 \leq k \leq N-1$, $0 \leq i \leq N-1$ and integer k is relatively prime to the length N. The parameters m, n and p in (37) take on real values

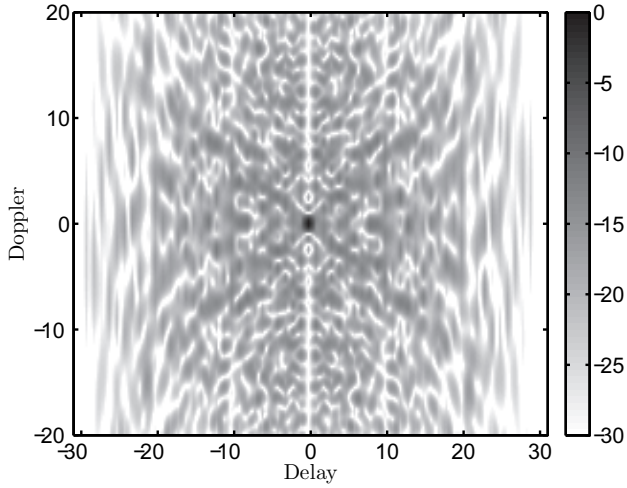

Figure 7: Synthesized CAF of Oppermann sequences with parameters $m, p = 1$, and $n = 3$.

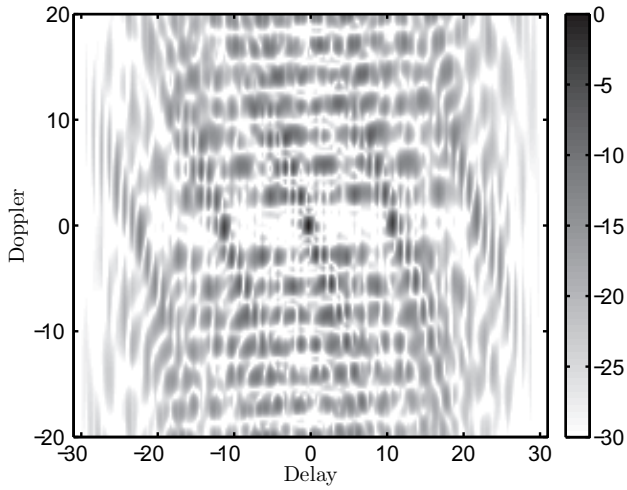

Figure 8: Synthesized CAF of Oppermann sequences with $\gamma = 0.05$ and using constraint (35).

and define a family of Oppermann codes.

The CAF for the case of Oppermann sequences with parameters $m, p = 1$ and $n = 3$ is shown in Fig. 7. The synthesized CAF of these Oppermann sequences is shown in Fig. 8, which approximates the desired CAF with a sidelobe free area around the neighbourhood of the origin. Relatively low sidelobe levels can be observed within the rectangular area close and around the origin with improved delay-Doppler characteristics compared to the CAF of the original sequence that is shown in Fig. 7. The zero-Doppler cut of the synthesized Oppermann sequence is shown in Fig. 9 which exhibits a low sidelobe level with respect to delay compared to the original Oppermann sequences.

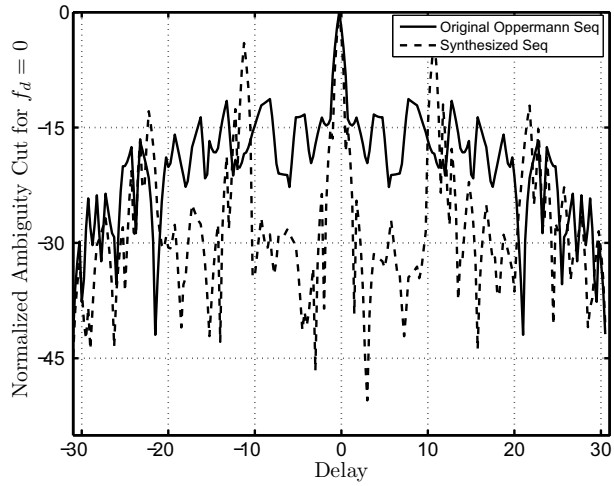

Figure 9: Normalized zero-Doppler cuts through the CAFs shown in Fig. 7 and 8.

6 Conclusions

In this chapter, the problem of synthesizing CAFs using a metaheuristic approach based on the echolocation of bats has been addressed. The fundamental problem in this context is to minimize the integrated square error between a desired CAF and a synthesized CAF. In particular, the IBA has been combined with a cyclic approach to solve this problem. By way of four examples, we have shown that the approach based on echolocation of bats can indeed synthesize CAFs that approximate CAF surfaces having a diagonal ridge and zero value elsewhere as well as CAF surfaces with a clear area around the origin. Our results indicate that the proposed approach is a promising technique for synthesizing CAFs. Further research will focus on more extensive studies of how to synthesize other complex functions and waveforms.

References

[1] Van Tress, H. L.: Optimum signal design and prcoessing for reverberation-limited environment. IEEE Trans. Military Electron. **9**(3), 212–229 (1965)

[2] Stoica, P., Li, J., Xue, M.: Transmit codes and receive filters for radar. IEEE Signal Process. Mag. **25**(6), 94–109 (2008)

[3] Blunt, S. D., Gerlach, K.: Adaptive pulse compression via MMSE estimation. IEEE Trans. Aerosp Electron. Syst. **42**(2), 572–584 (2006)

[4] Delong Jr., D. F., Hofstetter, E. M.: The design of clutter-resistant radar waveforms with limited dynamic range. IEEE Trans. on Inf. Theor. **15**(3), 376–385 (1967)

[5] Kay, S.: Optimal signal design for detection of Gaussian point targets in stationary Gaussian clutter/reverberation. IEEE J. of Sel. Top. Sign. Process. **1**(1), 31–41 (2007)

[6] Key, E. L.: A method of sidelobe reduction in coded pulse waveform. Tech. Report 209, M.I.T Lincoln Lab., Lexington, Mass (1959)

[7] Rummler, W. D.: A technique for improving the clutter performance of coherent pulse train signals. IEEE Trans. Aerosp Electron. Syst. **3**(6), 898–906 (1967)

[8] Stutt, C., Spafford, L. J.: A 'best' mismatched filter response for radar clutter discrimination. IEEE Trans. Inf. Theor. **14**(2), 280–287 (1968)

[9] Urkowitz, H.: Some high-velocity clutter effects in matched and mismatched receivers. IEEE Trans. Aerosp Electron. Syst. **4**(3), 481–485 (1968)

[10] Spafford, L. J.: Optimum radar signal processing in clutter. IEEE Trans. Inf. Theor. **14**(5), 734–743 (1968)

[11] Woodward, P.M.: Probability and information theory with applications to radar. Pergamon Press (1953). Reprint: Artech House, London (1980)

[12] Stoica, P., He, H., Li, J.: New algorithms for designing unimodular sequences with good correlation properties. IEEE Trans. Signal Process. **57**(4), 1415–1425 (2009)

[13] Wilcox, C. H.: The synthesis problem for radar ambiguity functions. MRC Tech. Summary Report 157, US Army, Univ. of Wisconsin, Madison, Wisconsin, USA, (1960). Reprint: Radar and Sonar, Part 1, The IMA Volumes in Mathematics and its Applications. Springer (1991)

[14] Gladkova, I., Chebanov, D.: On the synthesis problem for a waveform having a nearly ideal ambiguity function. In: International Conference on Radar Systems, Toulouse, France (2004)

[15] Stein, S.: Algorithms for ambiguity function processing. IEEE Trans. on Acoust. Speech, and Signal Process. **29**(3), 588–599 (1981)

[16] Sharama, R.: Analysis of MIMO radar ambiguity function and implications on clear region. In: IEEE International Radar Conference, Washington DC, USA (2010)

[17] Blau, W.: Synthesis of ambiguity functions for prescribed responses. IEEE Trans. Aerosp Electron. Syst. **3**(4), 656–663 (1967)

[18] Rihaczek, A. W., Mitchell, R. L.: Radar waveforms for suppression of extended clutter. IEEE Trans. Aerosp Electron. Syst. **3**(3), 510–517 (1967)

[19] Siebert, W.: A Radar Detection Philosophy. IRE Trans. on Information. Theory, **2**(3), 204–221 (1956)

[20] Sussman, S.: Least-square synthesis of the radar ambiguity function. IEEE Trans. Inf. Theor. **8**(3), 246–254 (1962)

[21] Wolf, J. D., Lee, G. M., Suyo, C. E.: Radar waveform synthesis by mean-square optimization techniques. IEEE Trans. Aerosp Electron. Syst. **5**(4), 611–619 (1969)

[22] He, H., Stoica, P., Li, J.: On synthesizing cross ambiguity function. In: IEEE International Conference on Acoustics, Speech and Signal Processing, Prague, Czech Republic (2011)

[23] Jamil, M., Zepernick, H.-J., Yang, X-S.: Lévy flight based cuckoo search algorithm for synthesizing cross-ambiguity functions, IEEE In: Military Communications Conference, pp. 823–828, San Diego, USA (2013)

[24] Jamil, M., Yang, X-S., Zepernick, H.-J.: Improved Bat-inspired metaheuristic algorithm with Lévy flights for global optimization problems, J. Appl. Softw. Comput. – Under Revision.

[25] Yang, X-S., Deb, S.: Cuckoo search via Lévy flights. In: Congress on Nature and Biological Inspired Computing, pp. 210-214, Coimbatore, India (2009)

[26] Yang, X-S.: Firefly algorithm, Lévy flights and global optimization. In: Bramer, M., Ellis, R., Petridis, M. (eds.) Research and Development in Intelligent Systems XXVI, pp. 209-218, Springer, Berlin (2010)

[27] Yang, X-S.: A new metaheuristic bat-inspired algorithm. In: Gonzalez et. al. J. R. (eds.) Nature Inspired Cooperative Strategies for Optimization, Studies in Computational Intelligence, pp. 65-74, Springer Berlin (2010)

[28] Gutowski, M.: Lévy flights as an underlying mechanism for global optimization algorithms. In: Proceedings National Conference on Evolutionary Computation and Global Optimization. Jastrzębia Góra, Poland (2001)

[29] Austin, D., Bowen, W. D., McMillan, J. I.: Intraspecific variation in movement patterns: Modelling individaul behaviour in a large marine predator. Oikos **105**(1), 15–30 (2004)

[30] Bartumeus, F., Peters, F., Pueyo, S., Marrase, C., Catalan, J.: Helical Lévy walks: Adjusting searching statistics to resource avaliability in microzooplankton. Proc. Nat. Acad. Sci. USA, **100**(22), 12771–12775 (2003)

[31] Humphries, N. E., Querioz, N., Dyer, J. R. M., Pade, N. G., Musyl, M. K., Schaefer, K. M., Fuller, D. W., Brunnschweiler, J. M., Doyle, T. K., Houghton, J. D. R., Hays, G. C., Jones, C. S., Noble, L. R., Wearmouth, V. J., Southall, E. J., Sims, D. W.: Environmental context explains Lévy and Brownian movement patterns of marine predators. Nature, **451**(7301), 1066–1069 (2010)

[32] Mårell, A. J., Ball, P., Hofgraad, A.: A foraging and movement paths of female reinedeer: Insights from fractal analysis, correlated random walks and Lévy flights. Can. J. Zoo. **80**(5), 854–865 (2002)

[33] Viswanathan, G. M., Afanasyev, V., Buldyrev, S. V., Murphy, E. J., Prince, P. A., Stanley, H. E.: Lévy flight search patterns of wandering albatrosses. Nature, **381**(6581), 413–415 (1996)

[34] Viswanathan, G. M.: Fish in Lévy-flight foraging. Nature **465**(7301), 1018–1019 (2010)

[35] Glover, F.: Tabu search - Part I. ORSA J. Comput. **1**(3), 190–206 (1989)

[36] Glover, F.: Tabu search - Part II. ORSA J. Comput. **2**(1), 4–32 (1990)

[37] Yang, X-S., He, X.: Bat algorithm review and and applications. Int. J. Bio-Inspired Comput. **5**(4), 141–149 (2013)

[38] Fienup, J. R.: Phase retrival algorithms: A comparison. Appl. Opt. **21**(15), 2758–2769 (1982)

[39] Overfield, J., Biskaduros, Z., Buehrer, R. M.: Geolocation of MIMO signals using the cross ambiguity function and TDOA/FDOA. In: IEEE International Conference on Communications, pp. 3648–3653, Ottawa, Canada (2012)

[40] Levanon, N., Mozeson, E.: Radar Signals. Wiley, New York (2004)

[41] Oppermann, I., Vucetic, B.S.: Complex spreading sequences with a wide range of correlation properties. IEEE Trans. Commun. **45**(3), 365–375 (1997)

ABSTRACT

The motivation of having a joint radar and communication system on a single hardware is driven by space, military, and commercial applications. However, designing sequences that can simultaneously support radar and communication functionalities is one of the major hurdles in the practical implementation of these systems. In order to facilitate a simultaneous use of sequences for both radar and communication systems, a flexible sequence design is needed.

The objective of this dissertation is to address the sequence design problem for integrated radar and communication systems. The sequence design for these systems requires a trade-off between different performance measures, such as correlation characteristics, integrated sidelobe ratio, peak-to-sidelobe ratio and ambiguity function. The problem of finding a trade-off between various performance measures is solved by employing meta-heuristic algorithms.

This dissertation is divided into an introduction and three research parts based on peer-reviewed publications. The introduction provides background on binary and polyphase sequences, their use in radar and communication systems, sequence design requirements for integrated radar and communication systems, and application of meta-heuristic optimization algorithms to find optimal sets of sequences for these systems.

In Part I-A, the performance of conventional polyphase pulse compression sequences is compared with Oppermann sequences. In Part I-B, weighted pulse trains with the elements of Oppermann sequences serving as complex-valued weights are utilized for the design of integrated radar and communication systems. In Part I-C, an analytical expression for the cross-ambiguity function of weighted pulse trains with Oppermann sequences is derived. Several properties of the related auto-ambiguity and cross-ambiguity functions are derived in Part I-D. In Part II, the potential of meta-heuristic algorithms for finding optimal parameter values of Oppermann sequences for radar, communications, and integrated radar and communication systems is studied. In Part III-A, a meta-heuristic algorithm mimicking the breeding behavior of Cuckoos is used to locate more than one solution for multimodal problems. Further, the performance of this algorithm is evaluated in additive white Gaussian noise (AWGN). It is shown that the Cuckoo search algorithm can successfully locate multiple solutions in both non-noise and AWGN with relatively high degree of accuracy. In Part III-B, the cross-ambiguity function synthesization problem is addressed. A meta-heuristic algorithm based on echolocation of bats is used to design a pair of sequences to minimize the integrated square error between the desired cross-ambiguity function and a synthesized cross-ambiguity function.

BLEKINGE TEKNISKA HÖGSKOLA · BTH ·

ISSN:1653-2090

ISBN: 978-91-7295-340-6

2017:07